

BEAM INSTRUMENTATION AND DIAGNOSTICS FOR HIGH LUMINOSITY LHC

M. Krupa*
CERN, Geneva, Switzerland

Abstract

The High Luminosity LHC project aims to increase the integrated luminosity of the LHC experiments by an order of magnitude. New and upgraded beam instrumentation is being developed to cope with much brighter beams and to provide the additional novel diagnostics required to assure safe and efficient operation under the new LHC configuration. This contribution discusses the various ongoing developments and reports on the results obtained with prototypes for transverse position, intra-bunch position, transverse size and profile, and beam halo monitoring.

INTRODUCTION

Since the first beam injection in 2008, the Large Hadron Collider (LHC) has delivered around 190 fb^{-1} of integrated luminosity to each of the two large experiments, ATLAS and CMS. This has led to numerous advancements in particle physics, the most notable being confirming the existence of the Higgs boson in 2012. To fully exploit the discovery potential of the LHC, the High Luminosity LHC (HL-LHC) project aims to achieve an additional 3000 fb^{-1} of integrated luminosity over twelve years of operation from 2026 which necessitates significant upgrades to the accelerator [1].

The two high-luminosity Interaction Regions (IR) of the LHC housing the ATLAS and CMS experiments will undergo major changes during the HL-LHC upgrade. The main change will be a complete replacement of the low-beta Inner Triplets (IT), with higher gradient quadrupoles to allow a further squeezing of the beams to produce even smaller beams at the collision point. In order to reliably collide these exceptionally small beams, extraordinary control of the beam orbit will be necessary.

Moreover, transverse deflecting RF cavities, referred to as crab cavities, will be installed on each side of ATLAS and CMS to perform bunch crabbing. Each bunch will be exposed to a modulating RF field, tilting the bunch transversely to allow the bunches to cross head-on at the collision point even for they approach each other at an angle. After the collision the bunches are rotated back to their original orientation by the crab cavity on the other side of the experiment. This operation maximises the geometric overlap between the colliding bunches which would otherwise be reduced due to the crossing angle.

In the high luminosity era, the LHC bunch intensity will be increased by a factor of two leading to much higher power stored in the beams. The machine protection requirements will therefore become stricter. This particularly concerns the allowed beam halo population since it will become possible

to lose the entire halo within a very short timescale in case of a crab cavity failure. Furthermore, increased radiation levels due to the higher beam intensity and the increased luminosity pose additional requirements on any equipment installed for HL-LHC.

To cope with the above challenges, both new and upgraded beam instrumentation is under development with the initial plans and early progress described in [2] and [3]. The following sections review the current state of these projects.

BEAM POSITION MONITORING

Interaction Regions

There are currently four types of Beam Position Monitors (BPMs) under development for the HL-LHC with their arrangement shown in Fig. 1. The seven BPMs closest to the collision point on each side of the experiments are installed in the new higher gradient, inner-triplet quadrupoles, in a region where both beams circulate in a common vacuum chamber. They must be able to clearly distinguish between the positions of the two counter-propagating particle beams, for which the solution is to use directional couplers. In such beam position monitors the passing particle beam couples to four long antennas (often called striplines) parallel to the beam axis. Each antenna is connectorised on both ends, and has the particularity that the majority of the beam signal is visible only on the upstream end with only a much smaller parasitic signal leaking to the downstream end. This feature, referred to as directivity, allows both beams to be measured by a single array of antennas, and is achieved by a careful RF design complemented by 3D electromagnetic simulations [4]. A 3D model of the most complicated HL-LHC directional coupler BPM is shown in Fig. 2.

To reduce the cross-talk between the signal from one beam and the other due to the limited directivity of such a stripline BPM, the HL-LHC directional coupler BPMs will be intentionally installed in locations where the bunches of the two beams arrive at different times. With bunches separated by 25 ns the maximum time difference between two counter-propagating beams arriving at a given position is 12.5 ns. Due to the HL-LHC beam optics and hardware constraints, it is not possible to install all the BPMs at ideal locations. However, the temporal separation between the beams at a BPM location will always be greater than 3.9 ns which is approximately 3 times longer than the bunch length.

Besides the directive couplers, a set of more conventional capacitive button BPMs is also under development.

The superconducting IT magnets incorporate tungsten shielding blocks which protect them from the high-energy collision debris [5]. Likewise, some of the cryogenic BPMs

* michal.krupa@cern.ch

OVERVIEW ON THE DIAGNOSTICS FOR EBS-ESRF

L. Torino*, N. Benoist, F. Ewald, E. Plouviez, J. Poitou, B. Roche, K.B. Scheidt, F. Taoutaou, F. Uberto, European Synchrotron Radiation Facility, 38000 Grenoble, France

Abstract

On December 2018 the ESRF was shut down and the 28 years old storage ring was entirely dismantled in the following months. A new storage ring, the Extremely Brilliant Source (EBS), that had been pre-assembled in 2017 and 2018, is presently being installed and the commissioning will start in December 2019. EBS will achieve a much reduced horizontal emittance, from 4 nm to 150 pm, and will also provide the x-ray users with a more coherent synchrotron radiation beam. In this paper, we present an overview of the diagnostics systems for this new storage ring.

INTRODUCTION

After one year to replace the full storage ring, the commissioning of the Extremely Brilliant Source (EBS) will start in December 2019 [1].

The full EBS upgrade process foresees also the upgrade, modernization and the adaptation of the diagnostics systems dedicated to monitor the electron beam characteristics with the utmost precision and resolution. Table 1 lists the components of the diagnostics system for EBS. A more detailed description of the individual systems will follow.

Table 1: Components of EBS Diagnostics

Quantity	Component
320	Beam Position Monitors (BPMs)
5	Striplines
2	Shakers
3	Special BPM blocks
6	Current Transformers (PCT, ICT, FCT)
128	Beam Loss Detectors (BLDs)
5	Emittance Monitors
1	Bunch Purity Monitor
1	Visible light beamline

BEAM POSITION MONITORS

A detailed review of the EBS BPM system can be found in [2]. The electronics has been extensively tested on the previous ESRF storage ring.

BPM Blocks

EBS will host 320 BPMs distributed as 10 per cell. Due to the shape of the vacuum chamber, the BPMs blocks are designed with two different geometries:

- Large (6 BPMs per cell) with a button diameter of 8 mm, a horizontal distance between buttons of 23 mm, and a vertical one of 13.34 mm;
- Small (4 BPMs per cell) with a button diameter of 6 mm, a horizontal distance between buttons of 12.5 mm, and a vertical one of 9.62 mm.

The compactness of the BPMs causes a reduction of the zone where the so called Delta over Sum (DoS) formula is accurate enough to calculate the beam position. This has been studied using BPMLab [3] which also provided suitable sets of 2D polynomials to extend the linear range of the beam position response.

Electronics

The BPMs will be read by a hybrid system composed by 6 Libera Brilliance and 4 Libera Spark per cell. Both of the electronics produce data-streams and buffers with identically synchronized sampling rates. The distribution of the electronics along a cell is presented in Fig. 1.

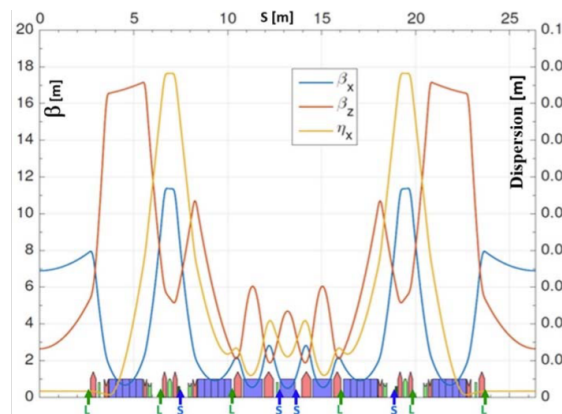


Figure 1: Distribution of the Libera Brilliance (L, green) and the Libera Spark (S, blue) along a cell.

All the BPMs will be used during machine operation for slow orbit acquisition and for orbit correction. The 192 BPMs equipped with Libera Brilliance will also provide position data at 10 kHz on an independent network for the Fast Orbit Feedback. Some of these latter BPMs (between 10 and 30) will also be used for machine interlock purposes.

Preparation and Implementation

After the installation of the blocks into the chambers, the button to button transmission has been measured using the Lamberson method [4] to estimate the offset induced by the difference in button sensitivity. The same measurement will be performed once the installation and the bake-out are completed in order to verify the behaviour of each block. A

* laura.torino@esrf.fr

OVERVIEW OF THE BEAM INSTRUMENTATION AND COMMISSIONING RESULTS FROM THE BNL LOW ENERGY RHIC ELECTRON COOLING FACILITY*

T. Miller[†], Z. Altinbas, D. Bruno, J. C. Brutus, M. Costanzo, C. Degen, L. DeSanto, K. A. Drees, A. V. Fedotov, W. Fischer, J. M. Fite, D. Gassner, X. Gu, J. Hock, R. Hulsart, P. Inacker, J. Jamilkowski, D. Kayran, J. Kewisch, C. Liu, K. Mernick, R. Michnoff, M. Minty, S. K. Nayak, L. Nguyen, P. Oddo, R. H. Olsen, M. Paniccia, W. Pekrul, I. Pinayev, V. Ptitsyn, V. Schoefer, S. Seletskiy, H. Song, A. Sukhanov, P. Thieberger, J. Tuozzolo, D. Weiss, BNL, Upton, NY, USA

Abstract

The Low Energy RHIC Electron Cooling (LEReC) facility [1] at BNL demonstrated, for the first time, cooling of ion beams using a bunched electron beam. LEReC is planned to be operational to improve the luminosity of the Beam Energy Scan II physics program at RHIC in the following two years. In order to establish cooling of the RHIC Au ion beam using a 20 mA, 1.6 MeV bunched electron beam; absolute energy, angular and energy spread, trajectory and beam size were precisely matched. A suite of instrumentation was commissioned [2] that includes a variety of current transformers, capacitive pick-up for gun high voltage ripple monitor, BPMs, transverse and longitudinal profile monitors, multi-slit and single-slit scanning emittance stations, time-of-flight and magnetic field related energy measurements, beam halo & loss monitors and recombination monitors. The commissioning results and performance of these systems are described, including the latest design efforts of high-power electron beam transverse profile monitoring using a fast wire scanner, residual gas beam induced fluorescence monitor, and Boron Nitride Nano-Tube (BNNT) screen monitor.

INTRODUCTION

Electron cooling of ion beams has been demonstrated long before now but with DC beams. As higher energy electron beams are needed to cool higher energy ion beams, RF acceleration becomes a necessary method. LEReC is the first electron cooler to employ RF acceleration of electron bunches [3, 4], paving the way toward the development of future higher energy electron coolers. The LEReC accelerator is based on a 400kV DC gun with laser-driven [5, 6] photocathode [7], and an SRF booster with a set of three normal conducting RF cavities [8] with which to provide a control of “RF gymnastics” to effectively tune the beam in the longitudinal phase space [9]. The machine layout is shown in Fig. 1. The LEReC beam contains a complex bunch structure defined by the 704 MHz fiber laser producing bunch trains of 40-ps bunches at ~9 MHz to effectively overlap the ion bunches in RHIC, as described in detail in [4].

LEReC was successfully commissioned in 2018 [10] and demonstrated cooling during the 2019 RHIC run with Au ions [4]. Table 1 summarizes the design parameters of the electron beam in the cooling section (CS). Although the designed charge per bunch was obtained, it was found that

a lower charge of around 75 pC was most optimal for cooling so far.

Table 1: Electron Beam Parameters in the CS

Electron beam energy, MeV	1.6-2.6
Charge per single bunch, pC	130-200
Number of bunches in macrobunch	30-24
Total charge in macrobunch, nC	3-5
Average current, mA	30-55
RMS normalized emittance, μm	< 2.5
Angular spread, mrad	< 0.15
RMS energy spread	< 5×10^{-4}
RMS bunch length, cm	3
Length of cooling sections, m	20

BEAM INSTRUMENTATION SYSTEMS

All instruments and associated systems, depicted in Fig. 1, have been described previously in detail in [2]. Descriptions of updates to each instrumentation system are elaborated on in the sections that follow along with the latest commissioning results.

Gun Instrumentation

Laser Exit Monitoring & Cathode Imaging

A laser exit table sits at the laser exit port to receive the drive laser reflected off of the mirror polished surface of the cathode substrate to minimize beam halo & tails otherwise generated by scattered light reaching the cathode. A power meter measures the exit-laser power to predict a loss of light inside the cathode laser chamber. A camera monitors the laser spot on the power meter to allow an operator to check for clipping of the laser spot.

The surface of the cathode substrate, a polished molybdenum puck with an activated cathode spot, held in the DC gun, is imaged, as shown in Fig. 2a. This imaging is used for alignment and automated tracking of the laser spot during automated quantum efficiency (QE) scans. The cathode is illuminated on-axis by an LED spotlight with adjustable spot size to minimize glare from surrounding reflective surfaces. A 2 MP GigE camera, AVT model Manta G201B, is fitted with a Navitar 6x ZoomXtender [11] lens assembly (working distance of 0.3 – 16 m) to image the 25-mm cathode substrate at a distance of 1 m.

BEAM INSTRUMENTATION AT THE FERMILAB IOTA RING*

N. Eddy[†], D. R. Broemmelsiek, K. Carlson, D. J. Crawford, J. Diamond, D. R. Edstrom, B. Fellenz, M. A. Ibrahim, J. Jarvis, V. Lebedev, S. Nagaitsev, J. Ruan, J. K. Santucci, A. Semenov, V. Shiltsev, G. Stancari, A. Valishev, D. Voy, A. Warner, Fermilab, Illinois, USA
 N. Kuklev, I. Lobach, University of Chicago, Illinois, USA
 S. Szustkowski, Northern Illinois University, Illinois, USA

Abstract

The Integrable Optics Test Accelerator (IOTA) is a storage ring located at the end of the Fermilab Accelerator Science and Technology (FAST) facility. The complex is intended to support accelerator R&D for the next generation of particle accelerators. The IOTA ring is currently operating with 100 MeV electrons injected from the FAST Linac and will also receive 2.5 MeV protons from the IOTA Proton Injector currently being installed. The current instrumentation and results from the first electron commissioning run will be presented along with future plans.

INTRODUCTION

The Integrable Optics Test Accelerator (IOTA) is a storage ring which is a component of the Fermilab Accelerator Science and Technology (FAST) facility. The facility is dedicated entirely to research and development for the next generation of particle accelerators. IOTA is a storage ring with a circumference of 40 meters which can store beams at momenta between 50 and 200 MeV/c. The main goals for IOTA are to demonstrate the advantages of nonlinear integrable lattices [1,2] for high intensity particle beams and to demonstrate new beam cooling methods [3].

FAST has begun operations with electron beam from the super-conducting linear accelerator [4]. The electron linac provides a lot of flexibility to adjust the energy and intensity of the injected electron beam to match the beam envelope within the IOTA ring for commissioning as well as different experimental setups. The key features are the electron gun, capture cavities, and super-conducting Tesla style cryomodule with eight accelerating cavities.

Once injected into IOTA, the electron beam is cooled by synchrotron radiation to very low emittance. This allows a wider range of diagnostics tools which provide more accurate measurements than are possible with the proton beams. The electron beam operation is critical for precision understanding of the IOTA lattice and operations with the key focus being nonlinear integrable optics and optical stochastic cooling.

The layout of the ring is shown in Figure 1. The main design parameters for the IOTA ring are shown in Table 1. Some of the key elements are a dual frequency Radio Frequency (RF) accelerating cavity, horizontal and vertical strip-line kickers, 8 bend dipoles each with a horizontal trim, 39 quadrupole magnets powered in pairs, and 20

skew-quadrupole magnets each with horizontal and vertical trim magnets.

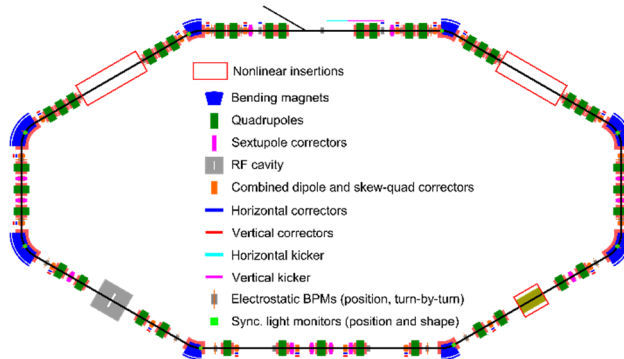


Figure 1: The layout of the IOTA ring.

Table 1: IOTA Design Parameters

Parameter	Value
Ring Circumference	39.97 m
Momentum Acceptance	50-200 MeV/c
Electrons	150 MeV/c
Protons	70 MeV/c
RF Frequency (electrons)	30.034 MHz
RF Frequency (protons)	2.19 MHz
RF Voltage	1 kV
Harmonic Number	4
Bunch Length (electrons)	10-20 cm
Tune (horizontal, vertical)	5.3, 5.3
Synchrotron Frequency	43 kHz

BEAM INSTRUMENTATION

The IOTA ring is equipped with a Direct Current Current Transformer (DCCT), 8 Synchrotron Light Monitor stations, 21 Beam Position Monitors (BPM), and a resistive Wall Current Monitor (WCM). In the course of the first run both a longitudinal and a transverse feedback system were also implemented.

DCCT Intensity Monitor

The IOTA DCCT is a Bergoz MPCT-RH-113 model, which was purchased for Booster R&D project in 1999. It was never used operationally and removed from the beamline in 2016. When the unit was retrieved, the signal cable was damaged from radiation a few inches from the sensor head. Unlike the new MPCT, the cable came right out of the sensor without a DB connector on that end. An attempt was made to repair the cable, but it turned out the wires

* Work supported by Fermi Research Alliance, LLC under Contract No. DE-AC02-07CH11359 with the U.S. Department of Energy, Office of Science, Office of High Energy Physics.

[†] eddy@fnal.gov

CHARACTERIZATION AND FIRST BEAM LOSS DETECTION WITH ONE ESS-nBLM SYSTEM DETECTOR

L. Segui*, H. Alves, S. Aune, J. Beltramelli, Q. Bertrand, M. Combet, A. Dano-Daguze, D. Desforge, F. Gougnaud, T. Joannem, M. Kebbiri, C. Lahonde-Hamdoun, P. Le Bourlout, P. Legou, O. Maillard, A. Marcel, Y. Mariette, J. Marroncle, V. Nadot, T. Papaevangelou, G. Tsiledakis, IRFU-CEA, Université Paris-Saclay, F-91191, Gif-sur-Yvette, France
I. Dolenc Kittelmann, T. J. Shea, European Spallation Source ERIC, Lund, Sweden

Abstract

The monitoring of losses is crucial in any accelerator. In the new high intensity hadron facilities even low energy beam can damage or activate the materials so the detection of small losses in this region is very important. A new type of neutron beam loss monitor has been developed specifically targeting this region, where only neutrons and photons can be produced and where typical Beam Loss Monitors (BLM), based on charged particle detection, could not be appropriate because of the photon background due to the RF cavities. The BLM proposed is based on gaseous Micromegas detectors, designed to be sensitive to fast neutrons and with little sensitivity to photons. Development of the detectors presented here has been done to fulfil the requirements of ESS and they will be part of the ESS-BI systems. The detector has been presented in previous editions of the conference. Here we focus on the neutron/gamma rejection with the final FEE and in the first operation of one of the modules in a beam during the commissioning of LINAC4 (CERN) with the detection of provoked losses and their clear separation from RF gammas. The ESS-nBLM system is presented in this conference in a separate contribution.

INTRODUCTION

A new type of beam loss monitor (BLM) based on the detection of fast neutrons have been conceived, constructed and characterized. Moreover, the response of a pre-series detector to beam losses and RF gammas background has been tested at Linac4, at CERN. Such detector has been developed in the context of an in-kind contribution from CEA-Saclay to ESS, constituting one of the ESS Beam Instrumentation (ESS BI) systems, namely the neutron sensitive BLM (nBLM) system [1].

The proposed detector aims to extend the sensitivity in the low energy region of an hadron accelerator. In such region only gammas and neutrons can be used as beam losses signature. The goal is to detect the produced fast neutrons while having a low sensitivity to gammas that are also produced by the RF cavities. Moreover, the detector will exhibit low sensitivity to thermal neutrons which will have lost their location information due to their moderation and they can be also produced by the surroundings.

Two complementary types have been proposed, both based on Micromegas detectors as readout. The project

started in July 2016 and in the last two years, after the conceptual design phase, the detectors have been characterized at different irradiation facilities. In the following section the geometry and operation of the modules will be explained in detail. Afterwards, experimental results showing discrimination of neutrons from gammas will be presented. Finally, the first beam loss detection at LINAC4 (CERN) will be shown, as proof of detector capabilities.

DETECTOR CONCEPT AND DESIGN

The nBLM proposed is based on Micromegas readout [2]. They are gaseous amplification structures part of the MPGD family (Micro-Pattern Gaseous Detectors), successors of the wire chambers, with high gain, fast signals, and a very good spatial and energy resolution.

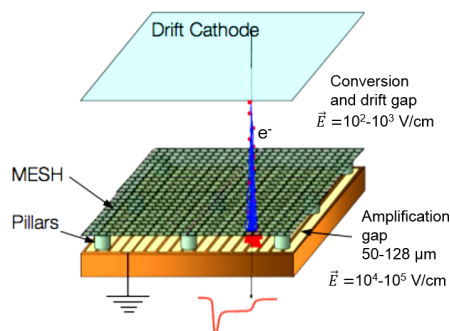


Figure 1: Sketch of Micromegas detector operation.

Micromegas devices operate with two regions separated by a micromesh: the conversion region and the amplification region (see Fig. 1). The detector itself consists on a mesh suspended over an anode by insulator pillars, usually made by lithographic process [3, 4]. It operates always with a third parallel plate as cathode. The conversion region is defined between the cathode and the mesh, and is where the primary electrons are produced when a charged particle ionizes the gas (usually an electric field of $\sim 100 \text{ V/cm} - 1000 \text{ V/cm}$ is applied). The amplification region is defined between the mesh and the anode and is where an avalanche of electrons is produced that will induce a detectable signal in both the mesh and the anode. In this region the electric field is much higher, usually of $\sim 1 \times 10^4 \text{ V/cm} - 1 \times 10^5 \text{ V/cm}$ to produce the avalanche. The amplification gap is usually of $50 \mu\text{m} - 125 \mu\text{m}$ while the conversion distance varies according to the application. The anode can be made by strips or pixels as well.

* laura.segui@cea.fr

Content from this work may be used under the terms of the CC BY 3.0 licence (© 2019). Any distribution of this work must maintain attribution to the author(s), title of the work, publisher, and DOI

ONLINE TOUSCHEK BEAM LIFETIME MEASUREMENT BASED ON THE PRECISE BUNCH-BY-BUNCH BEAM CHARGE MONITOR*

B.Gao[†], Y.B.Leng, F.Z.Chen, Shanghai Advanced Research Institute,
 Chinese Academy of Sciences, Shanghai, China

Y.M.Zhou¹, Shanghai Institute of Applied Physics, Chinese Academy of Sciences, Shanghai, China
¹also at University of Chinese Academy of Sciences, Beijing, China

Abstract

Beam lifetime is a very important issue at high current operation of light source. Most of the existing lifetime monitor can only be measured for average lifetime. However, the life-related physical formula is only strictly established for a single bunch. In order to describe the behaviour of all electron bunches completely and accurately, a precisely bunch-by-bunch charge monitor has been developed at SSRF. Two-phase sampling based peak seeking method is introduced to avoid the influence of longitudinal oscillation on the sampling point, thanks to this, the resolution of the BCM was below 0.02%. Utilizing the advantages of BCM's high refresh rate and high resolution, the system can meet the requirement of monitor the bunch-by-bunch beam lifetime, measure Touschek lifetime and vacuum lifetime. In this paper, experiments and analysis will be described in detail.

INTRODUCTION

The beam current and its lifetime are two of the most important parameters of an electron storage ring. They are used to not only characterize the beam quality and machine status, but also to quantify the injection efficiency for weighing the injector/storage-ring matching.

The average beam current is measured to control injections during top-up operations, calculate the average lifetime and stability of the beam, and calculate the injection efficiency to determine whether the beam loss during an injection is tolerable.

The charges of the bunches are used to check the filling pattern and determine how to make the next injection to achieve the designed pattern, such that the desired filling pattern and the operation mode can be sustained.

The total lifetime in an electron storage ring consists of the lifetime of the beam electron residual gas scattering, the electron-electron scattering within the bunch, also the quantum excitation. There might also come a situation in which the values of the Touschek lifetime, vacuum lifetime, and quantum lifetime are needed, especially during machine studies.

The contribution to the total beam lifetime can be described as:

$$\frac{1}{\tau_{total}} = \frac{1}{\tau_{quantum}} + \frac{1}{\tau_{touschek}} + \frac{1}{\tau_{vacuum}}. \quad (1)$$

Where τ_{total} the total lifetime, the indices quantum,

Touschek and vacuum denote the different components of the lifetime. Among them, Touschek lifetime is related with the beam charge, and the other two independents of the beam charge. Hence, the above formula can be rewrite as:

$$\frac{1}{\tau_{total}} = k_{touschek}Q + \frac{1}{\tau_{vacuum+quantum}} \quad (2)$$

Touschek lifetime is the most important mechanism for long-term particle losses in a storage ring. The online bunch-by-bunch Touschek lifetime monitor can provide a toolkit for complete and accurate representation of the behaviour of all electron bunches; it is also a precise bunch-by-bunch beam charge monitor, which can be used to do accurate measurement, correlation analysis and transient instability study of a single bunch.

The current of the beam injected into the storage ring typically decays exponentially over time. The goal of this system is to achieve on-line beam life measurement, and the injection period of SSRF running in top-up mode is about 5 minutes, so BCM must at least be able to distinguish the change of a single bunch charge at 1 minute during the period of decay.

Assume that when the current is 240mA and the beam life is 20 hours. According to the theoretical formula, in the decay mode, the change in flow intensity should be as shown in Fig. 1 below.

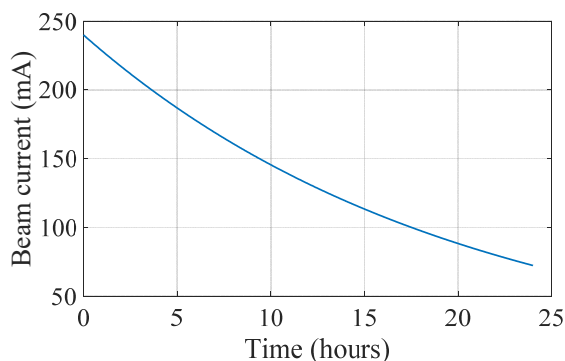


Figure 1: Current change diagram in the decay mode.

In this mode, the amount of current change in a minute is probably 0.2 mA. Assuming that each bunch changes the same value, the amount of change in the charge of 500 bunches should be 0.4 pC, for a 500 pC bunch, the amount of change is about 0.1%. Hence, the resolution of the BCM should be better than 0.1%, and the refresh rate should be higher.

In order to realize the online bunch-by-bunch lifetime monitor, four necessary conditions must be available:

* Work supported by National Ten-thousand Talents Program

[†] gaobo@zjlab.org.cn

DEVELOPMENT OF A PASSIVE CAVITY BEAM INTENSITY MONITOR FOR PULSED PROTON BEAMS FOR MEDICAL APPLICATIONS

P. Nenzi[†], A. Ampollini, G. Bazzano, F. Cardelli, L. Picardi, L. Piersanti, C. Ronsivalle, V. Surrenti, E. Trinca, ENEA C.R. Frascati, Frascati, Italy

Abstract

In this work the design of a passive cavity beam intensity monitor to be used in the TOP-IMPLART medical proton linac for the on-line measurement of beam current is presented. It will be used to monitor the beam between modules and at the linac exit. TOP-IMPLART produces a pulsed proton beam with 3 μ s duration at 200 Hz repetition rate with a current between 0.1 μ A and 50 μ A. The current required for medical applications is less than 1 μ A and has to be known with an accuracy better than 5%. Large dynamic range and space constraints make the use of usual non-interceptive beam diagnostics unfeasible. The proposed system consists of a resonant cavity working in the TM010 mode, generating an electromagnetic field when the beam enters the cavity; a magnetic pickup senses an RF pulse whose amplitude is proportional to the current. The RF pulse is amplified and subsequently detected with zero-biased Schottky diodes. The cavity operates in vacuum when used in the inter-module space. The work reports also the results of preliminary measurements done on a copper prototype in air at the exit of the TOP-IMPLART linac to test the sensitivity of the system on the actual 35 MeV proton beam.

INTRODUCTION

The use of proton beams for cancer treatment presents advantages over conventional (photon based) particle therapy. Protons lose their energy in a narrow range of depth near their stopping range. This characteristic yields to a more conformal mapping of the treatment volume with the possibility of sparing nearby organs. Most of the commercial medical accelerators for proton therapy consist of circular accelerators (cyclotrons and synchrotrons).

However, it is identified the need of developing more compact and more efficient accelerators that can reduce the duration of the treatment, improve the precision of dose delivery, and lower the overall cost of the facilities. It is with this aim that TOP-IMPLART (Terapia Oncologica con Protoni, Intensity Modulated Proton Linear Accelerator for Radiotherapy) program is developing a fully linear solution for proton therapy. The accelerator, bearing the same name, is under construction at the ENEA Frascati Research Center. It is a compact pulsed RF linac, consisting of a 7 MeV Hitachi-AccSys PL7 injector (425 MHz) followed by an S-band booster (2997.92 MHz) accelerating the beam up to 150 MeV. TOP-IMPLART, recently, achieved an energy of 35 MeV with the successful commissioning of its first booster section, consisting of four SCDTL (Side Coupled Drift tube Linac) modules powered by a single 10 MW

peak power klystron [1]. The accelerator delivers its proton beam in 1 μ s to 4 μ s long pulses (FWHM) with a Pulse Repetition Frequency in the 10 to 100 Hz range.

The peak pulse current can be set between 0.1 μ A and 50 μ A changing the injected current. The output current range is broader than the one needed for therapeutic applications, that lies between 0.1 μ A and 1.0 μ A, because TOP-IMPLART beam is used also for non-biological experiments, requiring higher proton fluence [2]. Pulse current is an important parameter for machine control; therefore, non-interceptive current monitor shall be installed along and at the output of the linac. Measurements of currents lower than 10 μ A, which is the typical limit of commercial AC current transformers, has been performed during linac commissioning, on the extracted beam, with the ionization chambers used for dose delivery control. However, this type of diagnostic cannot be inserted in the inter-module space in vacuum. For this reason a high sensitivity, short, non-interceptive detector based on a passive resonant cavity has been developed.

RESONANT CAVITY BEAM INTENSITY MONITOR

A radiofrequency cavity working in the TM010 mode whose resonance frequency is tuned to the micro-bunch frequency of the beam ($1/T_b$ in Fig. 1) can be used as a beam intensity monitor [3].

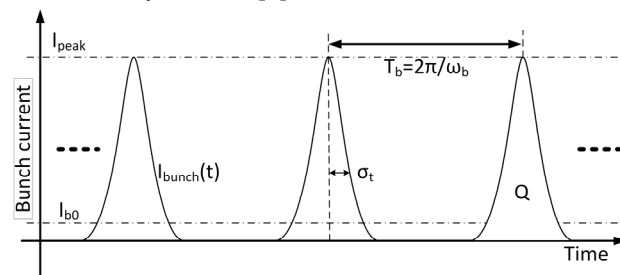


Figure 1: Proton beam structure (micropulse).

The particle beam passing through the cavity excites an electromagnetic field whose azimuthal magnetic component is picked up and converted into an electric signal proportional to the pulse current. According to [4], the power extracted from the cavity can be expressed as:

$$P = (a_1)^2 (R_s/Q_0) T^2 Q_{load} \frac{\beta}{(1+\beta)} \cos^2 \varphi, \quad (1)$$

where a_1 is the first term of the Fourier series expansion of the beam current signal, R_s is the shunt impedance of the cavity, T is the transit time factor, Q_0 and Q_{load} are the unloaded and loaded quality factors, respectively, and β is the coupling coefficient between the loop and the cavity.

Work funded by Innovation Department of Regione Lazio Government
[†] paolo.nenzi@enea.it

ESTIMATION OF LONGITUDINAL PROFILES OF ION BUNCHES IN THE LHC USING SCHOTTKY-BASED DIAGNOSTICS

K. Lasocha¹, D. Alves, CERN, Geneva, Switzerland

¹also at Institute of Physics, Jagiellonian University, Kraków, Poland

Abstract

The Large Hadron Collider (LHC) Schottky monitors have been designed to measure various parameters of relevance to beam quality, namely tune, momentum spread and chromaticity. We present another application of this instrument - the evaluation of longitudinal bunch profiles. The relation between the distribution of synchrotron amplitudes within the bunch population and the longitudinal bunch profile is derived from probabilistic principles. Our approach, limited to bunched beams with no intra-bunch coherent motion, initially fits the cumulative power spectral density of acquired Schottky spectra with the underlying distribution of synchrotron amplitudes. The result of this fit is then used to reconstruct the bunch profile using the derived model. The obtained results are verified by a comparison with measurements from the LHC Wall Current Monitors.

INTRODUCTION

The Large Hadron Collider (LHC) transverse Schottky system, whose main objective is to provide the beam operators with non-invasive, bunch-by-bunch tune and chromaticity measurements was commissioned in 2011 [1]. In the meantime, the system has undergone major upgrades in order to improve signal quality [2]. Still, although qualitatively its chromaticity estimates seem to agree with trends from other measurement techniques (as verified in dedicated experiments), the quantitative discrepancies observed still need to be fully understood [3]. Studies are therefore underway in order to better understand the spectra obtained, will, under the assumption that there is no coherent intra-bunch motion. It should be noted, however, that the LHC Schottky monitors are designed for transverse measurements, and as such are not optimised for measurements in the longitudinal plane.

LONGITUDINAL BUNCH PROFILE

In hadron machines such as the LHC, where radiation losses are small, the RF phase difference, $\Delta\phi_{RF}$, between a given particle within the bunch and the synchronous particle obeys the pendulum equation [4, Eq. (9.51)]

$$\frac{d^2\Delta\phi_{RF}}{dt^2} + \omega_{s_0}^2 \sin(\Delta\phi_{RF}) = 0 \quad (1)$$

where ω_{s_0} is the nominal synchrotron frequency. For RF harmonic h , revolution frequency ω_0 and time amplitude (maximum time difference between a given particle and the synchronous particle) of synchrotron oscillations $\widehat{\tau}$, we have that the particle's synchrotron frequency is given

by:

$$\omega_s = \frac{\pi}{2\mathcal{K}\left[\sin\left(\frac{h\omega_0\widehat{\tau}}{2}\right)\right]} \omega_{s_0}, \quad (2)$$

where $\widehat{\Delta\phi_{RF}} = h\omega_0\widehat{\tau}$ is the RF phase amplitude of synchrotron oscillations and $\mathcal{K}([0, 1]) \rightarrow [\pi/2, \infty]$ is the complete elliptic integral of the first kind [5, p. 590]. This comes from the general theory of an arbitrary-amplitude pendulum [6].

From [7] we know that the time difference τ between a particle performing synchrotron motion and the synchronous particle is described by a simple harmonic motion, i.e.:

$$\tau = \tau(\widehat{\tau}, \phi_s) = \widehat{\tau} \cos(\omega_s t + \phi_s). \quad (3)$$

The longitudinal bunch profile can be interpreted as the probability distribution of τ . We shall denote this distribution by $\mathcal{B}(\tau)$. The assumption of no coherent intra-bunch motion implies that the distribution of initial synchrotron phases, ϕ_s , is uniform and independent of the distribution of synchrotron amplitudes $\widehat{\tau}$. Furthermore, under stationary conditions, the longitudinal bunch profile is independent of time. Therefore, the probability of finding a particle with time difference τ with respect to the synchronous particle depends only on its amplitude of oscillation $\widehat{\tau}$:

$$\mathcal{B}(\tau) = \int_0^\infty g_{\tau, \widehat{\tau}}(\tau, \widehat{\tau}) d\widehat{\tau} = \int_{|\tau|}^\infty g_{\tau, \widehat{\tau}}(\tau, \widehat{\tau}) d\widehat{\tau},$$

where $g_{\tau, \widehat{\tau}}(\tau, \widehat{\tau})$ is the joint probability density of a particle having amplitude $\widehat{\tau}$ and time difference τ . The second equality comes from the fact, that $g_{\tau, \widehat{\tau}}(\tau, \widehat{\tau}) = 0$ for $|\tau| > \widehat{\tau}$. Derivation of $g_{\tau, \widehat{\tau}}(\tau, \widehat{\tau})$ is not straightforward, as τ and $\widehat{\tau}$ are not independent, but it can be derived from the joint distribution of initial synchrotron phases and amplitudes $g_{\phi_s, \widehat{\tau}}$. We can write

$$g_{\phi_s, \widehat{\tau}}(\phi_s, \widehat{\tau}) = g_{\phi_s}(\phi_s) g_{\widehat{\tau}}(\widehat{\tau}) = \frac{g_{\widehat{\tau}}(\widehat{\tau})}{2\pi},$$

as these random variables are independent and ϕ_s is uniformly distributed. In addition, let us define the transformation

$$u = (u_1, u_2) : (\phi_s, \widehat{\tau}) \mapsto (\tau, \widehat{\tau})$$

where u_1 is defined by Eq. (3) and u_2 is the identity function of $\widehat{\tau}$. The relationship between the joint distributions of two sets of random variables related by a known transformation function is given in [8, p. 201]. Using this, we obtain

$$g_{\tau, \widehat{\tau}}(\tau, \widehat{\tau}) = \frac{2g_{\phi_s, \widehat{\tau}}(\phi_s, \widehat{\tau})}{\sqrt{\widehat{\tau}^2 - \tau^2}} = \frac{g_{\widehat{\tau}}(\widehat{\tau})}{\pi\sqrt{\widehat{\tau}^2 - \tau^2}}$$

OVERVIEW OF BUNCH-RESOLVED DIAGNOSTICS FOR THE FUTURE BESSY VSR ELECTRON-STORAGE RING*

G. Schiwietz[†], J.-G. Hwang, M. Koopmans, M. Ries
 Helmholtz-Zentrum Berlin für Materialien und Energie GmbH,
 Albert-Einstein-Str. 15, 12489, Berlin, Germany

Abstract

The upgrade of the BESSY II light source in Berlin towards the Variable pulse-length Storage-Ring BESSY VSR leads to a complex fill pattern [1-3]. This involves co-existing electron bunches with significant variations of their properties. Among many other boundary conditions, this calls for bunch resolved measurements with sub-ps time resolution and micrometer spatial resolution.

Currently, we are constructing a diagnostic platform connected to new dipole beamlines for visible light as well as THz measurements. The mid-term aim is a 24/7 use of beam-diagnostic tools and the development of advanced methods for specific purposes. Recently, we have set-up a sub-ps streak camera [4] and we are investigating other innovative methods for bunch-length [5] as well as lateral size determination using visible light [6,7] at the first of our new diagnostic dipole beamlines. Preliminary results as well as our concepts for achieving high sensitivity, good signal-to-noise ratio and time resolution will be presented and discussed below.

TRANSITION FROM BESSY II TO BESSY-VSR OPERATION

The current BESSY II electron-storage ring of the Helmholtz-Zentrum Berlin (HZB) is operated at the electron energy of 1.7 GeV for a cavity frequency of 500 MHz. The typical ring current is 300 mA. Different optics modes are available and various bunch-filling patterns are distributed within the 400 buckets that are separated by approximately 2 ns.

The upgrade of the BESSY II light source towards the Variable pulse-length Storage-Ring BESSY VSR [1-3] involves a triple-cavity structure at high mean electric field strengths. Thus, the bunch lengths may be significantly reduced at fixed bunch-charge values, see Fig. 1. This means that time-dependent X-ray experiments (coincidences, pump/probe measurements, etc., see ref. [8]) will gain time resolution, whereas precision spectroscopy and scattering experiments running in parallel profit from stable large mean currents for a matched bunch pattern.

Superposition of 0.5 GHz (BESSY II) and additionally 1.5 GHz and 1.75 GHz SRF (superconducting RF) at high voltages leads to a beating pattern of the field gradients and a corresponding formation of alternating short and long buckets every 2 ns. This will be the basis of an even more complex filling pattern with co-existing electron bunches that differ significantly regarding their bunch

length, bunch charge as well as transverse profile and charge density. Thus, bunch resolved diagnostics of lateral size, position and bunch length with high sensitivity, good signal-to-noise ratio and high time resolution are demanded. This calls for new or at least improved properties of the future beam-diagnostics hardware.

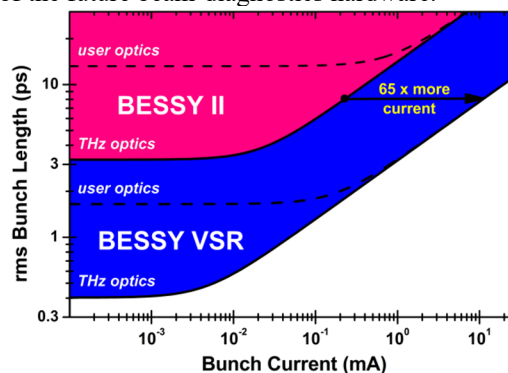


Figure 1: Comparison of standard user optics as well as THz optics for BESSY II with the future BESSY-VSR system, considering realistic SRF boundary conditions.

BUNCH-RESOLVED OPTICAL DIAGNOSTICS

New Platform and Beamlines

The diagnostic platform features visible-light output ports from two dipole beamlines (see Fig. 2) equipped with X-ray blocking baffles. Each outlet of the evacuated beamlines is fed through a radiation labyrinth and ends in a wedged glass window. The design target of the VSR diagnostic systems is 24/7 availability, robustness and sufficient space for future R&D.

One beamline (*Sector12-Dip1.2*) will be equipped with planar precision mirrors optimized for phase stability for the transverse size monitor (see next subsection). Another beamline (*Sector12-Dip1.1*) is optimized for high photon yields (opening angles of 20×5.6 mrad) and consists of precise ellipsoidal and toroidal focusing mirrors. This beamline is in operation since January 2019 and it is coupled to one optical table, mainly for bunch-length measurements (see further below). Both optical tables are air damped against the influence of ground vibrations and during the next few months they will be encased by an air-conditioned hutch against the influence of dust, external sound and unwanted stray light. Additional space is available outside the hutch for computer controls, work benches and storage.

A third beamline (*Sector12-Dip2.1*) will be used exclusively for THz intensity measurements and spectral THz

[†] schiwietz@helmholtz-berlin.de

* Work supported by the German Bundesministerium für Bildung und Forschung, Land Berlin and grants of Helmholtz Association

Content from this work may be used under the terms of the CC BY 3.0 licence (© 2019). Any distribution of this work must maintain attribution to the author(s), title of the work, publisher, and DOI

SAFETY CLASSIFIED SYSTEM USING BEAM INTENSITY MONITORING FOR THE RESPECT OF NUCLEAR REQUIREMENTS OF SPIRAL2 FACILITY

P. Anger, C. Berthe, F. Bucaille, V. Desmezières, C. Haquin, C. Jamet, S. Leloir, G. Normand, J.C. Pacary, S. Perret-Gatel, A. Savalle
 GANIL Laboratory, Caen, France

Abstract

The SPIRAL2 Facility at GANIL is based on the construction of a superconducting ion CW LINAC (up to 5 mA - 40 MeV deuteron beams and up to 1 mA - 14.5 MeV/u heavy ion beams) with two experimental areas called S3 and NFS.

The building, the accelerator and experimental equipment studies started in 2009. For safety-classified system using beam intensity monitoring, SPIRAL2 project system engineering sets up a specific reinforced process, based on V-Model, to validate, at each step, all the requirements (technical, nuclear safety, quality, reliability, interfaces...) from the functional specifications to the final validation.

Since 2016, the main part of the safety devices is installed and is currently under testing. These tests which are pre-requisites to deliver the first beam will demonstrate that both functional and safety requirements are fulfilled.

This contribution will describe the requirements (operation field, limitation of equipment activation...), the technical studies, the failure mode and effects analysis, the tests, the status and results of the SPIRAL2 Machine Protection System using AC and DC current transformers to measure and control the beam intensity.

INTRODUCTION

Officially approved in May 2005, the GANIL SPIRAL2 radioactive ion beam facility (Fig. 1) was launched in July 2005, with the participation of French laboratories (CEA, CNRS) and international partners. In 2008, the decision was taken to build the SPIRAL2 complex in two phases: A first one including the accelerator, the Neutron-based research area (NFS) and the Super Separator Spectrometer (S3), and a second one including the RIB production process and building, and the low energy RIB experimental hall called DESIR [1][2][3].

In October 2013, due to budget restrictions, the RIB production part was postponed, and DESIR was planned as a continuation of the first phase.

The first phase SPIRAL2 facility is now built, the accelerator is installed [4]. The French safety authority agreement is now validated and the accelerator is under testing with the aim of obtaining the first beam for physics (NFS) in 2019 [3].

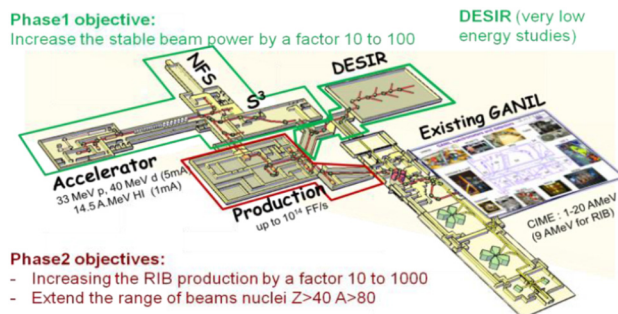


Figure 1: SPIRAL2 project layout, with experimental areas and connexion to the existing GANIL.

PROBLEMATIC

The GANIL/SPIRAL2 facility is considered as an “INSTALLATION NUCLEAIRE DE BASE” (INB), administrative denomination. According to the French law (law n°2006-66, decree 63-1228 and 2007-1557). The GANIL is under the control of the French Nuclear Safety Authority. The classification of the SPIRAL2/GANIL facility in the INB field is due to the characteristics of the beams at the last acceleration state and the use of actinide target.

SPIRAL2 will produce different beams (protons, deuterons and heavy ions) at very high intensity. Table 1 recalls the main beam characteristics.

Table 1: Beam Specifications

Beam	P	D ⁺	Heavy Ions
Max. Intensity	5 mA	5 mA	1 mA
Max. Energy	33 MeV	20 MeV/A	14.5 MeV/A
Max. Power	165 kW	200 kW	45 kW

The goals are to protect workers, public and environment against all risks identified and to reduce as low as possible frequencies and consequences of incidents and accidents.

Concrete building (14.000 m3) and an 8 meters underground beam axis, without beam power control is not sufficient for protection against external exposure to ionizing radiation. Controlling the accelerator device activation due to beam losses (beam losses limited to 1 W/m for D⁺ beams), along with the target and Beam dump activation as well as the operating range is then required.

To control the beam power for this goal, a dedicated and Safety Machine Protection System (MPS) is required.

CURRENT PER BUNCH DISTRIBUTION MEASUREMENT AT ESRF

L. Torino*, B. Roche, B. Vedder
European Synchrotron Radiation Facility, 38000 Grenoble, France

Abstract

During the last run of the ESRF machine, several instrumentation improvements have been carried out in order to be exported on the new EBS storage ring. In particular, the top-up operation mode has been implemented and it demanded for an accurate, fast, and reliable measurement of the current per bunch distribution. In this proceeding, we describe the characteristics and the performance of the setup chosen to perform this measurement, which consists in a stripline, connected with a high dynamic range oscilloscope and a dedicated data analysis. We also comment on the integration of the measurement in the top-up routine to selectively refill less populated bunches.

INTRODUCTION

The European Synchrotron Light Source (ESRF) is going through an upgrade phase, which will lead to the Extremely Brilliant Source (EBS). The new hybrid multi bend achromat lattice will reduce the horizontal emittance from 4 nm to 150 pm to provide the user with a more coherent photon beam [1]. The reduction in emittance, however, also cause a reduction of lifetime and for this reason EBS will operate in top-up mode.

This operation mode has been implemented and commissioned during last runs of ESRF. In order to guarantee a more uniform filling pattern and to enhance the beam stability, an injection routine to selectively refill the emptiest bunches has been developed and a diagnostics tool to measure the current per bunch distribution was needed.

The longitudinal structure of ESRF and EBS is composed by 992 buckets separated by 2.8 ns, defined by the 352 MHz RF-cavity system. The most typical operation mode of ESRF-EBS is the so called “7/8+1” filling mode, which consists in 190 mA of current distributed uniformly in a continuous train covering the 7/8 of the available bunches and delimited by two 1 mA “marker” bunches. A single bunch of 8 mA is located in the center of the gap to allow users to perform timing experiments. This particular filling mode foresees a ratio of 40 between the single bunch and the bunches of the train.

Due to this configuration, a new current per bunch monitor was developed to provide a good dynamic range to distinguish the main train from the noise, without saturating the single bunch. Moreover the acquisition and the data analysis had to be fast enough to provide a continuous, online monitoring. The device has been commissioned on ESRF and will be re-installed on EBS.

* laura.torino@esrf.fr

EXPERIMENTAL SETUP

The experimental setup consists on a stripline coupled to a high dynamic range oscilloscope. Data are then directly acquired by the Tango control system, treated and are available to users through an application.

Stripline

An horizontal stripline has been chosen to perform this measurements because the sensitivity of such a pickup is high and allows to have a strong signal even at low current. This stripline was originally designed to kick the beam, i.e. it has both an input and output port on each blade. For current per bunch measurement, only the input port is connected to the scope. The output one is connected to a coaxial cable terminated with a 50 Ω load in order to avoid undesired reflections. The signal coming out from the stripline is quite strong and has to be attenuated before being fed to the scope. A 30 dB attenuator was installed in the tunnel, close to the stripline port, and a second 10 dB attenuator was inserted before the scope. These attenuators also ensure that the signal acquired will not be polluted by reflection coming from bad mismatch between cables and the stripline or the scope ports.

Oscilloscope

The requirements for the readout electronics were the following:

- High dynamic range, in order to be able to properly separate the signal from the noise, also when operating in 7/8+1;
- High sampling rate, in order to obtain enough samples of the single 2.8 ns bucket over the total $\approx 3 \mu\text{s}$ beam length;
- Few GHz bandwidth in order to avoid the attenuation of the main 352 MHz signal;
- Possibility of acquiring data online and to easily integrate the device in the Tango operative system.

To cope with this requirements the LeCroy WavePro 254 HD oscilloscope has been chosen [2].

The selected oscilloscope has a bandwidth of 2.5 GHz, which is enough to observe the 352 MHz beam structure. The sampling rate of 20 GSa/s provides 56 samples per bucket. The vertical dynamic range of 12 bit allows to measure bunches with very different population. The possibility of manipulating the signal by filtering, averaging, or performing other mathematical calculation is also offered. Finally the device can be connected to the control system through an Ethernet port.

BEAM CURRENT MEASUREMENTS WITH SUB-MICROAMPERE RESOLUTION USING CWCT AND BCM-CW-E

F. Stulle*, L. Dupuy, E. Touzain, Bergoz Instrumentation, Saint Genis Pouilly, France
W. Barth¹, P. Forck, M. Miski-Oglu¹, T. Sieber, GSI, Darmstadt, Germany
¹also at Helmholtz Institute Mainz, Mainz, Germany

Abstract

The CWCT current transformer and its accompanying BCM-CW-E electronics allow accurate, high-resolution beam current measurements. This is achieved by combining a high-droop current transformer with low-noise sample-and-hold electronics. Thanks to a fast response time on the microseconds level the system can be applied not only to CW beams but also macropulses. Pulse repetition rates may range from 10 MHz to 500 MHz, rendering CWCT and BCM-CW-E suitable for a wide variety of accelerators. We report on test bench measurements achieving sub-microampere resolution. And we discuss results of beam measurements performed at the cw-LINAC, GSI.

INTRODUCTION

A growing number of particle accelerators is used worldwide for a growing variety of applications. Each of the applications has its own peculiarities which the particle beam, e.g. the particle species and energy, needs to be adapted to. This leads to a diversified accelerator landscape with a large variety of particle beam characteristics.

While beam instrumentation has been developed for most of these particle beams, in some cases existing solutions are either not optimum or not at all applicable due to the particle beam characteristics or the accelerator environment. Consequently, the development of improved beam instrumentation remains important for new and existing accelerators.

One recurring topic for new developments is the measurement of average beam currents. Especially average current measurements of CW beams, i.e. long streams of particle pulses, are challenging, because these are (quasi) DC currents.

Passive beam instrumentation coupling either capacitively, e.g. the pick-up electrodes of beam position monitors, or inductively, e.g. current transformers, to the electromagnetic fields of the particle beam cannot detect DC fields.

Only when using active sensors, e.g. DCCTs based on the fluxgate principle [1], DC beam currents can be measured non-invasively. Unfortunately, such sensors tend to be highly sensitive to the accelerator environment and too slow for some applications.

However, if a CW beam consists of well separated pulses using a passive current transformer and appropriate signal analysis can be sufficient to deduce the average current from the detected AC signal. The idea is to detect in between consecutive pulses the baseline of the transformer's

output signal, e.g. with a fast sample-and-hold circuit. This results a signal proportional to the average input current.

Such a measurement system has been developed by Bergoz Instrumentation and first results have been reported in [2]. It consists of a passive current transformer (CWCT) and analog electronics (BCM-CW-E) to process the CWCT's output signal. Due to its fast response time on the microsecond level, it can be used for CW beams and long macropulses. Table 1 summarizes CWCT and BCM-CW-E design specifications. Figure 1 shows photographs.

Table 1: CWCT and BCM-CW-E Design Specifications

Bunch repetition rate	10 MHz — 500 MHz
Current measurement range	10 μ A — 200 mA
Response time (full bandwidth)	1 μ s (10% — 90%)
Output noise (10 kHz bandwidth)	1 μ A _{rms}
Output noise (100 Hz bandwidth)	0.5 μ A _{rms}
Output voltage (in 1 M Ω)	-4 V — +4 V
Controlled via	TTL or USB



Figure 1: CWCT and BCM-CW-E.

Following successful first beam measurements at UNILAC, GSI [2], the BCM-CW-E electronics was further improved. Using a newly developed test bench at Bergoz Instrumentation enhanced stability and resolution are observed. Test bench measurements are discussed in the next section.

To demonstrate the improved performance with beam, CWCT and BCM-CW-E electronics were installed at the cw-LINAC [3], which is currently under development at GSI and HIM. This linac will provide CW ion beams mainly dedicated to GSI's super heavy elements (SHE) program. Consequently, in the future a measurement system for average currents of CW beams will become mandatory. Existing ACCTs could only be used for macropulse studies.

* stulle@bergoz.com

DEVELOPMENT AND CALIBRATION OF A MULTI-LEAF FARADAY CUP FOR THE DETERMINATION OF THE BEAM ENERGY OF A 50 MeV ELECTRON LINAC IN REAL-TIME

C. Makowski[†], A. Schüller, Physikalisch-Technische Bundesanstalt (PTB), Braunschweig, Germany

Abstract

The Physikalisch-Technische Bundesanstalt (PTB), Germany's national primary standard laboratory, operates a research electron LINAC with variable energy (0.5 – 50 MeV). A 128-channel Multi-Leaf Faraday Cup (MLFC) has been developed to measure the energy and the pulse charge in real time during the preparation or optimization of an electron beam of specific desired energy. The thickness of the entire leaf stack of the MLFC is sufficient to stop a 50 MeV electron beam. A dedicated electronic device has been developed for sequential readout of the charge collected by the leaves after each beam pulse. The range of the electrons and thus the distribution of the charge on the leaves depends on the energy. The MLFC was calibrated by recording charge distributions from monoenergetic electron beams of known energy. The MLFC is mounted at the end of the accelerator structure and replaces the beam dump. Energy, pulse charge and beam power from the MLFC measurement are displayed in real-time so that the influence of any manipulation of parameter setting on energy and beam power during beam preparation can be evaluated immediately.

INTRODUCTION

The preparation of an electron beam of specific desired energy and beam power at a LINAC is an optimization problem with many parameters. All parameters which influence the HF power (as e.g. via the high voltage at the modulator) as well as the number of charged particles in a bunch to be accelerated (as e.g. via the gun emission) also change the energy of the beam. It is therefore very helpful to be able to measure the energy in real-time during the adjustment of a setting.

The range of charged particles and thus the initial distribution of the charge in a solid depends on their energy. By means of a MLFC it is possible to measure nearly instantaneously the amount of deposit charge as function of the range [1-3]. The corresponding energy can be determined from this charge distribution. MLFCs are already used in proton beam facilities for energy and range modulation measurements [4-7]. For proton beams are even two different types of MLFCs commercially available [8-9].

In this work we present a MLFC designed for electron beams up to 50 MeV with a dedicated self-developed readout device based on inexpensive electronic circuits for fast sequential readout of the 128 MLFC channels.

DESIGN AND OPERATING PRINCIPLE

The MLFC detector consists mainly of 128 galvanically insulated Al plates in a stack perpendicular to the beam. The Al plates act as capacitors and store the charge portion deposit by the beam pulse in each plate until their sequential readout. From the distribution of the charge on the plates or in the 128 corresponding readout channels, respectively, the beam energy is determined.

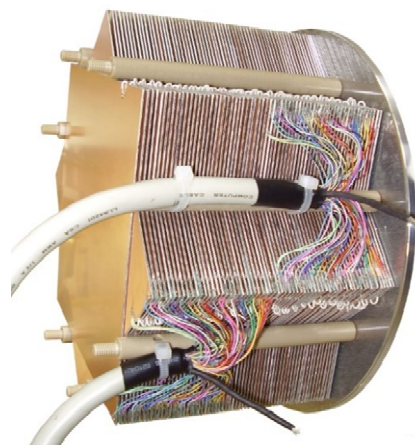


Figure 1: MLFC detector consisting of 128 leaves.

Figure 1 shows the MLFC detector without its housing. The dimensions and the total thickness of the leaf stack was chosen in such a way that it is large enough to absorb all primary electrons with the highest planned energy (50 MeV) and without scattered electrons leaving the detector laterally; On the other hand, the leaves are thin enough so that the charge distribution from an electron beam with the lowest planned energy (5 MeV) is still well resolved by the first 15 MLFC channels.

Each of the 128 MLFC leaves (15x15 cm) consists of a 0.625 mm Al plate, which acts as the actual beam absorber, a thin insulating layer (125 μm glass fibre) and a thin metal layer (35 μm Cu) on earth potential for shielding of the electric field from the charge stored at the Al plate. A further thin insulating layer (75 μm polyamide) works as galvanic insulation against the subsequent leaf. The insulation resistance of the Al plates is $> 2 \text{ G}\Omega$, so that the collected charge is stored virtually loss-free until its readout. Thanks to this feature, it is not necessary to read out all 128 plates parallel at the same time. Instead, signal acquisition can be done using a single charge integrator with a multiplexer. This simplifies the design, because otherwise 128 separate integrators would be necessary which have to be individually calibrated.

[†] email address

christoph.makowski@ptb.de

RADIATION HARDNESS INVESTIGATION OF ZINC OXIDE FAST SCINTILLATORS WITH RELATIVISTIC HEAVY ION BEAMS

P. Boutachkov*, A. Reiter, B. Walasek-Höhne, M. Saifulin, GSI, Darmstadt, Germany
E.I. Gorokhova, Shvabe, St. Petersburg, Russia
P.A. Rodnyi, I. Venevtsev, Polytechnic University Peter the Great, St.Petersburg, Russia

Abstract

At GSI ion beams of many elements, from H up to U, are produced with energy as high as 4.5 GeV/u with the SIS-18 synchrotron. For absolute beam intensity and micro-spill structure measurements a BC400 organic scintillator is used. Due to the low radiation hardness of this material, alternative inorganic scintillators like ZnO:Ga and ZnO:In were investigated. The properties and possible application of these novel radiation hard fast scintillators will be discussed. Their response to Sn, Xe and U ion beams will be reported.

USE OF FAST SCINTILLATORS AT GSI/FAIR

The complete range of possible beam intensities at GSI/FAIR cannot be covered by one detector type. The task is accomplished by a combination of three detectors, a plastic SCintillator (SC), an Ionization Chamber (IC) and a Secondary Electron Monitor (SEM). The SC detector utilizes the interaction of the ion beam with a scintillator which generates photons. A photomultiplier tube (PMT) converts the light into an electrical signal. The detector produces one pulse for each detected ion. In contrast the IC and SEM detectors generate a current proportional to the beam intensity. The systematic errors in the calculation of the beam current are removed by calibration of the IC versus a SC detector. Next, at higher beam intensities, the current determined by SEM is compared to the reading of the calibrated IC detector.

The plastic scintillator has to be exchanged regularly, due to radiation damage. The typical dose at which an exchange has to be performed is 40 kGy. This dose is regularly reached, therefore we started an investigation of an inorganic material which can substitute the plastic scintillator.

ZINC OXIDE RESPONSE TO HEAVY IONS

Zinc oxide (ZnO) is known as an efficient phosphor. It exhibits two emission bands, a fast decaying narrow band located near the absorption edge of the crystal and a broad band, with maximum usually in the green-yellow spectral range. The typical decay time of the broad band is of order of ms while the narrow one decay in less than a ns. Producing large area ZnO based scintillator is challenging. In the recent year there have been breakthroughs in manufacturing ZnO optical ceramics. The combination of nano-materials with improved manufacturing technology led to fast ZnO based scintillators with area of order of 5 cm², disks with diameter

of 25 mm. A key part of the production is the introduction of doping which suppresses the long lived green-yellow spectral component and enhances the fast narrow band luminescence, see Ref. [1, 2] and the references within for more details.

In this paper we present an investigation of the new ceramic scintillators with heavy ions. A schematics of the experimental setup is shown in Fig. 1. The heavy ion beam from SIS-18 comes from the right, it passes into air through a 100 μm steel window. It is collimated to a spot with a diameter of 5 mm by the Aluminum collimator. An ionization chamber is used to determine the dose deposited by the beam into the studied samples. The samples are inserted into the beam with a remotely controlled manipulator, indicated as target ladder in the figure. A photomultiplier detects the scintillation light.

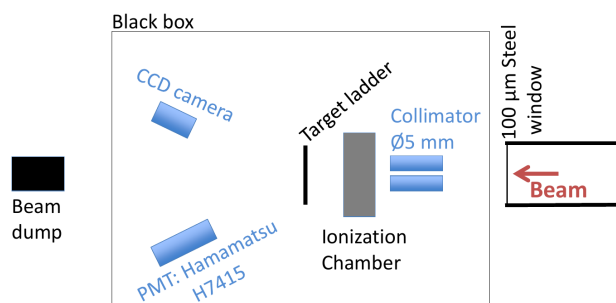


Figure 1: A schematics of the experimental setup. See the text for details.

A CCD camera and a Cromox screen installed on the target ladder were used for beam tuning. The charge collected from the IC was measured with a charge to frequency converter [3] which was calibrated versus a plastic scintillator installed on the target ladder.

ZnO ceramic scintillators doped with In and Ga were investigated with relativistic Xe and U ions. The response to 300 MeV/u ¹²⁴Xe ions of 1 mm thick BC400 plastic scintillator and 0.4 mm thick ZnO:Ga and ZnO:In ceramics is shown in Fig. 2. The observed rise and decay times are faster than the one of BC400 plastic scintillators. The PMT signals are transmuted over 75 m long cable to the oscilloscope used to record them. This is reflected in their shape.

In Fig. 3 the light yield of the ZnO ceramics is compared to the one of BC400 scintillator. We have to investigate the light yield from heavy ions as function of ZnO thickness and energy loss in the material. Nevertheless, the 300 MeV/u ¹²⁴Xe data shows that the light yield from 0.4 mm ZnO:In is 10% higher than the one from 0.4 mm BC400 scintillator.

* P.Boutachkov@gsi.de

COMMISSIONING OF THE BEAM LOSS MONITORING SYSTEM FOR THE HADES BEAM-LINE AT GSI

P. Boutachkov*, M. Sapinski, S. Damjanovic, B. Walasek-Höhne, GSI, Darmstadt, Germany

Abstract

The High Acceptance Di-Electron Spectrometer experiments at GSI (HADES) require high-intensity heavy ion beams. Monitoring and minimization of the beam losses are critical for the operation at the desired beam intensities. FAIR-type Beam Loss Monitor (BLM) system based on sixteen plastic scintillator detectors is installed along the beam line from the SIS-18 synchrotron to the experiment location. The detectors are used in counting mode, with maximum counting rate of order of 20 MHz. The system has been commissioned during the 2018 beam time. Details on the detector setup, its calibration procedure and how it can be used for quantitative beam loss determination are presented.

BLM DETECTOR

A photograph of the detector components is shown in Fig. 1. The light from $20 \times 20 \times 75 \text{ mm}^3$ BC408 plastic scintillator is converted in an electrical signal by a Hamamatsu R6427-20 photomultiplier (PMT). The PMT active area is 25 mm. The selected photomultiplier has a large dynamic range, low leakage current and gain variation of less than 50% between different PMTs. An active voltage divider (AVD) was developed at GSI to power the PMT. The main features of the divider are:

- limited (maximum) average anode current, hence the longevity of the PMT is ensured
- improved gain stability
- operating at 10^7 counts per second (cps) counting rates, at current of 0.7 mA provided from the power supply.
- total current required of only 0.7 mA for the operation of the voltage divider

For operational considerations and possible radiation damage of the electronics the PMT signal is sent over a long cable, on average 150 m, to data acquisition system based on level discriminators and a counters [1]. The typical signal width after shaping from the cable is of order of 20 ns. Hence, due to pile-up, for normally distributed 10^7 signals per second, the data acquisition system will count on average 8×10^7 pulses.

BLM PLACEMENT AND CALIBRATION

The BLM detector are placed around the aperture limitations of the HADES beam line. Details about the beam line layout and beam optics are presented in Ref. [2]. There are always at least two detectors near an expected beam loss location. A photograph of one of the BLM at the beam line is shown in Fig. 2. The active volume of each detector is placed symmetricly relative to the aperture limitation, reducing the signal dependence on possible asymmetric beam



Figure 1: An assembled BLM detector is shown to the right of the photograph. In the middle the scintillator, photomultiplier and voltage divider are shown. A disassembled active voltage divider is placed to the left of the photograph.

losses. For example at the location shown in Fig. 2 the beam loss is expected to occur due to the small vertical aperture of the upstream magnet vacuum chamber, therefore the BLM is placed in the horizontal plane. This layout reduces the total number of BLM detectors needed for the beam line optimization.

The distance of the detector to the beam axis was chosen based on FLUKA [3,4] simulations of the particle shower created during a beam loss. The detectors are attached to the beam tube at a distance of 0.3 m from the beam axis. Depending on the nearest upstream magnet they are installed at about half a meter from the nearest upstream quadrupole or a meter from the nearest upstream dipole magnet. The exact positions are determined based on mechanical constrains. This placement leads to suppression of the signals from heavy ions of 3 orders of magnitude versus the signal from protons and neutrons. Moving the detector away from the heavy ion shower allows to operate the PMT at the same voltage independent of the accelerated ion species. The detector were not mounted further away as it is advantageous to keep them in the proton shower created by the lost particles. This point will be discussed in next section on quantitative determination of the beam loss.

The detector system was calibrated with a ^{137}Cs γ -source. The discriminator thresholds of all detectors were set to the same value. Their high voltages were adjusted until the same predetermined counting rate was reached with the γ -source mounted on the top of each detector. Fig. 3 shows the fit

* P.Boutachkov@gsi.de

VERSATILE BEAMLINE CRYOSTAT FOR THE CRYOGENIC CURRENT COMPARATOR (CCC) FOR FAIR*

D. M. Haider[†], F. Kurian, M. Schwickert, T. Sieber, F. Ucar
GSI Helmholtzzentrum für Schwerionenforschung, 64291 Darmstadt, Germany
T. Koettig, CERN, 1211 Geneva 23, Switzerland
T. StoeHLker^{1,2}, V. Tympel, Helmholtz Institute Jena, 07743 Jena, Germany
J. Golm, Institute of Solid State Physics, 07743 Jena, Germany
M. Schmelz, R. Stolz, V. Zakosarenko³, Leibniz IPHT, 07745 Jena, Germany
H. De Gersem, N. Marsic, W.F.O. Mueller, TU Darmstadt, 64289 Darmstadt, Germany
¹also at GSI Helmholtzzentrum für Schwerionenforschung, 64291 Darmstadt, Germany
²also at Institute for Optics and Quantum Electronics, 07743 Jena, Germany
³also at Supracon AG, 07751 Jena, Germany

Abstract

The Cryogenic Current Comparator (CCC) extends the measurement range of traditional non-destructive current monitors used in accelerator beamlines down to a few nano-amperes of direct beam current. This is achieved by a cryogenic environment of liquid helium around the beamline, in which the beam's magnetic field is measured with a Superconducting Quantum Interference Device (SQUID), which is itself enclosed in a superconducting shielding structure. For this purpose, a versatile UHV-beamline cryostat was designed for the CCCs at FAIR and is currently in production. It is built for long-term autonomous operation with a closed helium re-liquefaction cycle and with good access to all inner components. The design is supported by simulations of the cryostat's mechanical eigenmodes to minimize the excitation by vibrations in an accelerator environment. A prototype at GSI has demonstrated the self-contained cryogenic operation in combination with a 15 l/day re-liquefier. The cryostat will be used in CRYRING to compare the FAIR-CCC-XD with newly developed CCC-types for 150 mm beamlines. Both will supply a nA current reading during commissioning and for the experiments.

INTRODUCTION

The non-destructive measurement of DC beam currents of a few nano-ampere with a Cryogenic Current Comparator (CCC) has been a goal at GSI since the 1990s [1]. Among many other advantages that come with the precision of nano-ampere, this low detection threshold brings an immense benefit during the commissioning of accelerators and allows the monitoring of weak (slowly-extracted) ion beams. Therefore, up to five CCCs will be installed in the FAIR accelerator complex in Darmstadt, Germany. The first of them will become part of the low energy storage ring CRYRING in summer 2020 in order to supply several experiments with precise current readings. The extremely

high sensitivity is achieved by moving the principle of 'classic' current transformers into a cryogenic environment, using superconductors to detect the magnetic field of the passing ion beam. A SQUID measures the azimuthal magnetic field down to fractions of a flux quantum (2.07 E 15 Wb) while being surrounded by a complex superconducting shield that attenuates (>130 dB) all other field components. Similar to a current transformer the CCC encloses the beamline in order to detect the azimuthal field. However, it is a significant challenge to provide a stable cryogenic environment that can house the CCC as close to the beamline as possible during a beamtime of several months without any direct access to the system. Furthermore, it was shown that the CCC is very sensitive to changes of temperature and pressure. In fact, there is a drift of the current signal of 73.7 nA/mbar or an average of 33.5 nA/mK [2]. The cryogenic infrastructure of the FAIR facility is not built to ensure the stability required. Therefore, a beamline cryostat with an independent cooling cycle based on a local helium re-liquefier has been designed together with the company ILK Dresden. The closed cooling concept has been tested in a prototype at GSI. A lot has been learnt from the cryostat built for the CCC at the Antiproton Decelerator at CERN [3].

The high sensitivity to magnetic fields coincides with a susceptibility to mechanical vibrations. At the moment, the current resolution is limited by the background noise of ~30 pA/√Hz at frequencies between 5 Hz and 100 Hz [4], while the white noise is at 3 pA/√Hz up to 100 kHz. A significant part of the background at low frequencies can be linked to mechanic oscillations of the environment. Therefore, a study of the mechanical resonances needs to be part of the design process of the cryostat in order to minimize their impact on the quality of the signal.

In the following, an overview of the thermal design followed by the results of a FEM study to determine the resonant behaviour is given. An additional approach to minimize the current noise and to increase the sensitivity by modifying the CCC itself is presented in [5]. For a more detailed explanation of the measurement principle and a summary of previous installations please refer to [2, 6].

* Work supported by AVA – Accelerators Validating Antimatter the EU H2020 Marie-Curie Action No. 721559 and by the BMBF under contract No. 05P155JRBA and 5P185JRBI.

[†] d.haider@gsi.de

Content from this work may be used under the terms of the CC BY 3.0 licence (© 2019). Any distribution of this work must maintain attribution to the author(s), title of the work, publisher, and DOI

FIRST MEASUREMENTS OF A NEW TYPE OF CORELESS CRYOGENIC CURRENT COMPARATORS (4C) FOR NON-DESTRUCTIVE INTENSITY DIAGNOSTICS OF CHARGED PARTICLES*

V. Tympel[†], T. Stöhlker^{1,2}, Helmholtz Institute Jena, 07743 Jena, Germany
 J. Tan, CERN, CH-1211, Geneva 23, Switzerland

N. Marsic, W.F.O. Müller, H. De Gerssem, Department of Electrical Engineering and Information Technology, TU Darmstadt, Germany

D. Haider, M. Schwickert, T. Sieber, GSI Helmholtzzentrum für Schwerionenforschung, 64291 Darmstadt, Germany

J. Golm, M. Stapelfeld, F. Schmidl, P. Seidel, Institute of Solid State Physics, 07743 Jena, Germany

M. Schmelz, T. Schönau, S. Anders, J. Kunert, R. Stolz, V. Zakosarenko³, Leibniz Institute of Photonic Technology, Leibniz-IPHT, 07745 Jena, Germany

¹also at GSI Helmholtzzentrum für Schwerionenforschung, 64291 Darmstadt, Germany

²also at Institute for Optics and Quantum Electronics, 07743 Jena, Germany

³also at Supracon AG, 07751 Jena, Germany

Abstract

The non-destructive and highly sensitive measurement of a charged particle beam is of utmost importance for modern particle accelerator facilities. A Cryogenic Current Comparator (CCC) can be used to measure beam currents in the nA-range. Therein, charged particles passing through a superconducting toroid induce screening currents at the surface of the toroid, which are measured via Superconducting Quantum Interference Devices (SQUIDs). Classical CCC beam monitors make use of a high magnetic permeability core as a flux-concentrator for the pickup coil. The core increases the pickup inductance and thus coupling to the beam, but unfortunately also raises low-frequency noise and thermal drift. In the new concept from the Leibniz Institute of Photonic Technology the Coreless Cryogenic Current Comparator (4C) completely omits this core and instead uses highly sensitive SQUIDs featuring sub-micron cross-type Josephson tunnel junctions. Combined with a new shielding geometry a compact and comparably lightweight design has been developed, which exhibits a current sensitivity of about 6 pA/sqrt(Hz) in the white noise region and a measured shielding factor of about 134 dB.

INTRODUCTION

The accurate and non-destructive beam intensity measurement of small currents below 1 μA is a challenge. An excellent way to do this is to measure the azimuthal magnetic field of the charged particle beam and to compare that with fields of known electrical currents. Since the magnetic fields are very small, SQUIDs are used for field detection and massive superconductors for suppression of interference fields.

* Work supp. by BMBF 05P15SRBA, 05P18RDRB1, 05P18SRB1

† volker.tympel@uni-jena.de

History and Design

Classical CCCs for beamlines, developed in the 70s at Physikalisch-Technische Bundesanstalt (PTB) [1] and beginning in the 90s at GSI [2], have three main components: the superconductive meander structure for filtering the azimuthal field component, the pickup coil for the magnetic coupling with the SQUID, which carries out the actual current measurement and is located in the so-called SQUID cartridge (see Fig. 1).

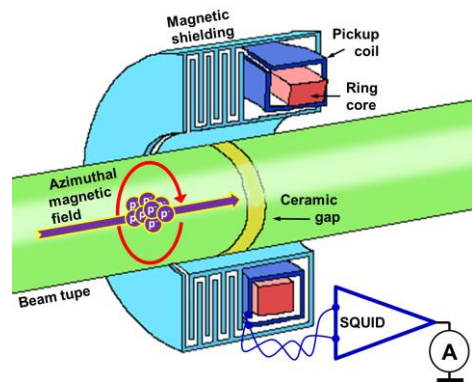


Figure 1: Classical CCC design for beamlines.

Meander Structure

The meandering structure is a shortened design of two long, coaxial superconducting tubes that realize the extraction of the azimuthal magnetic field component by shielding other components. The arrangement of the meanders was often perpendicular to the beam tube as shown in Fig. 2 (a) and called ring topology. This design has been applied to the CERN-Nb-CCC, which is currently installed at CERN-Antiproton Decelerator (AD), and to the GSI-Nb-CCC-XD, which has an inside diameter that allows it to be used on 150 mm beam tubes of the FAIR project.

RETRIEVING BEAM CURRENT WAVEFORMS FROM ACCT OUTPUT USING EXPERIMENTAL RESPONSE FUNCTION FOR USE IN LONG PULSE ACCELERATORS

Y. Hirata[†], J. Franco Campos, A. Kasugai, Rokkasho Fusion Institute, National Institutes for Quantum and Radiological Science and Technology, Aomori 039-3212, Japan

Abstract

Current transformers (ACCT/DCCT) are used as non-interceptive means of beam current measurement in many accelerators. In the case of long pulse to CW accelerators for fusion neutron sources such as IFMIF, A-FNS, etc., current measurement using current transformers for pulses with around 10-100 ms or longer suffer such problems as drooping and the measurement accuracy is deteriorated. So, improving the accuracy for long pulse beams is highly required. We have proposed a method for retrieving the beam currents from the ACCT output using a transfer function obtainable from simple experiments. It was confirmed from numerical calculation that beam currents longer than a second could be theoretically retrieved. The effects of associated circuits and cables such as stray capacitance, inductance and magnetic materials nearby are inherently included in the transfer function. We are working for implementing this method into FPGA. For calculation convenience, the transfer function is converted into a form of impulse response function and the convolution with the digitized ACCT output is to be carried out to retrieve the beam current. The theory, algorithm and design will be discussed.

INTRODUCTION

Current transformers (ACCT/DCCT) are used as non-interceptive means of beam current measurement in accelerators. Current measurement using current transformers (CTs) for long pulses with 10-100 ms or longer suffers such problems as droops.

In the case of long pulse to CW accelerators for fusion neutron sources such as IFMIF, A-FNS, etc., the deterioration of measurement accuracy could be crucial and improving the accuracy for long pulse beams, or at least in the gap uncovered by the ACCT and DCCT, is highly required.

Measurement errors with an ACCT for long pulses are due to the fact that this measurement is based on the current induction through transformers and is considered inevitable. Ideally the output of ACCT is supposed to be the derivative of the beam current, so the integrator at downstream will give back the beam current. In reality, however, the output signal from the ACCT is not an ideal derivative. There is influence from the cable stray impedance, capacitance, inductance, associated amplifier, etc.

The electrical circuits connected to CTs have been improved in order to reduce drooping and to obtain a waveform as close as to the original beam current waveform, but the decay time of the circuit can be extended up to as

long as 1 second or could be a little longer [1,2,3]. Moreover, there is need to reduce the influence of the magnetic materials nearby [2, 4].

In our previous study [5], a method for obtaining the beam current waveforms from the waveform of ACCT output signals have been proposed. Since the ACCT and associated electrical circuits can be considered as a linear system, there must be a unique transfer function that connects the input and the output. This transfer function and the backward transfer function can be obtained numerically from simple experiments. The conversion from the output waveform to the input waveform is "ideal" since it is free from restrictions of real circuits.

This method has several advantages: (1) no detail information about the ACCT and the electronics is necessary; (2) the transfer function is easy to obtain from simple experiments with a function generator and an oscilloscope other than the ACCT and an amplifier; (3) effects of stray capacitance, inductance and magnetic materials nearby are inherently reflected in the transfer function; (4) the use of FFT speeds up the calculation for obtaining the transfer function.

On the other hand, it does not allow a continuous or sequential beam retrieving since the retrieval can be done only over a certain time period which is the time window for FFT. Sequential retrieval is more convenient to be implemented with FPGA and for use in practical occasions.

In this paper, the viability of sequential retrieval of beam current waveform from the ACCT output is examined. We reformulated the theory in [5] into a convolutional form using response functions. An algorithm for FPGA was clarified and a simple program was made to check the validity of the algorithm.

It is said to be typical that a response function obtained from DFT (digital Fourier transformation) suffers some ghost signal problems coming from its periodic nature. A method for reducing this kind of ghost signals has also been examined.

This paper is organized in the following manner. Theory and an algorithm to be implemented will be given in the next chapter, followed by the check of its validity using data obtained in simple tests. Conclusions will be offered in the last chapter.

THEORY

A method presented in [5] for retrieving a beam waveform function from the observed ACCT output using a transfer function is a signal processing effective for the

DESIGN AND PROPERTIES OF A NEW DCCT CHAMBER FOR THE PF-RING AT KEK

R. Takai*¹, T. Honda¹, Y. Tanimoto¹, T. Nogami, T. Obina¹

High Energy Accelerator Research Organization (KEK), Tsukuba, Ibaraki, Japan

¹also at SOKENDAI (The Graduate University for Advanced Studies), Tsukuba, Ibaraki, Japan

Abstract

A DC current transformer (DCCT) for the PF-ring was renewed during the 2018 summer shutdown. A vacuum chamber for the new DCCT was designed based on a circular duct with an inner diameter of 100 mm and has a structure housing a toroidal core inside of electromagnetic shields. The geometry of the ceramic break for interrupting the wall current flow was optimized using a three-dimensional electromagnetic field simulator, and the break was fabricated considering some technical limitations. Both ends of the ceramic break were short-circuited in a high-frequency manner by a sheet-like capacitive structure to suppress the radiation of unneeded higher-order modes (HOMs) into the core housing. The ceramic break is also equipped with water-cooling pipes on metal sleeves brazed to the both ends to efficiently remove the heat generated by HOMs. The new DCCT chamber has been used already in user operation without any problems. A temperature rise near the ceramic break is still approximately 6 °C, even when a 50-mA isolated bunch is stored.

INTRODUCTION

In the Photon Factory storage ring (PF-ring), which is a dedicated light source of KEK, two DC current transformers (DCCTs) have been installed to measure the stored beam current in the ring [1]. It has been more than 20 years since the main DCCT for user operation was installed, and there is concern for failure due to aging. In addition, heat generation of the DCCT chamber caused by the higher-order modes (HOMs) emitted from the stored beam has become an issue for the filling pattern with a highly charged isolated bunch because the sectional shape of the chamber does not match the adjacent beam ducts. Because the stored current measured by the DCCT is one of the most important parameters in accelerator operation, we decided to update this old DCCT. For the toroidal core and signal-detection circuit of the components, an in-air model of the New Parametric Current Transformer (NPCT) and its electronics manufactured by Bergoz Instrumentation, which have been used successfully in many accelerators including the PF-ring, were adopted [2]. A vacuum chamber paired with the commercial core was designed and fabricated based on a circular duct with an inner diameter of 100 mm according to the duct shape at the installation site.

In this report, the detailed design of the new DCCT chamber with the ceramic break and its properties measured in different filling patterns are described.

DESIGN OF CERAMIC BREAK

To detect the electromagnetic field emitted from electron beams by the DCCT core placed outside of the beam duct, a part of the metal duct needs to be replaced by a ceramic to break the wall current flow accompanied with the beam propagation. However, because unneeded HOMs exceeding the measurement bandwidth of the DCCT are emitted into the core housing and can cause serious duct heating or electric discharges only by breaking the flow, both ends of this ceramic break are often short-circuited at high frequency by imparting an appropriate capacitance. The value of the capacitance C is determined by the cutoff frequency considering the measurement bandwidth and the impedance of the cavity structure formed by the core housing. For the core of the Bergoz Instrumentation, C is recommended to be set within the following range [3]:

$$10 \text{ nF} \leq C \leq 220 \text{ nF.} \quad (1)$$

In the case of DCCT chambers that have been used in the PF-ring, including the sub-DCCT, an alumina ceramic disk with a thickness of 0.5 mm is used as the ceramic break [4]. The ceramic disk has a hole corresponding to the adjacent duct shape at the center. Both sides of the disk are metalized, and a 0.5-mm-thick Kovar sleeve is brazed on each side. Such a structure where the thin ceramic disk is sandwiched between the metal sleeves is very effective for suppressing the duct heating because it is possible to reduce the beam-coupling impedance. However, because the outer diameter of the ceramic disk becomes much larger than that of the beam duct to realize the capacitance of the order of Eq. (1), there are some difficulties in manufacturing, cost, and handling. Therefore, a cylindrical ceramic break, which is also used in the Photon Factory Advanced Ring (PF-AR) and SuperKEKB (former KEKB) storage rings, was adopted for the new DCCT chamber [5]. In this method, the capacitance is secured by wrapping the exterior of the ceramic break with a sheet-like capacitive structure.

The beam simulation was conducted to evaluate the power loss generated when the beam propagated in a DCCT chamber by using a three-dimensional electromagnetic field simulator “GdfidL” [6]. Figure 1(a) shows a schematic layout of the simulated chamber model. The cylindrical ceramic break, whose longitudinal length is L and transverse thickness is T , is interposed in the middle of a circular duct

* ryota.takai@kek.jp

A DUAL FUNCTIONAL CURRENT MONITOR FOR STRIPPING EFFICIENCY MEASUREMENT IN CSNS*

W. L. Huang[†], R. Y. Qiu, F. Li, A. X. Wang, M. Y. Liu, M. Y. Huang, T. G. Xu
Institute of High Energy Physics, Chinese Academy of Sciences, Beijing 100049, China
Spallation Neutron Source Science Center, Dongguan 523803, China

Abstract

China Spallation Neutron Source (CSNS), the biggest platform for neutron scattering research in China, has been finished construction and already in user operation stage by the end of 2017. During the multi-turn charge-exchange injection, H⁻ stripping by a carbon primary stripper foil (100 μg/cm²) and a secondary stripper foil (200 μg/cm²) is adopted for this high intensity proton synchrotron. In order to evaluate the stripping efficiency and the foil aging, a dual-function low noise current transformer and corresponding electronics are designed to measure the ultra-low intensity of H⁻ and H⁰, which are not stripped completely by the 1st foil but totally stripped charge changing to H⁺ and delivered to the IN-DUMP. The self-designed CT sensors made of domestic nanocrystalline toroids, the noise analysis and elimination, measurement results and further improvement proposals are presented in this paper.

INTRODUCTION

As explained in Ref. [1], the beam density in hadron storage rings can be limited at injection by space charge or by the injector capacity. The H⁻ charge exchange injection technique is adopted to overcome the intensity limitation of the beam emittance increase with the number of injected turns and high losses at the septum. Thus, the multi-turn charge-exchange injection in spallation neutron sources is very common and proved to be effective.

China spallation neutron source (CSNS) consists of an H⁻ ion source, a 3-MeV RFQ, a 4-tank DTL which accelerates the H⁻ ions to 80MeV, an 80 MeV to 1.6 GeV RCS and a target station. Main parameters of CSNS are listed in Table 1. During the multi-turn charge-exchange injection, H⁻ stripping by a carbon primary stripper foil (100 μg/cm²) and a secondary stripper foil (200 μg/cm²) is adopted to fulfil a stripping efficiency of > 99.7%. The voltage curves of INBH and INBV magnets are optimized

Table 1: Main Parameters of CSNS[2]

Project Phase	I	II
Beam Power on target [kW]	100	500
Proton energy [GeV]	1.6	1.6
Average beam current [μA]	62.5	312.5
Pulse repetition rate [Hz]	25	25
Linac energy [MeV]	80	250
Linac type	DTL	+Spoke
Linac RF frequency [MHz]	324	324
Macropulse. ave current [mA]	15	40
Macropulse duty factor	1.0	1.7
RCS circumference [m]	228	228
harmonic number	2	2
RCS Acceptance [πmm-mrad]	540	540
Target Material	Tungsten	Tungsten

to paint the transverse phase space with a small beam loss [3].

In order to evaluate the stripping efficiency and the foil aging, a dual-function low noise current monitor (BCT+FCT) and corresponding electronics are designed to measure the ultra-low intensity of H⁻ and H⁰, which are not stripped completely by the 1st foil but totally stripped charge changing to H⁺ and delivered to the IN-DUMP. The layout of the injection region of CSNS is showed in Fig. 1.

BEAM TIME STRUCTURE

The H⁻ beam in the linac is chopped into micro bunches by a chopper located at the end of LEPT. The chopping factor is adjustable for different operation modes. For example, a chopping factor of 50% is adopted for user mode in normal operation and 75% for single bunch mode in special operation for the back-n experiments, which

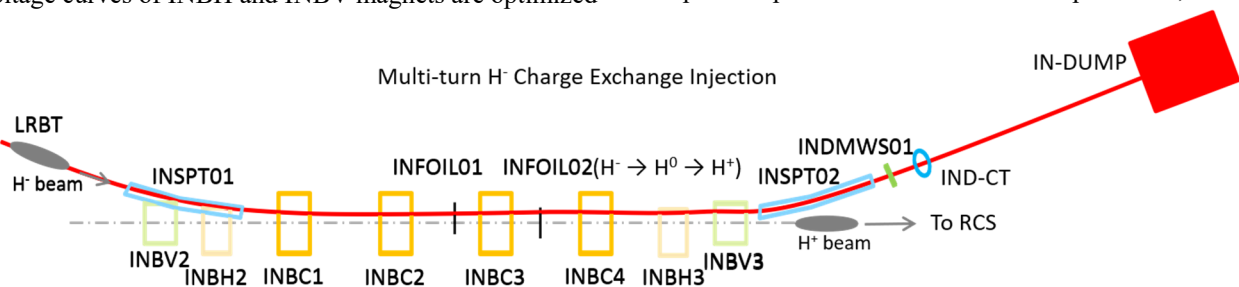


Figure 1: Layout of the injection region of CSNS.

* Work supported by National Natural Science Fund (No.11605214).

† huangwei@ihep.ac.cn

DEVELOPMENT OF COMPACT IONIZATION CHAMBERS FOR PARTICLE THERAPY FACILITIES*

M. Liu[†], C. X. Yin

Shanghai Synchrotron Radiation Facility & Shanghai Advanced Research Institute, Shanghai, China

Abstract

Dose monitors and position monitors are critical equipment for particle therapy facilities. Performance of the monitors affects precision of irradiation dose and dose distribution. Parallel plate ionization chambers with free air are adopted for dose monitors and position monitors. Radiation tolerant front-end electronics are integrated in the chambers, and the output of the chambers are digital signals. The structure of the monitors is compact and modularized. The ionization chambers are implemented successfully in Shanghai Advanced Proton Therapy Facility. The development details and implementation status are presented.

INTRODUCTION

Particle therapy facilities are dedicated accelerator facilities for cancer treatment. Compared with traditional radiotherapy, particle therapy has higher position accuracy transversely and longitudinally. In the course of treatment, radiation dose is mainly accumulated in malignant tumour. Cancerous cells are killed, while surrounding healthy tissue is spare. [1] During the delivery of radiation dose, beam parameters should be monitored in real time, especially in nozzle, which is the nearest part to patients.

Beam monitors are the core equipment of beam delivery system, by which beam from accelerator is converted to beam for treatment. The compact ionization chambers including front-end electronics were developed for particle therapy facilities. Parallel plate ionization chambers (PPIC) and multi-strip ionization chambers (MSIC, also a kind of PPIC) are used as the detectors, and radiation tolerant front-end electronics are designed to collect data and output digital signals.

Shanghai Advanced Proton Therapy Facility is under commissioning, which has a fix-beam room, a 180° gantry room and an ocular room. [2] The compact ionization chambers are implemented in the fix-beam room and the 180° gantry room. Both of the two rooms utilize active scanning technology for beam delivery. Compared with traditional passive scattering technology, the new technology has its advantages like providing more precise conformation [3], and yet raises more challenges to development of beam monitors.

SYSTEM DESIGN

For the nozzle which conducts spot-scanning dose delivery, scanning magnets moves particle beam discontin-

uously according to prescribed treatment plan. [4] Once preset dose value of current spot is reached, proton beam should be turned off and moved to next spot. The goal of irradiation is that the tumour receives a uniform dose distribution.

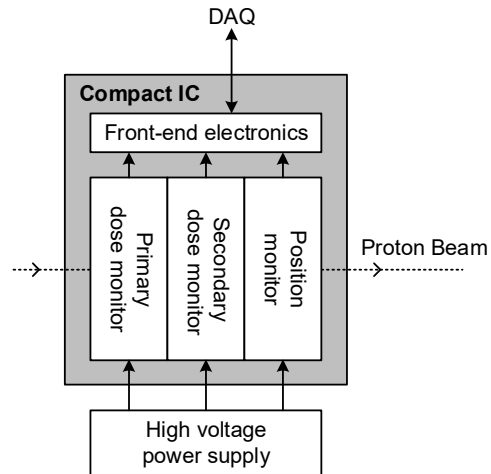


Figure 1: The structure of the compact ionization chambers.

The structure of compact ionization chambers is illustrated in Fig. 1. The dose monitors aim to achieve real-time dose measurement. The position monitor aims to achieve spot position and size measurement. Performance of the monitors affects treatment results severely. Characteristics of the beam monitors are shown in Table 1.

Table 1: Characteristics of the Compact Ionization Chambers

Parameter	
Dose relative accuracy	±2%
Dose relative resolution	±1% (2 sigma)
Dose data throughput	75kHz
Position accuracy	±0.5mm
Position resolution	±0.2mm (2 sigma)
Position data throughput	1.6kHz
Ion collection time	70 μs

Dose Monitor

Parallel plate ionization chambers with free air were used as the detectors of dose monitor, and the structure is illustrated in Fig. 2. The high voltage is -2500V. The material of the planes in PPIC is Kapton of 25μm, which is coated with Aluminium of 0.1μm. The gap between the high voltage plane and the signal pad is 5mm. According to spill strength range of the extracted beam, the collection efficiency is greater than 99%.

* Work supported by the Youth Innovation Promotion Association CAS (No. 2016238)

[†] liuming@zjlab.org.cn

FARADAY CUP SELECTOR FOR DC-280 CYCLOTRON

V. Aleinikov[†], S. Pachtchenko, K. Sychev, V. Zabanova, FLNR JINR, Dubna, Russia

Abstract

New isochronous cyclotron DC-280, the basic facility of Super Heavy Element (SHE) Factory was put into operation in the FLNR JINR on March 25, 2019. Key role in beam diagnostics for lossless transportation is played by Faraday cups. Five elements were installed along the two injection lines and 14 elements on the five transport channels to the experimental facilities. The software was developed to automatically select the active Faraday cup depending on its location and track the current on a single indicator. This paper describes basic principles and algorithm of the Faraday cup Selector module which is a part of the DC-280 cyclotron control system.

INTRODUCTION

The DC-280 cyclotron has been created and put into operation in the new experimental building of the FLNR. The main goals of Super Heavy Element factory [1] are:

- Synthesis of SHE and studying of their properties.
- Search for new reactions for SHE synthesis.
- Chemistry of new elements.

The SHE will increase the present rate of super heavy nuclei production by one-two orders of magnitude. This will enable studies of nuclear/atomic structures of heaviest atoms and open the door to the discoveries of the new elements above $Z=118$ and of isotopes closer to the predicted shell closure at $N=184$.

The main purpose of beam transport is lossless and high-quality delivery of accelerated particles to a target in a physical setup. By affecting the particles by the magnetic field of the correction magnetic elements (coils, solenoids, lenses, etc.), the operator focuses and holds the beam in the pipe. The result is measured by means of a variety of devices: current probes, Faraday cups, stoppers, luminophores and so on. Most of these elements are opaque for the beam and interrupt it on the way. Therefore, the only beam current measured on a device that was inserted first along the beam is significant. Eight multi-channel meters are used to measure current from 21 diagnostic devices. During beam transportation operator has to switch his attention among multiple displays of current meters. For the convenience of the operator it was decided to create a program that automatically determines the actual diagnostic device and toggles its measurement to one common monitor.

HARDWARE

The beam transport system consists of two lines from different ECR ion sources on HV platforms (DECRIS-PM 14 GHz and Superconducting ECR), a common injection line into the accelerator, extraction line and 5 beam lines

to the physical setups (see Fig. 1). To measure the ion currents and to determine the beam transverse position total 5 diagnostics units were installed in the injection system, 2 units in common extraction line and 12 units in five beam lines to the physical setups. Each diagnostic unit may contain Faraday cup together with ionization beam profile monitor, luminophore. Depending on the acceleration mode, ions pass from one of two ECR sources through the accelerator to one of five physical facilities.

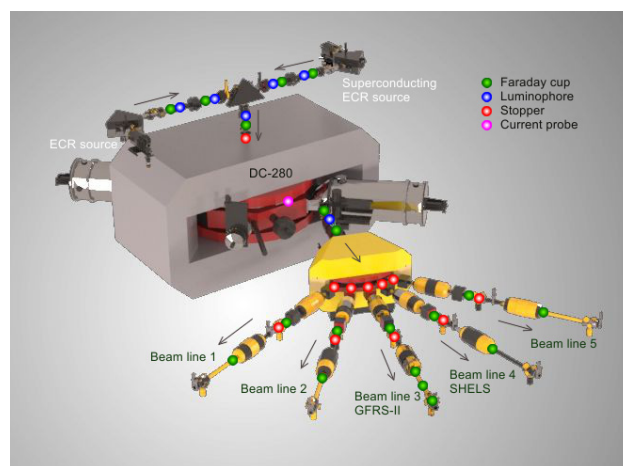


Figure 1: Beam diagnostics layout.

Key role in beam diagnostics for lossless transportation is played by Faraday cup. It was designed and manufactured in INR&NE department of the Bulgarian Academy of Sciences (Sofia, Bulgaria). Its design is shown in Fig. 2. Instruments for beam diagnostics are mechanically placed in the ion guide using a pneumatic drive mechanism.

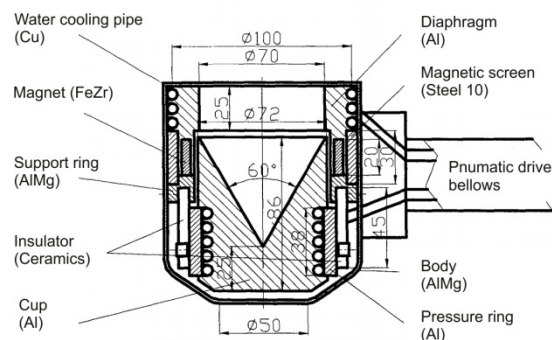


Figure 2: Faraday cup.

To measure the beam current, a specially developed module MI08-01 is used. It was designed and manufactured in FLNR JINR and meets SMARTBOX-6 system specifications [2]. The module has 8 input channels for connecting analog signals multiplexed to one measuring

[†] vitalirus@gmail.com.

DESIGN OF THE ESS MEBT FARADAY CUP

A. R. Páramo†, I. Bustinduy, D. de Cos¹, C. de la Cruz², I. Mazkiaran, R. Miracoli, V. Toyos,
 S. Varnasseri, Consorcio ESS-Bilbao, Zamudio, Spain

E. Donegani, J. P. Martins, European Spallation Source ERIC, Lund, Sweden

¹ also at Departamento de Física Aplicada II UPV/EHU, Vitoria, Spain

² also at Centro Nacional del Hidrógeno CNH2, Puertollano, Spain

Abstract

The European Spallation Source (ESS) is currently under construction and the Medium Energy Beam Transfer (MEBT) is developed by ESS-Bilbao as an in-kind contribution. In the MEBT a set of diagnostics is included for beam characterization, among them the MEBT Faraday Cup is used to measure beam current and as a beam stopper for the commissioning modes. The main challenges for the design and manufacturing of the Faraday Cup (FC) are the high irradiation loads and the necessity of a compact design due to the space constraints in the MEBT. We describe the design of the FC, characterized by a graphite collector, required to withstand irradiation, and a repeller for suppression of secondary electrons. For the operation of the Faraday Cup acquisition electronics and control system are developed, all systems have been integrated in the ESS-Bilbao ECR ion source to test operation under beam conditions. In this work, we discuss the design of the Faraday Cup, the results of the tests and how they agree with the expected performance of the Faraday Cup.

INTRODUCTION

The European Spallation Source (ESS) is currently under construction in Lund, Sweden [1,2]. The ESS linear accelerator (Linac) delivers 2 GeV protons to the tungsten target for neutron production. In the normal conducting Linac, the Medium Energy Beam Transport line (MEBT) matches, focuses and characterizes the proton beam before acceleration in the normal conduction DTLs and the superconducting cavities. To characterize the beam, the MEBT (see Figure 1) includes different kinds of diagnostics: Wire Scanners (WS), Beam Position Monitors (BPM), Beam Current Transformers (BCM), Collimation Scrapers (SC), a Slit and Grid Emittance Measurement Unit (EMU) and a Faraday Cup (FC).

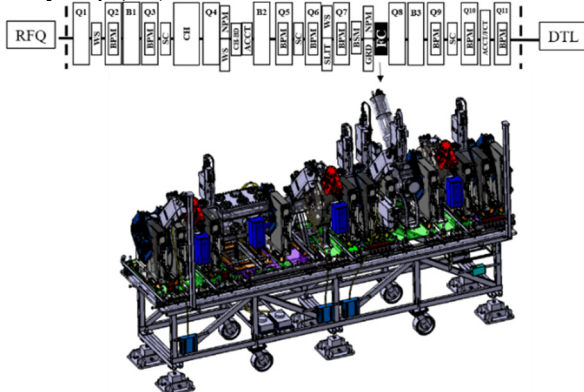


Figure 1: Scheme showing the ESS MEBT.

The MEBT will operate with a proton beam of 3.63 MeV and 62.5 mA peak current, and the FC will be used to measure the beam current and as a beam stopper during the MEBT commissioning.

In the Faraday Cup, the beam irradiates the collector and leads to high energy deposition during the pulse duration. As a result of the high currents (62.5 mA) and proton energies (3.63 MeV), the beam power is ~ 230 kW, that combined with a beam size of $\sigma_x \sim \sigma_y \sim 2.5$ mm [3], makes the requirements of the ESS MEBT Faraday Cup specially challenging.

Due to irradiation constraints, the operation of the FC is designed only for ESS commissioning modes: Fast tuning with pulses of 5 μ s at frequencies of 14 Hz and Slow Tuning with 50 μ s pulses at 1 Hz. The main operational parameters of the Faraday Cup operation are summarized in Table 1.

Table 1: Operational Parameters in the MEBT FC

Parameter	Value
Proton Energy	3.63 MeV
Intensity	62.5 mA
Beam Power	230 kW
Fast Tuning Mode	5 μ s - 14 Hz
Slow Tuning Mode	50 μ s - 1 Hz
Beam Size	$\sigma_x \sim \sigma_y \sim 2.5$ mm
Irradiation Power	5800 MW/m ²

The ESS MEBT Faraday Cup has an aperture of $\Phi 48$ mm, a total length of just 40 mm and is designed with a modular approach that allows for maintenance and replacement of its components, specially the collector which may undergo irradiation effects. A graphite collector is chosen due to its good capabilities to withstand the thermal shock of irradiation, selecting a high conductivity isostatic fine grain graphite SGL R7550, and with an indented profile similar to SNS DTL Faraday Cup [4] to reduce irradiation flux. A copper repeller is included for secondary electrons suppression operating at a nominal voltage of -1000 V and a refrigerated steel body allows for heat removal. The design of the Faraday Cup has been done by ESS-Bilbao and the manufacturing and assembly by the company Pantechnik. In Figure 2, we show the FC with its collector, repeller, insulators, refrigerated body and conduits.

For the operation of the Faraday Cup, integration with the electronics and control system is required. The different systems have been integrated and tested in the Bilbao ECR

CHARGE DETECTION SYSTEM FOR THE CLARA/VELA FACILITY

S. L. Mathisen^{1*}, Y. M. Saveliev¹, R. J. Smith¹, STFC, Sci-Tech Daresbury, UK
¹also at Cockcroft Institute, Sci-Tech Daresbury, UK

Abstract

The CLARA/VELA facility at Daresbury Laboratory combines an FEL test facility and an electron accelerator for scientific and industrial applications, capable of providing up to 40 MeV electrons, with an eventual goal of 250 MeV. Accurate measurement of the bunch charges in a wide range (1 - 250 pC) at a repetition rate up to 400 Hz is required. We present a new system of analogue electronics developed to interface with existing and future bunch charge measurement devices (wall current monitors, Faraday cups, etc.) to measure the bunch charges accurately and precisely. The system is based on a charge amplifier with switchable sensitivity, dark current gating and on-board self-calibration. Results of circuit simulations, offline calibration tests and online beam tests of a prototype system are presented.

INTRODUCTION

The CLARA front-end is the first phase of the CLARA 250 MeV FEL test facility, based at Daresbury Laboratory. The front-end was commissioned during 2018 [1] and used to provide high energy electrons for experiments using the VELA beamline during 2018 and 2019 [2]. The combined CLARA/VELA facility currently incorporates two Wall Current Monitors (WCMs), four Faraday Cups (FCs) and one Integrated Current Transformer (ICT) for bunch charge diagnostics, and plans for the full CLARA facility include several additional FCs and ICTs. The existing charge di-

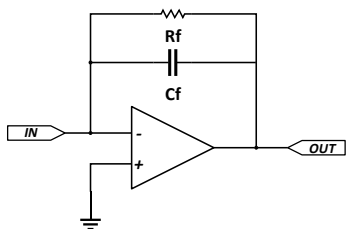
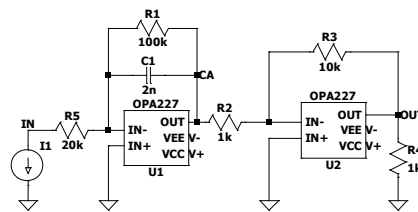


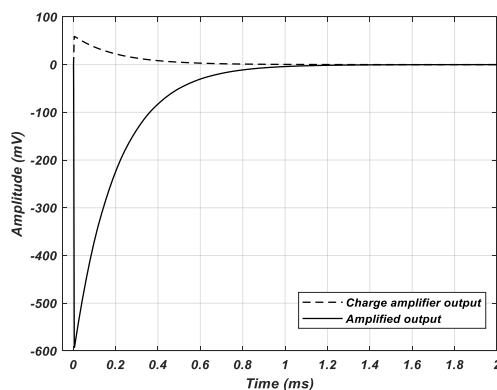
Figure 1: Practical charge amplifier circuit.

agnostics system installed on the CLARA/VELA FCs and WCMs is based on an *LC* integrator circuit with a resonance frequency of 30 MHz [3]. The implementation of this system used on VELA, and the CLARA front-end, lacks important features; such as online and automatic calibration, and remotely controlled sensitivity. This paper presents progress on an upgraded system for signal conditioning and charge detection for these systems, to improve the reliability and accuracy of bunch charge measurements available for commissioning and experimental exploitation of the CLARA beam.

* storm.mathisen@stfc.ac.uk



(a) LTspice model of a charge amplification circuit



(b) Pulse response of the above circuit

Figure 2: Simulation model of a charge amplification block, and the circuit response for a 120 pC pulse.

The upgraded charge detection system is based on a charge amplifier, effectively a current integrator, in which the voltage amplitude of the output is proportional to the injected charge. Additional features planned for the upgraded system include a current detection mode, dark current gating to avoid saturating the charge amplifier and differential signalling from the accelerator tunnel to protect against picked-up noise.

CHARGE AMPLIFIER

A basic, practical charge amplifier briefly consists of an operational amplifier, with an *RC* feedback network, as shown in Fig. 1. The sensitivity, v_o/Q_i , is inversely proportional to the feedback capacitance, C_f . The feedback resistance, R_f , prevents drift due to noise. The combination of capacitance and resistance values determines the fall time of the output signal.

PARTICLE INTERACTIONS WITH DIAMOND DETECTORS

C. Weiss ^{†1}, E. Griesmayer¹, P. Kavragin¹, M. Červ¹, CIVIDEC, Wien, Austria
¹also at TU Wien, Wien, Austria

Abstract

Chemical vapor deposition (CVD) diamond as radiation detector material has a wide range of applications, in particular for harsh radiation environments and at high temperatures. The sensitivity of diamond is exploited in measurements with charged particles, neutrons and photons.

Diamond detectors are used as beam loss monitors in particle accelerators, for photon detection in Synchrotron Light Sources, for neutron diagnostics in thermal neutron fields and for Deuterium-Deuterium (D-D) fusion and Deuterium-Tritium (D-T) fusion plasma neutrons.

In this paper we present the simulated and measured response functions of single-crystal (sCVD) diamond detectors to charged particles, heavy ions, thermal neutrons, fast neutrons, X-rays and gamma radiation. All measurements were performed with CIVIDEC diamond detectors and related electronics [1] at various research facilities.

CHARGED PARTICLES

Stopping Power

The interaction of charged particles with diamond sensors is based on the Bethe-Bloch formalism and was simulated with GEANT4 [2]. The minimum ionizing particle (MIP) energy for protons is 3 GeV, with a stopping power of 600 eV/μm in diamond. The MIP energy of electrons is 1.5 MeV with 570 eV/μm. The simulated stopping power in diamond is shown in Fig. 1, with examples for electron and proton facilities.

Electron facilities: DLS = Diamond Light Source (3 GeV), SP8 = Spring 8 (8 GeV), SLC = SLAC Linear Collider (47 GeV), LEP = Large Electron Positron Collider (105 GeV).

Proton facilities: MED = Medical Proton Therapy Facilities (250 MeV), SPS = CERN Super Proton Synchrotron (450 GeV), TVT = Tevatron (1 TeV), LHC = Large Hadron Collider (7 TeV).

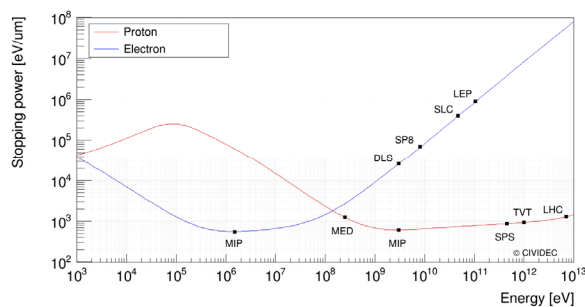


Figure 1: Bethe-Bloch function for electrons (blue) and protons (red) indicating the MIP energy and references of accelerator facilities.

[†] christina.weiss@cividec.at

Landau Distribution

The deposited energy spectrum by charged particles in diamond has a characteristic shape of a Landau distribution. The simulated most probable value (MPV) for MIP particles is 2.8 fC in 500 μm diamond, which corresponds to 17·500 electron-hole pairs, and to 35 eh-pairs/μm with the ionization energy of 13 eV/eh-pair in diamond.

The response of a diamond detector to a ⁹⁰Sr source, 0.5 MeV electrons (Fig. 2), is similar to the spectrum of MIP particles, with an MPV of 3.8 fC.

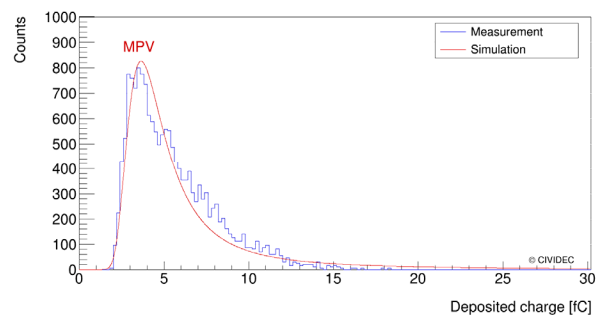


Figure 2: Deposited charge spectrum of ⁹⁰Sr β-particles in 500 μm diamond. The measured (blue) and the simulated Landau distribution (red).

Heavy-Ion Spectroscopy

The deposited energy spectrum from a ²³⁸Pu α-source (Fig. 3), emitting 5499 keV (71%) and 5456 keV (29%) α-particles, was measured in vacuum [3]. The simulated spectrum with GEANT4 includes ionization fluctuations of 5.6 keV FWHM, the electronic noise of 14.1 keV FWHM and energy straggling of 9.4 keV FWHM in the electrodes of the diamond sensor.

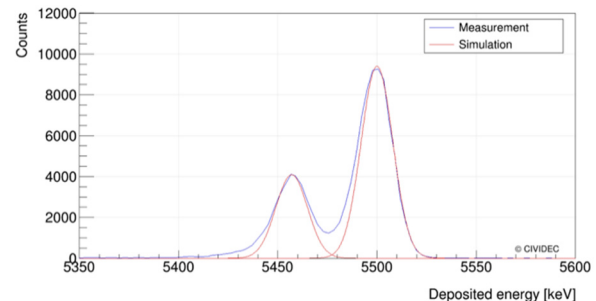


Figure 3: Deposited energy spectrum of ²³⁸Pu α-source in diamond. The main measured peak with 21 keV FWHM compares well to the expected theoretical value of 19 keV.

NEW BEAM LOSS MONITOR SYSTEM AT SOLEIL

N. Hubert, M. El Ajjouri, D. Pédeau, Synchrotron SOLEIL, 91192 Saint-Aubin, France

Abstract

SOLEIL is currently upgrading its Beam Loss Monitor (BLM) system from pin-diode detectors to plastic scintillators associated with photosensor modules. This new kind of monitor, associated to its dedicated electronics, can be used to record slow or fast losses. Monitors have been calibrated with a diode and with a cesium source. Both methods are compared. After preliminary tests, a first set of 20 new BLMs have been installed on 2 cells of the storage ring. Installation setup, calibration procedure and first measurements are presented.

INTRODUCTION

In the storage ring, the electron beam is subject to Touschek effects and to interactions with the residual gas, causing particle losses and impacting the lifetime. These losses may be regular or irregular, fast or slow, localized or distributed.

During SOLEIL installation in 2006, 36 coincidence pin-diode loss monitors [1] have been installed around the storage ring. This system has been in operation during 12 years but with some limitations: only slow losses are detected and the high directivity of the sensor makes the comparison between two detectors quite difficult. The count rate is indeed very sensitive to the orientation of the detector with respect to the loss source.

Recently, a new BLM system based on plastic scintillators has been tested and validated [2]. Two cells of the storage ring have been equipped with twelve (in cell 01) and eight (in cell 04) new monitors.

SYSTEM DESCRIPTION

The new BLM system had to fit the following requirements:

- Good (<10% error) relative calibration between the detectors to allow a comparison of the losses amplitudes around the machine.
- Possibility to provide slow and fast losses measurement with the same detector.

Based on the work conducted by ESRF [3] and preliminary tests at SOLEIL [2], we have installed BLM modules made of a scintillator and a photomultiplier. The plastic scintillator is a 10 mm high rod (EJ-200 [4]) wrapped into a high reflectivity aluminium foil to improve the photon flux towards the photomultiplier. The photomultiplier is a photosensor module from Hamamatsu (series H10721-110 [5]) that embed in a small case both photomultiplier and high voltage source.

Those two elements are integrated in a compact aluminium housing (Fig. 1).

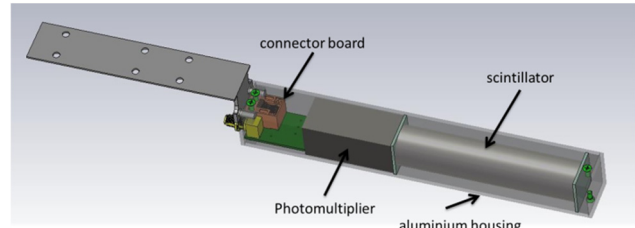


Figure 1: New BLM components integrated in aluminium housing.

The acquisition is performed by the Libera BLM electronic module which provides four 14 bits-125 MS/s ADCs together with a power supply and again control for the photosensor modules [6].

CALIBRATION

Having a relative calibration between the modules in order to be able to compare the losses amplitude measured by different detectors was one of the motivations for the upgrade of the system. We ideally targeted a relative calibration between all detectors better than 10%.

From manufacturing, the dispersion in the relative sensitivity between photosensors is very large with up to 50 % variations (Fig. 2).

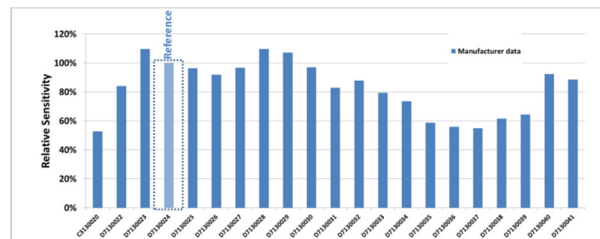


Figure 2: Photosensor relative sensitivities.

In order to verify those values, two different calibration methods have been applied, using either a LED or a cesium source.

LED (diode) Calibration Method

A dedicated housing has been manufactured to install a diode emitting at 455 nm, i.e. close to the maximum of the photosensor spectral response (250 nm to 650 nm). The output flux of the diode can be adjusted with a dedicated power-supply, whereas the photosensor is connected to the Libera BLM for acquisition and gain control (Fig. 3).

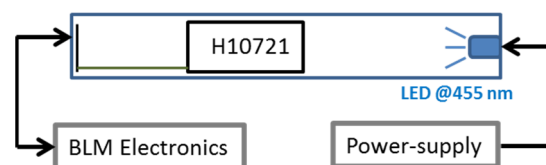


Figure 3: Setup for the calibration with a LED (diode).

Content from this work may be used under the terms of the CC BY 3.0 licence (© 2019). Any distribution of this work must maintain attribution to the author(s), title of the work, publisher, and DOI

DEVELOPMENT AND EVALUATION OF AN ALTERNATIVE SENSOR LIFETIME ENHANCEMENT TECHNIQUE USED WITH THE ONLINE-RADIATION-MONITORING SYSTEM (DosiMon) AT THE EUROPEAN XFEL AT DESY, HAMBURG

Frank Schmidt-Foehre, Shaghayegh Arab, Dirk Noelle, Rainer Susen (DESY, Hamburg)

Abstract

The European XFEL (E-XFEL), that started operation in September 2017 at the DESY/XFEL site in Hamburg/Germany uses a single-tunnel concept, forcing all frontend machine devices and electronics to be located inside the accelerator tunnel. Electro-magnetic showers, mainly produced by gun dark-current, RF cavity field-emission and beam-losses expose these devices to damaging irradiation. The new Online-Radiation-Monitoring-System (DosiMon) is mainly used for surveillance of radiation sensitive permanent magnet structures, diagnostic devices and rack-housed electronics. The integrated dose from Gamma- and optional future Neutron-radiation measurements can be monitored online by the DosiMon system. Safety limits ensure the correct function of monitored devices, provided by lifecycle estimations as measures for on time part exchange, to prevent significant radiation damage. A first expansion state currently enables more than 500 gamma measuring points. The development of a new sensor lifetime enhancement technique for the utilized RadFet sensors is presented together with corresponding evaluation measurements.

INTRODUCTION

The European XFEL located between the DESY campus at Hamburg and Schenefeld at Schleswig-Holstein [1,2], has been in operation since 2017, providing high duty cycle, ultra-short and extreme brilliant X-Ray beams at wavelengths about 0.5 Å. Up to 27000 pulses per second are possible due to the super conducting 17.5 GeV linac, provided by an electron beam with the corresponding time structure. The beam can be distributed into 3 undulator sections of about 200 m length, which consist of 21 to 35 undulators each. The installation of all parts including the electronics was chosen to be inside of a single tunnel system due to the overall length of the facility of about 3.4 km located in the city area of Hamburg. The environmental conditions of the single tunnel installation made it necessary, to control beam losses and radiation damage. Hence a new Embedded Radiation-Monitor-System (DosiMon) had been developed for measurement of γ -radiation at various appropriate electronics-internal and rack-external measurement points and dose levels.

The DosiMon-System uses several different sensors to ensure safe and reliable γ -radiation measurement at hundreds of measurement points, distributed along the E-XFEL. While RadFet-type solid-state radiation sensors are used for online measurement of γ -radiation [3], well-known TLD (Thermo Luminescent Detector) sensors are used to provide sporadic reference measurements of ac-

cumulated γ -dose for comparison, cross-reference and -calibration checks.

Motivation

The fingertip-sized, online-readable RadFet-type RFT-300-CC10G1 sensors from REM Oxford Ltd. [4] have been successfully used in the original version (here called pre-series version) of the DosiMon system since the first orientational measurements and have consequently been selected as appropriate γ -radiation sensors for series production [5]. The sensor principle and key parameters are described in [4,6]. After some minor manufacturing and application issues were found during the implementation phase of pre-series devices, the RadFets were redesigned in close collaboration between DESY and the supplier company REM, to form the newest RadFet series version currently in widespread use at the E-XFEL. The demanding number of E-XFEL testpoints in combination with upcoming new accelerator projects with high demands on testpoint numbers shift a re-use of RadFets into focus. In 2016, the manufacturing company went out of business, so that further delivery of these RadFets tends to become more difficult in the future. Based on estimations and simulations for upcoming electromagnetic shower production at different testpoints along the E-XFEL, several generations of RadFet sensors have initially been purchased according to lifetime estimations.

On the other hand, the RadFet-supplier REM Oxford Ltd. recommended not to refurbish used (i. e. pre-irradiated) RadFets due to functional chip degradation, induced by the necessary heat-up process for the reduction of stored charge [7]. Early tests at the manufacturer with re-configuration temperatures around 250 °C had functionally destroyed the RadFet device.

Refurbishment



Figure 1: Climate cabinet with dose measurement setup.

FIRST TESTS USING SIPM BASED BEAM LOSS MONITORS AT THE EUROPEAN XFEL

T. Wamsat*, P. Smirnov

Deutsches Elektronen-Synchrotron DESY, Hamburg, Germany

Abstract

The European XFEL uTCA based Beam Loss Monitor System (BLM) is composed of about 470 monitors using photomultiplier tubes (PMTs). BLMs installed in the SASE undulator intersections show high signals at electron energy higher 16 GeV or photon energy higher 14 keV due to background synchrotron radiation which directly affects the PMT. The amplitude of this signal can get that high that, also without using any detector material, the BLMs get blind for real losses. Also different lead arrangements did not shield the signal sufficiently.

First tests show that a Silicon photomultiplier (SiPM) is not affected. Also there are several advantages to use SiPM, they are cheaper by factor of 40 and operating voltage is below 35V. First test results will be presented and how it can get implemented in the existing BLMs and BLM system.

DETECTORS

The Beam Loss Monitor (BLM) system at the European XFEL is the main system to detect losses of the electron beam, thus to protect the machine hardware from radiation damage in particular the permanent magnets of the undulators. As part of the Machine Protection System (MPS) [1] the BLM system delivers a signal which stops the electron beam as fast as possible in case the losses get too high.

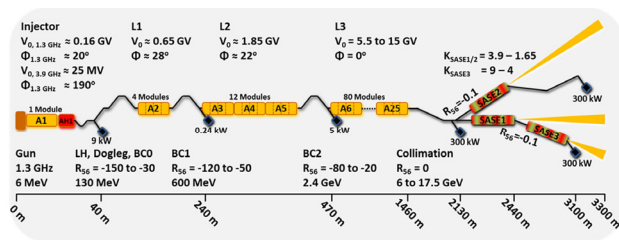


Figure 1: Schematic overview of the European XFEL accelerator [2].

About 470 BLMs are installed along the XFEL Linac which schematically is shown in Fig. 1. The BLMs are positioned at locations near the beamline, where losses can be expected or where sensitive components are installed, thus most of the BLMs are installed in the

undulator area. The BLM includes either an EJ-200 plastic scintillator or a SQ1 quartz glass rod. The latter are used mainly in the undulator intersection. Scintillators are also sensitive to hard x-rays which are produced within the undulators, whereas quartz rods work with Cherenkov effect, that is sensitive to particle losses only.

Metal Channel type photomultipliers (PMTs) are used for readout. This type of PMTs has excellent immunity to magnetic fields up to 10 mT, what is very important for accelerator measurements.

TASKS

SASE test at 16.5 GeV has shown the following problem:

- at very closed undulator gap (9 keV photon energy) the rear BLMs of SASE1 have shown high signals and turned off the beam. In the setting the magnetic field was very strong and the critical energy was very high.
- at 15 keV and further opening of undulator the problem disappeared

We are dealing here with very hard spontaneous radiation which affects the PMT. Photoeffect produces secondary electrons directly in the PMT, what in turn generates false BLM signals. This fact was proven in BLM without optical radiator (Cherenkov or scintillator).

Any attempts to shield PMT area with lead plates gave no significant effect.

Another way to solve the problem is to use another light detector type like SiPMs.

Figure 2 shows the mounting of BLMs in the undulator intersection where the problems appears.



Figure 2: BLMs in undulator intersection.

* thomas.wamsat@desy.de

NEUTRON SENSITIVE BEAM LOSS MONITORING SYSTEM FOR THE ESS LINAC

I. Dolenc Kittelmann*, F. S. Alves, E. Bergman, C. Derrez, V. Grishin,
K. Rosengren, T. J. Shea, ESS ERIC, Lund, Sweden
Q. Bertrand, T. Joannem, P. Legou, Y. Mariette, V. Nadot, T. Papaevangelou,
L. Segui, IRFU, CEA, Gif-sur-Yvette, France
W. Cichalewski, G. W. Jabłoński, W. Jałmużna, R. Kiełbik, TUL, DMCS, Łódź, Poland

Abstract

The European Spallation Source (ESS), currently under construction in Lund, Sweden, will be a neutron source based on partly superconducting linac, accelerating protons to 2 GeV with a peak current of 62.5 mA, ultimately delivering a 5 MW beam to a rotating tungsten target. For a successful tuning and operation of a linac, a Beam Loss Monitoring (BLM) system is required. The system is designed to protect the machine from beam-induced damage and unnecessary activation of the components. This contribution focuses on one of the BLM systems to be deployed at the ESS linac, namely the neutron sensitive BLM (nBLM). Recently, test of the nBLM data acquisition chain including the detector has been performed at LINAC4, at CERN. The test represents first evaluation of the system prototype in realistic environment. Results of the test will be presented together with an overview of the ESS nBLM system.

INTRODUCTION

The European Spallation Source (ESS) is a material science facility, which is currently being built in Lund, Sweden and will provide neutron beams for neutron-based research [1]. The neutron production will be based on bombardment of a tungsten target with a proton beam of 5 MW average power. A linear accelerator (linac) will accelerate protons up to 2 GeV and transport them towards the target through a sequence of a normal conducting (NC) and superconducting (SC) accelerating structures (Fig. 1).

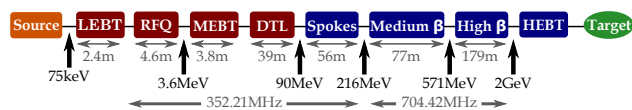


Figure 1: The ESS linac layout [1]. Red colour represents the NC and blue the SC parts of the linac.

As in case of all future high-power accelerators, ESS linac operation will be limited by beam losses if machine activation is to be kept low enough for hands-on maintenance. Moreover, loss of even a small fraction of intense ESS beam can result in a significant increase of irradiation levels, ultimately leading to damage of the linac components. Beam Loss Monitoring (BLM) systems are designed to provide information about beam loss levels. Thus, they play an important role in machine fine tuning as well as machine

protection from beam-induced damage by detecting unacceptably high beam losses and promptly inhibiting beam production.

Two types of BLM systems differing in detector technology have been conceived at ESS. The neutron sensitive BLM (nBLM) system is based on 82 neutron detectors primarily covering the lower energy part of the ESS linac. Conversely, the Ionisation Chamber based BLM (ICBLM) system consists of 266 ionisation chambers located almost exclusively throughout the SC parts of the linac [2].

This contribution aims to report an overview of the nBLM system design. In addition to this, results of the test performed with the first prototype in realistic environment are presented.

DETECTOR DESIGN

The nBLM system is based on neutron-sensitive Micromegas devices [3], specially designed to primarily cover the lower energy part of the ESS linac. Monte Carlo simulation studies were used to optimise the detector design and locations in order to assure coverage and redundancy for the machine protection purposes and provide spatial resolution for the diagnostic purposes [4, 5].

One of the challenges when measuring beam losses in a linac is related to the RF-induced background. This background is mainly due to the electron field emission from RF cavity walls resulting in bremsstrahlung photons created on the cavity or beam pipe materials [6]. For this reason, the nBLM detectors are designed to be sensitive to fast neutrons and exhibit low sensitivity to low-energy photons. Additionally, the signals due to thermal neutrons are suppressed as they may not be directly correlated to the beam losses. This is achieved by equipping the detector with suitable absorber and neutron converter materials.

Two types of nBLM detectors with complementary functionality have been developed. Fast detectors (nBLM-F) aim to detect fast losses when high particle fluxes due to accidental beam losses are expected. On the other hand, slow detectors (nBLM-S) primarily aim to monitor slow losses when low particle fluxes are expected. Details of the final detector module design and performance are available at this conference in a separate contribution [7].

Time characteristics of nBLM-F and nBLM-S signal pulses are the same, however neutron moderation in case of nBLM-S delays a big part of events by amount of time ranging from tens of ns to $\sim 200 \mu\text{s}$. A typical signal pro-

* irena.dolenckittelmann@esss.se

IONISATION CHAMBER BASED BEAM LOSS MONITORING SYSTEM FOR THE ESS LINAC

I. Dolenc Kittelmann*, F. S. Alves, E. Bergman, C. Derrez, V. Grishin, T. Grandsaert, T. J. Shea, ESS ERIC, Lund, Sweden
 W. Cichalewski, G. W. Jabłoński, W. Jaźmużna, R. Kiełbik, TUL, DMCS, Łódź, Poland

Abstract

The European Spallation Source, currently under construction in Lund, Sweden, will be a neutron source based on partly superconducting linac, accelerating protons to 2 GeV with a peak current of 62.5 mA, ultimately delivering a 5 MW beam to a rotating tungsten target. One of the most critical elements for the protection of an accelerator is its Beam Loss Monitoring (BLM) system. The system is designed to protect the machine from beam-induced damage and unnecessary activation of the components. This contribution focuses on one of the BLM systems to be deployed at the ESS linac, namely the Ionisation Chamber based BLM (ICBLM). Several test campaigns have been performed at various facilities. Results of these tests will be presented here together with an overview of the ESS ICBLM system.

INTRODUCTION

The European Spallation Source (ESS) is a material science facility, which is currently being built in Lund, Sweden and will provide neutron beams for neutron-based research [1]. The neutron production will be based on bombardment of a tungsten target with a proton beam of 5 MW average power. A linear accelerator (linac) will accelerate protons up to 2 GeV and transport them towards the target through a sequence of a normal conducting (NC) and superconducting (SC) accelerating structures (Fig. 1).

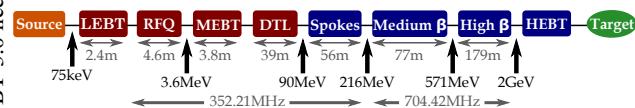


Figure 1: The ESS linac layout [1]. Red colour represents the NC and blue the SC parts of the linac.

A certain set of beam instrumentation is required for successful commissioning, tuning and operation of a linac. As part of this set, the Beam Loss Monitoring (BLM) system is designed to detect beam instabilities potentially harmful to the linac components and inhibit beam production before damage occurs. Additionally, the system provides information about the secondary particle rates close to the beam line during all machine modes of operation in order to enable tuning and keep the machine activation low enough for hands-on maintenance.

Two types of BLM systems differing in detector technology have been conceived at ESS. The Ionisation Chamber-based BLM (ICBLM) system employs 266 ionisation chambers

located almost exclusively throughout the SC parts of the linac. Conversely, the neutron sensitive BLM (nBLM) system consists of 82 neutron detectors primarily covering the lower energy part of the ESS linac [2].

This contribution aims to report an overview of the ICBLM system design. In addition to this, results of detector tests performed at various facilities will be discussed.

DETECTOR DESIGN

The ICBLM system is based on parallel plate gas ionisation chambers. The detectors were originally designed by CERN for the LHC BLM system and fabricated by Institute for High Energy Physics (IHEP), Protvino, Russia between 2006 and 2008. The LHC type chambers were selected as the ICBLM detectors due to their fast response, stable gain and large dynamic range of 10^8 (pA–mA). In addition to this, they require little maintenance. Hence, in 2014 a new production line was set up for ESS, CERN and GSI needs [3]. However, certain modifications to the original detector design have been carried out for this production by ESS and IHEP. The modifications were required due to the issues with availability of certain components. Following the production and testing by IHEP, 285 chambers were received at ESS in July 2017.

The detectors are filled with N_2 gas at 1.1 bar, which is sealed in a 2 mm-thick stainless steel cylindrical container with inner length of 480 mm (Fig. 2). The active volume of the detector consists of 61 parallel electrodes, where the gap between the electrodes serves to reduce the charge drift path and recombination probability, which results in desired linear response of the detector. The thickness of aluminium electrode is changed to 0.54 mm compared to 0.5 mm found in the LHC type. Moreover, the gap size is alternating between 5.75 mm and 5.71 mm as opposed to constant value of 5.75 mm in case of LHC type detectors. The latter represents the most significant difference in design compared to the original LHC detectors.



Figure 2: ESS ICBLM detector with (bottom) and without (top) metal casing.

* irena.dolenc kittelmann@ess.se

DEVELOPMENT OF NEW LOSS MONITOR ELECTRONICS FOR THE HIPA FACILITY

R. Dölling[†], E. Johansen, M. Roggli, W. Koprek, D. Llorente,
Paul Scherrer Institut, 5232 Villigen PSI, Switzerland

Abstract

A replacement for the ageing electronics of loss monitors at HIPA is under development. We discuss requirements, concepts and first tests of a prototype.

INTRODUCTION

Some 320 signal currents from ionization chambers, collimators, aperture foils, halo monitors and beam stoppers in the HIPA facility [1] are read out by several types of in-house developed CAMAC modules, which also generate interlocks to protect the machine from irregular beam. Most types are based on logarithmic amplifiers to cover the large dynamic range of signals. After 20 to 35 years of operation, the electronics approaches the end of its life cycle. With a limited number of spares, discontinued components, outdated standards, incomplete documentation and the system specialists all retired, maintenance gets increasingly difficult. At the same time the risk of causing significant downtime increases, since nearly all supported devices are, other than, e.g., profile monitors, essential for machine protection in normal operation. The need for a replacement of the ~190 involved CAMAC modules, including high voltage (HV) supplies for the ionization chambers (IC), is evident. However, with limited resources, it is still under discussion when it should take place.

We started a pre-project to evaluate a modern version of a logarithmic amplifier in combination with a system-on-module data processing unit and state of the art network connectivity. A single type of module should provide the needed wide current range, speed, computing capability and connectivity. Making use of modern technology capabilities, we intend to implement several improvements of the electronic functionalities [2]:

1. Refined rules for interlock generation to allow safe operation with fewer restrictions to operation.
2. Capability for checking the performance of detectors, cables and electronics when beam is switched off.
3. Storage of data series for post-interlock analysis and other studies.

In the long term, the new module can also be a part of the replacement of the remaining 36 CAMAC modules for the control of wire monitors and beam-induced fluorescence monitors.

REQUIREMENTS

Amplifier

Signal currents from the diagnostic devices, mostly loss monitors, are permanently measured and evaluated. ICs as

well as collimators and secondary emission foils all deliver positive currents, which need to be measured in the range of 20 pA to 20 mA.

A bandwidth of 50 kHz allows to switch off the beam fast enough to prevent thermal damage to accelerator components in case of accidental loss of the full and even focused beam. This is needed above 10 nA where the interlock levels are usually set. This bandwidth is also sufficient to resolve an, e.g., 40 μ s long beam pulse when pulsing the 870 keV beam line with 500 Hz for test purposes. Also the effects of the 7 ms long pilot pulses preceding the switching of the full beam to the ultra-cold neutron source [3], as well as conceivable, even shorter, single ‘explorative pulses’ for the study of new beam optics [4], are resolved.

With logarithmic amplifiers, care has to be taken to prevent latch-up from short negative current spikes, which are part of AC electromagnetic interference, which may cause a delayed response to following positive currents. Here a low-pass filtering and the permanent injection of a bias current of, e.g., +100 pA are helpful. Any hardware filters must be applied before the logarithmic amplifier to conserve average values.

To prevent ground loops, the amplifier ground is separated from rack ground (Fig. 1, a high impedance Z1 is required). The individual ground for each channel is provided via the shield of the long signal cable to the detector [5-7].

Bias Voltage

A voltage source applied between amplifier ground and the shield of the long cable, allows to bring the amplifier, and with it the connected collimator or secondary emission foil, to a bias potential (Fig. 1). This can be used for several purposes [2]:

1. Isolation check of collimator and cable, measured without beam (negative voltage).
2. Suppression of secondary electrons from collimators to get a more accurate reading of the stopped beam current fraction, especially in the 870 keV beam line and the first turns of the Injector 2 cyclotron, where the secondary electron yield is >1 (positive voltage).
3. As a side effect, in the 870 keV line, this may lower the degree of local space-charge compensation. The impact on beam emittance has to be evaluated.
4. Suppression of thermionic electrons from wire monitors and radial wire probes (positive voltage) [8].
5. To prevent crosstalk of secondary electrons in multi-electrode secondary emission monitors [9] (negative voltage).

A very low ripple of the voltage source is required to prevent artefacts in the current measurement [6]. A voltage

[†] rudolf.doelling@psi.ch

ENHANCEMENTS TO THE SNS* DIFFERENTIAL CURRENT MONITOR TO MINIMIZE ERRANT BEAM

W. Blokland[†], C.C. Peters, T.B. Southern, Oak Ridge National Laboratory, Oak Ridge, USA

Abstract

The existing Differential Beam Current Monitor (DBCM) has been modified to not only compare beam current waveforms between upstream and downstream locations, but also to compare the previous beam current waveform with the incoming beam current waveform. When there is an unintended change in the beam current, the DBCM now aborts the beam to prevent beam loss on the next pulse. This addition has proved to be crucial to allow beam during specific front-end problems. All data is saved when an abort is issued for post-mortem analysis. This paper describes the additions to the implementation, our operational experience, and future plans for the differential beam current monitor.

INTRODUCTION

The Differential Beam Current Monitor (DBCM) was implemented to abort beam in the Super-Conducting Linac (SCL) faster than the existing Beam Loss Monitors (BLM) [1,2]. The faster abort reduces the cavity degradation due to beam losses [3]. By comparing the incoming beam current (upstream) with the beam current leaving the SCL (downstream), beam loss anywhere in the SCL is detected. A dedicated optical fiber link sends an alarm directly to the Low Energy Beam Transport (LEBT) Chopper, see [4], to quickly abort the beam. The system can abort the beam in about 7 μ s total, including signal and beam travel times and computation time.

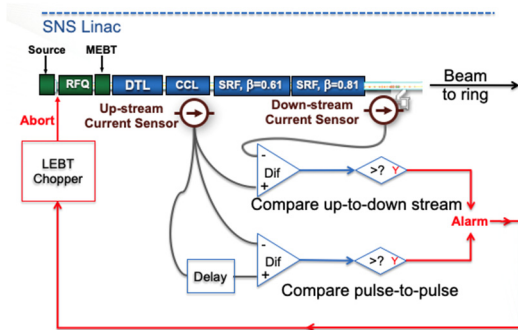


Figure 1: Differential Beam Current Monitor.

The layout of the DBCM is shown in Fig. 1. The upstream and the downstream beam current signals are compared, and an alarm is given if the difference exceeds a threshold. Note that with the single DBCM covering the whole SCL, there is no need to upgrade the abort response times for the many SCL BLMs.

Figure 1 also shows the new pulse-to-pulse comparison feature. The previously digitized current waveform is stored and compared sample-by-sample to the new pulse's current waveform.

The downstream sensor is a current toroid while the upstream sensor is a beam position pickup. The sum of the pickup plates signals is routed to a log amplifier to detect the Radio-Frequency (RF) signals envelope which is representative of the beam current. The DBCM converts the log signal to a linear signal to directly compare to the toroid's signal. Using the beam position pickup was necessary because suspected RF electrons burned a hole in the ceramic break of the upstream current toroid assembly and the assembly had to be removed, see Fig. 2.

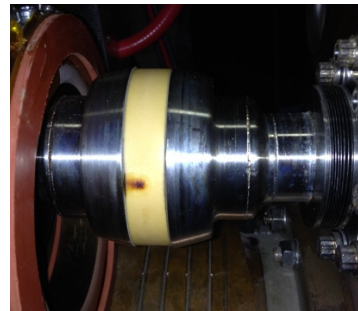


Figure 2: Damaged ceramic break.

ERRANT BEAM AND PULSE-TO-PULSE COMPARISON

There are two main sources of errant beam in the SNS linac: warm linac RF and the Ion Source.

The goal of the first iteration of the DBCM was to minimize the impact of beam loss from warm linac RF faults. Data analysis showed that the Drift Tube Linac (DTL) and Coupled Cavity Linac (CCL) cavities were the major cause for errant beam. As stated previously, the first iteration of the DBCM cut the beam turn off time in half. However, the need to lower SCL cavity gradients to maintain high reliability has continued.

The goal of the second iteration of the DBCM has been to minimize impact of beam loss from Ion Source malfunctions.

* This manuscript has been authored by UT-Battelle, LLC, under Contract No. DE-AC05-00OR22725 with the U.S. Department of Energy. The United States Government retains, and the publisher, by accepting the article for publication, acknowledges that the United States Government retains a non-exclusive, paid-up, irrevocable, world-wide license to publish or reproduce the published form of this manuscript, or allow others to do so, for United States Government purposes. The Department of Energy will provide public access to these results of federally sponsored research in accordance with the DOE Public Access Plan (<http://energy.gov/downloads/doe-public-access-plan>).

[†] blokland@ornl.gov

Content from this work may be used under the terms of the CC BY 3.0 licence (© 2019). Any distribution of this work must maintain attribution to the author(s), title of the work, publisher, and DOI

A LONGITUDINAL KICKER CAVITY FOR THE BESSY II BOOSTER

T. Atkinson*, M. Dirsat, A. Matveenko, A. Schällicke,
B. Schriefer, Y. Tamashevich, Helmholtz-Zentrum Berlin, Berlin, Germany
T. Flisgen, Ferdinand-Braun-Institut, Berlin, Germany

Abstract

As part of the global refurbishment of the injector at BESSY II, a new longitudinal kicker cavity and suitable feedback will be installed in the booster. Both a flexible bunch charge and spacing is essential for efficient injection. Such a cavity is needed to mitigate the unwanted coupled bunch instabilities associated with these elaborate filling patterns and the HOMs of additional accelerating structures. This paper covers the conceptual design, simulation strategy, manufacture and bench tests of the longitudinal kicker cavity before it is installed in the ring.

MOTIVATION

In a familiar fashion that characterized 3rd generation light sources across the world, injection into the BESSY II storage ring is from a low energy linac followed by a full energy booster synchrotron.

The present injection scheme is highly reliable [1], but a global upgrade is necessary for the BESSY VSR project [2]. The most prominent aspect with respect to the injector is the evidence that the bunch length on injection into the storage ring needs to be reduced from its present value, by at least a factor of two in order to keep the high injection efficiencies.

The preferred method to produce shorter bunches from the booster is an upgrade of the existing 500 MHz RF system. Two additional 5-cell PETRA cavities each driven by 80 kW transmitters have been purchased. In terms of beam commissioning, slowly increasing the total RF gradient each year by installing the additional cavities one after another, is a subtle way to actively control and diagnose the beam in all dimensions.

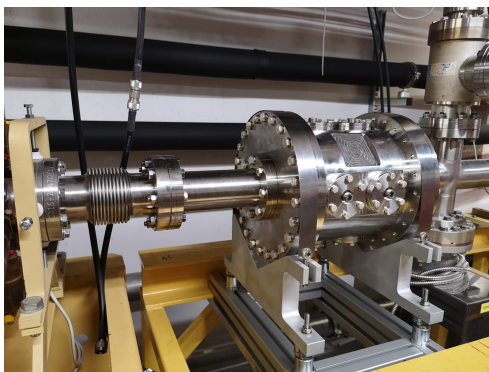


Figure 1: Longitudinal kicker cavity installed in the booster.

The 5-cell PETRA cavities were developed without supplementary features to reduce unwanted HOMs. Installing

* terry.atkinson@helmholtz-berlin.de

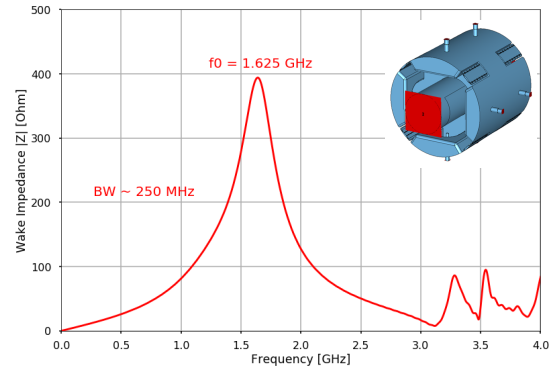


Figure 2: Longitudinal wake spectrum of the kicker cavity. Insert shows the vacuum model used for optimization.

such cavities will lead to higher ring impedance and enhance the longitudinal instabilities resulting in a larger effective emittance of the multi-bunch injection that we already witness in the booster [3]. A longitudinal kicker cavity, Fig. 1 was installed to mitigate these supplementary problems.

DEVELOPMENT OF DESIGN

The use of overloaded cavities and active feedbacks to compensate longitudinal instabilities at both the BESSY II and MLS storage rings is long established. [4] details the excellent performance at both storage rings and the additional bunch-by-bunch features the beam users could take advantage of. The cavity hardware presently installed at BESSY II was first commissioned almost two decades ago. Since the first design in 1995 at *DAΦNE* [5] the overloaded cavity has been modified and optimized to suit most light sources across the world. The base design for the longitudinal kicker to be installed in the booster was that used at Diamond Light Source (DLS) [6]. This design is an amalgamation over the years of high end computer simulations and multi-objective optimization to produce a low-Q, broadband device with little impedance at high frequencies suitable for modern storage rings.

The noticeable design modifications from the DLS baseline are that the beam pipe in the booster is round not tapered and the field enhancing nose stubs have been removed. The simulation strategy was based on optimizing each of the three main components consecutively. First the resonator is tuned to a fundamental frequency f_0 of 1.625 GHz, Fig. 2 (the upper band of the third RF harmonic). Next the feedthroughs and loaded waveguides were added to the model to optimize their positions with respect to each other and the resonator

FIRST BEAM-BASED TEST OF FAST CLOSED ORBIT FEEDBACK SYSTEM AT GSI SIS18

R. Singh^{*1}, S. H. Mirza^{1,2}, K. Lang¹, A. Bardorfer³, P. Forck¹,
 A. Doering¹, D. Rodomonti¹, D. Schupp¹, H. Welker¹, and M. Schwickert¹
¹GSI Helmholtzzentrum für Schwerionenforschung GmbH, Darmstadt, Germany
²Technische Universität Darmstadt, Darmstadt, Germany
³Instrumentation Technologies, Solkan, Slovenia

Abstract

The SIS18 synchrotron of GSI will serve as a booster ring for the SIS100 synchrotron in the FAIR project. In order to counter orbit distortion due to cycle-to-cycle hysteresis of the main magnets and stabilize the beam orbit during the full acceleration cycle, a global closed orbit feedback (COFB) system is being implemented in context of both synchrotrons. The primary design goal of the system is robustness against variations of the beam and machine settings. These variations are unavoidable due to large expected dynamic range in beam intensity and flexible machine settings at the FAIR facility. The detailed architecture of the system is discussed in this contribution. First beam-based tests for orbit correction were performed with a large spatial model mismatch, when the orbit response matrix corresponding to injection energy was used for the entire acceleration ramp only taking the beam rigidity into account. The result of these preliminary tests is also presented.

INTRODUCTION

The maximum beam intensities in FAIR (baseline) design goal are an order of magnitude higher in comparison to operational GSI facility [1,2]. This introduces stricter conditions for both machine protection and beam quality conservation in FAIR synchrotrons SIS18 and SIS100. These requirements translate directly into a better control of the closed orbit through SIS18 into SIS100. Further, the creation of fast dynamic orbit bumps and the possibility of orbit correction during the acceleration ramp impose a requirement of at least 100 Hz bandwidth taking model mismatch into account [3,4]. Although the COFB system is mainly conceptualized for SIS100, the prototyping is being performed at the operational SIS18 as further discussed in this paper.

SIS18 is a versatile synchrotron capable of accelerating particles ranging from protons to Uranium ions with a variety of charge states, with the maximum energy corresponding to the magnetic rigidity of 18 T-m. There is a (unique) optics transition from triplet to doublet quadrupole configuration during the acceleration ramp in order to incorporate a larger beam size due to multi-turn injection. This results in an on-ramp lattice model variation. A large dynamic range in beam intensity requested by experiments introduce more challenges, such as a) intensity dependent tune shifts, b) gain and offset calibration errors in the BPM system due to

amplifier gain ranges and c) coupling of dipole magnet fields into matching transformers of the BPM system especially for lower beam intensities. These conditions lead to different design goals of our COFB system in comparison to those implemented in the light sources and colliders where the beam settings and machine model are typically fixed as well as the reference orbit is expected to be static during the beam storage.

Consequently, we aim for a COFB system which is robust against the changes in orbit response matrix (ORM), reference orbit changes, cycle to cycle changes in beam intensity as well as BPM and steerer magnet hardware and communication failures. There are 12 shoe-box type pick-ups and 12 steerer (corrector) magnets per plane, symmetrically distributed in the 12 sections of the SIS18 lattice [5]. The feedback system is tuned to operate with these existing BPMs and steerer magnets. In the scope of this paper, we report on the hardware layout, infrastructure dependencies, design overview, and the first beam based test of the SIS18 COFB hardware.

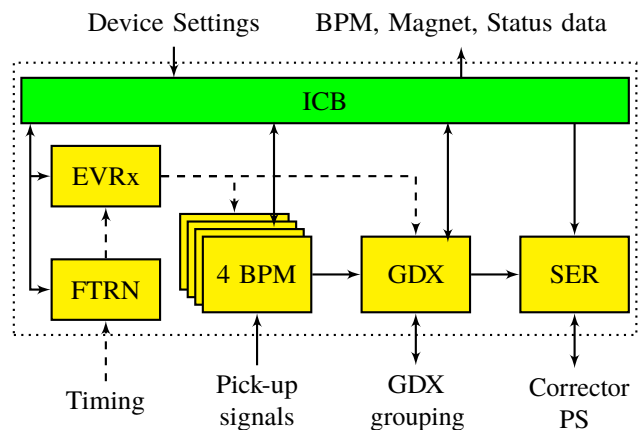


Figure 1: Libera Hadron hardware layout.

COFB HARDWARE LAYOUT

Libera Hadron platform B is the Slovenian in-kind contribution for beam position calculation and closed orbit feedback system targeted at SIS-100 and is utilized for these tests in SIS-18. It contains dedicated Beam Position Monitor (HBPM) modules for the data processing from upto four pick-ups, Gigabit data exchange (GDX) module for beam position data exchange with other GDX modules and feedback algorithm implementation and Serial communication

* r.singh@gsi.de

LONGITUDINAL BUNCH-BY-BUNCH FEEDBACK SYSTEMS FOR SuperKEKB LER

Makoto Tobiyama^{1,*}, John W. Flanagan¹, Tetsuya Kobayashi¹, Shinji Terui, KEK Accelerator Laboratory, 1-1 Oho, Tsukuba, 305-0810, Japan.

John D. Fox, Stanford University, Stanford, CA, U.S.A.

¹also Department of Accelerator Science, SOKENDAI, Japan.

Abstract

Longitudinal bunch-by-bunch feedback systems to suppress coupled bunch instabilities with minimum bunch spacing of 2 ns have been constructed in SuperKEKB LER. Through the grow-damp and excite-damp experiments with several filling patterns and the transient-domain analysis of unstable modes, the behaviors of possible impedance sources have been evaluated. The measured performance of the system, together with the performance of the related systems such as slow phase feedback to the reference RF clock are reported.

INTRODUCTION

The KEKB collider has been upgraded to the SuperKEKB collider with a final target of 40 times higher luminosity than that of KEKB. It consists of a 7 GeV high energy ring (HER, electrons) and a 4 GeV low energy ring (LER, positrons). About 2500 bunches per ring will be stored at total beam currents of 2.6 A (HER) and 3.6 A (LER) in the design goal. After the successful operation of phase-1 (without IR magnets), phase-2 (with superconducting final quadrupoles (QCSs) and Belle II detector but without inner-most sensors such as Pixel and SVDs), we have started the phase-3 operation with almost full-function of the Belle II detector from early March, 2019.

In the longitudinal plane, it is expected that the coupled-bunch instability (CBI) coming from the fundamental mode (-1, -2, and -3) will affect with medium beam current in both HER and LER. To cure the instability, the mode-by-mode feedback system in the LLRF [1] has been implemented. Growth time of other unstable modes from the imbalance in the HOM-cancelling in the cavities has been estimated slightly faster than the radiation damping time in LER with the maximum beam current of 3.6 A; 21 ms. At KEKB LER we did not need the longitudinal bunch feedback system up to the maximum beam current of 2 A. We are taking over the similar accelerating cavities (ARES) from KEKB so the threshold of the CBI is expected to be similar.

During the Phase-1 and Phase-2 operation, we have observed unexpected longitudinal coupled-bunch instabilities on LER starting much lower beam current, say, 600 mA. As the longitudinal motion strongly damage the luminosity in the collider, the suppression of the CBI is the must to get the higher luminosity.

We have prepared the longitudinal bunch-by-bunch feedback system (LFB) capable to handle the minimum

bunch spacing of 2 ns in LER. The bunch feedback system consists of position detection systems, high-speed digital signal processing systems with a base clock of 509 MHz, and wide-band longitudinal kickers fed by wide-band, high-power amplifiers. We describe here the design, commissioning and the present status of our longitudinal bunch feedback systems. Table 1 shows the main parameters of SuperKEKB HER/LER achieved up to now.

Table 1: Main Parameters of SuperKEKB HER/LER in Phase 3 Operation

	HER	LER
Energy (GeV)	7	4
Circumference (m)	3016	
Maximum beam current (mA)	1010	870
Max. bunch current (mA)	1	1.5
Bunch length (mm)	5	6
RF frequency (MHz)	508.886	
Harmonic number	5120	
Synchrotron Tune	0.028	0.024
Momentum compaction	0.00045	0.00032
L. damping time (ms)	29	23
Natural Emittance (nm)	4.6	3.2
Peak luminosity (cm ⁻² s ⁻¹)	1.23x10 ³⁴	
Bunch current monitor	1	1
Longitudinal bunch FB	0	1
No. of longitudinal kickers	0	4
No. of longitudinal amplifiers	0	8

OUTLINE OF LONGITUDINAL BUNCH FEEDBACK SYSTEM

Block diagram of the longitudinal bunch feedback system is shown in Fig. 1. All the transverse and longitudinal bunch feedback equipment including high-power amplifiers are installed in the Fuji straight section area [2].

Bunch Position Detector

The 2 GHz component of a bunch signal from button electrode is filtered using a comb-type bandpass filter,

* email address makoto.tobiyama@kek.jp

PRELIMINARY TEST OF XBPM LOCAL FEEDBACK IN TPS

P. C. Chiu, J. Y. Chuang, K. H. Hu, C. H. Huang, K. T. Hsu
 NSRRC, Hsinchu 30076, Taiwan

Abstract

TPS is 3-GeV synchrotron light source which has opened for public users since September 2016 and now offers 400 mA top-up mode operation. The requirements of the long term orbit stability and orbit reproducibility after beam trip have been gradually more and more stringent and become a challenge from users' request. Furthermore, the thermal effect would be expected to be worsen after 500 mA top-up operation which should deteriorate the orbit drift. The report investigates the long-term orbit stability observed from electron BPM and X-ray BPM and also evaluates the possibility of the local XBPM feedback to improve photon beam stability.

INTRODUCTION

FOFB and RF frequency compensation have been applied to stabilize the electron orbit [1][2] in TPS to achieve beam position stability less than 10% of the beam size. Besides, to monitor the position and stability of photon beams, two-blade type X-ray beam position monitors (XBPMs) are installed in beamline frontends and beamlines. It is observed that the thermal effect would cause the mid-term orbit disturbance at the first 30 minutes after the beginning of beam stored and long-term slowly drift for the following 4~5 hours before it achieves the equilibrium, especially in the vertical plane. Besides, there are also obvious daily position change along with temperature variations and periodic 4-minutes variation consistent with injection cycle. Furthermore, insertion device (ID) gap/phase change is also significantly affect position stability where it is partly caused by deformation and resulted in BPM mechanics displacement and partly still due to thermal effect. The position drift/fluctuation seemed to be able to be controlled below several microns or even sub-micron in electron BPM. However, the errors would be amplified several times observed at the end of beamline XBPM. To improve beamline XBPM position stability, the local XBPM feedback is proposed and tested in TPS beamlines. The XBPM feedback would include straight-line BPM and beamline XBPM to monitor photon position and adjacent 2~4 correctors for actuators to minimize photon position variation. Since the local XBPM feedback would be operated together with FOFB. The interferences between both could be sometimes occasionally resulted in conflict and diverge. Therefore, an extra process to check interference status and avoid instability would be an important concerns.

PHOTON BEAM POSITION MONITOR LAYOUT AND ELECTRONICS

There are seven beamline open to users in TPS now. For each beamline, there are different types of X-ray or photon beam position monitors are used to detect the synchrotron

radiation. The blade-type X-ray BPMs (XBPM) [3] is standard equipment installed at each front-end; quadrant PIN photodiode BPMs (QBPMs) [4] are adopted by few experimental end station. The layout of front-end instrumentation is shown as Fig. 1. XBPM1 is completed calibration and observed reliable for a while. However, the calibration of XBPM2 is not yet completed and it was observed that the horizontal and vertical readings of XBPM2 had serious coupling. Therefore, only XBPM1 is presented and included for feedback in this report. About acquisition electronics, three types of electronics had been used and evaluated. The first one uses the FMB Oxford F-460 to convert current to voltage and read the voltage with a NI-9220. The second type of electronics is a home-made device with a 0.5 Hz update rate. The third type is the commercial product and now our majority: Libera Photon which could provide different data flow for different purpose of analysis, including 10/25 Hz streaming, 5 kHz/578kHz waveform with trigger as well as post-mortem functionalities.

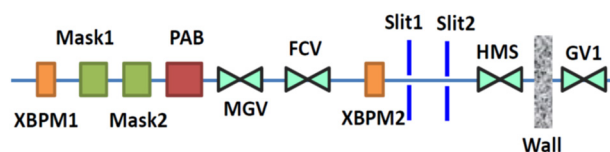


Figure 1: The layout of the front-end instrumentation.

OBSERVATION OF POSITION STABILITY FROM BPM AND XBPM

Position Drifts after Beam Restored

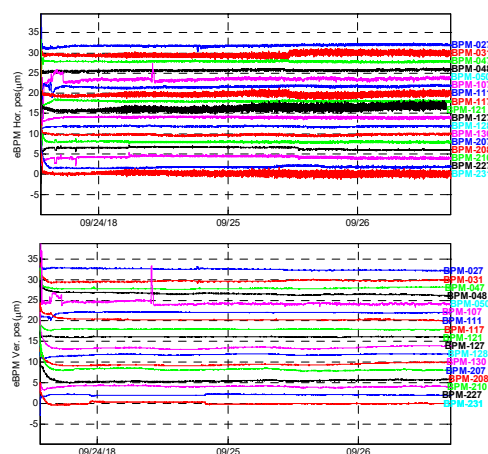


Figure 2: The upstream and downstream electron BPM reading nearby IDs for three days after beam restored.

It could be observed the upstream and downstream electron BPM nearby 7 IDs as Fig. 2 at first beginnings of beam stored, the position drift of some BPMs would be up to

OPTIMISATION OF THE ISIS PROTON SYNCHROTRON EXPERIMENTAL DAMPING SYSTEM

A. Pertica*, D. W. Posthuma de Boer, R. Williamson, ISIS, STFC,
Rutherford Appleton Laboratory, Oxfordshire, OX11 0QX, UK
J. Komppula, CERN, Geneva, Switzerland

Abstract

The ISIS Neutron and Muon Source, located in the UK, consists of a H^- linear accelerator, a rapid cycling proton synchrotron (RCS) and two extraction lines delivering protons onto two heavy metal targets. One of the limiting factors for achieving higher intensities in the accelerator is the head-tail instability present in the synchrotron around 2 ms after injection. In order to help mitigating this instability, an experimental damping system is being developed. Initial tests using a split electrode beam position monitor (BPM) as a pickup and a ferrite loaded kicker as a damper showed positive results. This paper describes the different developments made to the damping system and planned improvements to optimise its performance for use in user operations.

INTRODUCTION

The ISIS Synchrotron

The ISIS synchrotron accelerates two proton bunches, with a total of 3×10^{13} protons, from 70 MeV to 800 MeV at a repetition rate of 50 Hz, delivering a mean beam power of 0.2 MW to two tungsten targets. Protons are accelerated over 10 ms by first and second harmonic RF cavities, with a fundamental frequency sweep of 1.3 MHz to 3.1 MHz [1].

The Head-Tail Instability at ISIS

The head-tail instability is a primary concern for high intensity operation in many hadron synchrotrons including ISIS and its proposed upgrades [2]. The instability imposes an intensity limit through associated beam loss and the ensuing undesired machine activation.

Measurements on ISIS have consistently shown that the two proton bunches exhibit vertical head-tail motion at 1 – 2.5 ms through the 10 ms acceleration cycle [3,4]. The instability is suppressed by ramping the vertical tune down away from the integer ($Q_y = 4$) and making the longitudinal distribution asymmetric using the dual harmonic RF during the time of the instability. The longitudinal and vertical injection painting schemes also have a strong influence on the susceptibility to the instability. Lowering the tune further tends to induce beam loss associated with the half integer resonance [5] and other mitigation strategies have little effect on beam loss.

Figure 1 shows a typical vertical BPM sum and difference signal over several turns during the instability, with dual harmonic RF, indicating clear head-tail motion over a portion of the bunch. Measurements of the instability, made with

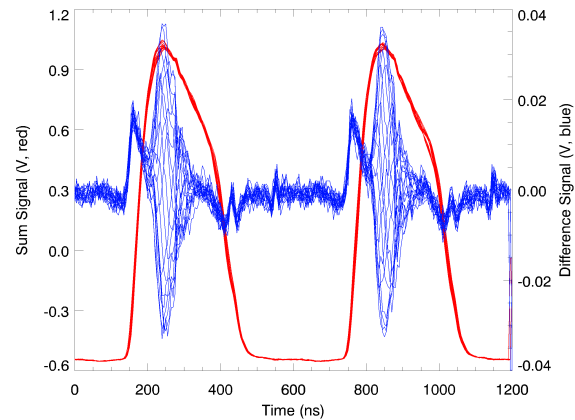


Figure 1: Sum (red) and difference (blue) vertical BPM signals over several turns around 2 ms through the acceleration cycle.

single harmonic RF and at low intensities, give a clear $m = 1$ mode structure whereas Sacherer theory [6] predicts a higher growth rate for $m = 2$. Studies are ongoing to determine the cause of the discrepancy.

The major challenge for damping the head-tail motion on the ISIS synchrotron is the fast ramping of both the accelerating frequency and the betatron tune.

THE ISIS DAMPING SYSTEM

Overview

A way of mitigating the head-tail motion is with the use of a transverse feedback system [7]. In ISIS, this has been possible by using one of the existing BPMs [8] as a pickup and the vertical betatron exciter [9] as a kicker, allowing for a reduced development time for a working prototype. The kicker is situated downstream of the selected pickup, providing a betatron phase advance of 266° for a vertical tune $Q_y = 3.80$ [10]. The processing electronics and power amplifiers are located 150 m away in an area free of ionizing radiation.

The ISIS BPMs are cylindrical split electrode type. The performance of such BPMs is characterised by the ratio of electrode voltage to incoming beam current [11]. The lower cut-off frequency of the BPM has been lowered to 11 kHz by terminating the capacitive electrodes into 100 k Ω resistors. Finite element simulations of a simplified version of this monitor were performed with both CST Particle and Microwave Studio to verify the expected performance. Low frequency results were obtained by scaling the whole geometry by a factor p and the termination impedance by a factor

* alex.pertica@stfc.ac.uk

FAST FEEDBACK USING ELECTRON BEAM STEERING TO MAINTAIN THE X-RAY BEAM POSITION AT A MONOCHROMATIC X-RAY DIAGNOSTIC AT DIAMOND LIGHT SOURCE

C. Bloomer*, G. Rehm, A. Tipper, Diamond Light Source Ltd, Didcot, UK

Abstract

A new feedback system is being developed at Diamond Light Source, applying a modulation to the position of the electron beam to keep the synchrotron X-ray beam fixed at a beamline X-ray diagnostic. Beamline detectors operating in the 100 - 1000 Hz regime are becoming common, and the X-ray beam stability demanded by beamlines is thus of comparable bandwidths. In this paper we present a feedback system operating at these bandwidths, using a diagnostic instrument permanently installed in the X-ray beam path to measure the error in beam position close to the sample point, and fast air-cored magnets to apply a small modulation to the electron beam to compensate. Four magnets are used to generate electron beam bumps through an insertion device straight. This modulation of the beam away from the nominal orbit is small, less than 10 microns, but should be sufficient to compensate for the bulk of the X-ray motion observed. It is small enough that the impact on the machine will be negligible. This system aims to maintain X-ray beam stability to within 3 % of a beam size, at bandwidths of up to 500 Hz.

INTRODUCTION

Beamlines are demanding greater positional stability of X-ray beams and at greater bandwidths than ever before. To meet this need a new system has been developed to improve the positional stability of a focussed X-ray beam. The system achieves this using a fast feedback scheme which monitors the X-ray beam position downstream of the monochromator, and makes small, fast adjustments to the X-ray beam source point. This system can reduce the X-ray beam motion at bandwidths of up to ~ 1 kHz. Presented in this paper are an outline of this system, Source Feedback From X-rays (SOFFOX), and the initial results.

The increases in stability requirements and increases in bandwidths are being driven by sub-micron sized synchrotron beams, and kHz detector rates [1–3]. It is extremely difficult for beamlines to correct beam motion at frequencies > 100 Hz with ‘conventional’ beamline feedback using optical components (monochromator crystals, mirrors, etc) to steer the X-ray beam. These components are difficult to move and manipulate at high enough frequencies to effectively counter beam motion. However, it is feasible to manipulate the electron beam at these bandwidths.

The I14 beamline at Diamond Light Source was chosen as the testbed for SOFFOX due to the extremely small X-ray beam sizes that it will employ, and due to the long length of

the beamline: 30m between the source and the monochromator, and 155m between the monochromator and the sample point [4]. There is the potential for even small position errors at the source point to result in large X-ray beam motion at the sample point.

Figure 1 presents an overview of the beamline and source point. SOFFOX uses four dedicated fast corrector magnets in the insertion device (ID) straight, capable of applying a horizontal magnetic field transverse to the electron beam path. Each is supplied with a high precision bipolar current supply. The corrector magnets are a simple air-cored Helmholtz coil design. The four magnets generate a closed bump in the electron beam orbit, inducing vertical steers of the electron beam through the source point without affecting the remainder of the orbit. The system is only designed to operate on the vertical component of the beam motion, and horizontal coupling should be minimised.

On the beamline, a single-crystal diamond X-ray beam position monitor (XBPM) [5] is used as the monitor. The XBPM signals are acquired into a custom μ TCA board at a rate of 100 kHz. An FPGA calculates the new feedback setpoint from the measured beam position, and transmits this new setpoint to the magnet power supplies. The μ TCA board and the magnet power supplies are linked by a low-latency, small form-factor pluggable (SFP) fibre optic network connection. The feedback is ultimately designed to operate only on the AC component of the X-ray beam motion, leaving the synchrotron fast orbit feedback (FOFB) and the beamline optics to correct DC errors.

This feedback system is agnostic to the source of the X-ray beam motion, reducing the impact of all disturbances, whether originating with the electron beam, or originating on the beamline. Similar feedback schemes, steering the electron beam to compensate for observed X-ray beam motion, have been implemented in the past [6]. However, to the best of the author’s knowledge, this is the first time such a scheme has been implemented using a monitor located downstream of the monochromator and operating at these bandwidths on a 3rd generation light source.

A great emphasis has traditionally been placed upon keeping the electron beam position stable during synchrotron operation. The decision to intentionally modulate the electron beam trajectory in order to improve the X-ray beam stability at the sample point is potentially quite heretical! However the authors hope to demonstrate that it is worthwhile to sacrifice the ideal of ‘a stable electron beam’, at least over some timescales, for the improved X-ray beam stability that this system provides.

* chris.bloomer@diamond.ac.uk

PRELIMINARY DESIGN OF Mu2E SPILL REGULATION SYSTEM (SRS)

M. A. Ibrahim[†], E. Cullerton, J.S. Diamond, K.S. Martin, P. S. Prieto, V.E. Scarpine, P. Varghese
 Fermi National Accelerator Lab, Batavia, IL 60510, USA

Abstract

Direct $\mu \rightarrow e$ conversion requires resonant extraction of a stream of pulsed beam, comprised of short micro-bunches (pulses) from the Delivery ring (DR) to the Mu2e target. Experimental needs and radiation protection apply strict requirements on the beam quality control and regulation of the spill. The objective of the Spill Regulation System (SRS) is to maintain the intensity uniformity of a stream of $\sim 25k$ pulses as $1e12$ protons are extracted at 590.08 kHz over a 43 ms spill period. To meet the specified performance, two regulation elements will be driven simultaneously: a family of three zero-harmonic quadrupoles (tune ramp quads) and a RF Knock-Out (RFKO) system. The SRS will use two separate control loops to control each regulation element simultaneously. It will be critical to coordinate the SRS processes within the machine cycle and within each spill interval. The SRS has been designed to have a total Gain-Bandwidth product of 10 kHz, which can be used to mitigate several sources of ripple in the spill profile.

OVERVIEW

The former Antiproton Source transport lines and storage rings have been upgraded and repurposed into the “Muon Campus” (Fig. 1) for experiments, such as g-2 and Mu2e.

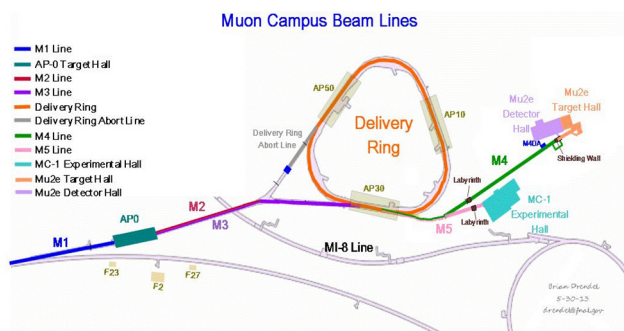


Figure 1: Muon Campus Map.

Mu2e proposes to measure the ratio of the rate of the neutrino-less, coherent conversion of muons into electrons in the field of a nucleus, relative to the rate of ordinary muon capture on the nucleus. This requires the resonant extraction of a stream of pulsed beam, comprised of short micro-bunches (pulses) from the Delivery Ring (DR) to the Mu2e target. Experimental needs and radiation protection apply strict requirements on the beam quality control and regulation of the spill [1].

* This manuscript has been authored by Fermi Research Alliance, LLC under Contract No. DE-AC02-07CH11359 with the U.S. Department of Energy, Office of Science, Office of High Energy Physics.

[†] cadornaa@fnal.gov

Accelerator Timeline for Mu2E Proton Delivery

Depicted in Fig. 2, Mu2e uses 8 kW of 8 GeV protons from the Booster. Two batches of $\sim 4e12$ protons are sent to the Recycler (RR). In the RR, the beam circulates and is then re-bunched by a 2.5 MHz RF system. The batch is divided into 8 2.5 MHz bunches. Extracted at MI-52 from RR, the reformatted bunches are transported to the DR via P1, P2, M1, and M3 beam transfer lines.

Once $1e12$ protons are injected into the DR, beam is then slow extracted to the Muon proton target at the DR revolution frequency of 590.08 kHz over a 43.1 ms spill period. Between each spill period, there is 5 ms reset period, in which there is no extraction. After the 8th spill, there is no beam in DR for 1.02 s. Dividing the total spill time by the length of the cycle, the spill duty factor is 27.1% [2].

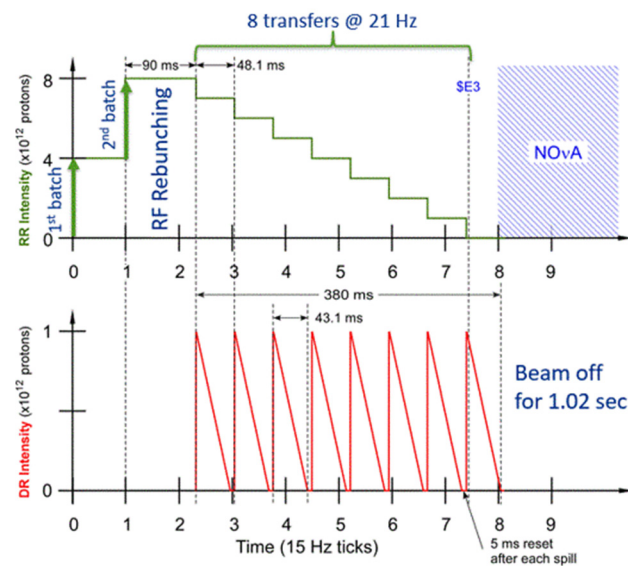


Figure 2: Mu2E Timeline.

Resonant Extraction in DR

By exciting 2 families of the harmonic sextupoles in the DR, the third integer resonant extraction condition is established [3]. Then, a family of 3 zero-harmonic quadrupoles (tune ramp quads) drives the machine tune to the exact resonance, gradually pushing the circulating beam into the resonance stop band. As unstable particles in the stop band drift towards the machine aperture, they get intercepted in the Electrostatic Septum (ESS) and are deflected towards the Mu2e target at the end of the extraction beam line.

SRS REQUIREMENTS

The SRS’s objective is to maintain the intensity uniformity of the stream of $\sim 25k$ extracted pulses from the DR

BEAM INSTRUMENTATION CHALLENGES FOR THE FERMILAB PIP-II ACCELERATOR*

V. Scarpine[†], N. Eddy, D. Frolov, M. Ibrahim, L. Prost, R. Thurman-Keup
 Fermi National Accelerator Laboratory, Batavia, IL USA

Abstract

Fermilab is undertaking the development of a new 800 MeV superconducting RF linac to replace its present normal conducting 400 MeV linac. The PIP-II linac warm front-end consists of an ion source, LEPT, RFQ and MEPT which includes an arbitrary pattern bunch chopper, to generate a 2.1 MeV, 2mA H- beam. This is followed immediately by a series of superconducting RF cryomodules to produce a 800 MeV beam. Commissioning, operate and safety present challenges to the beam instrumentation. This paper describes some of the beam instrumentation choices and challenges for PIP-II.

THE PIP-II ACCELERATOR

The PIP-II project at Fermilab is building a superconducting Linac to fuel the next generation of intensity frontier experiments [1]. Capitalizing on advances in superconducting radio-frequency (SRF) technology, five families of superconducting cavities will accelerate H⁻ ions to 800 MeV for injection into the Booster. Upgrades to the existing Booster, Main Injector, and Recycler rings will enable them to operate at a 20 Hz repetition rate and will provide a 1.2 MW proton beam for the Long Baseline Neutrino Facility. Table 1 list keep beam parameters for PIP-II.

Table 1. PIP-II Beam Parameters

Linac	PIP-II
Delivered Beam Energy (kinetic)	800 MeV
Particles per Pulse	6.7×10^{12}
Average Beam Current in the Pulse	2 mA
Pulse Length	550 μs
Pulse Repetition Rate	20 Hz
Bunch Pattern	Programmable
Booster	Value
Injection Energy (kinetic)	800 MeV
Extraction Energy (kinetic)	8 GeV
Particles per Pulse (extracted)	6.5×10^{12}
Beam Pulse Repetition Rate	20 Hz
Recycler Ring / Main Injector	Value
Injection Energy (kinetic)	8 GeV
Extracted Beam Energy	60-120 GeV
Beam Power (120 GeV)	1.2 MW
Cycle Time (120 GeV)	1.2 sec
Upgrade potential	2.4 MW

* This work was supported by the U.S. Department of Energy under contract No. DE-AC02-07CH11359.

[†] email address: scarpine@fnal.gov

Figure 1 shows the layout of the SC Linac [1], The β values represent the optimal betas where the corresponding cavity delivers the maximum accelerating voltage. A room temperature (RT) section accelerates the beam to 2.1 MeV and creates the desired bunch structure for injection into the SC Linac. In the SC section of the linac, strict particle-free and high-vacuum requirement place limitation on the design and type of beam instrumentation that can be used.

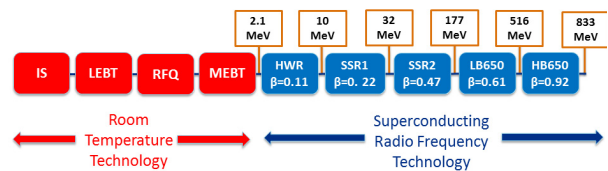


Figure 1: The PIP-II SC Linac technology map.

THE PIP-II INJECTOR TEST FACILITY

The PIP-II R&D strategy is designed to mitigate technical and cost risks associated with the project. One part of this strategy is to develop and operational test the PIP-II Front End covering the first 20 MeV in the PIP-II Injector Test (PIP2IT) facility [2].

The PIP2IT program will develop and perform an integrated system test of the room temperature warm front end (WFE), consisting of the ion source, LEPT, RFQ and MEPT [3], and the first two superconducting cryomodules. The ion source and LEPT operate with 30 keV H- beam up to 10 mA and the MEPT operates with 2.1 MeV H- beam up to 5 mA. The hardware layout is shown in Figure 2.

In addition, the MEPT section of the WFE operates a bunch-by-bunch chopper allowing for any arbitrary beam pattern [4]. For PIP-II beam operations, the chopper will reduce the beam current from 5 mA to 2 mA before injection into the SC linac.

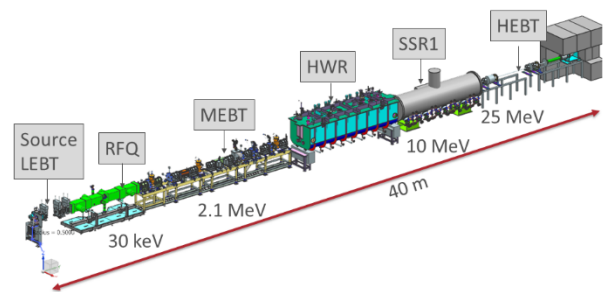


Figure 2: The beamline layout of the PIP-II Injector Test.

The warm front-end has a number beam diagnostic instruments to help prepare beam for the SC linac. Figure 3 shows the beamline layout of the PIP2IT WFE MEPT used for commissioning the MEPT.

ELECTRON BEAM DIAGNOSTICS CONCEPT FOR THE LWFA DRIVEN FEL AT ELI-BEAMLINES

K.O. Kruchinin*, D. Kocon, A. Molodozhentsev, ELI-Beamlines,
 Institute of Physics of the Czech Academy of Science, Prague, Czech Republic
 A. Lyapin, John Adams Institute at Royal Holloway University of London,
 Egham, United Kingdom

Abstract

Uniquely short high energy electron bunches produced by compact Laser Wakefield Accelerators (LWFA) are attractive for the development of new generation Free Electron Lasers (FEL). Although the beam quality of LWFA is still significantly lower than provided by conventional accelerators, with persistent progress seen in the area of laser plasma acceleration, they have a great potential to be considered the new generation drivers for FELs and even colliders. A new LWFA based FEL project called "LUIS" is currently being commissioned at ELI-beamlines in Czech Republic. LUIS aims to demonstrate a stable generation of X-ray photons with a wavelengths of 6 nm and lower, suitable for user applications. Electron beam diagnostics are absolutely crucial for achieving LUIS's aims. Low charge, poor beam stability and other beam properties inherent for a LWFA require rethinking and adaptation of the conventional diagnostic tools and, in some cases, development of new ones. In this paper we provide an overview of the electron beam instrumentation in LUIS with a focus on the current challenges and some discussion of the foreseen future developments.

INTRODUCTION

The beamline facility of the Extreme Light Infrastructure (ELI), located south-west of Prague, Czech Republic focuses on short pulse X-ray generation, particle acceleration and their applications using high power (PW-class) ultra-short (few fs) lasers [1]. Within this facility a dedicated Laser-Plasma Driven Undulator X-Ray Source (LUIS) beamline is being commissioned. The main parameters of

Table 1: Expected ELI LUIS Electron Beam Parameters

Parameter	Value	Units
Energy	350 – 600	MeV
Charge	1 – 100	pC
Rep. rate	up to 10	Hz
Bunch length	up to 30	fs
Norm. emittance	< 1	π mm mrad
Energy spread	< 5	%
Divergence at the source	< 5	mrad
Beam size at the source	~ 1	μ m
Beam size at the undulator	~ 100	μ m
Injection error	± 6	μ m

* konstantin.kruchinin@eli-beams.eu

the LUIS beamline are presented in Table 1. The goal for the LUIS project is to produce X-ray photons with a wavelength $\lambda = 1.9 - 6$ nm using short undulator (less than 1 m) and develop techniques to reach stable operation for user experiments. Development towards laser driven X-ray FEL is also considered.

In the following sections we will describe the key diagnostic systems which will be used for the LUIS electron beam characterization.

TRANSVERSE DIAGNOSTICS

To measure the beam envelope (transverse size and divergence) YAG:Ce screens will be used. Although there are some resolution issues with such systems [2] this is still suitable for low intensity beams and when the beam size is large. This will be true for the first stage of the LUIS commissioning where expected beam size will be a few hundreds of μ m. To achieve higher resolution OTR screens [3] can be used in the future.

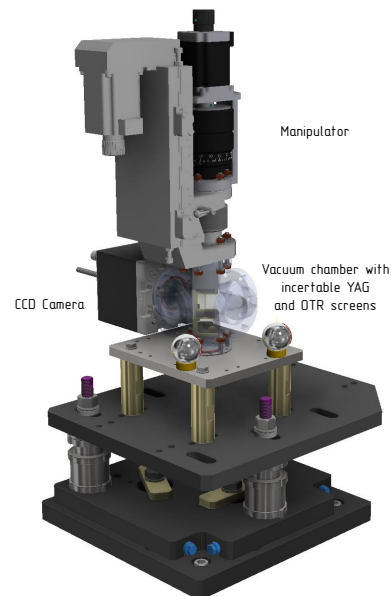


Figure 1: Model of the transverse diagnostics station.

For emittance measurements a "pepper-pot" technique will be used. This technique has been successfully demonstrated in several experiments for beams produced by the LWFA [4, 5]. Main advantage of the "pepper-pot" is the ability to measure emittance in both planes (vertical and horizontal) in a single shot. For characterization of the elec-

Content from this work may be used under the terms of the CC BY 3.0 licence (© 2019). Any distribution of this work must maintain attribution to the author(s), title of the work, publisher, and DOI

SPIRAL2 DIAGNOSTIC QUALIFICATIONS WITH RFQ BEAMS

C. Jamet[†], S. Leloir, T. Andre, V. Langlois, G. Ledu, P. Legallois, F. Lepoittevin, T. Le Ster, S. Loret, C. Potier de courcy, R.V. Revenko, GANIL, Caen, France

Abstract

The SPIRAL2 accelerator, built on the GANIL's facility, at CAEN in FRANCE is dedicated to accelerate light and heavy ion beams up to 5mA and 40 MeV. The continuous wave accelerator is based on two ECR ion sources, a RFQ and a superconducting LINAC. The beam commissioning of the RFQ finished at the end of 2018. This paper presents the Diagnostic-Plate installed behind the RFQ, with all associated accelerator diagnostics. Diagnostic monitors, measured beam parameters, results are described and analyzed. A brief presentation of the next steps is given.

INTRODUCTION

The SPIRAL2 facility is designed to produce deuteron and proton beams with the first ECR source and ion beams with the second source. The acceleration is given by a CW RFQ ($A/Q \leq 3$) and a high power superconducting linac. Table 1 recalls the main beam characteristics.

Table 1: Beam Characteristics

Beam	P	D+	Ions (1/3)
Max. Intensity	5 mA	5 mA	1 mA
Max. Energy	33 MeV	20 MeV/A	14.5 MeV/A
Max. Power	165 kW	200 kW	43.5 kW

The linac is composed of 19 cryomodules, 12 with one cavity ($\beta=0.07$) and 7 with 2 cavities ($\beta=0.12$).

The HEBT lines distribute the linac beam to a beam Dump, to the NFS (Neutron For Science) or S3 (Super Separator Spectrometer) experimental rooms.

Major challenges are to handle the large variety of beam characteristics (particle types, beam currents from few $10\mu\text{A}$ to few mA, wide energy range), the high beam powers (up to 200 kW CW) and the safety issues [1].

The first commissioning phase consisted to qualify the RFQ beams with a Diagnostic Plate (D-Plate), this injector commissioning took place from the end of 2015 up to 2018. The D-Plate was removed to install the full MEBT at the beginning of 2019.

Three different beams were chosen, Proton, Helium and Oxygen, to qualify the injector performances. Argon beam was also measured.

The 5mA proton beam is easy to produce but more difficult to transport in the LEBT due to the space charge forces. 4He^{2+} was selected to mimic the future deuteron beam without neutron production due to the d-d reactions.

It also allowed to test the heavy ion ECR source and LEBT1 [2].

The same accelerator frequency, on all the RF devices, is 88.0525 MHz.

The RFQ beam power is to 3.5 kW with 5 mA of protons and 7 kW with Helium. In order to limit the beam losses in the D-Plate and on the various interceptive diagnostics, the duty cycle applied on the chopper was usually around of few ms per few 100 ms.

INJECTOR AND D-PLATE DESCRIPTION

The injector schematic is given in Fig. 1.

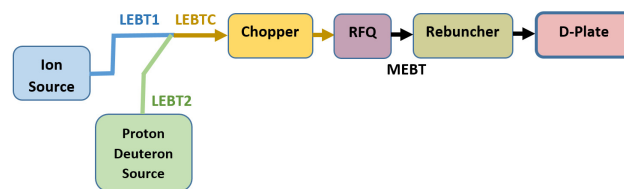


Figure 1: Injector Diagram.

The D-Plate (named BTI in French: Intermediate Test Bench) was defined to characterize the beams from the RFQ and also to qualify the SPIRAL2 diagnostic monitors.

Three quadrupoles, one rebuncher (Fig. 2) were installed behind the RFQ to tune the beam transport in both transverse and longitudinal planes. The D-plate allowed to measure:

- Intensities with Faraday cups, ACCT and DCCT,
- Transverse profiles with classical multi-wire profilers and Residual Gas Monitor (RGM)
- H and V transverse emittances with Allison type scanners
- Energies with a Time of Flight (TOF) monitor,
- Phases with the TOF and 2 BPMs
- Longitudinal profiles with a Fast Faraday Cup (FFC), and a Beam Extension Monitor (BEM)
- Beam position and ellipticity ($\sigma_x^2 - \sigma_y^2$) with the BPMs

The D-Plate was a workpackage supported by the French Laboratory IPHC. This CNRS laboratory had in charge the mechanical design and the supply of the D-Plate.

[†] christophe.jamet@ganil.fr

STATUS OF BEAM INSTRUMENTATION FOR FAIR HEBT

M. Schwickert[†], P. Boutachkov, T. Hoffmann, H. Reeg, A. Reiter, and B. Walasek-Höhne
 GSI Helmholtzzentrum für Schwerionenforschung, Darmstadt, Germany

Abstract

At present the Facility for Antiproton and Ion Research (FAIR) is under construction at the GSI site. As part of the FAIR project the beamlines of the High Energy Beam Transport (HEBT) section interconnect the synchrotrons, storage rings and experimental caves. The large range of beam energies (MeV to GeV) and beam intensities up to 10^{12} particles per pulse for uranium, or up to 2×10^{13} particles per pulse for protons, demand in many cases for purpose-built beam diagnostic devices. Presently, the main diagnostic components are being manufactured by international in-kind partners in close collaboration with GSI. This contribution presents an overview of the beam instrumentation layout of the FAIR HEBT and summarizes the present status of developments for HEBT beam diagnostics. We focus on the status of the foreseen beam current transformers, particle detectors, scintillating screens and profile grids.

STATUS OF FAIR ACCELERATORS

Presently, civil construction works of the northern section of the FAIR accelerator complex are progressing well [1]. This section is the first to be built and includes the underground ring building for SIS100, i.e. the main synchrotron of FAIR, as well as significant parts of the HEBT buildings. Also the interconnection between the existing GSI accelerator facility, which will serve as injector for the FAIR machines, is presently being prepared. The ring tunnel for the fast ramped super-conducting synchrotron SIS100, located 25 metres underground is already excavated and first sectors of the ring building are constructed. Construction works of the HEBT buildings have started too. The HEBT connects the synchrotrons with the super-fragment separator (S-FRS) for the production of rare isotopes, with the antiproton target and separator for the production of antiprotons, the collector ring (CR) for stochastic pre-cooling of rare isotopes and antiprotons and the high-energy storage ring HESR. In addition, HEBT beamlines provide beams to the fixed target experiments of APPA, SPARC and CBM. The main accelerator of FAIR will be SIS100, designed for production of up to 5×10^{11} U28+ ions/s with energies of 0.4-2.7 GeV/u. SIS100 beams can be extracted either in single bunches of 30-90 ns, or by slow extraction with extraction times of several seconds, for the production of radioactive ion beams in the S-FRS and various high energy experiments, like e.g. CBM or HADES. Efficient production of antiprotons will require 2×10^{13} protons per pulse at an energy of 29 GeV with a repetition rate of 0.1 Hz and a bunch length of 50 ns. After passing the large aperture antiproton separator line, secondary antiproton beams will be stored and pre-cooled in

[†] m.schwickert@gsi.de.

the CR and transported to the HESR for stacking, stochastic cooling and post-acceleration. The design of the FAIR facility foresees that all accelerators operate in a highly multiplexed mode, thus allowing sequential beam delivery to up to four different experiments inside one machine super-cycle. The complex modes of operation demand for well adopted beam instrumentation inside the HEBT beamlines.

HEBT BEAM DIAGNOSTICS

Beam instrumentation for the 1.5 km long HEBT beamlines has to cover both, slow and fast extracted beams, as well as a wide range of beam intensities. Thus dedicated instruments were developed for all modes of operation. Table 1 summarizes the diagnostic equipment of the HEBT. Especially high current operation requests for non-intercepting devices, like e.g. Beam Current Transformers, Beam Position Monitors or Ionization Profile Monitors.

Table 1: HEBT Diagnostic Devices

Device	Parameter	No. of pcs.
Resonant Transformer	Bunch / batch charge	25
Fast Current Transformer	Bunch current, time structure	11
Cryogenic Current Comparator	Beam current, spill structure	4
Particle Detector Combination	Beam current	16
Beam Position Monitor	Centre-of-mass	39
Multi-Wire Proportional Chamber / Ionization Chamber	Transverse beam profile, current	34
SEM-Grid	Transverse beam profile	51
Scintillating Screen	Transverse beam profile	18
Ionization Profile Monitor	Transverse beam profile	15
Beam Loss Monitor	Beam loss	30

Diagnostic Vacuum Chambers

As part of the Indian in-kind contribution to FAIR 70 diagnostic vacuum chambers for beam diagnostic devices will be manufactured. Presently, a commercial provider has been selected by the Indian shareholder and the first two prototype chambers are ready for delivery. Prior to series

Content from this work may be used under the terms of the CC BY 3.0 licence (© 2019). Any distribution of this work must maintain attribution to the author(s), title of the work, publisher, and DOI

THE BEAM DIAGNOSTICS TEST BENCH FOR THE COMMISSIONING OF THE PROTON LINAC AT FAIR

S. Udrea[†], P. Forck, C. M. Kleffner, K. Knie, T. Sieber, GSI Helmholtzzentrum für Schwerionenforschung GmbH, Darmstadt, Germany

Abstract

A dedicated proton injector for FAIR (the pLinac) is presently under construction at GSI Darmstadt. This accelerator is designed to deliver a beam current of up to 70 mA with a final energy of 68 MeV for the FAIR anti-proton program. For the commissioning of the pLinac a movable beam diagnostics test bench will be used to characterize the proton beam at different locations during the stepwise installation. The test bench will consist of all relevant types of diagnostic devices as BPM's, ACCT's, SEM grids, a slit-grid emittance device and a bunch shape monitor. Moreover, a magnetic spectrometer is supposed to measure the energy spread of the proton beam. Point-to-point imaging is foreseen to enable high energy resolution independently on the transverse emittance. Due to the limited space in the accelerator tunnel a special design must be chosen with the inclusion of quadrupole magnets. The present contribution gives an overall presentation of the test bench and its devices with a special emphasis on the magnetic spectrometer design.

INTRODUCTION

The FAIR [1] facility, presently under construction at GSI Darmstadt, is envisaged to provide both antiproton and ion beams. FAIR's accelerator complex will include two linacs as injectors: the existing UNILAC [2] and the pLinac [3], a new proton linac under construction. Both linacs inject into the present SIS18 synchrotron, which will act as an injector for the future SIS100 synchrotron.

The pLinac will consist of an RFQ followed by two 9 m long sections of Cross-bar H-drifttube (CH) accelerating structures working at 325.224 MHz and is designed to deliver a beam current of up to 70 mA at a macropulse length of 36 μ s and a typical bunch length of 100 ps [3,4]. The design energy is 68 MeV.

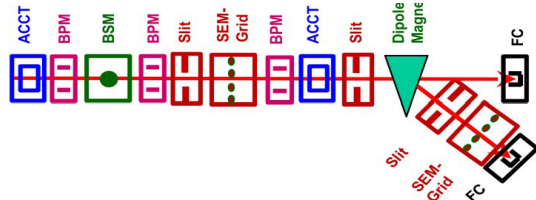


Figure 1: Schematic test bench overview.

During the stepwise commissioning phase a movable test bench will be employed to characterize the proton beam behind each cavity. The bench is foreseen to consist of all relevant types of diagnostic devices that have been developed for the pLinac (BPM's, ACCT's, SEM grids, a slit-grid emittance device and a bunch shape monitor) and additionally a magnetic spectrometer for measurements of

[†]s.udrea@gsi.de

the proton beam's energy spread. An overview of the planned bench is shown in Fig. 1.

STANDARD BEAM DIAGNOSTICS

We give here short descriptions of the main diagnostic devices which will also be installed along the pLinac beam line. For more details see [4].

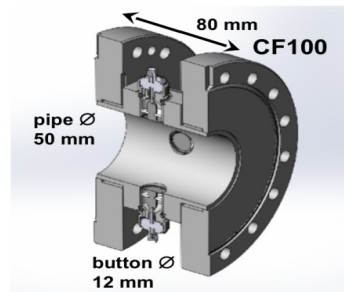


Figure 2: Cross section through a 'beam-line' BPM.

BPMs

The BPMs are of the button type and will be built in two mechanical designs – 'inter-tank' and 'beam-line' – and five different geometries. The 'inter-tank' ones are supposed to be mounted between the CH modules of the CH tanks while the 'beam-line' BPMs will be installed outside the tanks. For the test bench three 'beam-line' BPMs are foreseen with inner diameters of 50 mm and 12 mm wide buttons, see Fig. 2. They will be used both for position and mean energy measurements by the time of flight method [5].

ACCTs

The AC beam transformers (ACCTs) are built by Bergoz (see Fig. 3), were developed based on GSI specifications and are an improvement of a standard Bergoz model. The enhanced ACCT mainly differs from its predecessor by a larger bandwidth (3 MHz instead of 1 MHz), three measurement ranges (100/10/1 mA) instead of one, the availability of a test input and an improved magnetic shielding [6].



Figure 3: The ACCT developed by the Bergoz company.

BEAM DIAGNOSTICS FOR THE MULTI-MW HIGH ENERGY BEAM TRANSPORT LINE OF DONES*

I. Podadera[†], A. Ibarra, D. Jiménez-Rey, J. Mollá,
C. Oliver, R. Varela, V. Villamayor[‡], CIEMAT, Madrid, Spain
O. Nomen, D. Sánchez-Herranz, IREC, Sant Adrià del Besós, Spain

Abstract

In the frame of the material research for future fusion reactors, the construction of a simplified version of the IFMIF plant, the so-called DONES (Demo-Oriented Neutron Early Source), is under preparatory phase to allow materials testing with sufficient radiation damage for the new design of DEMO. The DONES accelerator system will deliver a deuteron beam at 40 MeV, 125 mA. The 5 MW beam will impact onto a lithium flow target to form an intense neutron source. One of the most critical tasks of the accelerator is the beam diagnostics along high energy beam transport, especially in the high radiation areas close to the lithium target. This instrumentation is essential to provide the relevant data for ensuring the high availability of the whole accelerator system, the beam characteristics and machine protection. Of outmost importance is the control of the beam characteristics impinging on the lithium curtain. Several challenging diagnostics are being designed and tested for that purpose. This contribution will report the present status of the design of the beam diagnostics, focusing on the high radiation areas of the high energy beam transport line.

INTRODUCTION

The linear accelerator for the IFMIF-DONES facility [1] will serve as a fusion-like neutron source for the assessment of materials damage in future fusion reactors. DONES will consist of a linear deuteron RF linear accelerator up to 40 MeV at full CW current of 125 mA. The facility is divided in three major systems: the particle accelerator, the target and the experimental material test area.

The accelerator system is based on the design of LIPAC [2], which is currently in its commissioning phase [3]. The accelerator will be made of 1) a Low Energy Beam Transport (LEBT) section at 100 keV to guide the low energy ions up to the RadioFrequency Quadrupole (RFQ) and match its injection acceptance, 2) an RFQ to accelerate the ions from 100 keV up to 5 MeV, 3) a Medium energy Beam Transport Line (MEBT) to match the RFQ extracted beam to the injection of the SRF Linac, 4) an SRF Linac of five cryomodules to bring the energy of the deuterons up to 40 MeV, 6) a High Energy Beam Transport (HEBT) lines to transport the beam from SRF Linac towards the lithium target or the beam dump transport line (BDTL), in pulsed mode.

Beam losses along all the accelerator should be kept below 1 W m^{-1} . Besides of the transport function, the HEBT will be mainly responsible of shaping the beam to the rectangle required by the lithium target. For this purpose, multipole magnets (dodecapoles and octupoles) are used along the beamline [4]. In order to fulfill this function, beam diagnostics will provide essential information both during the commissioning and operation phases for the tuning and safe operation of the accelerator.

HEBT REQUIREMENTS

The distribution of the monitors along the HEBT is based on the beam dynamics design requirements [4]. The beamline can be divided in three sections (Fig. 1): a section S1 before the dipole which directs the beam to the target, a section S2 which transforms the beam phase-space using octupoles and dodecapoles, and a section S3 which makes the beam imping in the right spot. This section passes through a separate room downstream the last magnetic expansion – the Target Isolation Room (TIR) – before colliding with the target.

Along section S1 the monitors are focused in monitoring the beam from the SRF Linac. The following properties should permanently monitored to be sured the right beam is delivered to the target: DC current, mean energy and transverse size.

In section S2 it is very important to control the profile and position of the beam at each multipole magnet. In section S3 the essential points are: 1) to point the beam to the center of the target. This can be achieved by using RF pickups tuned to the fundamental frequency, 2) to control the size and uniformity of the transverse profile. A complete discussion of the design of the beamline, including the remote handling requirements in the last sections, is given elsewhere [5].

The DONES environment pose several challenges to the beam diagnostics [6]. The present plan assumes the operation with deuterons from the earliest stage. However a preliminary operation with protons is highly probable/almost mandatory, as it has been found/estimated beneficial at LIPAC. First of all, the availability of the accelerator system [7] is very important to guarantee the irradiation dose rate to the material samples. The monitors should be robust enough to monitor continuously and with high reliability the important beam parameters used to control and protect the machine during operation and tuning status. Therefore, the monitors should withstand the severe environment conditions of the beamline, especially regarding the high neutron and gamma radiation. The present considerations are that

* Work carried out within the framework of the EUROfusion Consortium and funded from the Euratom research and training programme 2014-2018 and 2019-2020 under grant agreement No 633053

[†] ivan.podadera@ciemat.es

[‡] presently at Seven Solutions, Granada, Spain

STATUS OF THE FARADAY CUPS FOR THE ESS LINAC

E. Donegani*, C. Derrez, T. Grandsaert, T. Shea, European Spallation Source, Lund, Sweden
 I. Bustinduy, A. R. Paramo, ESS-Bilbao, Bilbao, Spain

Abstract

The proton linac for the European Spallation Source (ESS) is under construction on the outskirts of Lund (Sweden). Four Faraday Cups (FC) are meant to stop the proton beam and measure the beam current in the normal conducting linac section. The first Faraday cup is located in the LEBT and has been operational throughout the commissioning of the source and the LEBT. In June 2019, a second Faraday cup was installed in the MEBT and will undergo verifications without beam in fall 2019. The two most challenging FCs are currently in construction phase and will be installed in two DTL intertanks early in 2020. This contribution summarizes the latest milestones and challenges for the development and operation of all the ESS Faraday cups.

INTRODUCTION

The proton linac for the European Spallation Source (ESS) is currently under construction in Lund (Sweden). Once operational, ESS will be the most powerful and brightest spallation neutron source in the world, relying on an accelerator of protons up to an energy of 2 GeV. The ESS linac is mainly superconducting and has a normal conducting linac section as its injector. At the moment, the installation is progressing for the four normal conducting sections:

1. the Low Energy Beam Transfer (LEBT) line;
2. the Radio Frequency Quadrupole (RFQ);
3. the Medium Energy Beta Transfer (MEBT) line;
4. the Drift Tube Linac (DTL).

During the start-up and commissioning phases of the normal conducting linac, the beam current is measured either with non-interceptive [1] or interceptive devices.

Four Faraday cups (FC) are included in the latter category; they serve as beam destination and measure the beam current. Only the LEBT FC can withstand the nominal ESS beam pulses of 62.5 mA current, 6 ms width and 14 Hz repetition rate, as long as the maximum power density is within 14 kW/cm², which corresponds to a 3.7 mm RMS size for 75 keV protons. The other three FCs are specifically designed to withstand only the so-called ESS tuning modes:

- *slow* tuning: 50 μs long pulses at 1 Hz repetition rate;
- *fast* tuning: 5 μs long pulses at 14 Hz repetition rate.

In Table 1, the current status is summarized for each device. This contribution highlights the latest milestones and challenges either in the development or operation of the four FC systems.

* Corresponding author: elena.donegani@ess.se

Table 1: Status of the Four Faraday Cups for the ESS Linac and Energy of the Proton Beam They Are Exposed To

	FC Status	Proton energy (MeV)
LEBT	Operational	0.075
MEBT	Just installed	3.63
DTL2	Under production	21 or 39
DTL4	Under production	39 or 74

LEBT FC

The Faraday cup (FC) in the Low Energy Beam Transport (LEBT) line was designed at ESS [2] and produced in 2014 by Pantechnik [3]. The actual cup is entirely made of copper and water cooled. The cup is inserted or extracted from the beam line by means of a pneumatic actuator.

In 2017, the LEBT FC took part in the ion source and LEBT commissioning in Catania (Italy). From September 2018 to July 2019, it contributed to various types of characterizations of the source and LEBT at ESS in Lund [4]. The current readings from the LEBT FC and the two Beam Current Monitors (BCMs) upstream were compared in several source configurations.

A representative plot is presented in Fig. 1 (left), resulting from the scan of the two LEBT solenoids (namely, Sol1 and Sol2). In particular, the solenoid current was increased from 250 to 350 A, and from 160 to 380 A, for the first and second solenoid, respectively. It is worth noting that the maximum solenoid current is 500 A and the typical operational range is between 250 A and 300 A.

The FC was located about 600 mm downstream of the collimator exit at the end of the LEBT, with an aperture of just 14 mm in diameter. During the solenoid scan, a

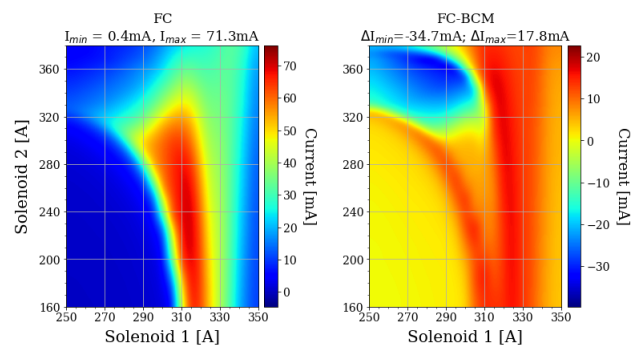


Figure 1: Beam current measurements resulting from solenoid scans: (left) in the LEBT FC and (right) difference between LEBT FC and BCM currents.

MAX IV OPERATIONS - DIAGNOSTIC TOOLS AND LESSONS LEARNED

B. Meirose*, V. Abelin, B.E. Bolling, M. Brandin, R. Høier, A. Johansson, P. Lilja, J. S. Lundquist, S. Molloy, F. Persson, J. E. Petersson, R. Svärd, MAX IV Laboratory, Lund University, Sweden

Abstract

New beam diagnostic and monitoring tools developed by the MAX IV Operations Group are presented. In particular, new beam position monitoring (BPM) and accelerator tunes visualization tools and other simple but useful applications are presented. We also briefly share our experience with the development of audible alarms, which help operators monitor various parameters of the machine, and explain how the implementation of all these tools have improved accelerator operations at MAX IV.

INTRODUCTION

The MAX IV laboratory [1, 2] is a synchrotron radiation laboratory in Lund, Sweden. MAX IV is the first Multi-Bend Achromat (MBA) Synchrotron Radiation Light Source in the world and provides scientists with the most brilliant X-rays for research. The laboratory was inaugurated in June 2016 and consists of two storage rings operated at 1.5 and 3 GeV providing spontaneous radiation of high brilliance over a broad spectral range. The 1.5 GeV ring has a circumference of 96 m and employs a double-bend achromat lattice to produce an emittance of 6 nm rad. The 3 GeV storage ring on the other hand is aimed towards ultralow emittance to generate high brilliance hard X-rays. The design of the 3 GeV storage ring includes many novel technologies such as MBA lattice and a compact, fully-integrated magnet design. This results in a circumference of 528 m and an emittance as low as 0.2 nm rad [3].

A linear accelerator (linac) works as a full-energy injector for the storage rings as well as to a Short Pulse Facility (SPF). The prime sources for synchrotron radiation at the rings are optimized insertion devices (IDs), providing intense X-ray light for each of the MAX IV beamlines.

MAX IV ACCELERATOR OPERATIONS

The Operations Group is responsible for delivering stable high-quality beams to the beamlines (users). Figure 1 shows the facility status in May 2019, when eleven beamlines had closed undulator gaps and open shutters, indicating that they were actively taking synchrotron light produced at the accelerators, all at the same time. As one can also see from the plot, the linac performed excellently as injector providing beam current top-up every 30 minutes, as well as high bunch charge (100 pC) to the SPF.

* bernhard.meirose@maxiv.lu.se



Figure 1: MAX IV status page in May 29, 2019.

BEAM POSITION MONITOR TIME EVOLUTION

BPM trends is a tool developed by the operations group that shows the storage rings beam positions over time (a real-time “sliding plot” during operations) as measured by all the rings’ BPMs. The vertical scale on the right (in μm) controls whether there is any deviation within the lower and upper limits set by the scale. Figure 2 shows a typical example of stable delivery, where all BPM readings show the beam is kept within the required limits (within $0\mu\text{m} \pm 0.3\mu\text{m}$, in this example) and are therefore shown in green. When the deviation is above the upper limit ($0.3\mu\text{m}$) the points are shown in red. An illustration of this fact is demonstrated in Fig. 3, where one can observe that small changes to one of the beamline’s gap in the 3 GeV storage ring can cause visible disturbances to the beam. In Fig. 4 it is noticeable that during injections a large vertical line can be observed in the 1.5 GeV ring BPM trends, due to the significant disturbances caused by the dipole kicker that it is used in the smaller ring. A similar line is not observed in Fig. 2 as the 3 GeV ring makes use of a multipole injection kicker (MIK), which accomplishes top-up injections without visibly disturbing the beam orbit.

ACCELERATOR TUNES VISUALIZATION

The accelerator tunes visualization makes use of similar concept as the BPM trends, but it monitors the synchrotron and betatron frequencies variations measured by MAX IV’s Bunch by Bunch (BBB) system [4]. Figure 5 shows (starting approximately at -40 min) a manual increase of the Master Oscillation (MO) RF of the 3 GeV storage ring in steps of 5 Hz in order to reach a vertical tune of 0.265. At -5 minutes one of the beamlines closes its undulator gap, causing the tune to shift, which is clearly visible at right end of the plot.

DESIGN AND DEVELOPMENT OF BEAM DIAGNOSTICS FOR AN FETS-FFA RING FOR ISIS-II UPGRADE STUDIES

E. Yamakawa*, JAI in Oxford University, Oxford, United Kingdom
 C. C. Wilcox, A. Pertica, S. Machida, RAL STFC, Didcot, United Kingdom

Abstract

The ISIS-II project aims to deliver a new spallation neutron source by 2034, driven by a 1.2 GeV proton accelerator capable of delivering a beam power of 1.25 MW with a repetition rate of 50 Hz or higher. One of the options for this future accelerator is a Fixed Field alternating gradient Accelerator (FFA). To demonstrate the suitability of FFAs for use in a user facility such as ISIS, there is a plan to construct a smaller scale proof of concept machine: FETS-FFA. Developing beam diagnostics for the FETS-FFA ring presents a challenge due to a large orbit excursion and aperture (60 mm x 700 mm). Diagnostics must cover the full size of beam chamber whilst still providing measurement sensitivity and resolution comparable to that seen in the ISIS synchrotron.

This paper presents the current design and development of beam diagnostics for the FETS-FFA ring, including finite element studies of Beam Position Monitors and Ionisation Profile Monitors.

INTRODUCTION

The feasibility studies for an intensity upgrade of ISIS, towards a 1.25 MW proton driver for neutron provision in Europe, was started in 2016 [1]. One of the options being considered is a Fixed Field Alternating gradient (FFA) ring [2, 3]. FFAs utilise static magnetic fields to accelerate a particle beam with a high repetition rate (~200 Hz), while achieving high beam intensities. In order to demonstrate the viability of an FFA for a high intensity user facility, the small-scale FETS-FFA ring will be built initially, before the final decision is made on which type of accelerating ring will be used in ISIS-II. The preliminary parameters of FETS-FFA are summarised in Table 1.

Table 1: Preliminary parameters of FETS-FFA ring

Beam energy range	3 - 30 MeV
Central radius	4 m
Orbit excursion	0.58 m
Bunch intensity N_p	10^{10} ppb
Harmonic number	2
RF bandwidth	4 - 7 MHz
Bunch length at 3 MeV, 30 MeV ($4\sigma_L$)	31 ns, 54 ns

A key challenge in the development of beam diagnostics for this ring (and other FFA's) is the requirement to measure across the large beam chamber width (~700 mm) whilst also achieving high measurement sensitivity and resolution, comparable to those achieved in the ISIS synchrotron. In this paper, the current designs of a Beam Position Monitor

(BPM) and Ionisation Profile Monitor (IPM) for FETS-FFA are presented.

BEAM POSITION MONITOR DEVELOPMENT

BPM development for the FETS-FFA ring has focused on a rectangular, electrostatic shoe-box type monitor (also known as a split-plate BPM) [4], with two pairs of electrodes to allow measurement in both the horizontal and vertical planes. This type of BPM has been installed and demonstrated in a proof-of principle FFA at KEK, in 2001 [5], and is the same style as the BPMs used at ISIS [6].

Assuming the beam is centred in a rectangular vacuum chamber, the maximum detected pick-up signal ($V(t)$) [4] is given by:

$$V(t) = \frac{1}{c\beta C} \frac{A}{2\pi(a+b)/4} I_{\text{beam}}(t), \quad (1)$$

where c is the speed of light, C the capacitance between the electrode and ground, A the area of the electrode, I_{beam} the beam current, a the vertical electrode separation and b the horizontal electrode separation. When measuring this voltage, the BPM acts as a first order high-pass filter, with a cutoff frequency given by $f_{\text{cut}} = 1/2\pi RC$. As a result, the termination impedance which the signal is measured across must be high, in order to give a low enough cutoff frequency for the bandwidth requirement of the FETS-FFA ring, as listed in Table 1.

The FETS-FFA ring requires such a large vacuum chamber because the beam orbit moves as the beam energy increases, over a range of about 600 mm. The preliminary design of the ring includes several straight vacuum chambers between each main magnet, and it is within these sections that the beam diagnostics will be installed. Each straight section is 0.75 m long, with an internal aperture of 778 mm x 138 mm, meaning any installed BPMs must have very large widths. Preliminary designs of the monitor have apertures of 710 mm x 70 mm, and electrode thicknesses of 4 mm. Figure 1 shows the preliminary design of the BPM, rendered in CST electromagnetic finite element software [7]. Inside the vacuum chamber, each electrode pair is formed by splitting a rectangular shaped electrode with a diagonal cut. This cut means that offsets in beam position from the centre of the monitor induce different strength signals on each electrode, yielding a beam position measurement. Electrical coupling between adjacent electrodes can reduce the measurement accuracy and sensitivity of these monitors, and this problem is exacerbated by the large electrode size required. To mitigate this, earthed guard-rings (the blue material in

* emi.yamakawa@physics.ox.ac.uk

DEVELOPMENT OF THE LINAC EXTENSION AREA 450-MeV ELECTRON TEST BEAM LINE AT THE ADVANCED PHOTON SOURCE*

W. J. Berg †, J. C. Dooling, S. H. Lee, Y. Sun, A. Zholents,
 Argonne National Laboratory, Lemont, IL 60439, USA

Abstract

A high brightness low-emittance electron beam line for accelerator-based R&D hardware experimentation and study of novel accelerator techniques is under development at the injection linac of the Advanced Photon Source (APS). The Linac Extension Area (LEA) beam line will operate up to the 450 MeV energy of the APS linac. The electron beam is generated from a photo-cathode (PC) RF gun delivering 300 pC of charge with a 3 ps rms bunch length and normalized slice beam emittance of $\sim 1 \mu\text{m}$. The bunch length can be compressed to 150 fs in a flexible chicane at a beam energy of 150 MeV. The APS linac contains an extensive set of conventional and advanced beam diagnostics including a recently commissioned s-band transverse deflecting cavity. The low-emittance electron beam is transported to an independent experimental tunnel enclosure that contains the LEA beam line. Implementing the LEA beam line separate from the APS injector complex allows for on-demand access to the area to perform work without interrupting beam operations of the APS. We discuss the overall scheme of the existing linac beam delivery and diagnostic systems, and report the design of the LEA beam line and initial planned experiments.

INTRODUCTION

The APS is preparing a Linac Extension Area (LEA) beam line to provide an experimental platform for hardware installations supporting the study of future concepts and novel accelerator techniques. The linac produces up to 450 MeV electrons from a high brightness low emittance PC RF gun (see Table 1). The electron beam is compressed by a flexible chicane positioned at the 150 MeV point and transported 90 m downstream to the LEA beamline [1]. The beam line extension area is located downstream of the APS injection linac in an independent building complex. This allows access to the beam line without impacting APS user operation runs. The LEA beamline is configured with a symmetrical beam lattice and diagnostics centered about the beam interaction region where an experimental vacuum chamber is installed to enhance ease of beam perturbation studies. The beam terminates into an energy spectrometer and beam dump. Downstream tunnel space capacity has been allocated after the beam dump to allow for the addition of future hardware installation opportunities and utilizing the electron beam. The first such plan is for incorporation of the Tapering Enhanced Stimulated Superradiant Amplification (TESSA) tapered undulator system, a collaboration between APS, UCLA, and RadiaBeam [2, 3].

* Work supported by the U.S. Department of Energy, Office of Science, under Contract No. DE-ACO206CH11357

† berg@anl.gov

Table 1: Linac Electron Beam Parameters

Parameter	Value	Note
Beam Energy	$\leq 450 \text{ MeV}$	Nominal
Bunch Charge	300 pC	Nominal
Bunch Length	3 ps rms	PC gun
Beam Emittance	$1 \mu\text{m}$	PC gun
Energy Spread	250 – 500 keV	Range

INJECTOR CONFIGURATION

Beam Generation

The electron beam is produced from a photo-cathode RF gun that was fabricated and installed into the linac in 2014, see Fig. 1 [4, 5]. A ND:Glass drive laser with a wavelength of 1066 nm, produces a 25 uJ/pulse in the ultra-violet (UV) at 266 nm to the copper cathode at a variable repetition rate. The PC gun generates an electron beam pulse of 300pC charge and bunch length of 3ps with an rms emittance of $1 \mu\text{m}$. The beam is accelerated by the first sectors of the s-band linac to the 150 MeV point and compressed to a bunch length of 150 fs in the flexible chicane. The beam can then be further accelerated by the next two linac sectors up to the nominal maximum linac energy of 450 MeV.

Beam Characterization and Transport

Multiple diagnostic systems have been developed to provide beam characterization including a coherent transition radiation (CTR) bunch length monitors located both before and after the chicane section, three screen emittance measurement station and s-band transverse deflection cavity (TCAV) as depicted in Fig. 2 [6, 7, 8]. The electron beam is matched for transport using the three screen in the accumulator ring bypass transport line and transported through the booster bypass transport to the LEA beam line tunnel.

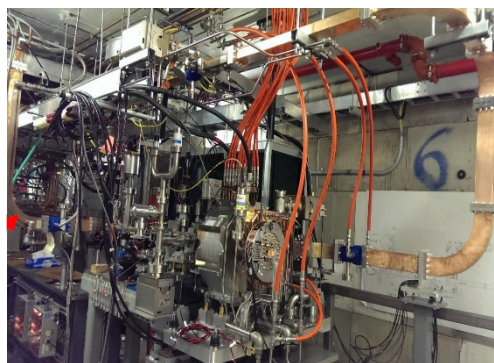


Figure 1: Image of PC Gun in Linac.

BEAM DIAGNOSTICS FOR STUDYING BEAM LOSSES IN THE LHC

B. Salvachua*, CERN, Geneva, Switzerland

Abstract

The LHC is well covered in terms of beam loss instrumentation. Close to 4000 ionization chambers are installed to measure global beam losses all around the LHC ring, and diamond detectors are placed at specific locations to measure bunch-by-bunch losses. Combining the information of these loss detectors with that from additional instrumentation, such as current transformers, allows for enhanced understanding and control of losses. This includes a fast and reliable beam lifetime calculation, the identification of the main origin of the loss (horizontal or vertical betatron motion or off-momentum), or a feedback to perform controlled off-momentum loss maps to validate the settings of the collimation system. This paper describes the diagnostic possibilities that open up when such measurements from several systems are combined.

INTRODUCTION

The Large Hadron Collider (LHC) is designed to provide proton-proton collisions at the unprecedented beam energy of 7 TeV. It is hosted in the former LEP tunnel [1], about 100 m underground, and has a circumference of 26.7 km. In order to keep the proton beams on a circular trajectory at such high energies, 1 232 superconducting dipole magnets are used; each cooled down to 1.9 K and providing a magnetic field up to 8.33 T.

Even a small deposition of beam energy of the order of 100 mJ/cm³ [2], risks to initiate a quench of the LHC magnets, resulting in a loss of superconductivity. This corresponds to a tiny fraction of the circulating beam, with the LHC operating regularly with stored beam energies of around 300 MJ. Figure 1 shows the total stored beam energy reached during LHC Run 2 (2015-2018) as a function of time when running at a collision energy of 13 TeV (6.5 TeV per beam).

In order to fulfill the machine protection requirements for the LHC, the beam has to be extracted within 3 LHC turns (1 LHC turn corresponding to 89 μs), in case of losses exceeding given thresholds. The fast detection of beam losses all along the machine is therefore crucial in order to ensure the protection of the LHC magnets and other equipment and guarantee a high operational efficiency. For this reason, more than 4 000 beam loss detectors are installed, covering all the critical loss locations. This includes the cold superconducting magnets, transfer lines for losses during beam injection, the dump lines for losses during extraction, and more than 100 LHC collimators monitoring the losses from beam halo cleaning. In addition to triggering a beam abort, the LHC beam loss monitoring (BLM) system provides additional information about the beam loss characteristics such as loss patterns or loss location. We describe here the use of the LHC BLM system for advanced beam diagnostics, covering both the standard ionization chamber detectors and the fast, bunch-by-bunch diamond-based beam loss detectors.

BEAM LOSS IONIZATION CHAMBER

The main LHC BLM system is composed of around 3 600 ionization chambers (IC BLM) and 400 secondary emission detectors (SEM) located throughout the LHC ring [3, 4]. Together they provide an overall view of the beam losses in the machine at any given time. Figure 2 shows an example of this view; the x-axis represents the position of each monitor in the LHC ring and the y-axis shows the beam loss measured at each monitor normalized to the maximum measured beam loss. The insertion regions (IRs) are marked: the experimental insertions are IR1, IR2, IR5 and IR8; the main collimation locations are insertions IR3 (momentum cleaning) and IR7 (betatron cleaning); the acceleration with radio-frequency cavities (RF) are located

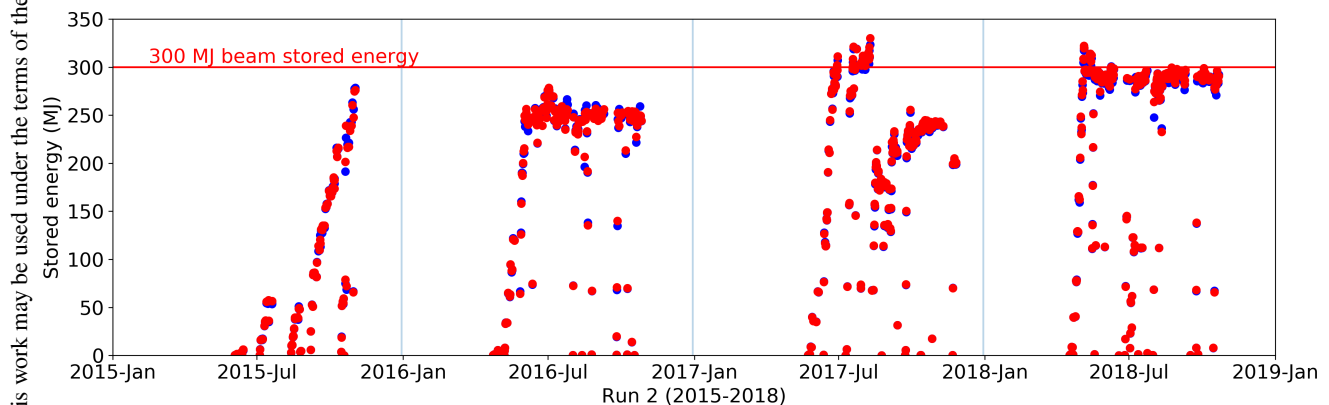


Figure 1: Maximum stored beam energy at the LHC over time during Run 2, each point represents one fill, for Beam 1 (blue points) and Beam 2 (red).

* belen.salvachua@cern.ch

BEAM-LOSS DETECTION FOR LCLS-II*

Alan S. Fisher[†], Christine I. Clarke, Bryce T. Jacobson, Ruslan Kadyrov,
Evan Rodriguez, Leonid Sapozhnikov, and James J. Welch
SLAC National Accelerator Laboratory, Menlo Park, California 94025, USA

Abstract

SLAC is now installing LCLS-II, a superconducting electron linac driven by continuous RF at 1.3 GHz. The 4-GeV, 120-kW beam has a 1-MHz maximum rate and can be switched pulse-by-pulse to either of two undulators, to generate hard and soft x rays. Two detector types measure beam losses. Point beam-loss monitors (PBLMs) set limits at critical loss points: septa, beam stoppers and dumps, halo collimators, protection collimators (which normally receive no loss), and zones with weak shielding. PBLMs are generally single-crystal diamond detectors, except at the gun, where a scintillator on a PMT is more sensitive to the low-energy (1 MeV) beam. Long beam-loss monitors (LBLMs) use 200-m lengths of radiation-hard optical fiber, each coupled to a PMT, to capture Cherenkov light from loss showers. LBLMs protect the entire 4-km path from gun to beam dump and locate loss points. In most regions two fibers provide redundancy and view the beam from different angles. Loss signals are integrated with a 500-ms time constant and compared to a threshold; if exceeded, the beam is stopped within 0.2 ms. We report on our extensive tests of the detectors and the front-end signal processing.

INTRODUCTION

SLAC has removed the first km of its 3-km copper electron linac, completely emptying this part of the tunnel and the Klystron Gallery above it for the first time since construction in the 1960s. Half the cryomodules of the new LCLS-II superconducting-RF (SRF) linac are now in the tunnel. In addition, two variable-gap undulators, for hard and soft x rays are replacing the fixed-gap LCLS undulator.

The superconducting linac, driven with continuous-wave (CW) 1.3-GHz RF, will produce 4-GeV bunches with variable spacing at rates of up to 1 MHz. The new machine raises the maximum beam power from 500 W to 120 kW. An 8-GeV upgrade will later double this power. The need to prevent damaging beam loss has grown proportionately.

Previous Beam-Loss Detectors

Beam-loss detection at SLAC has long depended on gas-filled ionization chambers. “Protection ionization chambers” (PICs) are point beam-loss monitors (PBLMs), placed at likely loss locations such as collimators. Long beam-loss monitors (LBLMs) detect losses over tens of meters, using “long ionization chambers” (LIONS), which are hollow gas-dielectric (Heliac) coaxial cables. Because the ion transit through both types is slow, 1 to 5 ms, ions will accumulate during high-loss bursts from a high-rate

beam. As presented previously [1], the resulting space charge can screen the bias field inside the detector and suppress its response. This paper reports on the faster alternatives planned for LCLS-II [2], discussing both the design considerations and the testing necessary to gain approval for a new safety system.

BCS, MPS, and Diagnostics

The new loss detectors avoid past duplication by simultaneously serving three functions [2]: as inputs to the Beam Containment and Machine Protection Systems (BCS and MPS), and as beam diagnostics.

The BCS halts the beam if the loss level might harm people or safety devices. Because it requires robust and simple signal processing, with no knowledge of bunch timing and no software, loss signals are passively integrated on a capacitor with a 500-ms time constant. If this capacitor voltage exceeds a threshold, a shut-off command is issued.

The MPS is allowed greater flexibility to avoid damage from losses: it can trip the beam off or reduce its repetition rate, and recovers faster from trips. It shares the BCS time constant but with a lower trip threshold. A buffered copy of the integrated BCS signal is passed to the MPS.

Finally, the high-frequency component of the LBLM output will be digitized at 370 MHz and used as a diagnostic waveform, for beam-loss localization and for beam-profile measurements with fast wire scanners. The arrival time of a loss peak at the digitizer relative to the arrival of the electron bunch in the same region indicates the position of the loss. During a wire scan, software extracts the loss signal from the waveform and correlates it with the wire position to determine the bunch profile, without need for a dedicated detector. The software provides three sampling windows, configurable in width and delay, to numerically integrate loss peaks and subtract pedestal.

LONG BEAM-LOSS MONITORS

In place of LIONS, LCLS-II will use optical fibers as LBLMs. A loss shower passing through a fiber emits Cherenkov light, a portion of which is captured in a fiber mode and carried to a photomultiplier (PMT) at one end. For sensitivity, each fiber is relatively thick—with diameters of 600, 660, and 710 μm for the core, cladding, and buffer, respectively—and is encased in a 2-mm jacket of black polyurethane, for protection and opacity. The fiber, type FBP-600660710 from the Polymicro division of Molex, uses a special, radiation-resistant quartz. This and related types were subjected to extensive tests of radiation hardness for use in the end cap of the CMS detector on the LHC at CERN [3-5]. The FPB type was found to be superior, especially for red wavelengths around 700 nm.

* SLAC is supported by the U.S. Department of Energy, Office of Science, under contract DE-AC02-76SF00515.

[†] email address afisher@slac.stanford.edu

BEAM LOSS MEASUREMENTS USING THE CHERENKOV EFFECT IN OPTICAL FIBER FOR THE BINP E-E+ INJECTION COMPLEX

Yu.I. Maltseva*, V.G. Prisekin, A.R. Frolov

Budker Institute of Nuclear Physics SB RAS, Novosibirsk, Russian Federation

Abstract

Optical fiber based beam loss monitor (OFBLM) has been developed for the 500 MeV BINP Injection Complex (IC). Such monitor is useful for accelerator commissioning and beam alignment, and allows real-time monitoring of e-e+ beam loss position and intensity. Single optical fiber (OF) section can cover the entire accelerator instead of using a large number of local beam loss monitors. In this paper brief OFBLM selection in comparison with other distributed loss monitors was given. Methods to improve monitor spatial resolution are discussed. By selecting 45 m long silica fiber (with a large core of 550 μm) and microchannel plate photomultiplier (MCP-PMT), less than 1 m spatial resolution can be achieved.

INTRODUCTION

Beam loss diagnostics is one of the most important tasks during machine commissioning and operation. Beam loss monitors (BLMs) are useful for real-time beam loss monitoring during beam alignment and advanced beam diagnostics. The most common BLMs are long and short ion chambers, scintillation and Cherenkov radiation counters, secondary emission chambers and PIN-diodes. For the past two decades, a distributed BLM based on the Cherenkov effect in the OF is widely used as an alternative method to the local BLMs.

This type of BLM has been developed at several facilities such as CTF3 (CERN), Australian Synchrotron (ANSTO), ALICE (Cockcroft Institute), FLASH (DESY), SPring-8 (RIKEN/JASRI), IC (BINP) [1–7], etc.

Compared with other distributed beam loss monitors such as long ionization chamber and scintillating fiber, monitor based on the OF has the following advantages: fast response time of less than 1 ms, near-zero sensitivity to background signal (mainly gamma radiation) and synchrotron radiation, unlike scintillating fiber. The OF is insensitive to the magnetic field, but it is susceptible to radiation damage (except silica fiber), which limits its lifetime. Moreover, due to the fast process of the Cherenkov light generation (< 1 ns), this device allows detecting turn-by-turn beam losses in storage rings. The main disadvantage of all distributed BLMs is an issue with signal calibration due to signal distortion by transmitting it over long distances.

PARTICLE LOSS DETECTION

The basic idea behind the OFBLM is to detect a burst of the Cherenkov radiation (CR) generated in the OF by

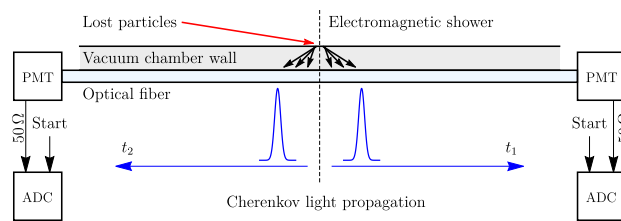


Figure 1: Beam loss detection with the OFBLM.

means of relativistic particles created in electromagnetic shower after highly relativistic beam particles (electrons or positrons) hit the vacuum pipe. Some of the CR photons propagate in the fiber and can be detected by a photodetector, e.g. PMT. Scheme of the OFBLM is presented in Fig. 1.

In our case, the timing of the PMT signal together with the beam injection/extraction trigger gives the location of the beam losses along the beamline. And the signal form gives us information about the number of registered lost particles.

The optical signal can be detected at either downstream or upstream ends of the fiber. Since beam velocity βc is greater than speed of light c/n in the OF, number of samples per meter can be written as: $1/s_d \approx f(n-1)/c$ and $1/s_u \approx f(n+1)/c$ for downstream and upstream fiber end, respectively, where n – core refractive index, f – ADC sampling frequency.

Hence, for $n = 1.5$ five times greater monitor spatial resolution can be achieved by detecting the CR at the upstream end of the fiber compared with the downstream one. Despite upstream signal sensitivity is ~ 10 times lower than downstream one, the former is preferable.

MONITOR REQUIREMENTS

Since 2016 the IC supplies two BINP colliders with high energy electron and positron beams via recently constructed K-500 beam transfer line [8–10]. It consists of two successive 300 MeV electron linac and 500 MeV positron linac and dumping ring (DR). The DR stores electron or positron beams for further extraction to the K-500 beam transfer line.

During 2018/2019 season facility operated at 400 MeV with linac repetition rate of up to 2 Hz for electrons and 5 Hz for positrons. Extraction repetition rate is up to 1 Hz. Beam production parameters are 2 – 5 nC (with bunch train of < 1 ns), which correspond to a 20 – 40 mA circulating beam in the 27.4 m DR. The typical value of beam losses during the transfer to the users is near 50%.

The main requirements for the OFBLM at the IC are the following:

- spatial resolution of < 1 m due to magnet spacing;

* yu.i.maltseva@inp.nsk.su

COMMISSIONING OF THE ARIEL E-LINAC BEAM LOSS MONITOR SYSTEM

M. Alcorta*, D. Dale, A.D. D'Angelo, H. Hui, B. Humphries, S.R. Koscielniak, K. Langton,
A. Lennarz, R.B. Nussbaumer, T. Planche, S.D. Rädcl, M. Rowe
TRIUMF, 4004 Wesbrook Mall, Vancouver BC, V6T 2A3, Canada

Abstract

The commissioning of the Advanced Rare Isotope Laboratory (ARIEL) facility at TRIUMF is underway. The 30 MeV e-linac has successfully been commissioned to 100 W, and to further increase the power to 1 kW the beam loss monitors (BLM) of the Machine Protection System (MPS) must be fully operational. There are currently two types of BLMs employed in the e-linac; long ionization chambers (LIC) and scintillators, consisting of a small BGO coupled to a Photo-Multiplier Tube (PMT). A front-end beam loss monitor board was designed at TRIUMF to meet the strict requirements of the BLMs: a trip of the beam occurs on 100 nC in 100 ms of integrated beam loss, and the trip must occur in $< 10 \mu\text{s}$. This contribution reports on the status of the 1 kW BLM system commissioning and gives an outlook as the power is increased to the full 300 kW.

INTRODUCTION

The ARIEL facility [1] at TRIUMF is currently in its early commissioning phase. The ARIEL project itself consists of many phases: Phase 1 covers the construction of the electron-linac beamline in the electron hall and commissioning up to 100kW, and Phase 2 includes the construction and commissioning of the beamline up to the 100 kW electron converter target for the production of Radioactive Ion Beams (RIB) using photo-fission. Other phases include a beamline switch-yard, high resolution spectrometer, a charge breeding facility, and the construction of an additional proton beam line for the production of RIB using the Isotope Separation On-Line (ISOL) method. The total available power of the electron beam is 300 kW (10 mA cw beam current at 30 MeV), but the beam dump and the electron converter target will limit the operation to 100 kW for the foreseeable future. Currently ARIEL is in phase 1, and the power is limited to 100 W until the Machine Protection System (MPS) is fully commissioned.

The MPS for ARIEL [2] consists of several different aspects, including beam loss monitors, beam position monitors, and administrative controls. As the final line of defense in case of an errant beam spill, the requirement on the BLMs is that they must trip the accelerator if an integrated beam spill of 100 nC in 100 ms occurs. This can take place by the following two beam spill scenarios at the extremes of time and loss: the full 10 mA electron beam is spilled in $10 \mu\text{s}$, or $1 \mu\text{A}$ of beam spill sustained loss over 100 ms. This trip level is defined as a catastrophic loss event and

requires that the beam be turned off in $10 \mu\text{s}$, calculated as the time required to raise the temperature of the material to 200°C in a worst-case scenario.

The BLMs also protect against chronic loss of the electron beam, defined as losses below the catastrophic level but greater than 1 W/m , or $\sim 30 \text{ nA/m}$ average beam loss. Unlike a catastrophic loss scenario which can cause immediate damage to the accelerator, a chronic beam spill is a concern for long-term activation of components for hands-on maintenance. Therefore it does not require an immediate trip, and instead will send out warnings to the operators on duty and reduce the duty factor if necessary.

The commissioning of the MPS BLMs in the electron hall is being done in stages. The first stage involves increasing the beam power from 100 W to 1 kW, starting with the low-energy section (ELBT) at 300 keV, followed by the medium energy section (EMBT) at 10 MeV, and finally the high energy section (EHAT) at 30 MeV. Figure 1 shows a layout of the electron hall which indicates the different areas separated by energy. The low-energy and medium-energy sections have been fully commissioned and are ready for 1 kW beam power, while the high energy section BLM commissioning is underway.

BEAM LOSS MONITORS

There are two types of BLMs employed at in the e-linac: LICs (see Fig. 2) and PMTs, the latter consisting of a 1 cm^3 BGO scintillator coupled to a PMT (see Fig. 3). The length of the LICs is variable, ranging from 0.5 m to 3 m, depending on sensitivity and space requirements. The LICs are filled with a constant flow of Argon gas for prompt charge collection. A positive high voltage is applied to the outer conductor, and the signal is taken from the inner conductor. The PMTs use a modified base with three different gain settings, corresponding to 1 dynode, 2 dynodes, or 3 dynodes of amplification. The HV of the PMT can be varied to adjust the gain setting as well. The PMTs are equipped with an LED housed inside the device, which is used for calibration purposes and for self-checks to ensure each PMT is properly working. Both types of BLMs have demonstrated a range of 10^6 , from $\sim 100 \text{ pA}$ to $\sim 100 \mu\text{A}$. This large sensitivity meets both the catastrophic and the chronic beam loss requirements.

TRIUMF BEAM LOSS MONITOR MODULE

The TRIUMF Beam Loss Monitor module (TBLM) [3], shown in Fig. 4, is a front-end electronics board developed

* malcorta@triumf.ca

SCREENS FOR HIGH PRECISION MEASUREMENTS*

B. Walasek-Höhne[†], P. Forck, GSI, Darmstadt, Germany
K. Höhne, FAIR, Darmstadt, Germany
G. Kube, DESY, Hamburg, Germany
R. Ischebeck, PSI, Villingen, Switzerland

Abstract

Scintillation screens made of various inorganic materials are widely used for transverse beam profile diagnostics at all kinds of accelerators. The monitor principle is based on the particles' energy loss and its conversion to visible light. The resulting light spot is a direct image of the two-dimensional beam distribution. For large beam sizes standard optical techniques can be applied, while for small beam sizes dedicated optical arrangements have to be used to prevent for image deformations. In the modern linac based light sources scintillator usage serves as an alternative way to overcome limitations related to coherent OTR emission. Radiation damages and intensity based saturation effects, in dependence of the screen material, have to be modelled. In this proceeding, an introduction to the scintillation mechanism in inorganic materials will be given including practical demands and limitations. An overview on actual applications at hadron and electron accelerators will be discussed as summary of the Joint ARIES-ADA Workshop on 'Scintillation Screens and Optical Technology for transverse Profile Measurements' held in Krakow, Poland [1].

INTRODUCTION / APPLICATION

Scintillators are used since the early days of nuclear physics. In hadron and electron accelerators they are used for transverse beam profile measurements and in high energy physics for particle detection and tracking.

Profile measurements are important for controlling the spatial distribution of the particle beam, as well as the matching of different sections of the accelerator. The performance and safe operation of particle accelerators is closely connected to the matching of the transverse beam distribution. Scintillating screens are a direct, but intercepting, method to observe transverse beam profiles. A measurement can hardly be more intuitive than to see a beam spot right in the centre of a scintillating screen. One typical realisation is shown in Fig. 1. For this reason many investigations have been done over years to achieve precise monitoring of the particle distribution along accelerator chains with scintillating screens.

Over the last century a large number of organic and inorganic scintillators in all physical states were discovered. In diagnostics inorganic solid state scintillators, such as crystals, powder crystals or ceramics, are mainly used. The response of scintillating materials depends on beam parame-

ters such as energy, intensity, ion species and time structure. Therefore, scintillating materials have to be tailored with respect to specific application demands required at accelerator facilities. Due to the direct beam interaction, many investigations described in this paper were performed for particle fluxes much higher than for typical scintillator applications in medical imaging or high energy physics. Table 1 gives a simplified overview of scintillator usage in beam diagnostics at ion and electron accelerators, and typical high-energy physics applications, e.g. PANDA detector at FAIR.

Precise measurements of the size, profile and position of a particle beam striking a scintillating screen requires a carefully designed optical system to transfer the scintillation light to the camera, so the true particle distribution can be reconstructed. Aim is to capture a clean, sharply focused image of the scintillation plane, free of distortion, optical aberrations, non-linearity, or optical backgrounds.

SCINTILLATION

A beam of ionizing radiation passing through a scintillator generates electronic excitations. The relaxation of electronic excitations involves complex mechanisms which can be described using a scheme of the electronic band structure of the crystalline scintillator. As proposed by Vasil'ev [2], the general time-dependent scheme of scintillation can be described in five main stages. The first stage starts with the production of primary excitations (deep core holes and hot electrons) by interaction of ionizing particles with the material. In a very short time (10^{-16} - 10^{-14} s) a large number of secondary electronic excitations is produced by inelastic electron-electron (e-e) scattering and Auger processes with creation of electrons in the conduction band and holes in core and valance bands. This multiplication is stopped when the energy of electrons and holes becomes lower than the threshold of e-e scattering and Auger relaxation. The second stage deals with the thermalization of electrons and holes with the production of e.g. phonons. In the third stage localization of the excitations through their interaction with stable defects and material impurities can take place. It may occur together with formation of self-trapped excitons (trapping due to lattice relaxation, not attributed to crystalline defects or impurities) and holes in the crystal lattice, the capture of electrons and holes by traps, etc. As a result, these centers have localized states in the band gap. The two last steps are related with migration of relaxed excitations and radiative or/and nonradiative recombination of localized excitations (fourth stage). The localization of excitations is sometimes accompanied by a displacement of atoms (defect creation,

* This project has received funding from the European Union's Horizon 2020 programme under Grant Agreement No 730871

[†] b.walasek@gsi.de

FERMI-PSI COLLABORATION ON NANO-FABRICATED WIRE-SCANNERS WITH SUB-MICROMETER RESOLUTION: DEVELOPMENTS AND MEASUREMENTS

G.L. Orlandi*, S. Borrelli, C. David, E. Ferrari, V. Guzenko, B. Hermann,
O. Huerzeler, R. Ischebeck, C. Lombosi, C. Ozkan-Loch, E. Prat
Paul Scherrer Institut, 5232 Villigen PSI, Switzerland
M. Ferianis, G. Penco, M. Veronese
Elettra-Sincrotrone Trieste S.C.p.A, 34149 Basovizza, Trieste Italy
N. Cefarin, S. Dal Zilio, M. Lazzarino
IOM-CNR Laboratorio TASC, c/o Area Science Park - Basovizza, 34149 Trieste, Italy

Abstract

Wire-scanners with micrometer resolution are in operation at SwissFEL and FERMI for measurements of the beam emittance and for beam profile monitoring. In addition, both laboratories are developing and testing innovative nano-fabricated wire-scanners capable of providing sub-micrometer resolution and being quasi non-destructive to the beam. Nano-fabricated wire-scanners with a free-standing design and a sub-micrometer resolution has been already successfully tested. In the present work, innovative nano-fabricated wire-scanners joining both features of a free-standing design and sub-micrometer resolution are presented. Experimental tests carried out at SwissFEL demonstrated the capability of such innovative wire-scanner solutions to resolve transverse profiles of the electron beams with a size of 400 – 500 nm without incurring in any resolution limit constraint and with a minimal beam perturbation. An overview on current status and results along with future developments of these nano-fabricated wire-scanners are here presented.

PREMISE

The present proceeding is intended to be a guide to the reader of the slides of the talk presented in this conference as well as a short introduction to a manuscript submitted to a peer-reviewed journal for a publication [1,2]. The talk given in the present conference is a revised and enlarged version of a previous talk just given a week ago in another conference [3]. The reader of the present proceeding will hopefully pardon the authors for maintaining the same structure and contents [3] which in a time interval of only a week cannot reasonably benefit from any substantial improvement and update.

The present proceeding briefly reports on the recent experimental results obtained in the nano-fabrication and electron beam characterization of free-standing WS with sub-micrometer resolution. The free-standing WS prototypes - independently nano-fabricated at PSI and FERMI by means of lithographic techniques - can measure the transverse profile of an electron beam with a rms geometrical resolution

of about 250 nm. The experimental test of the PSI and FERMI WS prototype have been performed at SwissFEL, where electron beams with a vertical size smaller than 500 nm have been successfully and consistently resolved. All information and technical details on the nano-fabrication and experimental tests - carried out at SwissFEL - of the PSI and FERMI free-standing WS with sub-micrometer resolution are reported in a manuscript submitted to a peer-reviewed journal for a publication. For more details on the WS nano-fabrication and characterization, the reader is hence addressed to the archived version of the manuscript, to the paper submitted to the journal and to the slides of the conference talk [1,2]. In the present proceeding, the authors will summarize the main highlights, achievements and perspectives of the experimental work on free-standing WS with sub-micrometer resolution. In addition, the authors will briefly summarize the background experience of PSI and FERMI on nano-fabrication and test of WS. Results of satellite tests carried out at SwissFEL in parallel with the characterization of the free-standing WS will be reported as well. The introduction and the conclusion sections are directly derived from [1,2].

INTRODUCTION

Wire-scanners (WS) constitutes a precious complement to view-screens for monitoring the transverse profile of the electron beam in a linac [4–13]. Because of the multi-shot and mono-dimensional reconstruction of the beam transverse profile, WS are not timewise competitive with view-screens for beam finding and for matching the magnetic optics in an electron linac. WS are inappropriate for slice emittance measurements as well. Nevertheless, WS are a unique and essential diagnostics whenever the beam characterization requires a high spatial resolution along with a minimal invasivity to the beam operation. The spatial resolution of a WS depends on the measurement resolution of the wire positioning, on the possible wire vibrations and, finally, on the geometry of the wire. The geometrical resolution of a WS is inversely proportional to the wire width. This also determines the surface of impact of the wire with the electron beam and hence the wire transparency to the beam (also depending on the wire thickness for non-cylindrical wires).

* gianluca.orlandi@psi.ch

CHALLENGES IN CONTINUOUS BEAM PROFILE MONITORING FOR MW-POWER PROTON BEAMS

M. Friend*, High Energy Accelerator Research Organization (KEK), Tsukuba, Japan

Abstract

Continuous beam profile monitoring of the high-power proton beam is essential for protection of beamline equipment, as well as for producing high-quality physics results, in fixed-target extraction beamlines. Challenges in continuous profile monitoring include degradation of materials after long-term exposure to the proton beam, as well as beam loss due to that material intercepting the beam, which can additionally cause activation of nearby equipment. An overview of various profile monitoring techniques used in high-power neutrino extraction beamlines, issues faced so far at beam powers up to several hundred kW, and some possible future profile monitoring solutions for MW-class beamlines will be discussed.

HIGH-POWER EXTRACTION BEAMLINES FOR NEUTRINO EXPERIMENTS

The study of neutrinos by long-baseline neutrino oscillation experiments offers a unique opportunity to probe fundamental open questions in physics. One important open question relates to the possibility that CP violation in neutrinos may help explain the abundance of matter over anti-matter in the Universe.

Neutrinos are produced and detected in three distinct “flavors”, associated with each of the three charged leptons. It has been observed that when neutrinos propagate they can also change flavor, or “oscillate”, with a probability proportional to the distance traveled and inversely proportional to the energy of the neutrino. Long-baseline neutrino oscillation experiments, where a neutrino beam of one flavor is produced and, after traveling a distance of hundreds of kilometers, neutrinos of another flavor are detected, can therefore be used to probe the fundamental properties of the neutrino.

A high-power neutrino production beamline is essential for making a precise measurement of neutrino oscillations. A neutrino super beam is generally produced by a high-energy, high-intensity proton beam incident onto a long, radiation-tolerant target. Pions and other hadrons generated by this process are focused in a set of electro-magnetic focusing horns. The hadrons are then allowed to decay in a long decay volume, where pions decay into muons and muon-neutrinos. The muons are then stopped in a beam dump, while the remaining neutrinos travel through the earth as a relatively pure beam of muon-neutrinos.

Currently running neutrino oscillation experiments include the T2K experiment [1], with a beam produced at the

neutrino extraction beamline of the Japan Proton Accelerator Research Complex (J-PARC) Main Ring (MR) synchrotron in Japan, and the NO ν A experiment [2], which uses the NuMI beamline at Fermi National Accelerator Laboratory (FNAL) in the United States.

Plans exist to upgrade the J-PARC MR accelerator and neutrino beamline towards future measurements with higher neutrino fluxes [3], including for the future Hyper-Kamiokande experiment [4]. A new neutrino facility at FNAL, the LBNF facility for the DUNE long-baseline neutrino oscillation experiment, is also under design now [5].

Beam profile monitoring is essential to stably run these fixed-target neutrino production beamlines.

J-PARC and FNAL Proton Beams for Neutrino Extraction Beamlines

As summarized in Table 1, the J-PARC MR 30 GeV proton beam has an 8-bunch beam structure. The J-PARC MR currently runs at 485 kW with the plan to upgrade to 750+ kW by 2022 and 1.3+ MW by 2026. This will be achieved by increasing the beam spill repetition rate from the current one spill per 2.48 s, to 1.32 s and finally 1.16 s, along with increasing the number of protons per pulse (ppp) from $\sim 2.4 \times 10^{14}$ to 3.2×10^{14} .

The FNAL NuMI beamline utilizes a 700+ kW, 120 GeV proton beam with 588 bunches per spill. The beam intensity is 5.4×10^{13} ppp with a plan to increase to 6.5×10^{13} ppp. The duty cycle is 1.333 s, with plans to decrease to 1.2 s.

The beam spot size must be kept large enough to prevent damage to the target and beam window. The higher number of ppp and protons-per-bunch at the J-PARC neutrino extraction beamline necessitates a larger beam spot size than at NuMI.

Table 1: Specifications of the J-PARC MR and FNAL NuMI Proton Beams

	J-PARC MR	FNAL NuMI
Beam Energy	30 GeV	120 GeV
Beam Power	500 kW → 1.3 MW	700-750kW → 1 MW
Beam Intensity	2.4E14 ppp → 3.2E14 ppp	5.4E13 ppp → 6.5E13 ppp
Beam Bunches	8	588
Pulse Length	4.2 μ s	11 μ s
Duty Cycle	2.48 s → 1.16 s	1.333 s → 1.2 s
Beam Spot@Target	4 mm	1.3 → 1.5 mm

* mfriend@post.kek.jp

MEASURING THE BEAM PROFILE BY COUNTING IONIZATION ELECTRONS

H. Sandberg^{*1,2}, W. Bertsche², D. Bodart¹, B. Dehning¹, S. Gibson³,
S. Levasseur^{1,3}, K. Satou⁴, G. Schneider¹, J.W. Storey¹, and R. Veness¹

¹CERN, Switzerland

²University of Manchester, Cockcroft Institute, UK

³Royal Holloway, University of London, UK

⁴Accelerator Laboratory, KEK, Japan

Abstract

The principle of non-destructive beam profile measurement with rest gas ionization electrons has remained largely unchanged since the technique was first proposed in the late 1960's. Ionization electrons (or ions) are transported by an electrostatic field onto an imaging detector, where the spatial distribution of detected electrons is a direct measure of the transverse beam profile. The detector typically consists of one or more Micro-Channel Plates (MCP's) to amplify the signal, followed by either a phosphor screen and camera, or pickup electrodes. A long-standing problem is the ageing of the MCP's, which limits the accuracy of the beam profile measurement.

A new technique to detect ionization electrons has been developed at CERN, which uses a hybrid pixel detector to detect single ionization electrons. This allows the application of counting statistics to the beam profile measurement. It will be shown that a meaningful beam profile can be extracted from only 100 electrons. Results from the new instrument will be presented, which demonstrate the ability to measure the beam profile of single bunches turn-by-turn, which offers new opportunities for beam diagnostic insights.

IONIZATION PROFILE MONITORS

Ionization beam Profile Monitors (IPM's) have several strengths, the most important being the non-destructive nature of the measurement. This enables studies of the evolution of the beam profile throughout a full cycle. Many different techniques to detect ionization electrons have been studied over the years, but common to all is the need to amplify the ionization electron signal. To increase the signal strength it is usual to integrate over many turns and to add Micro-Channel Plates (MCPs) to amplify the original signal. The final detection of the amplified signal is done either optically - with a phosphor converter and intensified camera - or with analog pickup electrodes and amplifiers. A problem with these amplifications is that each conversion of the signal will provide distortion and add noise, making it more difficult to understand the relationship between the detected signal and the original signal coming from the ionization process. In addition, during the integration window, the beam width and position must remain constant other-

wise the measured beam profile will be convoluted with any changes in these parameters.

To overcome these limitations, a new type of IPM has been implemented where the detection is performed using hybrid pixel detectors. The pixel detector enables direct detection of single ionization electrons with the added ability to filter out background particles. A more detailed description of the instrument, the so-called PS-BGI, can be found in [1].

BENEFITS OF COUNTING

Direct detection allows the use of counting statistics in the analysis of the recorded data. The basic idea is that discrete events occur independently of each other at a known average rate within a fixed window of time, with the time between two events considered as random. For the PS-BGI, the events are the detected ionization electrons from the pixel detector and the known rate comes from the ionization process. The time window is set by how long the detector is enabled which, for example, could be one turn or a number of turns. If the ionization electrons are spatially separated and limited in number, they can be considered independent given the large detection area of 14 mm × 56 mm. These arguments fit well to a Poisson distribution.

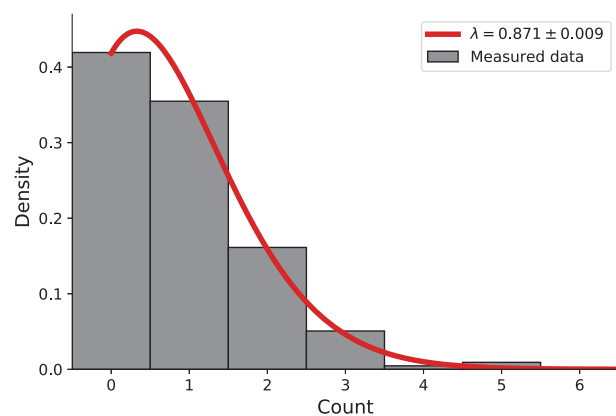


Figure 1: Measured counts from a single pixel column fitted with a Poisson distribution.

The Poisson distribution can be used to model the count of ionization electrons for a given transverse position. In the beam direction s , the count rate at a given transverse position is considered to be over the 14 mm length of the detector.

* hampus.sandberg@cern.ch

EXPERIMENTAL OBSERVATION OF SUBMILLIMETER COHERENT CHERENKOV RADIATION AT CLARA FACILITY

K. Fedorov*¹, P. Karataev, A. Oleinik³

John Adams Institute at Royal Holloway, University of London, Egham, United Kingdom

T. Pacey², Y. Saveliev²

ASTeC, STFC Daresbury Laboratory, Warrington, United Kingdom

A. Potylitsyn

Tomsk Polytechnic University, Tomsk, Russia

¹also at Tomsk Polytechnic University, Tomsk, Russia

²also at Cockcroft Institute, Warrington, United Kingdom

³also at Laboratory of Radiation Physics, Belgorod National Research University, Belgorod, Russia

Abstract

In current work we present the experimental results on Coherent Cherenkov Diffraction Radiation generation, observation and its further spectral analysis. All experimental work was performed at CLARA (Beam Area 1) facility (35 MeV beam energy at up to 10 Hz pulse repetition rate and sub-ps bunch length). For spectral analysis we used Martin-Puplett interferometer as it provides higher signal to noise ratio and allows us to perform charge normalisation. Furthermore we demonstrate the procedure of longitudinal beam profile reconstruction for a bunch with 0.6 ps Full Width at Half Maximum duration.

INTRODUCTION

Production and maintenance of short bunches in modern particle accelerators are forefront issues. Examples of accelerators that require short bunches are high quality particle physics facilities and linac-based fourth generation light sources. In practice, in order to verify the design and optimize the operation of such accelerators, it is necessary to obtain information on the bunch duration at various points along the accelerator beam line. Nowadays, the state of the art in non-invasive bunch length diagnostics is based on electro-optic technique. However, it is a cumbersome and an expensive device requiring a team of people to operate. The method of longitudinal beam profile diagnostic based on coherent radiation techniques is considered as one of the most perspective [1], because it could be embodied in a form of simple in use, robust and relatively inexpensive devices. Also, it has been theoretically demonstrated that coherent radiation techniques does not have any fundamental limitations for a bunch length diagnostics.

Nowadays, most studied coherent radiation technique is diagnostic with Transition Radiation (TR) [2], but its invasive nature excludes its use in modern and future facilities where the beam losses are limited. During past years reports about short bunches diagnostic based on Coherent Diffraction Radiation [3] mechanism have been also published. However, this methods suffers from coherent radi-

ation background (wakefields, synchrotron radiation, etc.) co-propagating along the beam and reflecting from the target. In this paper we report on another perspective method based on Coherent Cherenkov Diffraction Radiation (CChDR), which is induced by a charged particle traveling in the vicinity of a dielectric medium with the speed of particle higher than the speed of light inside this medium. First of all, this method promises relatively high intensity of coherent radiation, since according to the paper published by Tamm and Frank [4], the light intensity scales proportionally to the length of the radiator, which could be used to produce large photon flux by increasing the radiator size. Secondly, as it was shown later in 1955 by Linhart [5], Cherenkov Diffraction radiation could be induced by the interaction of electromagnetic field of the moving charged particle and atomic electrons on the surface of the dielectric, which opens the way for noninvasive diagnostic. Thirdly, CChDR is emitted at an angle θ , defined as $\theta = \cos^{-1} \frac{1}{\beta n}$, where n is the refractive index of radiator, and so could be separated from background radiation. In this work we report on successful implementation of diagnostics of 600 fs electron bunch via CChDR effect at CLARA machine at Daresbury laboratory. We will present the solution divided into three parts as follows:

- Theoretical calculation of ChDR single electron spectrum for the real experimental parameters;
- Experimental measurement of coherent ChDR spectrum at CLARA facility using Martin-Puplett interferometer as a most effective instrument for THz spectroscopy;
- Reconstruction of longitudinal beam profile using Fourier Transform and Kramers-Kronig phase analysis.

THEORETICAL BACKGROUND

Coherent radiation appears when the radiation wavelength is comparable to or longer than the charged particle bunch length. In this case the radiation photon yield is proportional to the number of electrons squared in contrast to the incoherent part of the spectrum, which is linear as a function

* fedorovkval@gmail.com

LONGITUDINAL PHASE SPACE RECONSTRUCTION FOR THE HEAVY ION ACCELERATOR HELIAC

S. Lauber^{*1,2,4}, K. Aulenbacher^{1,2,4}, W. Barth^{1,2}, C. Burandt^{1,2}, F. Dziuba^{1,2,4}, P. Forck²,
V. Gettmann^{1,2}, M. Heilmann², T. Kürzeder^{1,2}, J. List^{1,2,4}, M. Miski-Oglu^{1,2},
H. Podlech³, A. Rubin², M. Schwarz³, T. Sieber², S. Yaramyshev²

¹ Helmholtz Institute Mainz, Mainz, Germany

² GSI Helmholtzzentrum für Schwerionenforschung, Darmstadt, Germany

³ Goethe University, Frankfurt, Germany

⁴ Johannes Gutenberg University, Mainz, Germany

Abstract

At the GSI Helmholtzzentrum für Schwerionenforschung in Darmstadt, Germany, a prototype cryomodule (Advanced Demonstrator) for the superconducting (SC) continuous wave (CW) Helmholtz Linear Accelerator (HELIAC) is under construction. A transport line, comprising quadrupole lenses, rebuncher cavities, beam correctors and sufficient beam instrumentation has been built to deliver the beam from the GSI 1.4 MeV/u High Charge Injector (HLI) to the Advanced Demonstrator, which offers a test environment for SC CW multigap cavities. In order to achieve proper phase space matching, the beam from the HLI must be characterized in detail. In a dedicated machine experiment the bunch shape has been measured with a non destructive bunch shape monitor (BSM). The BSM offers a sufficient spatial resolution to use it for reconstruction of the beam energy spread. Therefore, different bunch projections were obtained by altering the voltage of two rebunchers. These measurements were combined with dedicated beam dynamics simulations using the particle tracking code DYNAMION. The longitudinal bunch shape and density distribution at the beginning of the matching line could be fully characterized.

INTRODUCTION

Super Heavy Element (SHE) research performs particle collision experiments with medium to heavy ions on heavy targets to cause fusion evaporation reactions. Extremely small cross-sections make a long beam time crucial the experiments [1, 2]. Whilst the GSI Universal Linear Accelerator (UNILAC) [3–7] is upgraded as an exclusive injector for the Facility for Antiproton and Ion Research (FAIR) [6, 7], a new SC CW heavy ion linear accelerator is built at GSI to keep the SHE research competitive. This project is carried out by GSI and HIM [8, 9] under key support of the GUF [10, 11] and in collaboration with the Moscow Engineering Physics Institute (MEPhI) and the Moscow Institute for Theoretical and Experimental Physics (KI-ITEP) [12, 13]. For different modern facilities worldwide, the operation of CW-Linacs is crucial, as for the Spallation Neutron Source (SNS) in the U.S. [14], or medium energy applications in isotope generation, material science and boron-neutron capture therapy [15]. All these ambitious projects strongly rely on

proper beam diagnostics, as minimal beam loss is a key quality to the machines as well as for superconducting multigap cavities [16].

Helmholtz Linear Accelerator

In the future, a new warm injector has to provide a 1.4 MeV/u CW heavy ion beam for the SC HELIAC [17]. It comprises of a Radio Frequency Quadrupole (RFQ) and an Interdigital H-Mode cavity (IH) together with two rebuncher cavities. Four cryomodules with compact SC CH cavities, SC solenoids and SC rebunchers [11] form the SC HELIAC section. Key features of the accelerator are a variable output energy (see Table 1) and the capability to provide for CW operation, while keeping the momentum spread low. The accurate implementation of the beam dynamics design is crucial for the CW-Linac project, as beam losses must be minimized to avoid the degradation of the superconducting cavities. Therefore, robust beam diagnostic methods are required, for the commissioning and routine operation.

The HELIAC stays in line with diverse ambitious Linac projects at GSI, namely the FAIR proton Linac [18], the UNILAC proton beam delivery [19–21], the linear heavy ion decelerator HITRAP (Heavy Ion TRAP) [22] and the LIGHT (Laser Ion Generation, Handling and Transport) facility for laser acceleration of protons and heavy ions [23].

Table 1: HELIAC Design Specifications [17]

	Value
Mass/charge	≤ 6
Frequency	216.816 MHz
Maximum beam current	1 mA
Injection energy	1.4 MeV/u
Variable output energy	3.5 MeV/u to 7.3 MeV/u
Output energy spread	± 3 keV/u
Repetition rate	continuous wave
Temperature	4 K

Demonstrator Environment

During 2017 and 2018, the novel CH design has been tested and validated in two measurement campaigns, with CH0 being the first of series to be extensively examined [17, 24, 25]. Beam from the injector HLI has been

* s.lauber@gsi.de

KALYPSO: LINEAR ARRAY DETECTOR WITH CONTINUOUS READ-OUT AT MHz FRAME RATES

Ch. Gerth*, B. Steffen, Deutsches Elektronen-Synchrotron DESY, Hamburg, Germany
M. Caselle†, L. Rota‡, Karlsruhe Institute of Technology (KIT), Eggenstein-Leopoldshafen, Germany
D.R. Makowski, A. Mielczarek, Lodz University of Technology (TUL), Łódź, Poland

Abstract

The novel linear array detector KALYPSO has been developed for beam diagnostics based on 1-dimensional profile measurements at high-repetition rate free-electron lasers (FEL) and synchrotron radiation facilities. The current version of KALYPSO has 256 pixels with a maximum frame rate of 2.7 MHz. The detector board, which comprises the radiation sensor, analog signal amplification, and analog-to-digital signal conversion, has been designed as a mezzanine card that can be plugged onto application-specific carrier boards for data pre-processing and transmission. Either a Si or InGaAs sensor can be mounted for the detection of visible or near infrared radiation. Results obtained in several beam diagnostics applications at the European XFEL and FLASH are presented to demonstrate the powerful capabilities of the KALYPSO detector.

INTRODUCTION

KALYPSO, a linear array detector - sometimes also denoted as 1D detector or line scan camera - has been developed for beam diagnostics applications based on the measurement of 1-dimensional distribution at high-repetition rates. A continuous data read-out at frame rates of up to 2.7 MHz has been achieved at the storage ring KARA [1]. In this paper we present results obtained at the Free Electron Laser at Hamburg (FLASH) [2] and European XFEL (EuXFEL) [3]. At FLASH, KALYPSO has been utilised to monitor the spectral distributions of FEL radiation pulses at an online spectrometer. At EuXFEL, electro-optical spectral decoding has been applied for the measurement of longitudinal bunch profiles, and near-infrared spectra of coherent diffraction radiation have been recorded for the study of micro-bunching instabilities.

DETECTOR SYSTEM OVERVIEW

The detector has been designed in a modular architecture: the radiation sensitive part, analog signal amplification, and analog-to-digital signal conversion are placed on a mezzanine card [1], which can be plugged onto application-specific carrier boards. A FPGA mezzanine card (FMC) carrier board has been developed for data acquisition and transmission to the accelerator front-end electronics in Micro Telecommunication Computing Architecture (MicroTCA.4)

standard [4] for integration into the control system and synchronisation to the accelerator timing system. The signal transmission via optical fibres enables a separation of a few hundred meters between the FMC carrier and the accelerator front-end electronics. A picture of the FMC carrier equipped with the KALYPSO mezzanine card is shown in Fig. 1.

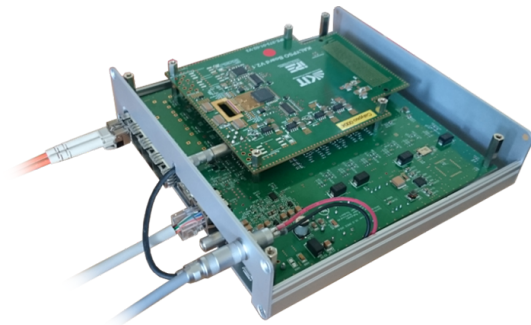


Figure 1: Photograph of the FMC carrier equipped with the KALYPSO mezzanine card.

A block diagram of the detector system is depicted schematically in Fig. 2. Currently, micro-strip sensors with 256 pixels and a width of 50 μm can be mounted on the KALYPSO mezzanine card. Up to now, two types of sensors have been employed: Si sensors for the detection of visible radiation, and InGaAs sensors that are sensitive in the wavelength range 900 nm to 1.7 μm . Each pixel of the sensor is bonded to an input channel of two modified versions of the GOTTHARD chip [5] that comprise analog signal amplification and 16:1 multiplexers. The resulting 16 differential outputs of both GOTTHARD chips are connected to a commercial 16-channel ADC (AD9249, Analog Devices) with 14-bit resolution that is operated at a sampling rate of 54 MHz. Compared to the original GOTTHARD chip, the correlated-double-sampling stage and automatic gain switching have been omitted in order to achieve a maximum frame rate of 2.7 MHz.

The FMC carrier [6] incorporates a FPGA (7-series Artix, Xilinx) and a DDR3 memory for data acquisition from the ADC on the KALYPSO mezzanine card as well as data processing and transmission via optical links to the accelerator front-end electronics. The accelerator front-end electronics is realized with a commercially available MicroTCA.4 board (MFMC, AIES) equipped with a FMC board for fast SFP communication (FMC-2SFP+, CAENels) which is connected via an optical fibre to one optical link of the FMC carrier. The total latency for data acquisition and processing of one frame with 256 pixels is less than 1 μs . This low

* christopher.gerth@desy.de

† Now at Gesellschaft für Schwerionenforschung, Darmstadt, Germany

‡ Now at SLAC National Accelerator Laboratory, Menlo Park, California, United States

DIRECT-SAMPLING COARSE BUNCH ARRIVAL TIME MONITOR IN THE FREE ELECTRON LASER FLASH BASED ON THE FAST DIGITIZER IMPLEMENTED IN THE FMC VITA 57.1 STANDARD

J. Zink*, M. K. Czwalinna, M. Fenner, S. Jablonski, J. Marjanovic, H. Schlarb
DESY, Hamburg, Germany
F. Gerfers

Dept. of Computer Engineering and Microelectronics, TU Berlin, Berlin, Germany

Abstract

At the free-electron lasers FLASH and European-XFEL bunch arrival times are monitored with a high-accuracy electro-optical based data acquisition system (BAM). Due to only a couple of picoseconds time measurement range of this system, large timing changes might cause the monitor to fail. To remove any ambiguity and for health status monitoring a high-speed direct-sampling FPGA mezzanine card (FMC) and an analogue RF front-end was added. The circuitry has lower precision than the electro-optical based BAM, but it can determine bunch arrival time with respect to a reference signal over a large time range, i.e. of the order of 1 ms. After restarts or larger energy changes during operation, the electron bunch arrival time may have been changed by tens or even hundreds of picoseconds, which causes that the BAM is out of its operation range and needs to be recalibrated. With the solution developed, the BAM gets the coarse bunch timing from the digitizer and adjusts its optical delay lines accordingly. This allows for finding the operation point fast and automatically. Performance data of the fast direct-sampling digitizer FMC and first measurement data from FLASH will be presented.

INTRODUCTION

In modern linear accelerators like *Free-Electron-Laser in Hamburg* (FLASH) or the *European X-Ray Free Electron Laser* (E-XFEL) one of the most critical systems is the *Low-Level-RF* (LLRF) control system. In FLASH and E-XFEL these systems are realized using the *Micro Telecommunication Computing Architecture* (MTCA.4). For measuring the pick-up signals coming from the accelerating superconducting cavities, a mixer is used to convert the 1.3 GHz signals down. Down converted signals are then fed into a digitizer. For several diagnostic applications like coarse *Bunch Arrival Time Monitor* (BAM) [1–3] or *Higher Order Mode* (HOM) sampling a cheaper and more simple solution is needed.

The mixer approach needs a very stable and accurate *local oscillator* (LO) signal, which generation can be expensive. To overcome this disadvantage, a direct-sampling digitizer based on an ADC with up to 1 GS/s was developed at DESY in 2018. First prototypes was tested and the second revision is in development right now. Figure 1b shows the first revision of the digitizer in ANSI/VITA 57.1 2010 FMC form



Figure 1: DFMC-DS500 digitizer board (a) top view (b) bottom view.

factor. BAM and HOM are realized as first test applications to see if the board can achieve the desired performance.

The new digitizer can be easily integrated in the existing MTCA infrastructure and is used in combination with the DESY *Advanced Mezzanine Card* DAMC-FMC25 FMC carrier board.

THEORETICAL ESTIMATION OF DIGITIZER PERFORMANCE

Before starting to measure the performance of the board a rough estimation of the resolution and SNR can be done. The frequency of the BAM and HOM signals is well known and always above 1 GHz. The BAM front-end has a bandpass filter with $f_c = 2.38$ GHz. The digitizers SNR and aperture

* johannes.zink@desy.de

A COMMON DIAGNOSTIC PLATFORM FOR ELETTRA 2.0 AND FERMI

G. Brajnik*, S. Cleva, R. De Monte, D. Giuressi, Elettra-Sincrotrone Trieste, Trieste, Italy

Abstract

Elettra 2.0 is the project of upgrading the current synchrotron light source to a low emittance machine. In this framework, various components of diagnostics have to be refurbished due to the obsolescence of the same or due to the tight requirements of the new accelerator. In this paper we present a high performance FPGA-based (Altera/Intel Arria 10) digital board developed internally, capable of hosting two FMC modules, equipped with DDR3 ram and 10 Gb/s Ethernet links. The presence of the FMC connectors allows a flexible use of the board: various configurations of A/D and D/A converters (different number of channels, resolution, sampling rate) can be obtained, also with various I/O ports for trigger and synchronisation. These features make it applicable as a base platform for various applications not only for Elettra (electron and photon BPMs, DLLRF systems, etc.) but also for Fermi (cavity BPMs, bunch arrival monitor, link stabiliser). The peripherals on board have been fully debugged, and probably a new version with a SoC (System on Chip) will be released in the next future.

INTRODUCTION

In a previous paper [1] we introduced a prototype of an electron Beam Position Monitoring system based on pilot-tone compensation, fully integrated in the Global Orbit Feedback system (GOF) of Elettra. In order to separate the analog and digital subsystems of the prototype, a modular design has been implemented. In this manner we had the chance to design, test and improve the analog signal conditioning subsystem, whose main goal was to feed any suitable digital acquisition system. The analog front end is still under testing even by external institutes, but up to now it has always shown remarkable performances [1]. For the first in-house evaluation of the front end, we put together a set of evaluation boards that globally acted as a digitiser; the drawback of this approach was the phasing out of various constituting devices, so they were not recommended for new designs. The evident lack of technology which was lived up to expectations, pushed us to develop in-house a suitable board with conversion and processing equipment powerful enough to be adopted as a generic board for a number of different diagnostics applications, both for Elettra 2.0 and Fermi accelerators. Taking into account that the operation of both accelerators relies on old equipment whose failure rate is supposed to increase over time, the design of this new generic board fulfils two goals: upgrade the full set of Elettra BPMs in the short time, replace the remaining acquisition systems in the long time.

* gabriele.brajnik@elettra.eu

DIGITAL PLATFORM FOR EBPM

The prototype is based on an Altera Stratix III FPGA, whose functional blocks are:

- two separate digital receivers (the first for beam signal, the second for the pilot tone) with CIC and FIR filters;
- two UDP Ethernet cores with SFP modules (Gigabit Ethernet);
- an external memory controller (1 GB of DDR2).

That design uses about 50 000 logic elements, 2 Mbit of embedded memory (FIFOs) and 88 DSP blocks. The incoming signals are digitised by four LTC2209 (16-bit, 160 MS/s), driven by a low jitter sampling clock synchronised with the machine clock of Elettra.

The new eBPMs, based on the incoming platform, should:

- house two complete BPM systems, optimising hardware, logic resources and interlock capabilities (angle detection);
- collect ADC raw data in a DDR SDRAM for post mortem and turn-by-turn beam analysis;
- share the acquired data by high speed links for reduced latency (10 Gbit/s);
- undersample the inputs by high-linearity 16-bit ADCs;
- drive the ADCs with a low jitter clock synchronised with the external reference (machine clock);
- export several digital I/Os (trigger, interlock, post mortem, ...);
- use four LTC2107 ADCs (16-bit, 210 MS/s). They have been already tested on an in-house developed FMC module and have shown better overall performances than the previously adopted LTC2209.

REPLACING DIAGNOSTICS IN ELETTRA AND FERMI

Since their first operation (1993 Elettra, 2010 Fermi), both lightsources rely on various equipment fully developed and built in-house. Due to ageing, it is mandatory to service partially or totally the installed equipment; the list of the systems involved in diagnostics tasks that need to be refitted is reported below:

- Low-Level RF system (LLRF - Elettra): it controls phase and amplitude of the RF power applied to the cavities that maintain stable the energy of the beam;
- RF Cavities Monitor (Elettra): it monitors the operating parameters of the cavities (vacuum, reflected power, temperature) and generates an interlock whenever required;
- Beam Dump Monitor (Elettra): it is a distributed system that acquires a number of critical operating parameters at turn-by-turn data rate, such as RF cavities power, beam current, radiation, interlock system. These data are sampled with a common timebase, aimed to bet-

HIGH-SPEED BEAM SIGNAL PROCESSOR FOR SHINE *

L.W. Lai[†], Y.B. Leng,
SSRF, Shanghai Advanced Research Institute, Chinese Academy of Sciences,
Shanghai, China

Abstract

A CW hard X-ray FEL is under construction in SSRF, which pulse rate is designed to 1MHz. A new high-speed sampling BPM signal processor is under development to meet the high performance requirements of beam position measurement system. The processor's sampling rate can be up to 500MHz, and beam position information of each bunch (1MHz rate) can be retrieved with the power of FPGA. Time stamp is aligned with the position data for offline analysis. The processor is designed to be a common signal processing platform for beam diagnostics. The first application is cavity BPM, and other applications, including button BPM, stripline BPM, and even wire scanner processor will be developed based on this platform. At the same time, a RF direct sampling processor is designed for cavity BPM signal processing. This novel technology will greatly simplify the cavity BPM electronic system, and make the system design more efficient and more flexible.

INTRODUCTION

SHINE is the abbreviation of Shanghai High repetition rate XFEL and Extreme light facility. SHINE is a 3110 meters long accelerator located at the 29 meters deep underground near SSRF. The energy is designed to be 8 GeV and repetition rate up to 1MHz. SHINE composed of a LINAC and 3 undulator lines, and to be completed in 2025.

There will have more than 300 cavity BPMs, stripline BPMs and button BPMs distributed along the injector, LINAC and undulator. A general BPM signal processing platform(DAQ) is under development to meet the diverse BPM data acquisition and signal processing requirements. RF conditioning components locate in an independent module before the DAQ.

The DAQ will apply state-of-the-art technology today to ensure the high performance even after 2025. Including a powerful SoC FPGA and high sampling rate and high resolution ADC. DAQ will supply 1MHz rate bunch position data with aligned timing information.

*Supported by Youth Innovation Promotion Association,CAS (Grant No. 2019290).; The National Key Research and Development Program of China (Grant No. 2016YFA0401990, 2016YFA0401903).

[†] lailongwei@sinap.ac.cn; lailongwei@zjlab.org.cn

PROCESSOR STRUCTURE

The DAQ is designed to be a SoC FPGA based standalone instrument. Figure 1 shows the DAQ structure. A Xilinx Zynq SoC FPGA containing both Arm CPU and FPGA, which enables realtime signal processing, data transfer and system control on one chip. The FPGA makes the DAQ structure simple and stable. There have two FMC interfaces on the FPGA board supporting two FMC cards for special applications. One is ADC FMC card for analog signal digitizing. One is white rabbit FMC timing card providing timing information for each trigger. Besides are peripheral components such as DDR, connectors and indicators.

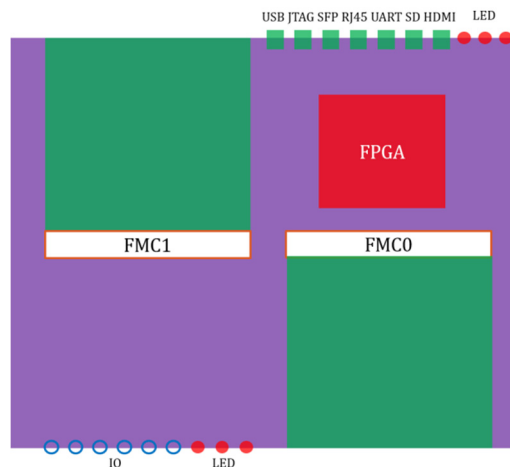


Figure 1: DBPM signal processing structure.

DAQ is designed to be 1U height. Figure 2 is the chassis size and the front panel and back panel. There have various connectors on the front panel, such as timing FMC card slot, JTAG, SFPx2, RJ45, UART, SD card slot, I/O, USB. Back panel have an ADC FMC card slot, and some I/O connectors.

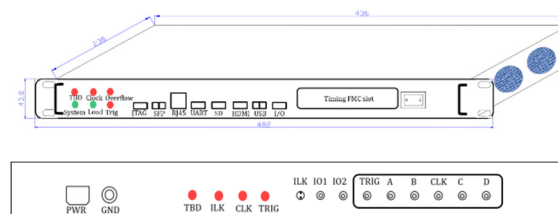


Figure 2: DAQ front and back panel.

PLC BASED FLEXIBLE AND SCALABLE VACUUM CONTROL AT THE ARGONNE TANDEM LINEAR ACCELERATOR SYSTEM (ATLAS)*

Y. Luo[†], C. Peters, S. Sharamentov, G. Bilbrough, C. Dickerson, M. Hendricks, A. Germain
Argonne National Laboratory, Argonne, IL, USA

Abstract

The beamline sections of an accelerator and different ion sources require a vacuum system capable of providing pressures down to 10^{-10} Torr. To control, monitor, and provide interlock protection of the vacuum equipment, a PLC-based vacuum control system was developed and tested at the Argonne Tandem Linear Accelerator (ATLAS). This system was designed to be highly flexible and scalable to meet the variety of equipment and configurations at ATLAS. The current FPGA-based system is reliable and fast, but is very difficult to maintain and upgrade. Particular attention was paid to the signal distribution to promote standard cable connections, minimize the usage of terminal blocks, and reduce the time to troubleshoot problematic channels. The system monitors the status of fast acting relays for interlock or control purposes, and utilizes RS-485 communication to gather lower priority information such as pump speeds or vacuum pressure readouts. The vacuum levels are monitored to interlock the high voltages of some beam instruments to protect against sparks as the Paschen minimum is approached. This paper mainly presents work on hardware interface to various vacuum devices.

INTRODUCTION

ECR (Electron Cyclotron Resonance) and EBIS (Electron Beam Ion Source) ion sources are used at ATLAS to generate beams along with other sources. There are two ECR (ECR2 and ECR3) sources and one EBIS here.

Paschen's law is an equation that describes the breakdown voltage between two electrodes in a gas as a function of pressure and gap length [1]. As shown in Fig. 1, the breakdown voltage drops dramatically when the vacuum condition of the system gets worse from high vacuum level. Without any protection, some beam instruments such as beam extractor, puller may generate high voltage (HV) sparks which could damage themselves or other beam components. So it is very important to interlock the HV bias of those beam instruments to the related vacuum levels to prevent HV sparks related to bad vacuum.

We have some aged in-house custom built vacuum hardware used for some other beam sections. It combined analog logic control circuitry and outdated FPGA (Field Programmable Gate Array) devices to control some specific vacuum devices. There are different revisions depending on their original intended purposes. For example, some chassis don't provide a remote vacuum pressure reading and some don't support a separate turbo pump, causing additional effort to integrate into the control system [2].

A new PLC (Programmable Logic Controller) based vacuum control system was proposed after communication with operators, engineers and management people. Then it was developed. The prototypes which were developed before finalized design requirement due to project schedule have been utilized in EBIS and ECR3. ECR3 is a newly developed ion source. The modified final design has been finished and will be deployed into other areas of ATLAS. The new system is highly flexible and scalable. The details are discussed below.

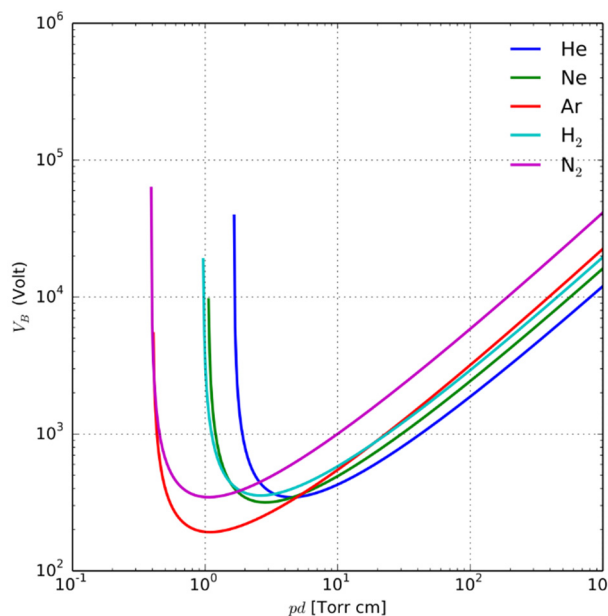


Figure 1: Paschen curves obtained for different gases.

DESIGN AND IMPLEMENTATION

The conceptual structure of the PLC based system is shown in Fig. 2. The PLC system used contains Modicon M340 system with Ethernet, RS-485 and some I/O modules, such as BMXDDI6402K and BMXDDO3202K. The PLC system communicates with the PLC interface, distributing output control and grouping input status signals. The interface chassis also provides RS-485 path for the PLC to collect pressure readout and other information. Then the valve and pump stations connect to the individual vacuum devices for controlling, status information collecting and RS-485 communication. Standard D-sub cables are used as much as possible to reduce the label time of making custom cables and costs. Most of the cables to the specific vacuum devices are also standard D-sub cables with one end re-terminated to the device's configuration.

* This work was supported by the U.S. DOE, Office of Nuclear Physics.

[†] Email: yluo@anl.gov

TRANSVERSE EMITTANCE MEASUREMENT OF A 2.5 MeV PROTON BEAM ON LIPAc, IFMIF'S PROTOTYPE

J. Marroncle, B. Bolzon*, P. Abbon, T. Chaminade, N. Chauvin, S. Chel, J.-F. Denis, A. Gaget
CEA-Saclay, Gif-sur-Yvette, France

P. Cara, IFMIF/EVEDA Project Team, Rokkasho, Aomori, Japan

J. M. Garcia, D. Jimenez-Rey, A. Ros, V. Villamayor, CIEMAT, Madrid, Spain

H. Dzitko, D. Gex, A. Jokinen, A. Marqueta†, F4E, Garching, Germany

L. Bellan, M. Comunian, E. Fagotti, F. Grespan, A. Pisent, F. Scantamburlo, INFN, Legnaro, Italy
A. Rodriguez, ESS-Bilbao, Zamudio, Spain

T. Akagi, K. Kondo, M. Sugimoto, QST, Rokkasho, Aomori, Japan

Abstract

IFMIF (International Fusion Materials Irradiation Facility) is an accelerator-driven neutron source aiming at testing fusion reactor materials. Under the Broader Approach Agreement, a 125 mA / 9 MeV CW deuteron accelerator called LIPAc (Linear IFMIF Prototype Accelerator) is currently under installation and commissioning at Rokkasho, Japan, to validate the IFMIF accelerator. During the deuteron beam commissioning at 5 MeV which started in June 2018, the horizontal and vertical transverse emittance of a 2.5 MeV proton beam have been measured downstream of the RFQ for different machine configurations. Such measurements were done with an emittance measurement unit composed of slits defining a beamlet of 200 μm width, then of steerers and finally of a SEM-Grid monitor. In this paper, the process and the system are first described. The secondary electron emission of SEM-Grid wires is then estimated based on measurements and results are close to the usual rule of thumb. Finally, emittance measurements are presented and comparisons with beam dynamics simulations show good agreement.

INTRODUCTION

The International Fusion Materials Irradiation Facility (IFMIF) is an accelerator-driven D-Li neutron source that will produce high energy neutrons at high intensity to characterize and qualify fusion reactor materials [1-3]. It aims of accelerating 125 mA/CW deuterium ion beam (D^+) up to 40 MeV. Its design performance will step forward present accelerator technological frontiers. It is presently in its engineering validation phase [4-7] with the Linear IFMIF Prototype Accelerator (LIPAc). The LIPAc aims to validate the IFMIF accelerators up to the first SRF Linac with a 125 mA / 9 MeV CW deuteron accelerator. It is being assembled, commissioned and will be operated in Rokkasho under the Broader Approach agreement, concluded between the European Atomic Energy Community (Euratom) and the Government of Japan.

After the injector commissioning phases A and B0 [8-10] with 140 mA/100 keV D^+ beam extraction, the LIPAc commissioning is currently in its phase B. This phase consists of accelerating D^+ beam through the RFQ up to 5 MeV

in pulsed mode at low duty cycle (0.1% in nominal) [11], and to transport the beam through the Medium Energy Beam Transport (MEBT) line and the Diagnostic Plate (D-Plate) up to the Low Power Beam Dump (LPBD). The commissioning of the MEBT line [12], to match the beam entrance characteristics into the SRF, and the commissioning of beam diagnostics are ongoing [13].

For a first tuning of the different subsystems, an equal perveance 70 mA/50 keV proton beam (H^+) has been successfully accelerated at the beginning of phase B (on 13th June 2018) up to 2.5 MeV through the RFQ [14]. The full characterization of the H^+ beam has been performed with a large variety of diagnostics located on the D-Plate. Among them, an emittance measurement unit (EMU) composed of slits, steerers and a SEM-Grid monitor had been set-up to allow horizontal and vertical emittance measurements without space charge issue. In this paper, the EMU is first described. Then, the beam profile measurements performed with the SEM-Grid alone are presented in order to give an estimation of secondary electron emission on wires. Finally, the emittance measurements are presented and compared to beam dynamic simulations.

EMITTANCE MEASUREMENT

Introduction

The emittance measurement in the D-Plate has to be made with 2.5 MeV H^+ beam and 5 MeV D^+ beam (D-Plate located currently downstream of the RFQ), and with 4.5 MeV H^+ beam and 9 MeV D^+ beam (D-Plate located in the future downstream of the SRF-Linac). The principle is depicted on Fig. 1 for a horizontal emittance measurement (X-axis). A short pulse length beam, coming from the left, is mainly stopped in a movable slit able to sustain high beam power deposition (aperture: 100 or 200 μm), leaving only a beamlet passing through it. The maximum pulse length is 100 μs (repetition rate of 1 Hz) assuming the nominal beam current of 125 mA. The beamlet profile is measured on the Y-SEM-Grid plane for each position of the vertical slit (Y-axis) moving transversely wrt X-axis. This method gives access to the angular divergence of the beam versus its transverse coordinate (X), from which the X-emittance is extracted.

The LIPAc's SEM-Grid monitor has large wire gaps (1, 2 and 3 mm), limiting the measurement resolution of the

* benoit.bolzon@cea.fr

† Presently at ITER, Cadarache, France.

TRANSVERSE PHASE SPACE SCANNER DEVELOPMENTS AT IPHC

F. Osswald[†], T. Adam, P. Graehling, M. Heine, C. Maazouzi, E. Traykov, Université de Strasbourg, IPHC, CNRS, UMR7178, 23 rue du Loess 67037 Strasbourg, France

Abstract

The Emittance characterization of charged particle beams is a standard and important tool to assess the performances of a facility. Due to emittance growth, beam losses, space charge and their incidence on beam matching and transport, the accurate measurement of the transverse phase space distribution of the charged particles is still an up-to-date issue. It enables detailed characterization of particle position and incidence distributions in addition to centroid position, profile, beam current and sectional shape measurement. It gives access to the particles distribution of the halo, a region of lower density important for high power accelerators and high intensity radioactive beams as they request reduced losses and damages thus less contaminated parts and nuclear waste for safe handling. Transverse phase space scanners are designed at IPHC and based on the Allison principle. They are currently used on different injection channels of large facilities as SPIRAL 2 and FAIR and will be used in the future on the DC280-SHE facility at JINR. A review of the IPHC's high resolution scanner design, development programme and future challenges are presented especially for beam halo analysis and "loss less" beam transport lines.

INTRODUCTION

The transverse phase scanner has been initially developed at IPHC in the 2000s for the SPIRAL 2 project then for FAIR with CEA-IRFU [1-5]. It is dedicated to low- energy ion-beam characterization. It is a slit-slit system based on Allison principle [6]. Each beamlet sampled by the entrance slit is analysed according to its incidence angle and energy. The analysis is performed by an electrostatic deflector composed of two parallel plates and a simple relation links the applied voltage to the angle. The beamlet current intensity is measured with a Faraday cup located after an exit slit. Another emittance-meter based on a slit-grid system has been developed at IPHC in the 80s and guided probably later choices [7].

DESIGN PARAMETERS

The main design parameters of the transverse phase scanner in Fig. 1 are shown in Table 1. To note that maximum beam size is 80 mm in diameter, beam power is limited to 300 W in DC mode and can be increased with duty cycle and defocusing of beam thus by decreasing the power density. The beam current intensity is fixed to the range between 10 μ A and 3 mA in accordance with the characteristics of the front-end electronics i.e. the current-voltage convertor.

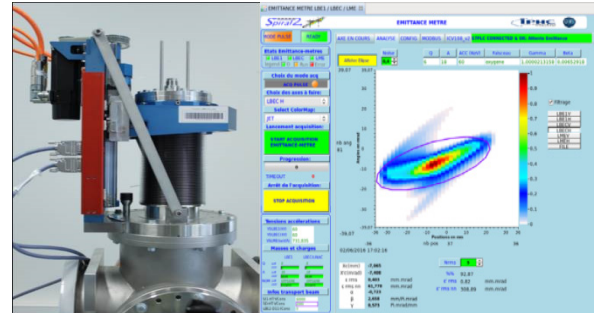


Figure 1: Transverse phase scanner mounted vertically – left part. Screenshot of 2D emittance figure on displayed control panel with computed data – right part.

OPTICAL PROPERTIES

The ions selected by the entrance slit are deflected by an electrostatic deflector composed of two parallel and polarized plates, see Fig. 2. The distribution of the positions of each beamlet is obtained with the measurement of the displacement of the motor. The simple relation in Eq. (1) between the applied voltage ($\pm V$), the accelerating potential (U) and the incidence angle (x' noted θ_A) is obtained with the equation of the motion of a charged particle in an uniform electric field and paraxial beam approximation. Simulations are performed with a 3D numerical model in order to assess the performances of the real system with slits and electron repeller limited apertures and fringe field of the deflector.

Table 1: Main Design Parameters

Scan plane	Horiz. or vertic.
Scan speed	Few min. - few hours
Scan length	≤ 123 mm
Resolution in position	100 μ m
Resolution in angle	1 mrad
Angular acceptance	+/- 100 mrad
Current intensity	10-3000 μ A
Power CW (DC)	≤ 300 W
Emittance normalized	0.01-1 π mm.mrad
Beam transverse envelop	≤ 80 mm in diam.
Time structure	DC or pulsed
Electron repeller	1 kV

THERMAL SIMULATIONS OF OPTICAL TRANSITION RADIATION TARGETS*

J. Pforr[†], M. Arnold, N. Pietralla, TU Darmstadt, Darmstadt, Germany

Abstract

The recirculating electron linac S-DALINAC provides beams with currents up to 20 μA and energies up to 130 MeV. It is planned to extend the beam diagnostics by adding multiple emittance measurement systems in order to investigate the emittance evolution along the beam line. The emittance measurement is based on the quadrupole scan technique and utilizes the existing quadrupoles and newly built optical transition radiation targets. As the targets are heated by the beam and destruction must be avoided, simulations of the thermal behaviour of the target were conducted. In particular, the dependence of the target temperature on the target design, but also variable parameters as beam spot size and current were investigated. This contribution will present these parameter studies.

NEW EMITTANCE MEASUREMENT SETUPS AT THE S-DALINAC

The S-DALINAC [1] is a thrice-recirculating electron linac. Its layout is shown in Fig. 1. In the injector, the electrons are accelerated to up to 10 MeV. Afterwards, the beam can be bent into the main accelerator, where an energy gain of 30 MeV per pass is possible. The three recirculation beam lines allow for four linac passes before the beam is extracted to the experimental hall [2].

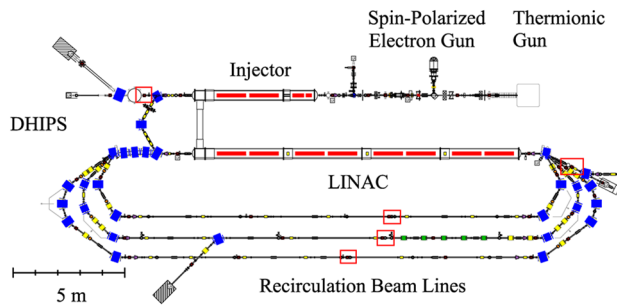


Figure 1: The layout of the S-DALINAC with three recirculation beam lines. The red boxes denote the positions of the new emittance measurement setups.

Our goal is to measure the emittance after each acceleration process. This shall allow to measure the emittance evolution along the beam line. Additionally, it would increase the reproducibility of the accelerator settings. The emittance measurement is based on a quadrupole scan [3] with optical transition radiation (OTR) targets. We installed one OTR target behind the injector, three in the recirculation beam lines and one in the extraction. Their positions are marked with red boxes in Fig. 1. For the quadrupole scan, we can use the existing quadrupoles. The targets are

observed by circuit board cameras, which are installed inside lead shielding as protection from radiation damage. These cameras are used routinely for other targets as well. Alternatively, we are testing a CMOS camera (FLIR BFLY-PGE-31S4M-C) that observes the target via mirror, so that it is not in the plane of the particle accelerator and there is more lead shielding possible. This camera was mainly chosen because many parameters, e.g. exposure time and gain, can be controlled remotely.

OPTICAL TRANSITION RADIATION

Transition radiation was predicted in 1947 by Ginzburg and Frank [4]. This radiation is created when a charged particle crosses the boundary between two media. The different permittivity of the media leads to a rearrangement of the electric field, and at the boundary, electromagnetic radiation is emitted. Since pioneering work was conducted in the 1970s [5], OTR is used for beam diagnostics. One advantage of OTR is that the emitted radiation is inherently proportional to the beam current, and the emission only takes place on the target surface. The emitted radiation is strongly directed, resulting in two cones of radiation in the backward halfspace, see Fig. 2. Its distribution was calculated in e.g. [6,7], but shall not be discussed here in detail. One notable aspect is the photon yield with a minimum frequency ω_{\min} , that can be expressed as [8]

$$\langle N_{ph} \rangle_{\omega > \omega_{\min}} \approx k \left[\left(\ln \frac{\gamma \omega_p}{\omega_{\min}} - 1 \right)^2 + \frac{\pi^2}{12} \right] \quad (1)$$

where γ is the relativistic factor, ω_p the plasma frequency and k a constant of proportionality. The plasma frequency is the oscillation frequency of electrons in the material.

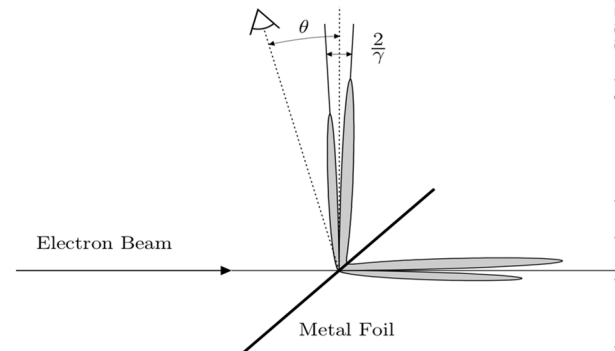


Figure 2: OTR intensity distribution for an electron beam crossing a metal foil. When the target is inclined by 45°, the radiation can be observed by a camera at 90° [9].

TARGET DESIGN

The requirements for the OTR targets include a high OTR yield, as the S-DALINAC is typically operating at

* Work supported by DFG through GRK 2128.
[†] jpforr@ikp.tu-darmstadt.de

DETERMINATION OF THE MOMENTUM SPREAD WHILE RUNNING IN THE ERL MODE AT THE S-DALINAC*

F. Schließmann[†], M. Arnold, M. Dutine, N. Pietralla, Institut für Kernphysik, Darmstadt, Germany

Abstract

The recirculating superconducting electron accelerator S-DALINAC at TU Darmstadt is capable to run as a onefold or twofold Energy Recovery Linac (ERL) with a maximum energy of approximately 34 MeV or 68 MeV in ERL mode, respectively. After the final acceleration in ERL mode, the momentum spread at the intended interaction point (IP) has to be determined. In order to investigate that momentum spread, a nondestructive measurement method is necessary. For this reason, it is planned to expand the beam horizontally in a section close to the IP by providing a well-defined horizontal dispersion. Using a wire scanner in this section for measuring the horizontal profile of the electron distribution, one can determine the momentum spread. The method of determining the momentum spread using the horizontal dispersion and the design of the wire scanner are presented.

INTRODUCTION

The S-DALINAC at TU Darmstadt is a superconducting electron accelerator with three recirculating beamlines [1]. A floorplan is shown in Fig. 1. The maximum energy gain is 130 MeV using all three recirculating beamlines for acceleration. Due to its recirculating scheme and a special path length adjustment system [2], the S-DALINAC is capable to run also as a onefold or twofold Energy Recovery Linac (ERL) [3]. The onefold ERL mode was already demonstrated in 2017 [2], while the twofold ERL mode is not yet demonstrated. When running in ERL mode, the electrons are accelerated, interact at an intended interaction point (IP) and are then guided back to the accelerator and will pass it with a phase shift of roughly 180° in order to be decelerated. In this way, the electrons will lose their energy which will be stored in the cavities and can be used in order to accelerate subsequent electrons. Since only a onefold or twofold ERL mode is available at the S-DALINAC, the maximum energy gain in ERL mode is 34 MeV or 68 MeV, respectively, instead of 130 MeV. In order to set up a stable and effective ERL mode, certain requirements for synchrotron phase and longitudinal dispersion are necessary. These also influence the momentum spread (see definition in the next section). The aim is not only to achieve an effective ERL mode but also to achieve a small momentum spread at the IP.

Therefore, it is important to measure the momentum spread while running in ERL mode. For this, it is necessary to use nondestructive measuring methods. If a destructive method will be used, not only the beam will be blocked but also the ERL mode gets destroyed and so only the momen-

tum spread generated by the conventional acceleration (CA) mode will be measured. At this time, it is still unknown whether the ERL mode leads to a different momentum spread than the CA mode, but since in the ERL mode the decelerated beam influences the electric field which accelerates the subsequent electrons, an impact on the energy gain and therefore on the momentum spread is expected. The influence of the ERL mode on the momentum spread can be determined by comparing the measured momentum spreads: once measured in ERL mode and once measured in the CA mode, i.e. with a beam blocked behind the IP. In the following, the definition of the momentum spread and the measurement method will be discussed in detail.

DEFINITION OF THE MOMENTUM SPREAD

Hereinafter, the subscript i indicates an individual electron. The relative momentum deviation δ_i is defined by $\delta_i := (p_i - p_0)/p_0$, where p_i is the electron's individual momentum and p_0 the design momentum. The quantity $\hat{\delta}$ denotes the centroid of the relative momentum deviation and is the arithmetic mean of all δ_i of the involved electrons. The standard deviation of all involved electrons' relative momentum deviation will be indicated by σ_δ and is the momentum spread, the quantity of interest. The hat as indicator for the centroid of a quantity and σ as indicator for the standard deviation of a quantity will be used in the following as well.

DETERMINATION OF THE MOMENTUM SPREAD

The aim is to measure the momentum spread σ_δ in a nondestructive way in order to keep the ERL mode alive. The best solution would be the usage of synchrotron radiation since it appears anyway while recirculating the beam. Mainly due to spatial constraints, it is unpractical to determine the momentum spread using the resulting synchrotron radiation in the intended section of the S-DALINAC. Furthermore, the horizontal dispersion in the dipole magnets is very small. Therefore, an alternative measurement method is necessary and that is the reason why a wire scanner will be used. A wire scanner is not perfectly nondestructive because it interacts with a part of the electron beam. Since it interacts only with a small fraction of the beam at a time (see details below), the vast majority of the beam remains unaffected and thus the ERL mode remains almost undisturbed. A wire scanner is therefore a good compromise and due to its specifications (see below) it can be considered as *quasi nondestructive*.

A wire scanner itself can be used to determine the transverse profile of the beam at position s . For a Gaussian beam profile in the horizontal plane, the standard deviation of it

* Work supported by BMBF through grant No. 05H18RDRB2 and DFG through GRK 2128.

[†] fschliessmann@ikp.tu-darmstadt.de

A FAST WIRE SCANNER SYSTEM FOR THE EUROPEAN XFEL

T. Lensch*, T. Wamsat, B. Beutner, Deutsches Elektronen Synchrotron, Hamburg, Germany

Abstract

The European-XFEL is an X-ray Free Electron Laser facility located in Hamburg (Germany). The 17.5 GeV superconducting accelerator will provide photons simultaneously to several user stations. Currently 14 Wire Scanner stations are used to image transverse beam profiles in the high energy sections. These scanners provide a slow scan mode for beam halo studies and beam optics matching. When operating with long bunch trains (>100 bunches) fast scans will be used to measure beam sizes in an almost non-destructive manner. This paper briefly describes the wire scanner setup and focusses on the fast scan concept and first measurements.

INTRODUCTION

The E-XFEL is a superconducting accelerator with an energy of up to 17.5 GeV. Within one RF pulse of 600 μ s up to 2.700 bunches can be accelerated. With a repetition rate of 10 Hz this corresponds to up to 27.000 X-ray pulses per second that can be distributed to the different undulator lines to allow for simultaneous operation of experiments [1]. Since spring 2019 the E-XFEL is operated with up to 600 bunches.

At the E-XFEL there are 14 wire scanner units installed. Each wire scanner unit consists of two motorized forks (horizontal and vertical plane). Each fork is driven by a separate linear servo motor. This 90° configuration of motors helps to avoid vibration influences. The wire position is measured with a linear ruler (Heidenhain) which has a resolution of 0.5 μ m. The motion unit is integrated by a custom front end electronic into the MTCA.4 [2] environment. A set of three 90° tungsten wires (50, 30 and 20 μ m) and two crossed 60° wires (10 μ m) is mounted on each titanium fork (see Fig. 1). This wire setup enables the users to make a 30° angled beam tomography with six scans at one location.

Wire scanner units are installed in groups of three upstream of the collimation section and upstream the undulator systems. Two locations in the post linac measurement section are equipped with an additional wire scanner unit each since summer 2019 to reduce the RMS error of the emittance measurement [3].

Several dedicated photo multiplier based detectors are installed downstream each set of wire scanner units. These fast 6-stage tubes are installed connected to a scintillating fiber wrapped around the beam pipe or connected to a scintillating paddel. Additionally regular beam loss monitors (BLM) can be used for loss detection [4] [5].

While slow scans with single bunches are a tool already used at the E-XFEL to measure beam halo distribution [6] and beam optics matching fast scans will allow to measure beam sizes in a non-destructive manner during user operation with long bunch trains.

* timmy.lensch@desy.de

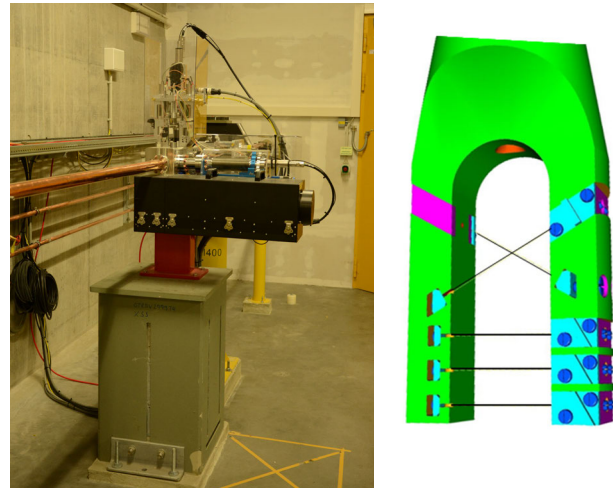


Figure 1: Left: wire scanner unit with horizontal and vertical plane installed in the E-XFEL with a screen station in the foreground. Right: 3D drawing of the fork with the different wires. Wire thicknesses from bottom to top: 50, 30 and 20 μ m) and two crossed 60° wires (10 μ m).

FAST SCAN

At the E-XFEL wire scanners had been developed to measure beam sizes within one long bunch train (bunch repetition rate up to 4.5 MHz) without interruption of user operation.

Technical Issues

To be able to hit bunches in fast scan mode the motor which drives the fork needs to be triggered with the general timing system. Using a custom trigger interface the motor controller is able to provide an adequate repetitive accuracy. Figure 2 shows the measured motor jitter of a fully assembled test setup.

The acceleration phase of the fork to the desired speed of 1 m/s takes about 20 ms. Depending on the z-position of the wire scanner unit and a region of bunches to be hit inside a bunch train an additional individual delay needs to be added to the timing trigger. Selection of the desired wire is also done by increasing this delay. Figure 3 shows complete strokes with different selection of wires. The area where the up to 600 μ s long electron beam is, is highlighted red.

Fast scans are only performed with a stroke out. After this motion the fork is directly moved back to the home position without hitting electron bunches again.

Correction of Bunch Position Offsets

During data acquisition the beam position at the wire might vary. Without correction the emittance could be over- or underestimated depending on the direction of the drift and the direction of wire motion. Figure 4 shows an orbit

Content from this work may be used under the terms of the CC BY 3.0 licence © 2019. Any distribution of this work must maintain attribution to the author(s), title of the work, publisher, and DOI

Content from this work may be used under the terms of the CC BY 3.0 licence (© 2019). Any distribution of this work must maintain attribution to the author(s), title of the work, publisher, and DOI

OBSERVATION OF SCINTILLATOR CHARGING EFFECTS AT THE EUROPEAN XFEL

A. Novokshonov*, B. Beutner, G. Kube
 Deutsches Elektronen Synchrotron (DESY), Hamburg, Germany
 S. Stokov, Tomsk Polytechnic University (TPU), Tomsk, Russia

Abstract

Scintillating screens are widely used for beam profile diagnostics at various kinds of particle accelerators. At modern linac based electron machines with ultrashort bunches as the European XFEL which is operated by DESY in Hamburg (Germany), scintillators help to overcome the limitation of standard OTR based monitors which is imposed by the emission of coherent radiation. The XFEL injector section is equipped with four off-axis screens allowing to perform online beam profile diagnostics, i.e. a single bunch out of a bunch train is kicked onto the screen and the profile is analyzed. However, during user operation a decrease of the SASE level was observed in cases that one of the off-axis screens were in use. The observation is explained by charging of scintillator screens: each deflected bunch hitting a screen causes ionization and results in electrostatic charging of the screen. The scintillator as good insulator keeps the charge for some time such that the non-deflected part of the bunch train feels their Coulomb force and experiences a kick, resulting in a drop of the SASE level. This report summarizes the observations at the European XFEL and introduces a simple model for quantification of this effect.

INTRODUCTION

The European XFEL is a free-electron laser located in Hamburg, Germany [1]. It is driven by a 17.5-GeV superconducting linac which operates at 10 Hz pulsed mode and delivers up to 2700 bunches per pulse.

The accelerator is equipped with scintillator screens in order to overcome the limitation of OTR caused by coherent effects [2, 3]. Most of the XFEL screen stations have a simple observation geometry which is introduced in Fig. 1: the electron bunch crosses the scintillator parallel to its surface normal; the light radiated from the scintillator is observed under an angle of 45°, then reflected by the mirror and focused onto a CCD via a wide-angle imaging lens. The CCD is oriented in Scheimpflug geometry in order to compensate the defocusing caused by depth-of-field effects.

In addition there is a number of screen stations that have additional so-called "of-axis" screens. In Fig. 2 the underlying scheme is plotted. The geometry for mirror, lens and CCD is the same than in Fig. 1, hence for simplicity only the is CCD depicted. Main difference is that the scintillator is slightly away from the bunch trajectory such that the majority of electron bunches pass nearby (blue dashed arrow), and only dedicated bunches will be kicked onto the scintillator

* artem.novokshonov@desy.de

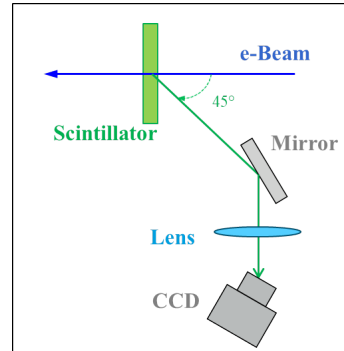


Figure 1: Standard scheme of scintillating screen monitors at the European XFEL.

(red dashed arrow) by a fast kicker magnet. The advantages of this setup are summarized in the following:

- A minimum perturbing online diagnostics may be performed by kicking only a single bunch out of a bunch train of up to 2700 bunches onto the scintillator. In addition, due to safety reasons the number of bunches which are allowed to hit a screen at 10 Hz repetition rate is restricted to a single one.
- Four off-axis screen monitors are paired together and can be operated in combination with a Transverse Deflection Structure (TDS). Besides conventional bunch profile measurements, this allows to measure longitudinal bunch profiles via streaking and to study online slice emittances in a minimum perturbing way.

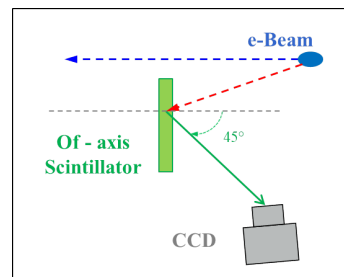


Figure 2: Of-axis screen scheme. Blue line: normal trajectory of electron bunches, red line: bunch trajectory of kicked ones crossing the scintillator.

The XFEL is operated with about 70 screen monitors, the majority is equipped with LYSO ($\text{Lu}_{1.8}\text{Y}_{0.2}\text{SiO}_5:\text{Ce}$) as scintillator material because of its good resolution as described in Ref. [4]. However, this material has other disadvantages, see e.g. Ref. [5]. Therefore the stations at which charging was observed utilize YAP ($\text{YAlO}_3:\text{Ce}$) as screen material.

IMAGE OF THE TRANSVERSE BUNCH PROFILE VIA COTR*

A. Potylitsyn[†], L. Sukhikh, T. Gusvitskii, Tomsk Polytechnic University (TPU), Tomsk, Russia
G. Kube, A. Novokshonov, Deutsches Elektronen Synchrotron (DESY), Hamburg, Germany

Abstract

The use of Optical Transition Radiation (OTR) monitors is a standard technique to measure transverse beam profiles at many electron accelerators. With modern accelerator technology it is possible to produce and accelerate even ultrashort electron bunches with sub-femtosecond duration. Such bunches interacting with the OTR target generate coherent optical transition radiation (COTR). For the COTR case, a reconstruction of the bunch profile from a recorded image using a conventional optical scheme is a task with inconclusive solution. In this paper we propose an approach which is based on the strict propagation of COTR fields through a focusing lens. As result we obtain a linear dependence of the measured rms image size on the bunch size.

INTRODUCTION

Optical transition radiation (OTR) monitors are widely used for transverse beam profile measurements of accelerated electron beams [1–4]. Such a technique can provide a sub-micron spatial resolution using the so-called “point spread function (PSF) dominated regime” [5]. In a recent publication [6] an approach based on the OTR characteristics using Zemax OpticStudio[®] [7] was developed which allows to take into account parameters of real optical systems. However, OTR monitors are able to measure only beam profiles for incoherent radiation, i.e. bunch length or bunch sub-structures have to be much longer than the OTR wavelength. Because of modern accelerator technologies as laser-driven plasma accelerators or free electron lasers [8–10] allow to generate sub-femtosecond and even attosecond electron bunches, they demand new diagnostic approaches [11]. Evidently, radiation in the visible spectral region of these bunches becomes coherent such that conventional OTR techniques cannot be applied any more. In this case, the radiation intensity depends on the squared number of electrons in the bunch, and the spectral-angular distribution of coherent OTR (COTR) is determined by the one of conventional incoherent OTR and the bunch form factor [12]. A profile image using COTR and measured with a standard optical system consisting of a focusing lens is a ring structure with a deep central minimum [13]. A few approaches were developed in order to reconstruct COTR generated bunch profiles using a conventional OTR monitor [13–16], but the approximations in use were rough, detailed simulations of this process meet a lot of troubles. In our work we give a consistent description of the optical scheme for COTR allowing to connect image parameters with the bunch size.

* This work was partly supported by the program “Nauka” of the Russian Ministry of Science, grant # 3.1903.2017

[†] potylitsyn@tpu.ru

MODEL

We consider the standard optical scheme which is illustrated in Fig. 1 together with the coordinate system in use. To simplify the final expressions describing the pattern in the detector plane and taking into account an initial beam profile, following Ref. [17] we use the dimensionless variables

$$\begin{aligned} \{x_T, y_T\} &= \frac{2\pi}{\gamma\lambda} \{X_T, Y_T\} \\ \{x_L, y_L\} &= \frac{\gamma}{a} \{X_L, Y_L\} \\ \{x_D, y_D\} &= \frac{\gamma}{a} \{X_D, Y_D\}, \end{aligned} \quad (1)$$

with γ the Lorentz factor, λ the radiation wavelength, and a the distance between target and lens. Cartesian coordinates indicated by small letters $\{x_i, y_i\}$ are dimensionless ones, by capital letters $\{X_i, Y_i\}$ dimensioned ones, the indices $i = T, L, D$ corresponds to target (T), lens (L) and detector (D) plane.

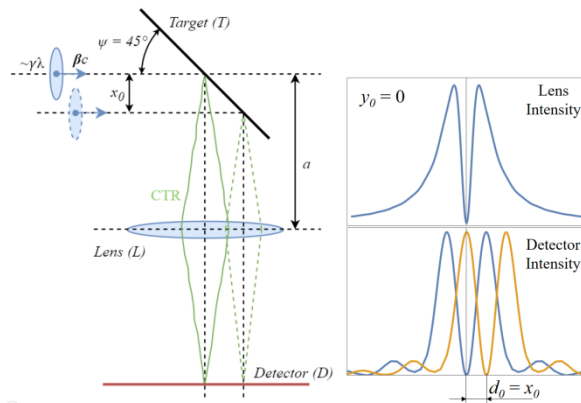


Figure 1: Typical scheme of OTR beam profile monitor.

In the limit of ultra-relativistic electron energies ($\gamma \gg 1$) the OTR process is described as a reflection of the electron field by a perfectly conducting target (an ideal mirror). For a particle passing through an optical system with trajectory coordinates $\{x_0, y_0\}$ relative to the optical axis (impact parameter $\sqrt{x_0^2 + y_0^2}$) it is straightforward to express the fields in the detector plane in paraxial approximation [17]:

$$\begin{aligned} E_{\{x,y\}}^D(x_D, y_D, x_0, y_0) &= \text{const.} \times \\ &\int dx_T dy_T \frac{\{x_T - x_0, y_T - y_0\}}{\sqrt{(x_T - x_0)^2 + (y_T - y_0)^2}} \times \\ &K_1 \left(\sqrt{(x_T - x_0)^2 + (y_T - y_0)^2} \right) \exp \left[i \frac{x_T^2 + y_T^2}{4\pi R} \right] \times \\ &\frac{4 \sin \left[x_m \left(x_T + \frac{x_D}{M} \right) \right]}{x_T + \frac{x_D}{M}} \times \frac{\sin \left[y_m \left(y_T + \frac{y_D}{M} \right) \right]}{y_T + \frac{y_D}{M}}. \end{aligned} \quad (2)$$

SLIT-BASED SLICE EMITTANCE MEASUREMENTS OPTIMIZATION AT PITZ

R. Niemczyk*, P. Boonpornprasert, Y. Chen, J. Good, M. Gross, H. Huck†, I. Isaev, C. Koschitzki, M. Krasilnikov, S. Lal, X. Li, O. Lishilin, G. Loisch, D. Melkumyan, A. Oppelt, H. Qian, H. Shaker, G. Shu, F. Stephan, G. Vashchenko, DESY, 15738 Zeuthen, Germany
 W. Hillert, University of Hamburg, 22761 Hamburg, Germany

Abstract

At the Photo Injector Test Facility at DESY in Zeuthen (PITZ) high-brightness electron sources are optimized for use at the X-ray free-electron lasers FLASH and European XFEL. Transverse projected emittance measurements are carried out by a single-slit scan technique in order to suppress space charge effects at an energy of ~20 MeV. Previous slice emittance measurements, which employed the emittance measurement in conjunction with a transverse deflecting structure, suffer from limited time resolution and low signal-to-noise ratio (SNR) due to a long drift space from the mask to the observation screen. Recent experimental studies at PITZ show improvement of the temporal resolution and SNR by utilizing quadrupole magnets between the mask and the screen. The measurement setup is described and first results are shown.

INTRODUCTION

Low transverse emittance is crucial for high-gain x-ray free-electron lasers (FEL) [1]. During the lasing process, the radiation is amplified by the electron beam within the cooperation length, which is often much smaller than the total bunch length. The transverse emittance inside this short longitudinal slice of the electron beam, i.e., the slice emittance, is more relevant for the FEL process than the projected emittance, thus of great interest for the FEL tuning [2].

At the Photo Injector Test Facility at DESY in Zeuthen (PITZ), see Fig. 1, RF electron guns are optimized and conditioned for use at the free-electron lasers FLASH and European XFEL in Hamburg [3]. Until now, the PITZ injector was experimentally optimized based on transverse projected emittance, as a reliable slice emittance diagnostics is still not established. Since the projected emittance optimization may not coincide with slice emittance optimization [4], the slice emittance diagnostics is in preparation.

For high-energy beams, where the space charge effect is negligible, the transverse emittance is usually mea-

sured with a quadrupole scan, where the emittance is reconstructed from beam images measured after propagation through different beam optics [5]. For a correct reconstruction the beam transport matrix has to be well-known.

At PITZ low beam energies of ~20 MeV and high bunch charges on the order of 1 nC complicate the beam transport due to strong space charge effects [6]. Therefore a single-slit mask is moved through the electron beam, allowing reconstruction of the phase space from the beamlet images on a screen downstream [7–9]. From the phase space the normalized transverse emittance

$$\epsilon_{n,x} = \beta\gamma\sqrt{\langle x^2 \rangle \langle x'^2 \rangle - \langle xx' \rangle^2}, \quad (1)$$

is calculated, where β is the mean electron velocity normalized to the speed of light, γ the average Lorentz factor and $\langle x^2 \rangle$, $\langle x'^2 \rangle$ and $\langle xx' \rangle$ the second-order beam moments [3].

Placing a transverse deflecting structure (TDS) downstream the slit mask, or operating an accelerating cavity off-crest while observing the beam image in a dispersive section allows for slice emittance measurements. Time-resolved emittance measurements with the booster are limited to ~2 ps [10], while slice emittance measurements with the TDS have already reached a resolution of down to ~1 ps [11].

However, the signal strength on the screen is low due to the small number of electrons passing the slit and the long drift length. Moreover, the TDS expands the beamlet in the vertical plane, leading to a low signal-to-noise ratio (SNR) which will underestimate the slice emittance due to signal removal during image noise subtraction. The use of quadrupole magnets between the slit mask and the observation screen reduces both the horizontal and vertical beta function at the measurement screen, which not only improves the time resolution, but also enhances the SNR for slice emittance measurements.

MEASUREMENT SET-UP

The RF electron gun operating at 1.3 GHz accelerates the electrons to an energy of ~6.3 MeV. A photocathode UV

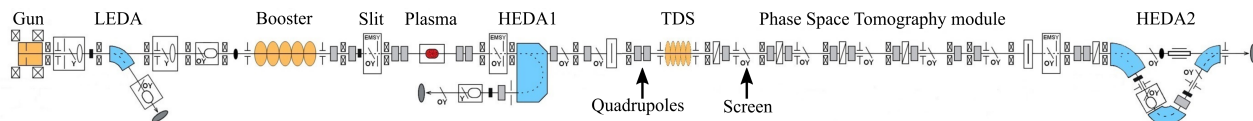


Figure 1: Schematic of the PITZ beamline.

* raffael.niemczyk@desy.de

† now at HZB

Content from this work may be used under the terms of the CC BY 3.0 licence (© 2019). Any distribution of this work must maintain attribution to the author(s), title of the work, publisher, and DOI

NEW COMBINED FUNCTION WIRE SCANNER-SCREEN STATION FOR THE HIGH RESOLUTION TRANSVERSE PROFILE MEASUREMENTS AT FERMI

M. Veronese*, A. Abrami, M. Bossi, S. Grulja, G. Penco, M. Tudor, M. Ferianis
Elettra-Sincrotrone Trieste S.C.p.A., Trieste, Italy

Abstract

We present the upgrade of the transverse profile diagnostics at the end of the FERMI Linac with a new high resolution instrumentation with the aim of improving the accuracy of the measurement of the twiss parameters and of the emittance. A scintillating screen, has been adopted instead of OTR screen due to known COTR issues. We used the same COTR suppression geometry that we had already implemented on our intra undulator screens and YAG:Ce as scintillating material. Screen based transverse profile diagnostics provide single shot measurements with a typical resolution of the order of tens of microns mainly due to refraction effects, geometry and other physical material properties. To extend the resolution to the micron level needed in case of low charge operation, we have equipped the same vacuum chamber with a wire scanner housing 10 μm tungsten wires. This paper describes the design and the first operational experience with the new device and discusses advantages as well as limitations.

INTRODUCTION

In a Free Electron Laser (FEL) it is of critical importance to have accurate knowledge of the optics along the machine to ensure stable operation of the machine. This translates in a significant effort from the electron beam instrumentation point of view in providing beam transverse profile measurement all along the FEL. For this reason modern FELs are equipped with instrumentation for transverse profile measurements all along the accelerator spanning from the injector to the very end of the accelerator. The two main types are wire scanners and view screens. Wire scanners have better resolution but can provide only 1D projection of the electron beam in a multi shot acquisition and thus are quite slow. View screens offer complete 2D distribution reconstruction in a single shot but have less resolution and may suffer from coherent optical transition radiation (COTR) or scintillator related limitations. At Fermi the initial design choice [1] for the linac was to have only view screens equipped with both YAG:Ce and OTR screens and no wire scanners. The screens have tilted at 45° screen with respect to the electron beam and with the imaging optics axis at 90° with respect to the electron beam. During operational experience at FERMI it became clear that COTR contamination was present on OTR screen making the unusable downstream the first bunch compressor (BC1) and also that it may also be present on YAG:Ce screen even with the laser

heater. At the end of the linac (1.5 GeV) where one of the key optics measurement is performed, it has become evident that the resolution of such view screen was not enough. To overcome such limitations in the undulator region the view screens were designed with a COTR suppressing geometry and better resolution [2]. A first experience with wire scanners was achieved with the tests of the PSI wire scanner prototype [3]. We recently decided to build an hybrid instrumentation hosting in a single vacuum chamber a wire scanner and a view screen. This paper describes its design and performances. The view screen which is used more often has a variable magnification to allow for high resolution for optics measurements and moderate resolution (but larger field of view) for longitudinal profile measurements when used in conjunction with the high energy RF deflector. Wire scanner can provide profile measurement with resolution of the order of few microns and is mandatory to be used for measurement at low charge (where the emittance drops and the screen resolution is insufficient) and is used for comparison with view screen in normal operation.

FERMI LAYOUT

FERMI is a seeded FEL based on the high gain harmonic generation (HG) scheme [4]. Two FEL lines, FEL-1 and FEL-2, are presently installed at the facility. FEL-1 is a single stage seeded FEL generating coherent light in the 65–20 nm wavelength range. FEL-2 is a double stage seeded FEL based on the fresh bunch injection technique [5, 6], where the additional stage extends the spectral range to 20–4 nm. At FERMI the electron bunch is generated at 10 Hz by a photo-injector GUN with energy of 5 MeV [7]. The electrons are accelerated by an S-band linac. The bunch length can be manipulated by means of a magnetic bunch compressor chicane (BC1). The microbunching present in the bunch can be mitigated before BC1 by a laser heater (LH) system. The final energy is up to 1.5 GeV in FEL operative conditions. After the acceleration, the electrons are injected into one of the two FEL lines (either FEL-1 or FEL-2). A layout of the FERMI FEL is shown in Fig. 1. The new combined function wire scanner plus screen station (MSCR-WS) is installed at the end of the linac before entering the Undulator Hall.

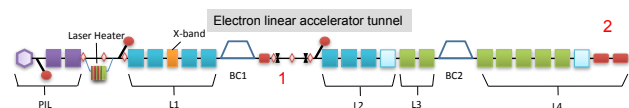


Figure 1: Layout of FERMI linac.

* marco.veronese@elettra.eu

WIRE SCANNER DIAGNOSTIC SYSTEM*

S. Grulja[§], S. Cleva, R. Demonte, M. Ferianis, Elettra Sincrotrone Trieste, Trieste, Italy

Abstract

Elettra Sincrotrone Trieste Research Center (Elettra) is one of the Italian Institutions, together with Istituto Nazionale di Fisica Nucleare (INFN) and Consiglio Nazionale delle Ricerche (CNR), committed to the realization of the Italian in-kind contributions for the European Spallation Source.

One part of the Elettra in-kind contributions to the proton accelerator is the construction of acquisition system for European Spallation Source (ESS) Wire Scanner (WS). This paper presents an overview of the diagnostic system of the ESS WS, including the first measurements with beam performed at CERN on LINAC4

OVERVIEW

The ESS diagnostic system adopts Wire Scanners for the measurement of the transverse beam profile [1] (Fig. 1). The purpose is to acquire and to made available to the ESS Integrated Control System (ICS) the signals either electrical or optical generated when a thin metal wire is scanned across the ESS accelerator beam. The amplitude of these signals is proportional to the charge density of the beam and the beam transverse profile may be obtained by plotting the signal amplitudes vs. the wire transverse position.

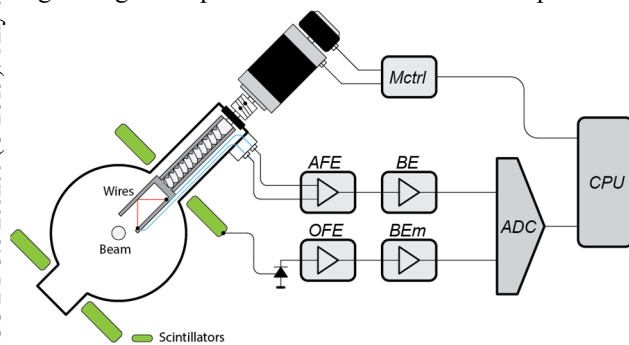


Figure 1: General Layout of wire scanner system.

The system acquires electrical and optical signal when a thin metal wire is scanned across the proton beam. The signal is proportional to the beam charge density. With obtained signal values the beam profile can be plotted.

The system is composed of custom developed hardware as Front Ends, Back Ends linked together and controlled by EPICS control and processing software.

The hardware components are Analog Front End (AFE), Back End (BE), Optical Front End (OFE) and Back End modified (BEm).

AFE-BE FOR THE CURRENT READ OUT

The Analog Front End (AFE) is used to read out the current from the wire intercepting the beam (Fig. 2).



Figure 2: Analog Front End.

It is located in the accelerator tunnel to minimize the signal loss connected to the associated Back End (BE) in the service gallery (Fig. 3).



Figure 3: Back End.

The Analog Front End (AFE) Trans impedance Amplifier (TIA) convert the ultra-low current generated in the wire into a voltage. This voltage is transmitted to the acquisition system at long distance, outside the machine tunnel (Fig. 4).

* Work supported by Elettra Sincrotrone Trieste
[§] sandi.grulja@elettra.eu -author

BEAM PROFILE MONITORS FOR THE CNAO EXPERIMENTAL LINE

C. Viviani[†], G. M. A. Calvi, L. Lanzavecchia, A. Parravicini, E. Rojatti, M. Manzini,

CNAO Foundation, Pavia, Italy

Abstract

The CNAO (Centro Nazionale di Adroterapia Oncologica) Foundation is the first Italian center for deep hadron-therapy. Since 2011, more than 2000 patients have been treated using Protons and Carbon ions. During the last 3 years an experimental line for research purposes has been built. The experimental line is equipped with three Scintillating Fibers with Photodiode array (SFP) detectors. The SFP is a profile and position monitor, whose sensitive part is made up of two harps of scintillating fibers. Each fiber is readout by a cell of a photodiode array. The SFP has been developed from the Scintillating Fibers harp Monitor (SFM) detector, the monitor presently installed along the CNAO extraction lines. The passage to the SFP results in a significant advantage in terms of cost, dimension, acquisition rate and flexibility. On May 19th, 2019 the first beam was extracted in the CNAO experimental room and the first in-line beam measurement with SFP was performed. The present work describes the SFP detectors, their achieved performances and the results obtained during experimental line commissioning.

DETECTOR OVERVIEW

The Scintillating Fiber with Photodiode array detectors (SFP) [1] are the beam profile monitors installed along the Experimental extraction line (XPR) of the CNAO (Centro Nazionale di Adroterapia Oncologica) accelerator (Fig. 1) [2].

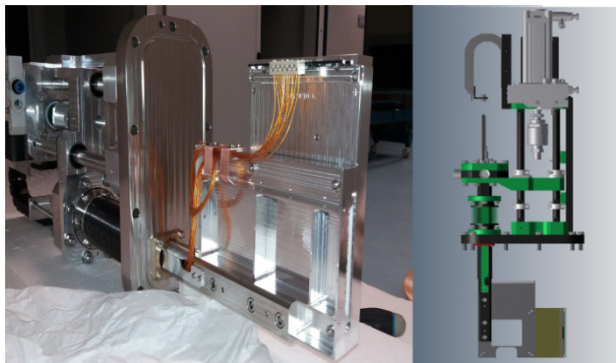


Figure 1: XPR layout with the SFP position

The SFP detector is the development of the Scintillating Fiber harp Monitors (SFM), the current profile/position monitors installed along the CNAO extraction lines. The main difference between SFM and SFP concerns the signal acquisition system: the CCD camera has been replaced by a photodiode array. The SFP working principle consists in the collection of light produced by the beam

crossing the scintillating fibers. The light is collected and converted in an electrical signal that depends on the number of particle crossing the sensitive area and on the beam energy. The integrated signal readout on the whole photodiode array gives the reconstructed profile of the beam. Three SFPs are mounted along the XPR line in order to reconstruct the beam trajectory (Fig. 2).

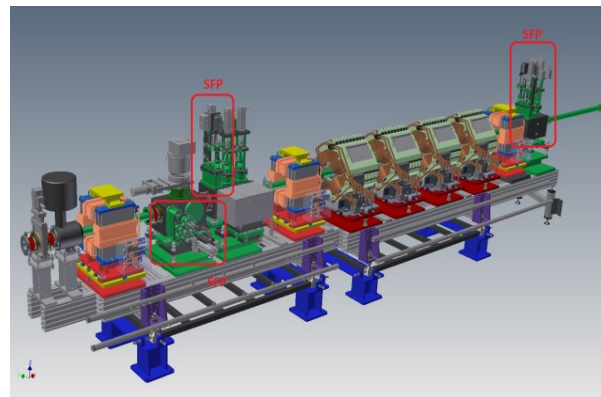


Figure 2: XPR layout with the SFP positions.

Mechanics

The sensitive area, whose dimensions are 64x64 mm², is made up of two orthogonal harps, with 128 fibers each. Fibers are arranged horizontally and vertically for vertical and horizontal profile measurements respectively. Scintillating fibers are of the SCSF-78 S type from Kuraray. They are 0.5 mm, square section plastic fibers. Each fiber is metalized all around in order to prevent signal cross-talk and light acquisition from other sources. Each harp is read-out by a photodiode array made up of 128 elements (mounted close to the beam line). The detector works under vacuum, with an expected vacuum pressure expected of 10 E-7 mbar. Signals are transmitted to the front end electronics by means of two vacuum connectors. The SFP can be moved into the beam trajectory by a pneumatic actuator (FESTO-DNC-50-100-PPV-ELH_2_03) and its position is checked by two mechanical limit switches that are engaged when the detector is IN or OUT respectively.

Electronics

As previously stated, the core of the SFP electronics readout is constituted by two photodiode arrays (Hamamatsu S8866-128-02), for the horizontal and the vertical plane respectively. Each array is associated with dedicated controller (Hamamatsu C9118). Consequently, one photodiode + controller system manages 128 fibers and has an independent readout. The photodiode integrated light is

[†] Claudio.viviani@cnao.it

THERMAL PERFORMANCE OF DIAMOND SR EXTRACTION MIRRORS FOR SuperKEKB

J. W. Flanagan^{†1}, M. Arinaga, H. Fukuma¹, H. Ikeda¹, G. Mitsuka, Y. Suetsugu¹

KEK, Tsukuba, Japan

E. Mulyani², BATAN, Yogyakarta, Indonesia

¹also at SOKENDAI, Tsukuba, Japan

²formerly at SOKENDAI, Tsukuba, Japan

Abstract

The SuperKEKB accelerator is a high-current, low-emittance upgrade to the KEKB double ring collider. The beryllium extraction mirrors used for the synchrotron radiation (SR) monitors at KEKB suffered from heat distortion due to incident SR, leading to systematic changes in magnification with beam current, and necessitating continuous monitoring and compensation of such distortions in order to correctly measure the beam sizes. To minimize such mirror distortions, quasi-monocrystalline chemical-vapor deposition (CVD) diamond mirrors have been designed and installed at SuperKEKB. Diamond has a very high heat conductance and a low thermal expansion coefficient. With such mirrors it is hoped to reduce the beam current-dependent magnification to the level of a few percent at SuperKEKB. Preliminary measurements of mirror distortion during SuperKEKB commissioning show very promising results with regard to thermal performance, though full beam currents have not yet been stored in the SuperKEKB rings. Measurements of the thermal deformation of the diamond mirrors will be presented in this paper, along with a description of the design of the mirrors and their mounts, and issues encountered during commissioning.

INTRODUCTION

Table 1: SR Source Parameters at KEKB and SuperKEKB

Parameter	KEKB		SuperKEKB	
	LER	HER	LER	HER
Energy (GeV)	3.5	8	4	7
Current (A)	2	1.4	3.6	2.6
Bending radius (m)	85.7	580	177.4	580
SR Power (W/mrad)	48	136	72	149

Visible-range SR monitors have been installed at SuperKEKB in both the 4 GeV positron Low Energy Ring (LER) and the 7 GeV electron High Energy Ring (HER). The SR monitors at SuperKEKB use source bends in the same locations as at KEKB, the 5 mrad “weak bends”

heading into the Fuji (LER) and Oho (HER) straight sections. The source bend parameters are shown in Table 1.

Heat deformation of the beryllium extraction mirrors was a very significant problem at KEKB, requiring complicated measures to measure and compensate for the distortion in real time in order to correct the beam-current dependence on the measured beam size [1]. Because the SR heat loads will be even higher at SuperKEKB, we have been pursuing the use of mirrors made of diamond, which has higher heat conductivity and lower thermal expansion coefficient than those of beryllium. Previous simulations have suggested that in the ideal case of a continuously monocrystalline mirror, the effective magnification changes due to thermal distortion as a result of absorbed incident SR power can be kept to the level of a few percent at the full design beam currents of SuperKEKB [2].

MIRROR AND HOLDER

The mirrors designed for SuperKEKB are made of CVD diamond, made by Cornes Technology and EDP Corporation. Each mirror is 20 mm wide x 30 mm tall, consisting of six 10 mm x 10 mm monocrystalline sections fused together, with a reflective surface made of 3 μm of gold. The thickness of the diamond substrate of each mirror is 0.5 mm. One of the mirrors is shown in Figure 1.



Figure 1: A 20 mm x 30 mm x 0.5 mm diamond mirror, consisting of six 10 mm x 10 mm monocrystals fused together, with 3 μm Au reflective coating. The light intensity pattern seen on the mirror surface comes from the reflector of the lamp used to illuminate it.

The mirror holder is a water-cooled split cylinder of soft copper, which grips the mirror on one edge only in order to

SYNCHROTRON RADIATION MONITOR FOR SuperKEKB DAMPING RING IN PHASE-III OPERATION

H. Ikeda ^{†,(A),B)}, J. W. Flanagan ^(A),B), H. Fukuma ^(A), H. Sugimoto ^(A),B), M. Tobiyama ^(A),B),
^{A)}High Energy Accelerator Research Organization (KEK), Tsukuba, Japan
^{B)}SOKENDAI, Tsukuba, Japan

Abstract

The SuperKEKB damping ring (DR) was commissioned in March 2019, before main ring (MR) Phase-III operation. The design luminosity of SuperKEKB is 40 times higher than that of KEKB with high current and low emittance. We constructed the DR in order to deliver a low-emittance positron beam. A synchrotron radiation monitor (SRM) has been installed for beam diagnostics at the DR. A streak camera and a gated camera were used for measurement of the damping time and the beam size. This paper shows the design of DR SRM and the result of the measurement.

INTRODUCTION

SuperKEKB is an electron-positron collider and constructed in 2011 towards the luminosity of $8 \times 10^{35} \text{cm}^{-2}\text{s}^{-1}$ that corresponds to 40 times higher luminosity as large as KEKB. The beam energies are 7 GeV and 4 GeV for the electron ring (HER) and the positron ring (LER), respectively. Phase-I was the test operation of the main ring (MR) for confirmation that there was no problem in accelerator from February 2016 through June [1]. We installed the Belle-II detector and remodelled injection region of an accelerator for Phase-II operation. The beam commissioning was from March 2018 to July [2]. It is necessary to squeeze the vertical beam size to nm level at the collision point to achieve the design luminosity. We built the damping ring (DR) in order to achieve a low-emittance positron beam and started the operation on February 2018[3,4]. Main design parameters of SuperKEKB MR and DR are shown in

Table 1. Phase-III operation was done from March 11th to July 1st2019. We started the collision data acquisition and aimed at improving the luminosity by increasing the beam currents and squeezing the beam size by beam tuning [5]. DR system works smoothly, and we measured DR parameters using a synchrotron radiation monitor at Phase-III operation.

SYNCHROTRON RADIATION MONITOR OF DAMPING RING

Main parameters of the DR synchrotron radiation monitor (SRM) are shown in Table 2. SRM uses the light from a bending magnet with a bending radius of 3.14m [6]. The magnet is located just after beam extraction point of DR. The beryllium mirror which we used in KEKB was installed to 0.5m downstream of the magnet to extract the light. That is a water-cooled mirror and the power from the light is 3.0W for maximum current of Phase-III that corresponds to 1/10 of KEKB LER. We don't need to care about the deformation of the mirror. Four transfer mirrors are set in the pit under the tunnel floor to the SRM room which is in the same level as that of the tunnel as shown in Fig.1. The mirrors are remotely controlled by the pulse motors to adjust the light axis by using real synchrotron radiation after the beam operation was started. The adjustment time was short since the alignment was done by a laser light at the construction of the light path.

Table 1: Design Parameters of SuperKEKB

Parameter	LER	HER	DR	Unit
Energy	4.0	7.0	1.1	GeV
Maximum stored current	3.6	2.6	0.070	A
Circumference	3016.315		135.5	m
Crossing angle	83			mrad
Number of bunches	2500		4	
Bunch current	1.44	1.04		mA
Coupling	0.27	0.28		%
Damping time (h/v/z)			11.5/11.7/5.9	ms
Emittance(h/v)	3.2/8.64	4.6/12.9	29.2/1500	nm/pm
β_x^*/β_y^*	32/0.27	25/0.3		mm
Bunch length	6	5	7.85	mm
Beam-beam parameter ξ_x/ξ_y	0.0028/0.0881	0.0012/0.0807		
Luminosity	8x10 ³⁵			cm ⁻² s ⁻¹

[†] email address: hitomi.ikeda@kek.jp

EXPERIMENTAL TESTS OF SCREEN MATERIALS FOR HIGH- PRECISION TRANSVERSE BEAM-SIZE MEASUREMENTS AT THE SuperKEKB INJECTOR LINAC

F. Miyahara[†], K. Furukawa, M. Satoh, Y. Seimiya, T. Suwada, High Energy Accelerator Research Organization (KEK), Tsukuba, Japan

Abstract

The SuperKEKB injector linac is required to deliver low-emittance electron and positron beams. Wire scanners are employed to measure Twiss parameters and to adjust beam optics conditions. Screen monitors also play important roles for single-shot measurements. However, the beam size became more than 10-times smaller compared with that of the KEKB injection. Beam tests have been performed in order to evaluate materials for high-precision transverse beam-size measurements at the injector. The main purpose of the beam tests is to quantitatively investigate the saturation effect of each screen material for generating the scintillation light, which is strongly depending on the beam fluence. Several scintillating screen materials including YAG:Ce, LYSO:Ce, BGO and aluminum ceramic doped chromium oxide (Al₂O₃:Cr) have been tested with high energy and high fluence. The results are compared with that obtained by the OTR measurement. The saturation of the luminescence was confirmed for all crystals and evaluated in fluence of the ~1 nC/mm².

INTRODUCTION

A very thin inorganic scintillator, YAG:Ce crystal is used in many facilities, is used to measure the charged particle beam profile or the temporal structure with the rf deflector. Beam profile measurement using a scintillating screen is easier to align the optical system than the optical transition radiation (OTR). In case of ultrashort bunch length, coherent OTR gives incorrect beam profile. By employing optimized imaging system, the resolution of the profile is comparable to the OTR screen monitor [1]. The response of YAG:Ce crystal to the high brightness electron beam was studied and the limitation of the resolution is discussed in Ref[2]. In case of YAG:Ce screen, the saturation becomes real at the electron beam fluence of the order ~0.04 pC/mm² for 100 MeV and this limit scales with energy. In the KEK linac, the electron beam with the bunch charge of 4 nC, the energy of 7 GeV and the normalized emittance of 40(Horizontal) / 20(Vertical) μm is required for SuperKEKB HER injection [3]. Because the beam size in the linac is ~100-200 μm , the fluence exceeds the limitation scaled by the beam energy. Thus, we have performed beam tests of scintillating screens, YAG:Ce, LYSO:Ce, BGO and Al₂O₃:Cr, to confirm the saturation of the light output to the high fluence electron beam [4]. Properties of those scintillators are summarized in Table 1.

The saturation of the luminescence of those scintillators, except for Al₂O₃:Cr, was observed at fluence of 1 nC/mm² for 1.5 GeV beam, but there was no reference measurement using the OTR screen. Thus, we have measured a beam profile measurement using those scintillating screens and an OTR screen.

Table 1: Properties of Scintillators

	τ_{decay} [ns]	λ_{max} [nm]	Light yield [10 ³ ph/MeV]	Density [g/cm ³]
YAG:Ce	70	550	17	4.6
LYSO:Ce	41	420	33	7.1
BGO	300	480	9	7.1
Al ₂ O ₃ :Cr ₂ O ₃	> ms	690	Large	4.0

EXPERIMENT

The KEK linac consists of 2 straight sections and 180 degrees arc section between them. The beam profile measurements were performed at a test beam line with a beam dump located downstream of the first straight section. The linac has an RF-gun for the generation of the low emittance electron beam and a thermionic gun for low current beam for PF/PF-AR storage rings or high bunch charge beam to produce a positron beam for SuperKEKB LER. In this experiment, a bunch charge of 1.15 nC beam generated by the rf-gun was used, and the beam accelerated up to 1.5 GeV. The experimental setup is shown in Fig. 1. The beam pass through a 30 μm thick stainless steel window and a blackout fabric to block the OTR generated at surface of the window. Scintillating screens and OTR screen are set on a motorized stage. The thickness of these scintillating screens is 0.1 mm. Two imaging system are located in the direction of 90 (OTR screen) and 19 (scintillating screens) degrees to the beam line respectively. The layout of the imaging system is also shown in the figure. To avoid saturation of the CCD and adjust quantity of light on the CCD for each scintillating screen, the variable neutral density (ND) filters is used. Because Al₂O₃:Cr has a long decay time, signal level of pixel outputs were adjusted by exposure time (500 μs for the Al₂O₃:Cr, 50 μs for other screens). The CCD camera has a sensor resolution of 659x493 pixels (cell size 7.4 μm) and 12bit ADC. The bandpass filter is used for limiting wavelength region for the OTR and Al₂O₃:Cr. The

[†] fusashi.miyahara@kek.jp

DEVELOPMENT OF A GATED IPM SYSTEM FOR J-PARC MR

K. Satou[†], J-PARC/KEK, Tokai, Japan

Abstract

In the Main Ring (MR) of Japan Proton Accelerator Research Complex (J-PARC), a residual-gas ionization profile monitor (IPM) is used to measure bunched beam profiles. After injection, the beam widths of the first ~20 bunched beams are analysed to correct the Quadruple oscillation. While only a few dozen profiles are required for this correction, the present IPM automatically measures all bunched beams, more than 2E6 bunches from injection to the extraction, because the present IPM operates using DC. This system is undesirable due to the limited lifetime of the Micro Channel Plate (MCP) detector; the more particles the MCP senses, the more it loses gain flatness and thus lifetime. To improve this situation, a gated IPM system has been developed, in which the High Voltage (HV) is operated in pulse mode. Results of performance analysis of a new HV power supply, improvement of the electrodes, and particle-tracking simulation considering the space-charge-electric field of the bunched beam are described.

INTRODUCTION

In the Main Ring (MR) of Japan Proton Accelerator Research Complex (J-PARC), three residual-gas Ionization Profile Monitors (IPMs) have been used: a horizontal type IPM (D2HIPM) and a vertical type IPM (D2VIPM) have been installed in a straight line named Ins_B where the dispersion function is zero; while another horizontal type IPM (D3HIPM) has been installed in the arc section, named Arc_C, where the dispersion function is non-zero. The Twiss parameters at these IPMs are $(\beta_x, \beta_y, \eta) = (12.1 \text{ m}, 27.3 \text{ m}, 0 \text{ m})$, $(13.1 \text{ m}, 21.6 \text{ m}, 0 \text{ m})$, and $(8.4 \text{ m}, 15.5 \text{ m}, 2.0 \text{ m})$ for D2VIPM, D2HIPM, and D3HIPM, respectively. Details on these IPMs are presented in [1-3].

The IPMs can be operated in ion-collection mode using a strong High Voltage (HV) maximum $\pm 50 \text{ kV}$ without a guiding magnetic field (B field). Only D2HIPM has a magnetic system of maximum 0.2 T, and can be operated in electron collection mode with the B field. For all three IPMs, the HV systems and magnetic system are operated under DC.

The chevron-type Micro Channel Plate (MCP) which has 32ch-strip anodes has been used as a particle detector; the width of each anode is 2.5mm. As the MCP is operated in analog mode, the output current distribution across the strips is a one-dimensional beam profile. Because the HV is in DC, the MCP should sense all ionized particles generated by the circulating bunched beams from the injection to the extraction, totalling more than 2E6 bunches. However, the MCP loses its gain flatness the more the charge is multiplied and extracted from the MCP. Moreover, from a

practical standpoint, the MCP detector is expensive and cannot be replaced frequently.

The idea of the gated IPM system [4] was developed at the Fermi National Accelerator Laboratory (FNAL) in the USA. In this system, HV gate pulses are used to accelerate the ionized particles onto the MCP detector. By changing the gate width and operational frequency, the operating duty of the IPM can be changed. For example, if it is operated with a duty ratio of 1/100, the lifetime of the MCP detector would become much longer. Moreover, changing the duty ratio can also improve the gain saturation effect [5], because low average output current is preferable for maintaining the gain stability.

To upgrade the existing IPM systems to the gated IPM system, modifications on the electrodes in the chamber were made, and a HV gate generator was developed. In this paper, the details of electrode modifications and the development of the HV gate generator are described.

IMPROVEMENT OF THE ELECTRODES

The electrodes used to generate flat external electric field, thus accelerating the charged particles onto the MCP detector, were improved as follows:

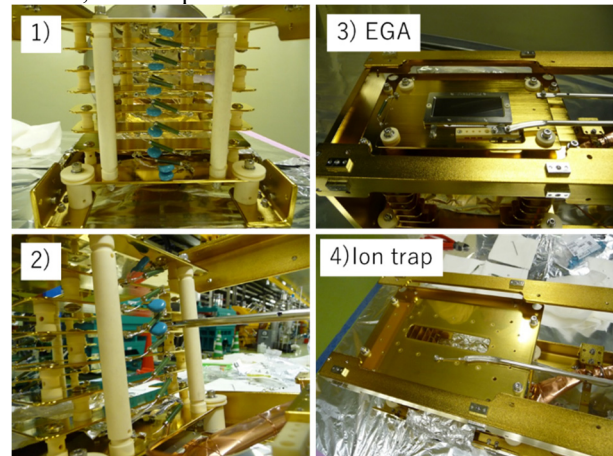


Figure 1: Modifications of the electrodes for gated IPM system. 1), 2) In total 11 capacitors were installed in parallel to the resistors. 3) The Electron Generator Array (EGA) previously installed to check the gain flatness of the MCP detector was removed and 4) an ion-trap structure was newly installed at the same position.

Impedance matching: The rectangular plates at each electrode step, which are used to improve the uniformity of the external electric field, were bridged with a resistor. In this study 100 M Ω resistors were used, except for in the last stage where a 50 M Ω resistor was used. To match the impedance and therefore shorten the rise and fall time for the $\pm 30 \text{ kV}$ gate pulse signals, 1 nF and 2 nF capacitors were set parallel with the 100 M Ω and 50 M Ω resistors, respectively, as shown as Figs. 1-1 and 1-2.

[†] kenichirou.satou@j-parc.jp.

DEVELOPMENT OF 16-ELECTRODES BEAM-SIZE MONITORS FOR J-PARC MR

M. Tajima*, T. Nakaya, Kyoto University, Kyoto, Japan

T. Toyama, T. Koseki, High Energy Accelerator Research Organization (KEK), Tsukuba, Japan

Abstract

For J-PARC Main Ring(MR), 16 electrodes beam-size monitors are developed aiming at measuring the beam sizes of high intensity beams up to 1.3 MW in 1.2 s cycle operation of the MR. Furthermore, with high accuracy measurements of beam sizes, the injection mismatch from the RCS is to be decreased. In the beam test in February 2019, the signal-noise ratio (SNR) of the 1st 16-electrodes monitor in bunch-by-bunch measurements was nearly 40 dB and lower than the design value 50 dB. To improve the SNR, we considered to develop new LPFs for anti-aliasing and attenuators system. In addition, the second monitor was installed in August 2019 and will be tested with beams in November.

INTRODUCTION

In 2018, the beam power of J-PARC MR is 490 kW and scheduled to be upgraded to 1.3 MW in 2021. For this, it is necessary to reduce beam losses and understand it. Therefore, the developments of new beam profile monitors are important.

Beam-profile monitors such as a Flying Wire Monitor [1] and an Ionization Profile Monitor [2] are already installed in MR. However, the two monitors have issues in measuring higher intensity beams. The former is that the wire gets easily burned out and the latter is that there is a sign of the saturation by a space charge effect. Therefore, we are developing 16-electrodes monitors (Figure 1) aiming at measuring the beam sizes of high intensity proton beams up to 4.2×10^{13} protons per bunch, which corresponds to 1.3 MW in 1.16 s cycle operation of the MR.

Measurements of Beam Sizes

The relation between induced voltage V_i ($i = 0, 1, \dots, 15$) in the electrode of ch i and transverse moments $Q, Q \langle x \rangle, Q \langle y \rangle, Q \langle x^2 - y^2 \rangle, Q \langle 2xy \rangle, \dots$ is given by:

$$\begin{pmatrix} g_0 V_0 \\ g_1 V_1 \\ \vdots \\ g_{15} V_{15} \end{pmatrix} = A \times \begin{pmatrix} Q \\ Q \langle x \rangle \\ Q \langle y \rangle \\ Q \langle x^2 - y^2 \rangle \\ Q \langle 2xy \rangle \\ \dots \end{pmatrix} \quad (1)$$

$\langle \rangle$ and Q show weighted mean of the charge distribution of beams and total charges.. The matrix A is calibration matrix 16×16 and obtained by wire calibration. The value g_i is the gain of ch. i and obtained by Beam Based Gain Calibration

* tajima.masanori.76r@st.kyoto-u.ac.jp

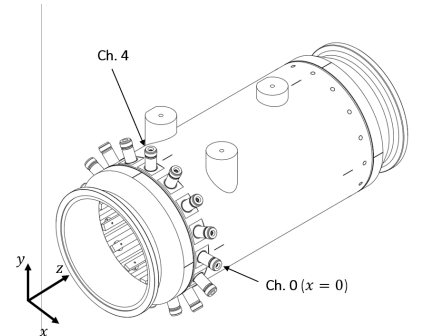


Figure 1: The drafting of 16-electrodes monitor by TOYAMA Co.,Ltd. The size is 500 mm length, 195 mm in outer diameter and 165 mm in inner diameter. Transverse moments of beam are calculated from induced voltages in 16 electrodes which are 320 mm long, 9.85 mm wide and 5.0 mm thick.

which is discussed later. In areas where dispersion functions are zero, the quadrupole moment $\langle x^2 - y^2 \rangle$ is given by:

$$\begin{aligned} \langle x^2 - y^2 \rangle &= \langle (x - \langle x \rangle)^2 - (y - \langle y \rangle)^2 \rangle + \langle x \rangle^2 - \langle y \rangle^2 \\ &= \beta_x \epsilon_x - \beta_y \epsilon_y + \langle x \rangle^2 - \langle y \rangle^2 \end{aligned} \quad (3)$$

where β_i ($i = x, y$) is the beta function and the ϵ_i is emittance. Hence, we could calculate transverse emittance from measurements of quadrupole moment in two locations which meet $\frac{\beta_{x,1}}{\beta_{x,2}} \neq \frac{\beta_{y,1}}{\beta_{y,2}}$ [3].

Signal Processing

Readout circuits for 16-electrodes monitors are consist of FPGA (VC707 evaluation board) and ADCs (LTM9011-14, 14-Bit, Input Range 2 Vp-p) [4]. The clocks of ADCs are synchronized with the 52th harmonic 88 MHz of the Acc. RF frequency (1.7 MHz). In bunch-by-bunch measurements, the Fourier amplitudes in the 2nd harmonic 3.4 MHz of the Acc. RF frequency are extracted by Goertzel algorithm [5] and used for calculations of transverse moments in FPGA. The frequency band of aliasing noises is 85 MHz. For the attenuations of these noises, low-pass filters (LPFs) are installed before ADC.

PERFORMANCE

Beam Test in February 2019

Beam test was done for Beam Based Gain Calibration (BBGC) which is discussed later. Beam parameters and waveforms in this time are given by Table 1 and Figure 2.

Signal-noise-ratio (S/N) was low, so fluctuations of quadrupole moment was large. (Table 2) In this time, the

DEVELOPMENT OF THE CALCULATION METHOD OF INJECTION BEAM TRAJECTORY OF RIKEN AVF CYCLOTRON WITH 4D EMITTANCE MEASURED BY THE DEVELOPED PEPPER-POT EMITTANCE MONITOR

Y. Kotaka[†], Y. Ohshiro, H. Yamaguchi, N. Imai, Y. Sakemi,
S. Shimoura, Center for Nuclear Study, University of Tokyo, Wako, Japan
T. Nagatomo, J. Ohnishi, T. Nakagawa, M. Kase, A. Goto, Riken Nishina Center, Wako, Japan
K. Hatanaka, Research Center for Nuclear Physics, Osaka University, Ibaraki, Japan
H. Muto, Suwa University of Science, Chino, Japan

Abstract

The Center for Nuclear Study, the University of Tokyo and RIKEN Nishina Center have been developing the AVF Cyclotron system at RIKEN. One of the important developments is to improve the transport system of the injection beam line. The transport efficiencies tend to decrease as beam intensities increase. To solve this problem, we developed the calculation method to trace a beam trajectory with a four-dimensional (4D) beam emittance measured by pepper-pot emittance monitor (PEM) as initial value. The reason for using the 4D beam emittance is that the transport system has rotating quadrupole magnets and solenoid coils, and that the space charge effect can be introduced. The beams through a pepper-pot mask can be detected on the potassium bromide fluorescent plate inclined 45 degree to the beam to be recorded by digital camera using developed PEM. We compared the calculated beam trajectory with the measurement of other beam diagnostics and quantified the degree of fit. It has been found that the degree of fit is improved by changing fiducial points on the fluorescent plate and optimizing the thickness of the fluorescent agent and the exposure time and gain of the digital camera.

INTRODUCTION

The Center for Nuclear Study, the University of Tokyo (CNS) and RIKEN Nishina Center have been expanding a variety of ion beams, increasing acceleration energy, and increasing beam intensity for RIKEN AVF Cyclotron [1, 2]. Among these, one of the important developments is to improve the transport system of the injection beam line.

Figure 1 shows injection beam line of AVF Cyclotron. Though there are 3 kinds of ion source, our target is 14 GHz electron cyclotron resonance ion source (ECRIS) named HyperECRIS developed by CNS.

According to the data from Sep. 2011 to Aug. 2013 when this study started, the average beam transport efficiency from 1st Faraday cup (FC_IH10) to 2nd Faraday cup (FC_I36), the center region, and the exit of extraction channel of accelerated beam were 64.7, 23.8, and 7.6 %, respectively. The center region is defined as the end of injection beam line. It is found most beams are lost in injection beam

line, and these values tend to decrease as beam intensities of FC_IH10 increase.

However, all the transport efficiencies include the attenuation of 83 % by buncher mesh set over FC_I36. Moreover, as beam is compressed in the beam direction by the buncher and accelerated 6 times by the high frequency electrode to the end of center region, the beam dropping off the accelerating phase is lost. As the causes of beam loss in the injection beam line are complicated, it is necessary to improve this beam trajectory.

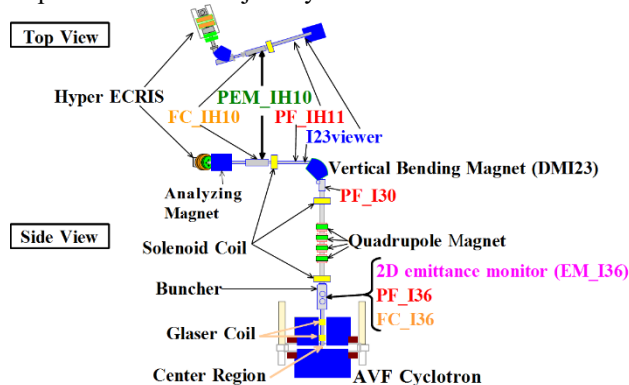


Figure 1: The injection beam line of the RIKEN AVF Cyclotron.

As the first step, we tried to understand the real beam transverse motion and the causes of beam loss. For this purpose, beam trajectory calculation is necessary. However, existing beam trajectory calculation codes are not useful because the beam intensity distribution generated by ECRIS is not gaussian, which means statistical approach is impossible. Therefore, we tried to develop the beam trajectory calculation method using the measured beam intensity distribution in the transverse phase space (x, x', y, y') (4D emittance) as the initial value by Lunge-Kutta method. As the second step, we will design beam trajectories which constrain beam loss and match the beam acceptance of AVF Cyclotron. Now, we completed to develop the beam trajectory calculation method including space charge effect.

PEPPER-POT EMITTANCE MONITOR

One reason for 4D emittance is that there are solenoid coils in the injection beam line. Another is that the beam line from analysing magnet to vertical bending magnet

[†] kotaka@cns.s.u-tokyo.ac.jp

TWO-DIMENSIONAL BEAM PROFILE MONITOR FOR ALPHA EMITTER

K. S. Tanaka*, H. Kawamura, M. Itoh, A. Terakawa, CYRIC, Tohoku University, Sendai, Japan
N. Ozawa, H. Nagahama, Y. Sakemi, CNS, University of Tokyo, Tokyo, Japan
K. Harada, Tokyo Institute of Technology, Tokyo, Japan
T. Hayamizu, RIKEN, Saitama, Japan

Abstract

We developed two-dimensional beam profile monitors for alpha-emitters along with other larger number of ions the experiment to measure the permanent electric dipole moment of the electron using francium (Fr) atoms at CYRIC in Tohoku university. Fr is produced by the fusion reaction between the oxygen beam from the cyclotron accelerator and the gold target, and a far larger number of other ions such as Na^+ or K^+ are also emitted from the target. It is difficult to measure the beam profile of Fr^+ since it is hidden by these ions. To measure the Fr^+ beam profile in this condition, we installed two beam profile monitors consisted of the micro-channel plate and phosphor screen. If we stop the beam after the injection to the monitor in sufficient time, we can only observe the fluorescence of the alpha particle emitted by Fr atoms on the surface of the plates. By using this monitoring system, we can optimize only the Fr^+ beam transportation and removed most of other ions by Wien filter.

INTRODUCTION

Search of the permanent electric dipole moment (EDM) using various kinds of atom and molecules has been carried out in recent years. The infinite value of electron EDM would imply of a new physics beyond the standard model of particle physics [1].

We are preparing the precise measurement of the EDM using a Fr in CYRIC. Fr is one of a suitable atom to search the electron EDM. It is the heaviest alkaline metal so that it has a large enhancement factor of EDM and can be applied laser cooling technique [2].

Fr is produced by nuclear fusion reaction between an oxygen beam (^{18}O) provided from CYRIC and gold target (Fig. 1). The intensity of the Fr production is limited such as 10^6 /s due to the intensity of the oxygen beam [3].

Fr is ionized by surface ionization on the gold target, and transport 12 m length to the measurement area which is free from the background noise of the cyclotron accelerator. The Fr^+ is accumulated to the Yttrium foil which has a small work function ($E_{WF} = 3.1$ eV). Then Fr atoms are release as a neutral atom by heating the foil and load to the laser-trapping area. The size of the yttrium foil is only 10 mm \times 10 mm, so that the control and focus of the Fr^+ beam to this small area is important to the efficiency of the number of the Fr loaded to the trapping area.

Also, we need to care about the other ions along with the Fr ions which cause atomic collisions in the trapping area. Typically, the intensity of Fr^+ beam is 10^6 /s and that of other ions (Na^+, K^+) are more than 10^{11} /s. Even light ions can be removed from the Fr^+ beam by Wien filter, ions which comparably close to the mass of Fr^+ such as Au^+ are difficult to remove. Hence beam profile of the Fr^+ is hidden by larger number of ions and unobservable with typical ways. Previously, the beam transport efficiency is measured by the rate of alpha decay from the Faraday cup by the solid-state detector (SSD) after the beam irradiation with enough time. However, this way only measure the total number of the Fr^+ but not measure the profile of the beam. This is the main reason that the optimization of the beam transportation was insufficient [4].

Therefore, we developed the new two-dimensional beam profile monitor for alpha emitter ion beam separated from the other ion beam by using the microchannel plate (MCP) and the phosphor screen.

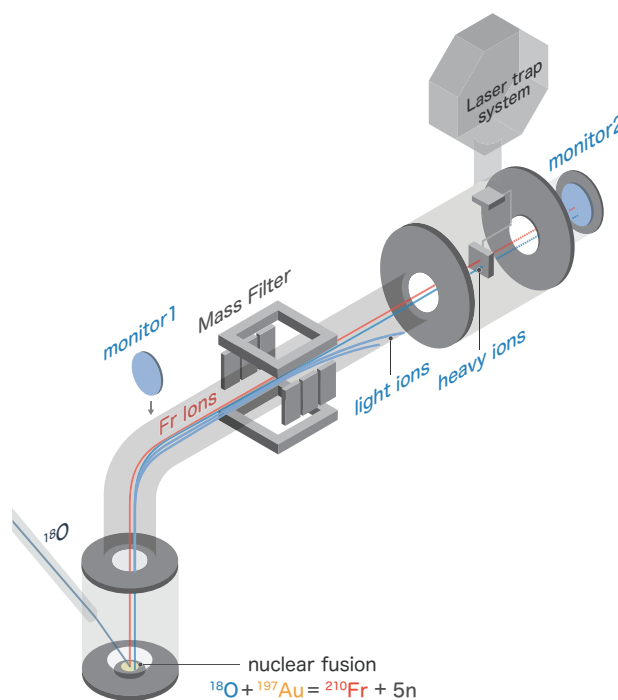


Figure 1: Fr^+ beamline at CYRIC. two beam monitors for alpha-emitter is installed on the beamline.

* tanaka@kaduo.jp

DEVELOPMENT OF BEAM INDUCED FLUORESCENCE MONITOR FOR NON-DESTRUCTIVELY PROFILING MW PROTON BEAM AT THE J-PARC NEUTRINO BEAMLIN

S. Cao*, M. Friend, K. Sakashita, High Energy Accelerator Research Organization, Tsukuba, Japan
M. Hartz¹, Kavli IPMU (WPI), University of Tokyo, Tokyo, Japan
¹also at TRIUMF, Vancouver, Canada
A. Nakamura², Okayama University, Okayama, Japan

Abstract

A Beam Induced Fluorescence (BIF) monitor is under development for non-destructively monitoring the future MW-power proton beam at the neutrino extraction beamline at J-PARC. The 30 GeV protons are bombarded onto a graphite target, producing one of the most intense neutrino beams in the world for the Tokai-to-Kamioka (T2K) long-baseline neutrino oscillation experiment, where beam profile monitoring is essential for protecting beamline equipment and understanding the neutrino flux. For the BIF monitor, gas is injected into the beam pipe and the spatial distribution of the fluorescence light induced by proton-gas interactions is measured, allowing us to continuously and non-destructively monitor the proton beam profile. However, the specifications of the beamline require us to carefully control the gas localization by pulsed injection. Radiation hardness of all monitor components and profile distortion caused by space charge effects must also be considered. We will show how to address these challenges and realize a working prototype.

J-PARC MW PROTON BEAM FOR NEUTRINO INTENSITY FRONTIER

Accelerator-Based Neutrino Research

One of the most striking discoveries of 20th century is that neutrino has non-zero mass, which contradict to the prediction of the so-called Standard Model of the elementary particles. The conclusion has been drawn from a well-established phenomenon, neutrino oscillation, in which neutrino, who is produced with a definite flavor (electron, muon, tau), can change into other flavors after traveling some distance. This quantum mechanic phenomenon has been realized as a great tool for exploring the fundamental laws of physics. One of the most stimulating physics is Charge-Parity (CP) violation in the leptonic sector. Recently T2K experiment provides a hint on this at 2σ C.L. [1]. The result is statistically limited and for providing a more significant sensitivity, higher intense neutrino beam(s) and bigger detector(s) are desired.

J-PARC, One of the Most Intense $\nu_\mu(\bar{\nu}_\mu)$ Beam

J-PARC Neutrino Experimental Facility has been built to deliver one of the most intense beams of $\nu_\mu(\bar{\nu}_\mu)$ for the neutrino research. Neutrino beam is made from the decay-in-flight of pions and kaons, which are produced when 30 GeV

proton beam from Main Ring (MR) are guided and hit on the graphite target. More detail description of the neutrino beam can be found at [2]. At present, J-PARC operate stably at around 485kW with an intensity of 2.5×10^{14} protons-per-pulse (ppp). The plan [3] is to upgrade to MW-power beam by reducing the cycle repetition from 2.48 s to 1.3 s, and increasing the beam intensity to 3.2×10^{14} ppp.

Present Beam Profile Monitors

There are two types of profile monitors being used at the J-PARC neutrino beamline: Segmented Secondary Emission Monitor (SSEM) and Wire Secondary Emission Monitor (WSEM). The detail can be found at [4]. Both are categorized as the destructive type of monitors. Each SSEM causes 0.005% beam loss and WSEM lessens it by a factor of ten. With MW-power beam, it is challenging to have a continuous operation of these conventional beam monitors due to the high irradiation, the risk of beamline component damage and the potential built-up residual dose which limits the machine maintenance time. Thus it is well-motivated for developing the non-destructive beam profile monitor(s).

DEVELOPMENT OF A BIF PROTOTYPE

Design Considerations

As discussed in [5], the space charge effect in the J-PARC neutrino beamline is too high to be counteracted by the typical Ionization Profile Monitors magnet. It thus was the practical choice to focus on a BIF-based prototype. To have enough photons for light detection system, the vacuum level near the fluorescence detection region must be degraded while maintaining an average vacuum level of 10^{-4} Pa at the ion pumps for the lifetime consideration and 10^{-6} Pa at the superconducting (SC) section for the safety reason. N_2 gas is selected due to its high light yield. Fluorescence spectral induced by proton- N_2 interactions spreads from 380 ns to 470 ns with a peak at ~ 390 ns. However, N_2 is relatively light and can be drifted largely due to the space charge field, consequently distorting the reconstructed profile. A fast photon catcher but non-vulnerable to the magnetic field is considered as a viable solution, which points us to Multi-pixel Photon Counter (MPPC). However, MPPC is not radiation-hard enough to function well and durably near the beamline environment. The practical use is to transport the light with radiation-hard optical fibers to sub-tunnel where the radiation level is suppressed and MPPC can be placed.

* cvson@post.kek.jp

DIAGNOSTIC BEAMLINES AT THE SOLARIS STORAGE RING

A. Kisiel, M. Ptaszekiewicz*, S. Cabala, A. Marendziak, A. Wawrzyniak†, I. Zadworny and T. Zbylut
 Solaris National Synchrotron Radiation Centre, Krakow, Poland

Abstract

Precise measurement and control of the electron beam emittance is a very important input to characterize the performance of any accelerator. Synchrotron radiation has been widely used as diagnostic tool to measure the transverse and longitudinal profile. Beam characterizations at the Solaris National Synchrotron Radiation Centre are provided by two independent diagnostic beamlines called PINHOLE and LUMOS beamline, respectively.

The PINHOLE beamline, depicts the electron beam by analyzing the emitted X-rays. However this method is predominantly applied to the middle and high energy storage rings. At Solaris storage ring with the nominal energy of 1.5 GeV and critical photon beam energy of c.a. 2 keV, the design of the beamline was modified to provide sufficient X-ray photon flux for proper imaging.

Second diagnostic beamline LUMOS, which will be operates in the visible region, was installed during summer shutdown 2019 and will be commissioned in next few months. The optical diagnostic beamline will be used not only for measure the transverse beam profile, but also for the bunch length measurements and study longitudinal beam dynamics.

Issues discussed include the general design philosophy, choice of instrumentation, and actual performance.

INTRODUCTION

The Solaris storage ring is designed to have small emittance (6nm rad), a 100 MHz pulsed electron beam, and maximum stored current of 500 mA, in order to produce bright beam of synchrotron radiation. More details about the machine layout and design can be found in [1–4] whereas the main storage ring design parameters are presented in Table 1.

Solaris has been operating with the beam in the storage ring since May 2015 and currently services two beamlines (PEEM/XAS with two end-stations, and UARPES with one end-station). Four beamlines are under construction (PHELIX, XMCD, SOLCRYS and SOLABS), two other (FTIR and POLYX) have received funding and will be installed and commissioned in next few years.

DIAGNOSTIC BEAMLINE PINHOLE

The first PINHOLE X-ray diagnostic beamline was installed and commissioned in the Solaris storage ring in the mid of 2018. This beamline has been designed to measure the transverse beam profile and to monitor the emittance and their stability during the beam decay. The source point for

Table 1: The SOLARIS Storage Ring Main Parameters

Parameter	Value
Energy	1.5 GeV
Max. current	500 mA
Circumference	96 m
Main RF frequency	99.931 MHz
Harmonic number	32
Horizontal emittance (without insertion devices)	6 nm rad
Coupling	1 %
Tunes Q_x, Q_y	11.22, 3.15
Natural chromaticity ξ_x, ξ_y	-22.96, -17.14
Corrected chromaticity ξ_x, ξ_y	+1, +1
Electron beam size (straight section centre) σ_x, σ_y	184 μm , 13 μm
Electron beam size (dipole centre) σ_x, σ_y	44 μm , 30 μm
Momentum compaction	3.055×10^{-3}
Total lifetime of electrons	13 h

the PINHOLE diagnostic beamline is the center of the bending magnet in cell 1 of the Solaris storage ring. The X-ray light is extracted from the source through a vacuum window. After exiting window, the X-ray passes through the pinhole cross and reaches the scintillator crystal where is converted to the visible light. The optical light from scintillator is imaged by a CCD camera.

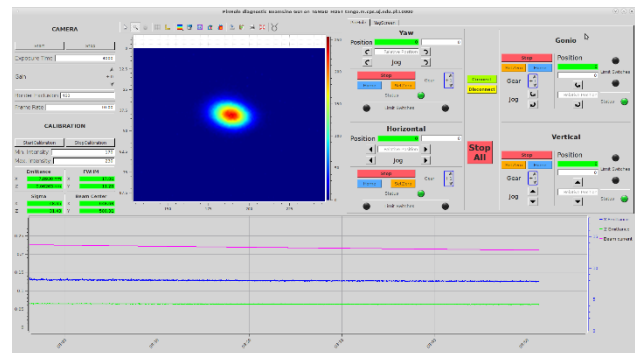


Figure 1: PINHOLE diagnostic Beamline GUI.

The acquired image is processed in a homemade developed software. This software consists of three layers: Taurus based GUI, TANGO Controls devices and PLC program. The PINHOLE diagnostic Beamline GUI on TANGO HOST is shown in Figure 1. Among the available options, the program fits Gaussian curves to determine the beam sigma's and calculates emittance, beam position and other parameters. All this data is stored in historical database.

* marta.ptaszekiewicz@uj.edu.pl

† adriana.wawrzyniak@uj.edu.pl

DEVELOPMENT OF A PRECISION PEPPER-POT EMITTANCE METER

G. Hahn*, Pohang Accelerator Laboratory (PAL), 37673 Pohang, South Korea
J.G. Hwang, Helmholtz-Zentrum Berlin (HZB), 12489 Berlin, Germany

Abstract

A fast single-shot emittance measurement device, a pepper-pot emittance meter, was developed to utilize it at the heavy ion therapy facility in Korea. In the manufacturing stage, in order to guarantee the hole quality of the holes in the pepper-pot mask, we fabricated two mask using different methods that are made of phosphor bronze by optical lithography process and SUS by laser cutting. After the comparison of each SEM (scanning electron microscope) measurement data, the phosphor bronze mask fabricated by lithography was found to be suitable. The rotation and translation matrices are applied on all images obtained by the camera to mitigate the relative angular misalignment errors between MCP, mirror, and CMOS camera with respect to the mask. By applying the instrument in the NFRI ion source, the four-dimensional phase-space distribution of ion beams is retrieved and compared with the result measured by using a slit-scan method. In this paper, we describe the fabrication process, data analysis method and beam measurement results of the developed emittance meter.

INTRODUCTION

Since the carbon ions in tumor therapy are the elevate relative biological effectiveness (RBE), enhancing the inactivation in the tumor volume while in the entrance channel RBE stays close to one. During the past decade, design and construction of synchrotron-based carbon-ion therapy facilities such as HIMAC, GHMC, SAGA HIMAT, iROCK and HIBMC in Japan, HIT, MIT and GSI in Germany, SPHIC and IMP in China, CNAO in Italy, MedAustron in Austria, and KHIMA in Korea have been carried out all over the world. The biological benefits of carbon ion therapy have been demonstrated in inoperable cases with various types of sarcoma, adenocarcinoma, adenoid cystic carcinoma and malignant melanoma arising from various sites that are well known as photon resistant tumors [1].

The Korea Heavy Ion Medical Accelerator (KHIMA) project was launched in Korea to develop and demonstrate accelerator technologies for a proton and carbon beam based therapy and it is currently under construction. Low-intensity proton and carbon beams with energy in the range of 110 to 430 MeV/u for carbon beams and 60 to 230 MeV for protons, which corresponds to water equilibrium beam range of 3.0 to 27.0 g/cm² are produced by the accelerator for a cancer therapy. The accelerator consists of a low energy beam transport (LEBT) line, radio-frequency quadrupole (RFQ) linear accelerator (linac), interdigital H-mode drift-tube-linac (IH-DTL), medium beam transport (MEBT) line, synchrotron, and high energy beam transport (HEBT) line [2].

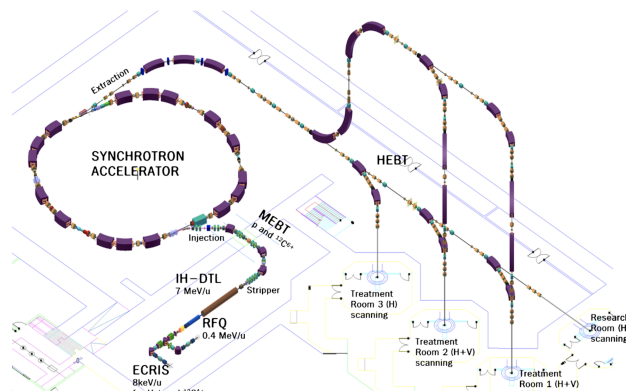


Figure 1: Layout of KHIMA project.

In the low energy beam transport line (LEBT) of the KHIMA accelerator (as shown in Fig. 1), two electron-cyclotron resonance ion sources (ECR-IS) are installed to produce the ³H⁺ beam with a nominal current of 328 e μA and ¹²C⁴⁺ beam with a nominal current of 122 e μA respectively, and the energy of ion beams is 8 keV/u that is determined by static extraction voltage [3]. It is important to precisely measure emittances between at the end of LEBT and at the entrance of RFQ, as the mismatching of the beam at this point determines most of the beam transmission ratio, and it affects the number of patients that can be treated. With the conventional diagnostic methodologies such as slit-scanning however it takes a relatively long time and space for accurate characterization of the beam properties at the LEBT section [4]. Therefore, we studied a pepper-pot meter that is a highly influential device to measure the emittance and Twiss parameter within a relatively short space of time.

This paper is structured as follows: First, we show the basic components of the pepper-pot meter, design criteria, and validation of the mask fabrication, which reduces the reconstruction error of emittance analysis of the device. Second, the method for image processing and reconstruction result of 4 × 4 symmetric moments beam matrix using experimental data with the 24 keV argon beam from ECR-IS are presented. Finally, our conclusion is given in the last section.

DESIGN AND FABRICATION

Design

The pepper-pot emittance meter consists of a mask with a pinhole array for deconvoluting the position and angular information of ion beams using a small opening, a micro-channel plate (MCP) for amplifying the signal intensity, phosphor screen for converting electrons to visible light and optics for measuring the profile. Since the ion beam intensity on the screen is reduced significantly by the mask, the MCP

* garam@postech.ac.kr

DOUBLE-WIRE VIBRATING WIRE MONITOR (DW-VWM) FOR BEAM HALO MONITORING IN HIGH-INTENSITY ACCELERATORS

D. Kwak¹, M. Chung¹, S.G. Arutunian², G.S. Harutyunyan², E.G. Lazareva², A.V. Margaryan²

¹ Ulsan National Institute of Science and Technology, 44919, Ulsan, Korea

² Yerevan Physics Institute, 0036, Yerevan, Armenia

Abstract

Double-Wire Vibrating Wire Monitor (DW-VWM) for beam halo monitoring in high-intensity accelerators is developed and manufactured. Compared with previously developed monitors, we increased the ratio of aperture to wire length by using small size magnets and shifting them to the ends of the wire. Besides, two vibrating wires are positioned on the same frame. The first wire is placed in the beam halo region for measurements, and the second wire, which is separated from the beam by a screen, is used to subtract background signal caused by ambient temperature shifts. Electronics of the DW-VWM consists of autogenerator unit placed near the monitor and frequency measurement unit placed in control room (100 m distance operation was tested). The nearest goal is to install the DW-VWM in the accelerator AREAL (Candle SRI) for profiling \sim pA mean beam current.

INTRODUCTION

The operating principle of Vibrating Wire Monitor (VWM) is based on the measurement of the change in the frequency of a vibrating wire, which is exposed to the beam. The heat transfer from beam to wire depends on particles and wire material parameters. Corresponding accuracy of resulting wire temperature is less than 1 mK [1]. In the proposed Double-Wire Vibrating Wire Monitor (DW-VWM) we introduced a second wire that can be separated from direct beam deposition by a screen. This wire is used to subtract measurement background. We also increased the ratio of aperture to wire length by using 5 mm x 5 mm magnets. After optimizing the parameters of the DW-VWM and selecting the proper material of the wire, we intend to install the sensor in the electron accelerator AREAL (Candle SRI) with 5 MeV of energy [2, 3] and measure the beam in range of pA.

DESIGN AND DISTINCTIVE FEATURES

The DW-VWM is installed inside the vacuum chamber of accelerator AREAL (see Fig. 1a). A schematic view of DW-VWM is presented in Fig. 1b.

Below we specify the distinctive features of DW-VWM.

Magnetic System and Wires

Aim of magnetic system is to generate oscillations on the second harmonic of natural frequency. Wire length is 22 mm. Optimal assembly of magnets is presented on the

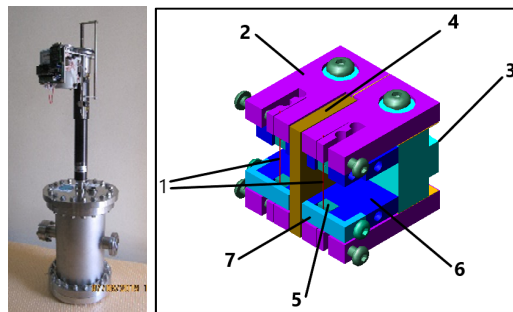


Figure 1: (a) Vacuum chamber of AREAL with step motor feed. (b) Main view of DW-VWM. Two wires (1) are tightened by four clips (2). Clips are fastened on the same frame from stainless steel (3). Between two wires inserted a removable screen (4) with thickness up to 4 mm. Magnetic field system consists of four assemblies of magnet poles and permanent magnets. The core of the system are permanent magnets (5) covered by magnetic steel (6 and 7). The bearing poles (6) are mounted on the bed (3).

left side of the Fig. 2 - the distance between centers of the magnets should be half of the wire length, i.e. 11 mm. For 5 mm size magnets the aperture in this case becomes only 6 mm. To enlarge the aperture, we shift magnets to the clips by 2.5 mm (right side of the Fig. 2). Distance between centers of magnets becomes 16 mm and aperture increases up to 11 mm.

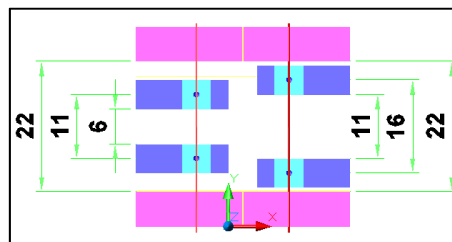


Figure 2: Two types of magnetic system for DW-VWM.

Electronics

New electronics of DW-VWM consists of two main boards: autogenerator unit placed near the VWM and frequency measurement unit placed in control room (100 m distance operation was tested). Autogeneration board is equipped with a scheme devoted to excite the oscillation generation by applying a short initiating pulse on the wire. Frequency measurement unit is equipped with FTDI1232C based USB interface (virtual COM port). Minimal measurement time is about 20 ms.

STRIPLINE-BASED NON-DESTRUCTIVE BEAM PROFILE MONITORING SYSTEM FOR MUON G-2/EDM EXPERIMENT AT J-PARC*

C. Sung, M. Chung[†]

Ulsan National Institute of Science and Technology, Ulsan, Republic of Korea

Selcuk Haciomeroglu, Yannis K. Semertzidis¹

Institute for Basic Science, Daejeon, Republic of Korea

¹also at Korea Advanced Institute of Science and Technology, Daejeon, Republic of Korea

Abstract

The muon g-2/EDM experiment at J-PARC aims to measure the muon magnetic moment anomaly, a_μ and electric dipole moment, d_μ by introducing an approach excluding any electric field with measurement goal of 450 and 70 ppb for statistical and systematic uncertainties of a_μ , respectively, and sensitivity of $1.5 \times 10^{-21} \text{ e} \cdot \text{cm}$ for d_μ . In order to match the phase space and acceptance for injection, the beam needs to be manipulated such that the X and Y components are coupled by means of skew quadrupole magnets through the transmission line. The XY coupling quality can affect the transmission and storage efficiency so that its failure causes systematic error. Since it is significant to monitor the XY coupling status during the beam operation, a non-destructive beam profile monitoring system is under development to investigate the XY coupling quality so as to reduce the source of systematic uncertainties. The device consists of stripline electrodes installed with 45° rotational symmetry. It will reconstruct the coupling parameters such as skew angle and beam size defined as $\sigma_x^2 - \sigma_y^2$ by using multipole analysis of image current. This work presents the simulation result on the reconstruction and the wire test result for the prototype device.

INTRODUCTION

The J-PARC is constructing a beamline described in Fig.1 to measure the electric dipole moment and anomaly of magnetic dipole moment of muon particle with high precision of 70 and 450 ppb, respectively, by producing reaccelerated thermal muon beam which has extremely small emittance of about $1.5\pi \text{ mm} \cdot \text{mrad}$ and momentum spread, $\delta p_t/p$, less than 10^{-5} [1].

The muons are required to have a small transverse emittance and the J-PARC has presented the first muon acceleration with a radio-frequency accelerator [2]. The reaccelerated muon beam is injected into the storage magnet after manipulating the phase space for the correlation of horizontal and vertical space, called an XY coupling, to prevent the vertical divergence of beam at the storage section which could be a source of systematic uncertainties on the measurement precision [3].

* Work supported by IBS. This work was also supported by the National Research Foundation of Korea (Grant No. NRF-2016R1A5A1013277).

[†] mchung@unist.ac.kr

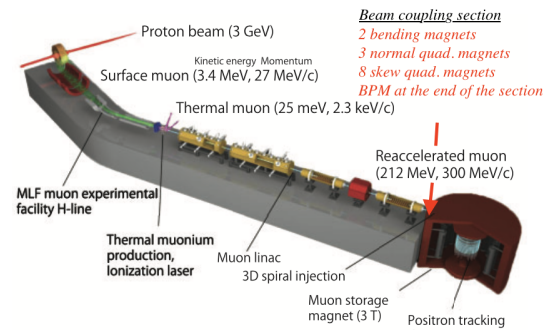


Figure 1: Schematic diagram of J-PARC muon g-2/EDM beam line. A muon beam is produced by using the laser ionization of Muonium and then accelerated through LINAC to $\beta \sim 0.94$. In the end, muons are injected into the solenoidal storage magnet after phase space manipulation by a series of skew quadrupole magnets which are not shown [1].

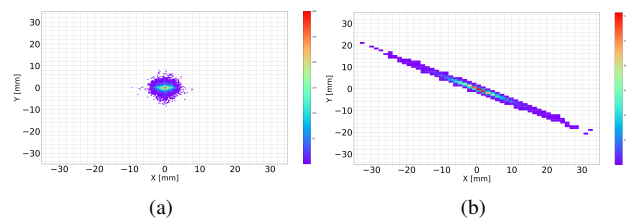


Figure 2: Beam distribution in real space (a) at the exit of LINAC where the distribution is azimuthally symmetric and (b) at the injection point after XY coupling.

Thus, the quality of XY coupling needs to be monitored for the beam transportation during a beam-operation to decrease the possible systematic uncertainties. A stripline beam position monitor would be implemented to reach the requirement of monitoring the XY coupling. The features of XY coupling such as the asymmetry of beam size and skew angle would be reconstructed by a method based on the multipole analysis of image currents over the circumference of vacuum chamber.

This paper will present on the multipole analysis of image currents for the method of how the XY coupled beam could be reconstructed. Next section, the mechanical dimension of prototype device will be shown and the wire test result

ANALYSIS OF HEAVY ION IRRADIATION FIELD NONUNIFORMITY USING TRACK DETECTORS DURING ELECTRONIC COMPONENTS TESTING

A.S. Bychkov[†], P.A. Chubunov, A.S. Konyukhov, A.A. Pavlov, ISDE, Moscow, Russia

Abstract

Determining the applicability of electronic components in spacecrafts involves conducting the tests using heavy ions. The Branch of URSC - ISDE and FLNR of JINR have created and operate the only in Russia test facilities based on the FLNR JINR accelerators allowing for heavy ion irradiation over a large area up to 200x200 mm. During simultaneous irradiation of several electronic components with heavy ions, it is necessary to ensure the device under test (DUT) location within the area of minimal nonuniformity. This problem is being solved by pretest determination of the irradiation field nonuniformity for each type of ion (Ne, Ar, Kr, Xe, Bi) and nonuniformity validation every 12 hours. Fluence is determined by a metrologically certified method using track detectors. In order to visualize the irradiation field nonuniformity, additional experiments were carried out with the irradiation of track detectors covering the entire irradiation area for each ion species. Based on the data obtained, a map of nonuniformity was plotted, which allows us to conclude that nonuniformity does not exceed 10% in the most frequently used areas of the irradiation field (100x150 mm) during SEE testing.

MANUSCRIPTS

This report presents the results of analysis of heavy ion irradiation field nonuniformity at various flow densities in test facilities to control resistance of electronic components (EC) to heavy ions (HI).

The assessment of the EC resistance to the effects of space ionizing radiation (SIP) is an integral part of the EC certification process for space applications. The procedure for confirming the EC resistance to the effects of SIP includes EC testing for single event effect assurance.

At this moment The Branch of URSC - ISDE and FLNR of JINR have created and operate the only in Russia test facilities (TF) based on the FLNR JINR accelerators allowing for heavy ion irradiation over a large area up to 200x200 mm.

The TF provides testing of all functional classes and constructive-technological versions (with the rarest exception) EC to all types of SEE. The TF allow to irradiate EC samples with C, O, Ne, Ar, Fe, Kr, Xe, Bi ions with a flux density in the range from 10 to 10⁵ particles / (cm² · s). Fluence is determined by a metrologically certified method using solid-state track detectors (TD) made of polymer membrane (Polyethyleneterephthalate and polycarbonate). TD are detectors of charged particles and

nuclear fragments, the registration of which is accompanied by the appearance of observable tracks repeating the trajectory of the particle.

The main goal of the further development TF is to increase their availability, stability of work, accuracy of characteristics control and, as a result, informativeness and reliability of tests, while reducing the cost of conducting them.

In the same time during simultaneous irradiation of several electronic components with heavy ions, it is necessary to ensure the device under test location within the area of minimal nonuniformity. This problem is being solved by pretest determination of the irradiation field nonuniformity for each type of ion (Ne, Ar, Kr, Xe, Bi) and nonuniformity validation every 12 hours.

To visualize irradiation field nonuniformity, additional experiments were performed with irradiation of the TD covering all irradiation area at the beginning, middle and at the end of the session on each type of ion at four flow densities (Table 1). In order to take a photo of the tracks and then count them, the irradiated samples were etched in an alkali solution, for the manifestation of “hidden” tracks left by the particles, after which a gold layer was applied to obtain a contrast image created on the computer screen with an electron microscope. Next, the tracks were counted using an electron microscope in accordance with the metrologically certified “Method for measuring the fluence of heavy charged particles using track membranes based on polymer films”.

Table 1: List of Flux Densities Used During Irradiation of Detectors

No. of density	Flux density ϕ , [particles/(cm ² ·s)]	Fluence Φ [particles/cm ²]
1	500	3x10 ⁵
2	5000	10 ⁶
3	10000	10 ⁷
4	50000	10 ⁷

Based on the data obtained, a map of nonuniformity was plotted (Fig. 1). The typical shape of the ion beam is in the form of a “Gaussian” curve with a “plateau” that is clearly distinguished in the central region of irradiation.

[†] npk1@orkkniikp.org

ELECTRON BEAM SIZE MEASUREMENTS USING THE HETERODYNE NEAR FIELD SPECKLES AT ALBA

M. Siano*, B. Paroli, M. A. C. Potenza, Università degli Studi di Milano, 20133 Milan, Italy
 U. Iriso, C. S. Kamma-Lorger, A. A. Nosych, ALBA, Cerdanyola del Valles, Barcelona, Spain
 S. Mazzoni, G. Trad, CERN, Geneva, Switzerland

Abstract

Experiments using the Heterodyne Near Field Speckle method (HNFS) have been performed at ALBA to characterize the spatial coherence of the synchrotron radiation, with the ultimate goal of measuring both the horizontal and vertical electron beam sizes. The HNFS technique consists on the analysis of the interference between the radiation scattered by a colloidal suspension of nanoparticles and the synchrotron radiation, which in this case corresponds to the hard X-rays (12 keV) produced by the in-vacuum undulator of the NCD-Sweet beamline. This paper describes the fundamentals of the technique, possible limitations, and shows the first experimental results changing the beam coupling of the storage ring.

INTRODUCTION

At the ALBA storage ring, beam size monitoring is routinely performed by means of an X-ray pinhole camera [1]. Furthermore, parallel reliable measurements are provided by Young interferometry with visible synchrotron radiation [2, 3]. A novel and unconventional interferometric beam size measurement technique is offered by the Heterodyne Near Field Speckle method (HNFS). It relies on the statistical analysis of the speckled intensity distribution generated by calibrated spherical nanoparticles of known properties enlightened by the Synchrotron Radiation (SR) extracted from the accelerator. It was developed almost twenty years ago at optical wavelengths as a particle sizing technique [4, 5] and then extended to the X-ray region of the spectrum [6]. More recently it has found applications in accelerator beam instrumentation [7–10] allowing to probe the SR two-dimensional (2D) transverse coherence described by the Complex Coherence Factor (CCF) [11, 12]:

$$\mu(\Delta\vec{r}) = \frac{\langle E(\vec{r})E^*(\vec{r} + \Delta\vec{r}) \rangle}{\sqrt{\langle I(\vec{r}) \rangle \langle I(\vec{r} + \Delta\vec{r}) \rangle}} \quad (1)$$

In Eq. (1), E is the electric field, $I = \langle |E|^2 \rangle$ is the associated intensity, $\vec{r} = (x, y)$ denotes transverse position on a x-y plane perpendicular to the propagation direction, and finally $\langle \cdot \cdot \cdot \rangle$ denotes ensemble averages. Under the conditions of validity of the Van Cittert and Zernike (VCZ) theorem [11, 12], the 2D transverse profile of the electron beam can then be retrieved from the measured 2D CCF.

We report here a proof of concept experiment for two dimensional beam size measurement using the 12 keV hard X-rays produced at the NCD-Sweet beamline at ALBA. The paper is organized as follows: after briefly reviewing the

fundamentals of the HNFS method, we describe the NCD-Sweet beamline and the experimental setup therein installed; then we show and discuss the first results obtained by changing the coupling in the storage ring; finally, we collect our conclusions.

THE HNFS TECHNIQUE

The HNFS technique relies on the self-referencing interference between the spherical waves scattered by the particles of the colloidal suspension and the transilluminating field. For a single scattering particle, the interference image is composed by circular fringes whose visibility is reduced according to the 2D CCF of the incoming radiation at the scattering plane. An example is shown in Fig. 1(a) where results of numerical simulations are reported for the case of incoming radiation endowed with larger coherence along the vertical direction. The random superposition on an intensity basis of many of these single-particle interferograms results in a stochastic intensity distribution known as heterodyne speckle field, as shown in Figs. 1(b) and (c).

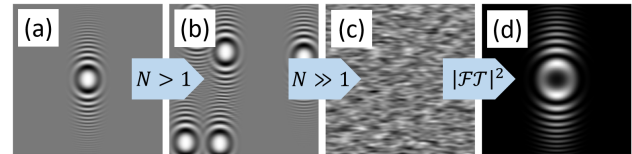


Figure 1: Fundamentals of the HNFS technique. (a) Single-particle interferogram for incoming radiation with larger coherence along the vertical direction. (b) and (c) The random sum of many single-particle interferograms generates a so-called speckle field. (d) The 2D power spectrum of heterodyne speckles allows to retrieve the interferometric information on coherence conveyed by the single-particle interference image.

Coherence information is retrieved by Fourier analysis of the speckle field – Fig. 1(d). In fact, the 2D power spectrum closely resembles the single-particle interferogram. It exhibits peculiar oscillations (Talbot oscillations) enveloped by the squared modulus of the radiation CCF [7–10]:

$$I(\vec{q}, z) = |\mu[\Delta\vec{r}(\vec{q}, z)]|^2 T(q, z) \quad (2)$$

where $I(\vec{q}, z)$ is the 2D spatial power spectrum of heterodyne speckles at a distance z from the scattering plane, $T(q, z) = 2 \sin^2[zq^2/(2k)]$ is known as the Talbot Transfer Function (TTF), \vec{q} is the Fourier wavevector, $q = |\vec{q}|$, $k = 2\pi/\lambda$ where λ is the radiation wavelength, and finally

$$\Delta\vec{r}(\vec{q}, z) = z \frac{\vec{q}}{k} \quad (3)$$

* mirko.siano@unimi.it

J-PARC TEST OF ESS BEAM ON TARGET DIAGNOSTICS PROTOTYPES APERTURE MONITOR AND GRID

C.A. Thomas*, J. Etxeberria, J. Paulo-Martin, H. Kocevar, E. Donegani
T. Shea, European Spallation Source ERIC, Lund, Sweden
Shin-ichiro Meigo, Motoki Ooi, JAEA/J-PARC, Tokai-mura
Haihua Niu, Bin Zhang, IMP/CAS, Lanzhou
Anders Johansson, Markus Törmänen, Lund University, Lund

Abstract

The ESS high power beam will be delivered to the spallation target with high degree of control. To this end, we have designed a suite of instruments which provide measurement of the beam characteristics in a drift space a few meters from the target. We present in the paper two of these instruments, the Aperture Monitor (APM) and the GRID. The APM is designed to measure the fraction of beam that goes through the defined aperture, and covers the range of time from intra-pulse at μs sampling time to many pulses over seconds. The GRID measures the projected horizontal and vertical profiles. We have been designing a prototype of these two instruments and installed them in the 3NBT dump line of J-PARC. In this paper we present in a first part the prototypes design. They are designed to test functionality of these instruments in a similar radiation environment as ESS. The 3NBT Dump line at J-PARC presents such an environment: it takes a 50 mA beam pulse from 50 μs to 500 μs , at energies from 400 MeV to 3 GeV; the location of the instrument is in front of the dump, although at 12 m, and 30 cm downstream a thin Al-window, which generates secondary particles. In the second part of the paper we report the results and the measurements performed to test the prototypes. Before concluding we will discuss the results and propose improvements to the instruments final design.

INTRODUCTION

The ESS accelerator delivers a high power beam to the spallation target that is 30% below the material rupture. As a consequence, a beam in errant condition, i.e. not matching the nominal condition, may bring a risk to the target. Preventing any risk condition to occur during the phases of tuning and neutron production is critical. A suite of instruments has been designed to that end [1]. It will measure the beam properties of any pulse delivered to the target, and permit to abort the pulse within 10 μs after detection of any errant beam condition. The suite of instrument is composed of beam on target imaging, a harp and aperture monitoring. The beam on target imaging is a critical instrument that will provide the main 2D information on the beam properties. For each pulse it will measure the position of the beam, the edges of the beam distribution, and the flatness of the current density distribution [2], with respect to the centre of the target wheel sector on which the pulse must be delivered. The

aperture monitoring is designed to detect any beam outside the nominal aperture. The harp is somehow redundant with the imaging, but it is complementary as it can detect the beam 1D profile within the pulse, thus detecting potential errant condition at the microsecond scale. In the following, we will focus on the harp and monitoring instrument. We will name the harp as the GRID, and the aperture monitoring as APM.

APM Functionality

The APM is designed to detect small fraction of the proton beam that is outside a defined aperture. The detection account for charges corresponding to 0.1% of the nominal beam current from 5 μs to minutes. To covers such a time span, the design incorporates 2 detections schemes, one is a metallic blade, from which the proton induced current is sampled at 1MS/s, and the second one is a thermocouple, which senses the charge induced temperature. The sampling rate of the temperature is expected to be in the range of 100 S/s. The temperature sensor can detect small amount of charge that can't be seen by the blade, which can accumulate creating damage on the long term.

GRID Functionality

The GRID is designed to provide the 1D projected profile of the beam on orthogonal axis. While the pulse is been delivered to the target, it measures the edges of the beam distribution, the flat top of the current distribution, and the position of the beam. In addition, the rasterising of the beam can be detected. The design is based on a harp of wires, from which the proton induced current is measured.

PROTOTYPE DESIGN

The location of these instruments in the close target region imposes some additional constraint, mainly due to the high radiation environment, that must be understood and taken into account. This is addressed by the choice of the materials, and by additional features to the current or temperature sensing. By this, we need to address the sensitivity of the instrument in radiation environment; the perturbation of the signal by radiation and general environment brought by pulsed high power beam, RF parasitic signals and charged secondary particles; the resistance of the instrument to any errant beam condition, in particular the most extreme where all the beam power is deposited on the instrument. This addresses primarily by modelisation of the instrument in

* cyrille.thomas@ess.se

Content from this work may be used under the terms of the CC BY 3.0 licence (© 2019). Any distribution of this work must maintain attribution to the author(s), title of the work, publisher, and DOI

LABORATORY AND BEAM BASED STUDIES FOR ASSESSING THE PERFORMANCE OF THE NEW FAST WIRE SCANNERS FOR THE CERN INJECTOR COMPLEX

J. Emery*, P. Andersson, W. Andreatza, J. M. Fernandez, A. Goldblatt, D. Gudkov, F. Roncarolo
J. L. Sirvent, J. Tassan-Viol, R. Veness, CERN, Geneva, Switzerland

Abstract

At CERN, fast beam wire scanners serve as reference transverse profile monitors in all synchrotrons. As part of the LHC Injector Upgrade project, a new generation of scanners has been designed to improve system reliability, precision and accuracy in view of higher brightness beams. This paper will discuss the performance achieved during both laboratory calibration and prototype testing with beam. The beam measurements performed in 2018 demonstrated excellent system reliability and reproducibility, while calibration in the laboratory showed that an accuracy below 10 μ m can be achieved on the wire position determination.

INTRODUCTION

Fast Beam Wire Scanner (BWS) systems are commonly used in synchrotrons to monitor transverse beam sizes. They are based on kinematic units designed to move very thin wires at high speed through a particle beam. The wire-beam interaction generates a shower of secondary particles that is typically measured by a scintillator coupled to a photo-multiplier tube. The correlation between the wire position and the intensity of the secondary particles shower allows the determination of the transverse beam size.

As part of the LHC injectors Upgrade (LIU) project at CERN, the 17 BWS systems presently installed in the CERN PSB, PS and SPS, historically using 3 different designs, will be replaced by a single, new generation of device that will start to be commissioned towards the end of 2020.

The new design aims at combining the movement accuracy of presently used linear systems that are limited in speed [1] with the high speed of rotative scanners [2, 3].

In addition the new design (see Fig. 1) will be made more robust by not including any moving vacuum bellows, a common source of failure on its predecessors. All moving parts (motor, resolver, optical encoder and fork) are on the same shaft on the vacuum side, while the motor stator coils are on the air side. A thin, magnetically permeable membrane allows magnetic energy transmission from stator to motor without the need for a vacuum feedthrough.

The use of a *direct drive* system, where the motor is directly coupled to the parts to actuate, leads to lower mass, lower friction and reduced mechanical play. With this arrangement, the angular position of the fork is driven without the translation stage or gearbox used on older systems, thus yielding enhanced accuracy and precision.

Wire Position Determination

The shaft angle, and thus the wire position, is measured by an optical encoder based on a reflective disk engraved with anti-reflective marks. The encoding of the marks during disk rotation gives the incremental angular position. The absolute angle is calculated from the encoding of specific reference marks. An extensive description of the optical encoder design can be found in [4].

Even though the mechanical design was optimized for high stiffness and low mechanical play [5,6], a laboratory bench is systematically used to verify the transverse wire position as a function of the angular position of the shaft for different wire speeds. This calibration allows any fork or wire deformation during the scan to be corrected.

Secondary Particles Detection

The beam-induced shower of secondary particles generated as the wire interacts with the beam will be measured by a scintillator located downstream of the beam-wire interaction point. In the current systems this scintillator is coupled to a Photo-Multiplier Tube (PMT), with selectable neutral density filters placed between the scintillator and the PMT to cover the signal generated by the wide variety of beams in the LHC injectors. For the LIU systems, the single PMT combined with neutral density filters, has been replaced with four PMTs linked to the same scintillator each with a fixed neutral density filter [4]. All 4 PMT signals are then digitised in parallel. Depending on the beam parameters, there will be always one optimal PMT which is not saturated and with enough signal to noise, that can be selected by software after the acquisition, eliminating the need to choose an appropriate optical density filter before each measurement. The new PMT setup includes custom

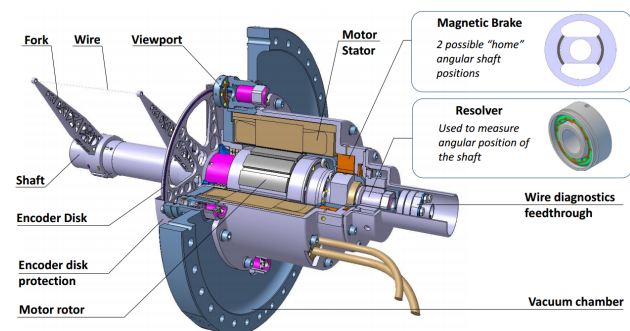


Figure 1: LIU wirescanner electro-mechanical mechanism and movement encoders.

* jonathan.emery@cern.ch

ANALYSIS OF QUADROPOLAR MEASUREMENTS FOR BEAM SIZE DETERMINATION IN THE LHC

D. Alves*, M. Gasior, T. Lefèvre, CERN, Geneva, Switzerland

Abstract

Due to limitations with non-invasive beam size diagnostics in the LHC, particularly during the energy ramp, there has been an interest to explore quadrupolar-based measurements for estimating the transverse beam size, and hence determining the transverse emittance. This technique is especially attractive as it is completely passive and can use the existing beam position instrumentation. In this work, we perform an analysis of this method and present recent measurements taken during energy ramps. Quadrupolar-based measurements are compared with wire-scanner measurements and a calibration strategy is proposed to overcome present limitations.

INTRODUCTION

Recently, there has been a rising interest in exploring the capabilities of existing beam position instrumentation for estimating transverse beam sizes in the LHC. These measurements are in fact very challenging in the LHC mainly due to the low relative sensitivity ($\approx 10^{-3} \text{ mm}^{-2}$) of the existing Beam Position Monitors (BPMs) to the quadrupolar moment. BPM systems equipped with the high resolution Diode Orbit and Oscillation (DOROS) electronics [1] have therefore been used. These systems are based on diode detectors with limited dynamic range. For this reason, the DOROS electronics makes use of a set of amplification stages with automatic gain adjustments ensuring that the diodes always operate in their linear regime [2].

Recently, encouraging results with this technique have been presented in [3] and [4]. In this work, we present a different approach for the absolute estimation of the transverse beam sizes, based on the cross-calibration of the various BPM systems against Wire-Scanner (WS) measurements.

PHYSICS

In the case of Gaussian-like transverse beam profiles, the quadrupolar moment Q is defined by [5]:

$$Q = Q_\sigma + Q_r = (\sigma_H^2 - \sigma_V^2) + (x^2 - y^2) \quad (1)$$

where $\sigma_{H,V}$ represent the RMS horizontal and vertical transverse beam sizes, x and y represent, respectively, the horizontal and vertical average beam positions, $Q_\sigma = \sigma_H^2 - \sigma_V^2$ and $Q_r = x^2 - y^2$.

Taking the usual multipole expansion of BPM amplitudes [5] we get, for each electrode:

$$H_1 = h_1 I (c_{0h} + c_{1h}x + c_{2h}Q + \dots) + k_1 \quad (2)$$

$$H_2 = h_2 I (c_{0h} - c_{1h}x + c_{2h}Q + \dots) + k_2 \quad (3)$$

$$V_1 = v_1 I (c_{0v} + c_{1v}y - c_{2v}Q + \dots) + w_1 \quad (4)$$

$$V_2 = v_2 I (c_{0v} - c_{1v}y - c_{2v}Q + \dots) + w_2 \quad (5)$$

where I is the beam intensity, the c coefficients are related to the geometrical/mechanical setup of the pick-up and the h , v , k and w coefficients are gains and offsets which are unknown functions of the bunch peak intensities and of the errors introduced by the electronics. Perfectly symmetric cabling and electronics, and zero offset on all 4 channels implies that $h_1 = h_2 = v_1 = v_2$ and $k_1 = k_2 = w_1 = w_2 = 0$. Furthermore, a perfectly symmetric pick-up implies that $c_{0h} = c_{0v} = c_0$, $c_{1h} = c_{1v} = c_1$ and $c_{2h} = c_{2v} = c_2$.

Under these ideal conditions, the quadrupolar moment can be derived from electrode measurements using Eq. (6):

$$R = \frac{\Sigma_H - \Sigma_V}{\Sigma_H + \Sigma_V} = \frac{c_2}{c_0} Q \quad (6)$$

where $\Sigma_H = H_1 + H_2$ and $\Sigma_V = V_1 + V_2$. In reality, however, the previous equation becomes more complicated and from Eqs. (2)–(5) we get:

$$R = \frac{\Sigma_H - \Sigma_V}{\Sigma_H + \Sigma_V} = \frac{A}{B} + \frac{C}{B} Q, \quad (7)$$

where:

$$A = (h_1 + h_2) c_{0h} - (v_1 + v_2) c_{0v} + (h_1 - h_2) c_{1h}x - (v_1 - v_2) c_{1v}y + \frac{k_1 + k_2 - w_1 - w_2}{I} \quad (8)$$

$$B = (h_1 + h_2) c_{0h} + (v_1 + v_2) c_{0v} + (h_1 - h_2) c_{1h}x + (v_1 - v_2) c_{1v}y + (h_1 + h_2) c_{2h}Q - (v_1 + v_2) c_{2v}Q + \frac{k_1 + k_2 + w_1 + w_2}{I} \quad (9)$$

$$C = (h_1 + h_2) c_{2h} + (v_1 + v_2) c_{2v} \quad (10)$$

If we now plug in theoretical values for the geometric constants of typical LHC BPMs:

$$\begin{aligned} c_1 &\approx 5 \times 10^{-2} c_0 \\ c_2 &\approx 3 \times 10^{-3} c_0 \end{aligned} \quad (11)$$

and consider small position displacements $|x| \lesssim 1 \text{ mm}$ and $|y| \lesssim 1 \text{ mm}$ as well as values of $|Q| \lesssim 10 \text{ mm}^2$ (e.g.

* diogo.alves@cern.ch

Content from this work may be used under the terms of the CC BY 3.0 licence (© 2019). Any distribution of this work must maintain attribution to the author(s), title of the work, publisher, and DOI

DEVELOPMENT OF MODULAR SPARE PARTS FOR THE PROFILE AND POSITION MONITORS OF THE 590 MeV BEAM LINE AT HIPA

R. Dölling[†], F. Marcellini, D. Kiselev, Paul Scherrer Institut, 5232 Villigen PSI, Switzerland
K. Zehnder¹, D. Berisha, J. Germanovic, ABB Technikerschule, 5400 Baden, Switzerland
¹also at Paul Scherrer Institut, 5232 Villigen PSI, Switzerland

Abstract

A new generation of monitor plugs is under development for the ageing wire profile monitors and beam position monitors which are inserted into massive shielding of the 590 MeV proton beam line at HIPA. The modular mechanical design, aspects of handling, vacuum compatibility, radiation hardness, shielding, cabling and monitor environment are discussed.

INTRODUCTION

Near to the meson production targets M and E, profile monitors (PM) and beam position monitors (BPM) in the 590 MeV beam line from the Ring cyclotron to the spallation neutron source SINQ are inserted into chimneys of the beam vacuum chamber, surrounded by the first shielding (Fig. 1). Monitor plugs contain motors, vacuum flange and feedthroughs at the top, accessible from the service floor, shielding iron, cables and mechanical transmissions in the middle, and wire forks and position pick-ups at the bottom, close to the beam pipe and exposed to much stronger radiation background. Three generations of plugs were designed in the 1980's and 90's, following different mechanical concepts, and after initial improvements all monitors were operated for many years with very few defects. However, in case of a defect, a repair of the lower parts of the plug is hardly possible due to the high activation level and the incongruous manipulator-compatible and modular design. Hence, a defect of a small part may lead to the disposal of a plug of, e.g., 1.7 tons. No complete spare plugs are available for the nine different types of plugs, which are adapted to the local environment. Four types do not include BPMs, which would allow automated centring of the beam to Target E and downstream. They may also contribute to an improved safety of SINQ operation [1]. This still has to be specified as part of a comprehensive evaluation of safety measures.

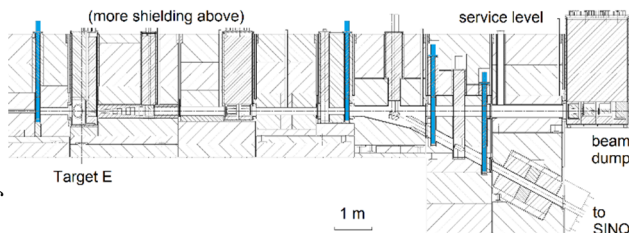


Figure 1: Generation 3 [2] monitor plugs at Target E and downstream. Generation 1 and 2 plugs are located upstream.

[†] rudolf.doelling@psi.ch

After two recent defects, we decided to develop a new generation of monitor plugs instead of copying the old designs, which are not documented in detail [3]. A single concept will be adapted to the different insertion environments. A strict modularity and manipulator compatibility will allow to exchange individual modules from a plug in case of a defect. This also enables later improvements and modifications. The new plug will include BPMs. With an ageing machine and limited resources, the affordability of such a development remains a point of controversial discussion.

MECHANICAL CONCEPT

The new monitor plug will consist of five building blocks [4]:

1. *PM module*, attachable by manipulator to the bottom of the shielding block. With a manipulator-detachable long *transmission rod* and a connector to which a cable module can be plugged into.
2. *BPM module*, attachable by manipulator to the shielding block. With a connector to which a cable module can be plugged into.
3. Two long, from top vertically removable *cable modules*, each housing four conductors. With electrical feedthroughs at the vacuum flange.
4. The main *vacuum flange* with the large *shielding block* mounted. Block with channels for cable inserts and transmission rod, plus a spare channel for later use (e.g., for a loss monitor). Flange with openings for drive module and cable inserts.
5. *Drive module* with motor, rotary vacuum feedthrough and linear stage with end switches, to which a transmission rod can be adapted.

Different from Generation 3, only a single PM module carries both rail guides with wire forks (Fig. 2). Forks with attached wires can still be dismantled separately by manipulator, using a snap fit. Unlike previous generations, horizontal and vertical profiles are measured synchronously. (Temperatures of the molybdenum double wires are well below thermionic emission. Hence, we expect only a minor crosstalk from secondary electrons.) Hereto the fork movement is coupled by a circumferential steel rope guided by four wheels. The use of the transmission rod instead of counter-moving steel ropes or strips, permits a relative simple exchange of the PM module by manipulator. However, at the cost of a slight positioning inaccuracy in the presence of temperature variations. The Generation 2 (see Fig. 9 of [5]) feature, having the forks mounted to a long sword which is retractable from outside through a large channel in the shielding block, was

PERFORMANCE OF AN IN-AIR SECONDARY EMISSION GRID PROFILE MONITOR AT THE ISIS NEUTRON AND MUON SOURCE

D. W. Posthuma de Boer*, C. Bovo, H. V. Cavanagh, B. Jones, A. Kershaw, A. Pertica
ISIS, STFC, Rutherford Appleton Laboratory, Oxfordshire, UK

Abstract

The ISIS neutron and muon source, located in the UK, consists of an H^- linear accelerator, a rapid cycling proton synchrotron and extraction lines to two target stations. A project is currently under way to replace the target assembly of the First Target Station (TS1) in order to secure its continued operation and improve operational flexibility. In addition to a number of other diagnostic tools, a new secondary emission (SEM) grid profile monitor is expected to be located within helium atmosphere of the new target assembly. To investigate the performance of an out of vacuum SEM grid, a prototype monitor was positioned in air between a beam exit window and a beam dump. Profile measurements taken with this monitor are presented, including tests at a range of bias voltages with a fast data acquisition system to investigate secondary signal sources.

INTRODUCTION

The ISIS Synchrotron

The ISIS synchrotron accelerates two bunches with a total of approximately 3×10^{13} protons from 70 MeV to 800 MeV at a repetition rate of 50 Hz delivering a mean beam power of 0.2 MW to two tantalum clad, tungsten targets; 1 in 5 beam pulses are delivered to target station 2 (TS2) and the remaining four to TS1. The target, reflector and moderator assembly (TRAM) of TS1 has been redesigned and will be replaced during the shutdown period from 2020 to 2021 [1].

A Near Target Profile Monitor

The TS1 target intercepts on average 160 kW and is susceptible to damage from over-focusing of the transverse beam size. The condition of the target is therefore monitored with thermocouples in contact with the tungsten plates and cooling water which flows between the plates is also monitored. Target halo monitors measure the approximate transverse beam size and position upstream of the target [2], and have been in use for a number of decades. A new profile monitor located near to the front face of the target would provide more detailed and faster transverse beam information and help to prevent over-focusing and improve positioning.

This near-target profile monitor (NTPM) will intercept four out of five beam pulses during routine operation and be located within the target assembly. The NTPM will be required to operate in the helium atmosphere of the target as-

sembly, which differs from the vacuum environment where these monitors are ordinarily used.

PROFILE MONITOR TESTING IN A GASEOUS ENVIRONMENT

The performance of a wire grid profile monitor in a gaseous environment was tested by positioning a spare monitor in the air between an exit window and a beam dump; Fig. 1 shows the machine components in the vicinity of the dump. The extracted beam travelled through two ordinary in-vacuum profile monitors, EPM1 & 2, before reaching the test in-air profile monitor and then the synchrotron room beam dump (SRBD). Figure 2 shows the layout in front of the SRBD, an air gap of approximately 30 cm separated the beam exit window from the front face of the SRBD.

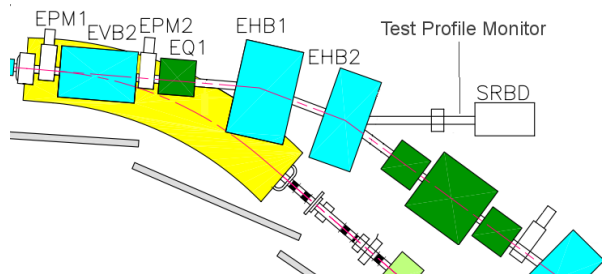


Figure 1: ISIS beam extraction line in the vicinity of the SRBD.

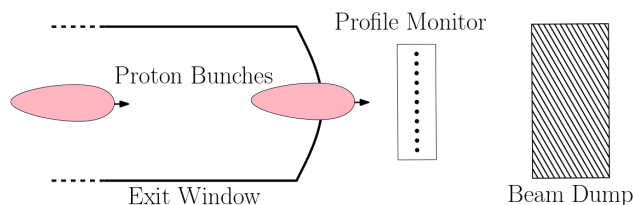


Figure 2: Approximate set-up in-front of the SRBD showing a beam exit window and the in-air profile monitor.

The test profile monitor was a dual plane wire grid with 24 signal wires per plane sandwiched between a series of biasing wires. The wires were SiC coated, carbon fibres with a diameter of 142 μm [3]. Signals from each wire were transported with individual coaxial cables to a data acquisition (DAQ) system in a shielded area. Two DAQ systems were available for this investigation: a slow system which output a voltage based on the integrated signal via a multiplexer, and a fast system which had ten synchronised National Instruments (NI) PXI-5124 scope cards. The fast sys-

* david.posthuma-de-boer@stfc.ac.uk

STUDIES OF THE TIME STRUCTURE OF IONISATION BEAM PROFILE MEASUREMENTS IN THE ISIS EXTRACTED PROTON BEAMLINE

C. C. Wilcox*, W. A. Frank†, A. Pertica, R. E. Williamson, STFC Rutherford Appleton Laboratory, Didcot, Oxfordshire, UK

Abstract

Ionisation Profile Monitors (IPMs) are used at the ISIS neutron and muon source to perform non-destructive transverse beam profile measurements. An in-house particle tracking code, combined with 3D CST modelling of the electric fields within the monitors, has been used to improve understanding of the various error sources within the IPMs, and shows close agreement with profile measurements in the synchrotron.

To allow for detailed benchmarking studies, an IPM has been installed in Extracted Proton Beamline 1 (EPB1), enabling comparison with secondary emission (SEM) grid measurements. However, the IPM measurements taken in EPB1 show increased levels of profile broadening at operational beam intensities, which are not reproduced by SEM measurements or simulation. To investigate these differences, studies of the time structure of measured profiles are being performed.

This paper details the development of new, high-speed multichannel data acquisition electronics, required to perform these studies. Resulting measurements are discussed, along with an analysis of the data's time structure and a comparison with that predicted by the IPM code.

INTRODUCTION

Profile measurements using Ionisation Profile Monitors (IPMs) are inherently affected by both the beam's space charge field and non-uniformities in the monitor's drift field distribution [1]. These effects alter the trajectories of residual gas ions within the monitors, causing them to diverge, broadening the measured profiles. Producing accurate simulation codes to analyse, quantify and correct for this effect is an area of active development at multiple hadron accelerator facilities [2].

A particle tracking code has been developed for ISIS IPMs, to simulate their internal residual ion motion and resulting profile measurements. Previous work and an outline of how this code functions are detailed in [3], though it has since been rewritten in Python. The code is benchmarked against a test IPM, installed in Extracted Proton Beamline 1 (EPB1), to allow for single-pass measurements to be taken and compared with profile data from nearby secondary emission (SEM) grids.

EPB1 transports an 800 MeV pulsed proton beam; each pulse consists of two 100 ns bunches separated by 225 ns. The ISIS synchrotron operates at a repetition rate of 50 Hz, with four of every five pulses extracted to EPB1. The minimum pulse spacing of 20 ms ensures that IPM measurements are unaffected by multi-pass effects. Typical beam intensities are $\sim 3 \times 10^{13}$ protons per pulse (ppp).

* christopher.wilcox@stfc.ac.uk

† william.frank@stfc.ac.uk

At operating intensities, profiles measured with the EPB1 IPM show unexpectedly high levels of broadening compared with both simulation and synchrotron IPM measurements. To further understand the effects occurring within the monitor, and to provide additional benchmarking data for the IPM code, high-speed data acquisition (DAQ) electronics have been developed to measure the time structure of the measurements taken by this monitor.

IPM CODE DEVELOPMENT

To allow for comparison with the measured time structure, a time-dependant approximation of the beam pulse structure has been added to the IPM simulation code. Two key effects are determined by this: beam-induced generation of residual gas ions and the impact of the beam's space charge field on ion motion within the IPM.

Two separate calculations of the electric field map within the monitor are computed, using CST EM Studio 2018 [4]. One utilises only the drift field electrode and IPM detector biases as electric field sources, while the other also includes the beam space charge field, with the input beam distribution determined by SEM profile monitor measurements. The ion tracking code only takes the space charge component of the electric field into account during the two 100 ns intervals in which a bunch is passing through the IPM. This is achieved by alternating between the two electric field maps at the relevant times during the tracking simulation. Similarly, the code generates residual gas ions continuously during these 100 ns time intervals, with the generated transverse ion distribution also determined by SEM monitor measurements.

DAQ SYSTEM REQUIREMENTS

Risetime and Bandwidth

ISIS IPMs use an array of forty 4800 series Channeltron Electron Multipliers (CEMs), supplied by Photonis [5], to detect residual gas ions. Each CEM is 6 mm wide, providing adequate measurement resolution for typical beam widths in the synchrotron and EPBs (50-120 mm). To estimate the required bandwidth for the DAQ system, the IPM simulation code was used to predict the time structure of the ion current input into the CEMs (Fig. 1a).

All residual gas ions generated in this simulation were H^+ ions (i.e. protons). In addition to being common within beampipe vacuums, the low mass and fast acceleration of H^+ by the drift field means the predicted time structure from this model represents the highest frequency content which the IPM should be expected to measure.

The frequency spectrum of this simulated ion current, obtained from a fast Fourier transform of the simulation output, yields a minimum required bandwidth of 3.5 MHz

SPATIAL RESOLUTION OF AN X-RAY PINHOLE CAMERA USING A MULTI-LAYER MONOCHROMATOR

L. Bobb*, G. Rehm, Diamond Light Source, Oxfordshire, U.K.

Abstract

X-ray pinhole cameras are widely used for beam emittance monitoring at synchrotron light sources. Due to the reduction in beam emittance expected for the many fourth generation machine upgrades, the spatial resolution of the pinhole camera must be improved accordingly. It is well known that there are many contributions to the point spread function. However, a significant contribution arises from diffraction by the pinhole aperture. Given that diffraction is dependent on the spectral distribution of the incident synchrotron radiation, the spatial resolution can be improved by using a monochromatic beam. For optimal performance, the photon energy should be matched to the pinhole aperture size. Here we investigate the spatial resolution of the pinhole camera as a function of photon energy using a multi-layer monochromator.

INTRODUCTION

Emittance monitoring is a crucial diagnostic instrument at synchrotron light sources. With the planned upgrades to fourth generation synchrotrons such as Diamond-II [1], which are in part motivated by a reduction in emittance to provide increased brightness on beamlines, the emittance monitoring capabilities must be upgraded accordingly. Given the reduced emittance, the transverse size of the electron beam in the storage ring will also decrease. Thus the spatial resolution of the diagnostic instrumentation must be improved to ensure accurate measurement of the emittance for feedback systems [2].

The point spread function (PSF) defines the spatial resolution of the diagnostic instrument. For X-ray pinhole cameras (XPCs), as shown in Fig. 1, it is well documented that each optical element will contribute to the overall PSF. The PSF from each optical element is assumed to be Gaussian such that the overall PSF is

$$\sigma_{\text{PSF}}^2 = \sigma_{\text{pinhole}}^2 + \sigma_{\text{camera}}^2 \quad (1)$$

with

$$\sigma_{\text{pinhole}}^2 = \sigma_{\text{diffraction}}^2 + \sigma_{\text{aperture}}^2 \quad (2)$$

and

$$\sigma_{\text{camera}}^2 = \sigma_{\text{screen}}^2 + \sigma_{\text{lens}}^2 + \sigma_{\text{sensor}}^2 \quad (3)$$

where the subscripts denote the optical element of the PSF contributions [3, 4].

The fundamental PSF of a pinhole camera comes from the requirement of a pinhole aperture to form an image. As shown in Eq. (2) this aperture causes geometrical and diffraction effects to the propagating X-ray wavefront and is

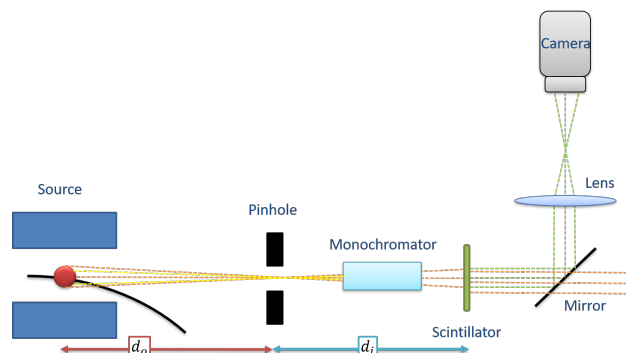


Figure 1: Schematic of an X-ray pinhole camera. The source-to-screen magnification is given by the ratio of the distances d_i/d_o .

one of the largest contributors to the overall PSF. Although the PSF contribution from the pinhole σ_{pinhole} cannot be avoided entirely, it can be minimised by matching the pinhole aperture size and photon energy [4].

PSF SIMULATION

Using XOP [5] a comparison of the spectral power distributions for the bending magnet source points in Diamond-I and Diamond-II is shown in Fig. 2. In all three cases similar spectral distributions are observed from 15 - 60 keV with the peak power in the 23 - 25 keV range. However due to the weaker magnetic field strengths of the Diamond-II dipoles ($B_{D1} = 0.76\text{ T}$, $B_{D4} = 0.70\text{ T}$), the total power is approx-

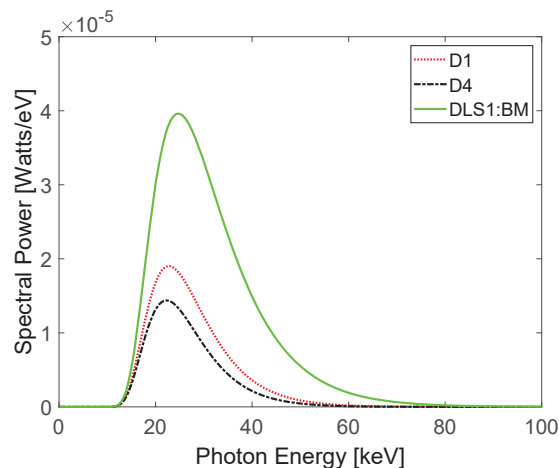


Figure 2: Comparison of the spectral power distributions, after 1 mm aluminium and 10 m air, of the bending magnet source points of Diamond-II (D1 and D4) with Diamond-I (DLS1:BM).

* lorraine.bobb@diamond.ac.uk

HORIZONTAL AND VERTICAL EMITTANCE MEASUREMENTS OF THE ADVANCED PHOTON SOURCE BOOSTER SYNCHROTRON BEAM AT HIGH CHARGE*

K. P. Wootton[†], W. J. Berg, J. R. Calvey, K. C. Harkay, A. Xiao, B. X. Yang
Argonne National Laboratory, Lemont, IL 60439, USA
A. H. Lumpkin, C.-Y. Yao, Argonne Associate of Global Empire, LLC,
Argonne National Laboratory, Lemont, IL 60439, USA

Abstract

In order to maximise the injection efficiency from the booster synchrotron into the proposed Advanced Photon Source Upgrade storage ring, beam-based optimisation of the booster electron optical lattice is anticipated. In the present work, we present non-destructive beam size and emittance measurements using the booster synchrotron light monitor and destructive quadrupole scan emittance measurements in the booster to storage ring transport line. Destructive measurements are performed with a 0.1 mm thickness Cerium-doped Yttrium Aluminium Garnet screen. In order to characterise performance, both the beam energy at extraction (5, 6 and 7 GeV) and the bunch charge are varied.

INTRODUCTION

The Advanced Photon Source Upgrade (APS-U) is a project to convert the existing facility to a high brilliance diffraction limited electron storage ring light source [1]. A distinguishing feature of multibend achromat lattices for diffraction limited storage rings is that the dynamic aperture is small enough that on-axis injection (rather than off-axis accumulation) becomes desirable [2, 3]. As a result, a high charge single bunch injector is an important feature of the design of the APS-U [4–7] and also the High Energy Photon Source [8, 9].

In order to efficiently inject into the APS-U storage ring, it is desired to monitor and optimise in particular the horizontal emittance of the high charge electron bunch extracted from the booster synchrotron. We consider several established diagnostics to measure the horizontal and vertical emittances in the booster [10]. For a non-destructive measurement of the stored beam in the booster, an optical synchrotron light monitor (SLM) was used [11, 12]. Destructive quadrupole scan emittance measurements of the electron beam emittance can be performed in the booster to storage ring transport line. The diagnostics used in this study are illustrated schematically in Fig. 1.

QUADRUPOLE EMITTANCE SCANS

Consider the beamline in Fig. 2. The beam encounters a quadrupole of length l_q and strength k that focusses the

beam in one dimension. The beam then traverses a drift of length d and is imaged on a screen.

The emittance is given by [13]:

$$\varepsilon = \sqrt{\Sigma_{0,11}\Sigma_{0,22} - \Sigma_{0,12}^2}, \quad (1)$$

The beam size at the screen ($\Sigma_{1,ij}$) can be expressed in terms of the beam size at the entrance of the quadrupole ($\Sigma_{0,kl}$) by [13]:

$$\Sigma_{1,11}(k) = \left(d^2 l_q^2 \Sigma_{0,11}\right) k^2 + \left(-2d l_q \Sigma_{0,11} - 2d^2 l_q \Sigma_{0,12}\right) k + \left(\Sigma_{0,11} + 2d \Sigma_{0,12} + d^2 \Sigma_{0,22}\right). \quad (2)$$

Uncertainties in the fitted parameters were determined by propagation of uncertainty. We follow an approach similar to Refs. [14, 15]. For a general parameter g , the uncertainty σ_g can be expressed by [15]:

$$\sigma_g^2 = \sum_{i=1}^n \left(\frac{\partial g}{\partial x_i}\right)^2 \sigma_{x_i}^2 + \sum_{i=1}^j \sum_{j=1, j \neq i}^j \left(\frac{\partial g}{\partial x_i}\right) \left(\frac{\partial g}{\partial x_j}\right) C(i, j) \quad (3)$$

where $\sigma_{x_i}^2$ are the variances of the fitted parameters x_i , and C is the covariance between them, which are determined when fitting Eq. (2) to measured beam moments. Because the terms $\Sigma_{0,ij}$ are not independent of one another, we partially differentiate the emittance with respect to each term.

$$\frac{\partial \varepsilon}{\partial \Sigma_{0,11}} = \frac{-\Sigma_{0,11} d^{-2} + \Sigma_{0,22} + 2\Sigma_{0,12} d^{-1}}{2\sqrt{\Sigma_{0,11}\Sigma_{0,22} - \Sigma_{0,12}^2}}, \quad (4)$$

$$\frac{\partial \varepsilon}{\partial \Sigma_{0,12}} = \frac{-2\Sigma_{0,11} d^{-1} - d\Sigma_{0,22} - 2\Sigma_{0,12}}{2\sqrt{\Sigma_{0,11}\Sigma_{0,22} - \Sigma_{0,12}^2}}, \quad (5)$$

$$\frac{\partial \varepsilon}{\partial \Sigma_{0,22}} = \frac{\Sigma_{0,11} - d^2 \Sigma_{0,22} + d \Sigma_{0,12}}{2\sqrt{\Sigma_{0,11}\Sigma_{0,22} - \Sigma_{0,12}^2}}. \quad (6)$$

The lattice parameters at the quadrupole are given by:

$$\beta(s) = \Sigma_{0,11} (\Sigma_{0,11}\Sigma_{0,22} - \Sigma_{0,12})^{-1/2}, \quad (7)$$

$$\alpha(s) = -\Sigma_{0,12} (\Sigma_{0,11}\Sigma_{0,22} - \Sigma_{0,12})^{-1/2}, \quad (8)$$

$$\gamma(s) = \Sigma_{0,22} (\Sigma_{0,11}\Sigma_{0,22} - \Sigma_{0,12})^{-1/2}. \quad (9)$$

* Work supported by the U.S. Department of Energy, Office of Science, Office of Basic Energy Sciences, under Contract No. DE-AC02-06CH11357.

[†] kwootton@anl.gov

DIGITAL CAMERAS FOR PHOTON DIAGNOSTICS AT THE ADVANCED PHOTON SOURCE*

K. P. Wootton[†], N. D. Arnold, W. J. Berg, T. L. Fors, N. S. Sereno, H. Shang, G. Shen, S. E. Shoaf, B. X. Yang, Argonne National Laboratory, Lemont, IL 60439, USA

Abstract

Cameras can be a very useful accelerator diagnostic, particularly because an image of the beam distribution can be quickly interpreted by human operators, and increasingly can serve as an input to machine learning algorithms. We present an implementation of digital cameras for triggered photon diagnostics at the Advanced Photon Source using the areaDetector framework in the Experimental Physics and Industrial Controls System. Beam size measurements from the synchrotron light monitors in the Particle Accumulator Ring using the new architecture are presented.

INTRODUCTION

Measuring the beam size of the high brightness beams produced by the Advanced Photon Source Upgrade (APS-U) will be accomplished with cameras at various points in the acceleration cycle [1, 2]. The existing Advanced Photon Source (APS) has many cameras used to image the electron beam throughout the accelerator complex. Image output from most cameras is National Television System Committee (NTSC) analogue video, from which individual frames are acquired using a DataCube Max Video MV200 system [3, 4]. In many other laboratories, digital cameras are used as part of the suite of accelerator diagnostics [5–9]. In anticipation of future capabilities for data acquisition and control of image data, potential need of a digital camera architecture is foreseen.

In the present work, we highlight recent work integrating digital camera control and data acquisition in the APS control system. Graphical and programmatic interface tools are outlined. A demonstration of digital camera use for the collection of beam physics data is presented.

SYSTEM ARCHITECTURE

We have deployed several digital cameras. At present the cameras used are FLIR Point Grey Research Grasshopper3 USB3 cameras. USB3 was selected for these locations because the communication protocol supports high frame rate output. The cameras are directly connected to soft input output controllers (IOCs) running on local personal computers.

We use areaDetector to interface with the cameras [10, 11]. The areaDetector package is used primarily as an Experimental Physics and Industrial Control System (EPICS) interface [12–15]. In addition, areaDetector modules provide

initial data processing and analysis before publication as process variables.

For timing synchronisation, the cameras are externally triggered. For a variable delay, we use a digital delay generator (Stanford Research System DG645) triggered from the timing system injection event.

GRAPHICAL USER INTERFACE

A Python-based graphical user interface (GUI) has been developed. This makes use of the pvaPy Python module for PV access. An example image of the GUI is shown in Fig. 1.

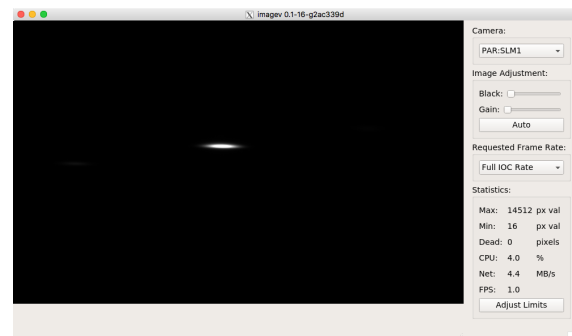


Figure 1: Python graphical user interface for digital cameras controlled by areaDetector.

PROGRAMMATIC INTERFACE

For programmatic access to digital camera data, a Self-Describing Data Sets (SDDS) function was written called sddsimagemonitor [16, 17]. The function provides similar functionality to sddswmonitor, optimised for cameras controlled through areaDetector.

Using sddsimagemonitor we were able to acquire images using channel access protocol at a high throughput of about 100 frames per second when the region of interest was cropped to 128×128 pixels. This may be useful for specific time-resolved studies.

EXAMPLE OF USE

We have used this system successfully to image the electron beam in the Particle Accumulator Ring (PAR) [18] and in the Booster Synchrotron [19] of the APS accelerator complex. An example of the electron beam size measured using the PAR synchrotron light monitor is illustrated in Fig. 2.

One nice feature of the digital cameras is the 12-bit analogue to digital converter. This allowed the acquisition of all eight images in Fig. 2 on the same intensity scale, with-

* Work supported by the U.S. Department of Energy, Office of Science, Office of Basic Energy Sciences, under Contract No. DE-AC02-06CH11357.

[†] kwootton@anl.gov

OBSERVATIONS OF LONG-RANGE AND SHORT-RANGE WAKEFIELD EFFECTS ON ELECTRON-BEAM DYNAMICS IN TESLA-TYPE SUPERCONDUCTING RF CAVITIES *

A.H. Lumpkin†, R. Thurman-Keup, N. Eddy, D. Edstrom, and J. Ruan
Fermi National Accelerator Laboratory, Batavia, IL 60510 USA

Abstract

The assessments of long-range and short-range wakefield effects in TESLA-type superconducting rf cavities at the Fermilab Accelerator Science and Technology Facility are described. A dipolar higher-order mode (HOM) of one cavity is shown to be in near resonance with the 3-MHz micropulse repetition frequency harmonic resulting in a clear sub-macropulse centroid oscillation of 100 kHz. In the short-range wakefield measurements, a head-tail transverse kick of $\sim 100 \mu\text{m}$ is seen in the streak camera images with 500 pC/b and offsets of $\sim 2 \text{ mm}$. A numerical model for the TESLA-type cavity is consistent with these latter results.

INTRODUCTION

Generation and preservation of bright electron beams are two of the challenges in the accelerator community given the inherent possibility of excitations of dipolar long-range wakefields (e.g. higher-order modes (HOMs)) and short-range wakefields due to beam offsets in the accelerating cavities. The Fermilab Accelerator Science and Technology (FAST) facility has a unique configuration of a photocathode rf gun beam injecting two TESLA-type single cavities (CC1 and CC2) in series prior to the cryomodule [1]. Beam propagation off axis in these cavities can result in emittance dilution within the macropulses and micropulses, respectively. Since such cavities form the drive accelerator for the FLASH FEL [2], the European XFEL[3], and the under construction LCLS-II [4], understanding the possible emittance dilution effects is of interest.

Two configurations of a Hamamatsu C5680 streak camera viewing a downstream OTR screen were utilized to track centroid shifts during the macropulse (framing mode) for the long-range case and during the micropulse for the short-range case (~ 10 -micron spatial resolution and 2-ps temporal resolution). Steering before CC1 resulted in a bunch centroid oscillation within the macropulse attributed to a near-resonance condition of an HOM with a beam harmonic that was detected by the downstream rf BPMs and the streak camera. Steering before CC2, we observed a head-tail centroid shift in the streak camera image $y(t)$ profiles which we attributed to a short-range wakefield effect. We will describe the potential emittance dilution effects we have seen in TESLA-type cavities due to off-axis beam trajectories.

* This manuscript has been authored by Fermi Research Alliance, LLC under Contract No. DE-AC02-07CH11359 with the U.S. Department of Energy, Office of Science, Office of High Energy Physics.

† lumpkin@fnal.gov

EXPERIMENTAL ASPECTS

The FAST Injector Linac

The FAST linac is based on the L-band rf photocathode (PC) gun which injects beam into two superconducting rf (SCRF) capture cavities denoted CC1 and CC2, followed by transport to a low-energy electron spectrometer. A Cs₂Te photocathode is irradiated by the UV component of the drive laser system described elsewhere [5]. The basic diagnostics for the studies include the rf BPMs located before, between, and after the two cavities as shown in Fig. 1. These are supplemented by the imaging screens at X107, X108, X121, and X124. The HOM couplers are located at the upstream and downstream ends of each SCRF cavity, and these signals are processed by the HOM detector circuits with the output provided online through ACNET, the Fermilab accelerator controls network. The HOM detectors' bandpass filters were optimized for two dipole passbands from 1.6 to 1.9 GHz, and the 1.3 GHz fundamental was reduced with a notch filter. The rf BPMs electronics were configured for bunch-by-bunch capability with reduced noise. At 2 nC per micropulse, the rms noise was found to be 25 μm in the horizontal axis (x) and 15 μm in the vertical axis (y) in B101 in the test with 4.5-MeV beam from the gun. The set of rf BPMS was critical for the HOM sub-macropulse beam effects. However, for the experiments on short-range transverse wakefields, we relied on a streak camera to provide the sub-micropulse spatial information.

Streak Camera Aspects

We utilized a C5680 Hamamatsu streak camera with S20 PC operating with the M5675 synchroscan vertical deflection unit that was phase locked to 81.25 MHz shown in Fig. 2. In addition, we used a phase-locked-loop C6878 delay box that stabilizes the streak image positions to about 1 ps temporal jitter over 10s of minutes. These steps enabled the synchronous summing of 50-150 micropulses or bunches (b) generated at 3 MHz by the photoinjector or the offline summing of 10-100 images to improve statistics in the sum images. We applied the principle to optical transition radiation (OTR) generated from an Al-coated Si substrate at the X121 screen location (see Fig.1) with subsequent transport to the beamline streak camera. Commissioning of the streak camera system was facilitated through a suite of controls centered around ACNET. This

Content from this work may be used under the terms of the CC BY 3.0 licence (© 2019). Any distribution of this work must maintain attribution to the author(s), title of the work, publisher, and DOI

TURN-BY-TURN SYNCHROTRON RADIATION TRANSVERSE PROFILE MONITOR FOR IOTA*

N. Kuklev[†], Y.-K. Kim, University of Chicago, Chicago, IL 60637, USA

Abstract

The Integrable Optics Test Accelerator is a research electron and proton storage ring recently commissioned at Fermilab. A key part of its beam diagnostics suite are synchrotron radiation monitors, used for measuring transverse beam profile, position, and intensity. So far, this system has used only visible light cameras, which are optimal for orbit measurements but do not provide turn-by-turn temporal resolution needed for beam dynamics analysis. Current electrostatic BPM system, while capable of turn-by-turn acquisition, will be pushed to its limits of accuracy and linearity by the requirements of planned nonlinear integrable optics experiments, and furthermore does not provide transverse profile data. To address these drawbacks, we present in this paper the design of a turn-by-turn BPM system based on a multi-anode photomultiplier detector. Extensive simulations are shown, combining both particle and optics tracking. A potential hardware and readout architecture is described. Statistical and systematic errors are explored. We conclude by outlining the prototype testing plans for run 2 in the fall of 2019, and other future work.

INTRODUCTION

The Integrable Optics Test Accelerator is a research electron and proton storage ring recently commissioned at Fermilab. It has a circumference of 40m, and is designed to use either 2.5 MeV protons provided by an RFQ injector, or up to 150 MeV electrons from FAST linac [1]. Over next few years, a comprehensive experimental campaign is planned including tests of techniques for improving beam intensity and stability (with integrable optics [2–4], and electron lenses [5]), a demonstration of optical stochastic cooling [6], single electron quantum optics and undulator radiation studies [7].

A wide variety of supporting instrumentation is installed in IOTA, with most capable of quick customization to suit specific experimental needs. One such system are synchrotron radiation monitors, used as transverse profile monitor (TPMs), for measuring transverse beam profile, position, and intensity. So far, this system has used visible light cameras, which are optimal for orbit measurements [8] but do not provide turn-by-turn temporal resolution due to CMOS technology and signal-to-noise limitations. However, such data is of interest for beam dynamics experiments, since the electrostatic BPMs (that provide TBT positions) have a high minimum current limit at which there exists significant

intra-beam scattering, preventing true ‘few-particle, pencil beam’ dynamics observations. Low current beam position data can improve and shorten measurements of dynamic aperture size/tune shifts, and in the ultimate limit of a single electron, would yield true single-particle dynamics. In this paper, we propose a TBT TPM system based on a multi-anode photomultiplier. In the following sections, detailed simulation and a potential hardware design are presented, along with some experimental plans for run 2.

Background and SR System Overview

Synchrotron radiation is produced by charged particles undergoing radial acceleration, and is a byproduct in any storage ring. It plays a large role in beam damping, and is also a commonly used diagnostic signal [9, 10]. SR intensity profile is strongly forward peaked, with total radiation power scaling as fourth power of particle energy. For IOTA, protons do not produce sufficiently intense or energetic SR signal, but for electrons, critical wavelength is in the UV range, allowing for simple and cost effective measurements with visible band optics.

IOTA ring contains 8 bending dipole magnets, with 4 each of 30 and 60 degree varieties, as shown in Fig. 1. All the vacuum chambers have downstream optically transparent windows, through which SR can be extracted. In 4 of 8 sections, radiation from potential insertion devices in the straights can also be observed.

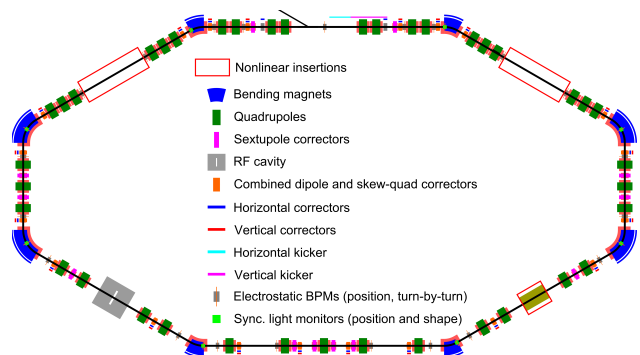


Figure 1: Layout of IOTA ring, with injection point in the upper central section. Main bends are in blue.

SyncLight system is comprised of 8 stations situated atop each of the dipoles. In base configuration, each station has two components - first is an optical periscope transport line consisting of two mirrors, an iris, and a lens, that captures SR and focuses it onto the detector, while using the iris to limit depth of field errors. Second and more extensive part is the modular detector station, that in its base configuration contains a low-noise CMOS camera, but also provides capability to add modules like color wheels, photomultipliers

* This work was supported by the U.S. National Science Foundation under award PHY-1549132, the Center for Bright Beams. Fermi Research Alliance, LLC operates Fermilab under Contract DE-AC02-07CH11359 with the US Department of Energy.

[†] nkuklev@uchicago.edu

FAST AND ROBUST WIRE SCANNERS WITH NOVEL MATERIALS FOR PROFILING HIGH INTENSITY BEAMS

M. Ruelas, A. Laurich, T.J. Campese, J.K. Penney, G. Andonian¹

RadiaBeam Technologies, Santa Monica CA, USA

J. Gubeli, K. Jordan, J. Yan, Jefferson Lab, Newport News VA, USA

L.R. Scammell, C.F. Huff, R.R. Whitney, BNNT LLC, Newport News VA, USA

¹also at University of California Los Angeles, CA USA

Abstract

Wire scanners are robust devices for beam characterization in accelerator facilities. However, prolonged usage with intense particle beams leads to wire damage, requiring replacement and beam diagnostic downtime. The fast, robust wire scanner was recently designed and engineered with swappable and modular wire cards, that can accommodate different wire materials under tension. Testing is currently underway at the Jefferson Laboratory (JLab) Low Energy Recirculating Facility. During the course of the diagnostic development and commissioning, we will test Tungsten, Carbon, and boron-nitride nanotube in wire form. The latter is particularly relevant as early results on the material show that it has very high thermal thresholds and may withstand the high-power of the beam during regular operations. This paper will report on the system design and engineering, and preliminary results with operation on the beamline.

INTRODUCTION

Transverse profile diagnostics for high intensity particle beams are critical for quality beam operations and incorporation into feedback controls [1]. Wire scanners allow for beam scanning at high powers by moving a rigid wire across the beam and measuring detector response downstream. However, the wires tend to degrade over prolonged exposure to the beam. In this wire-scanner project, the wires are mounted on a modular card-mount, and will be driven at very high speed, with precision control and readback on position. The modular card permits rapid swapping of the wires with minimal downtime. Additionally, the wire-scanner is mounted with boron nitride nanotubes (BNNT) in thread-form, which holds the promise for prolonged usage in high power beams, due to the higher thermal load handling of the material [2, 3].

General Considerations

The final design of the wire scanner that was developed is shown in Figure 1. The scanner consists of two linear motion stages mounted on a strongback. Direct-drive linear motors provide fast, smooth motion compared to ball screw systems. The wire-card is mounted axially in a large interaction chamber. Two in-vacuum bellows, on either side of the chamber, allow for full retraction of the wire-card for beam clear operation in both directions. The central chamber includes multiple feedthroughs and viewports for optical characterization of the wires, as well as for collection of

light emitted from the wire during the interaction. The large upper port also serves as the access port, both for initial assembly and for the eventual exchange of wire cards.

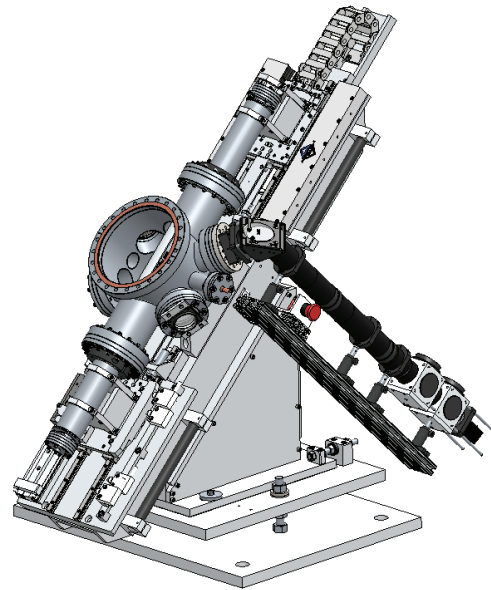


Figure 1: Scale model of wire-scanner. Central chamber incorporates wire mounting card that is precision controlled using linear stages. Optical transport provides imaging of the wires during the interaction and collection of spectral information.

Wire Card Mount

The main engineering directives for the wire-card design are modularity, accommodation of thin wires, and rapid, reproducible replacement. The card is designed to hold wires as small as 10 μm diameter, for high resolution operations [4]. Multiple wire card mounts are available and the modularity allows for use of different wire materials and sizes. The card also accommodates different wire materials, such as tungsten (W), carbon (C), and BNNT threads, with constant and controllable tensioning.

The wire-card holds coplanar wires, suspended across an open fixture, with one wire oriented horizontally, one oriented vertically, and the third at 45° (Fig. 2). The set of wires is swept through the beam diameter during operation of the wire scanner, and provides horizontal, vertical and

MULTIPLE SYNCHROTRON LIGHT MONITORS FOR TRANSVERSE MATCHING AND MONITORING AT CEBAF

B.G. Freeman, J. Gubeli, and M.G. Tiefenback, Jefferson Lab, Newport News, VA, USA

Abstract

Beam setup at the Continuous Electron Beam Accelerator Facility (CEBAF) involves threading beam through the machine and monitoring global transfer functions to identify and address cumulative lattice errors. Transverse beam emittance may grow by as much as two orders of magnitude, mediated by synchrotron radiation. Re-matching the enlarged beam phase space into successive re-circulation arcs minimizes this emittance growth but requires knowledge of the actual beam distribution. This is now accomplished through quadrupole scans using wire profile monitors, the most time-consuming activity in our setup process. We propose to use Synchrotron Light Monitors (SLMs) to image the beam at homologous points in the four super-period re-circulation arc lattices. Benefits include real-time monitoring of beam parameters and reduced elapsed time for initial setup. These SLMs will be installed in Arc 7 of the CEBAF machine, where Synchrotron Radiation contributes moderately to emittance growth. One of four required SLMs will be installed and commissioned this year, with the rest being installed next year.

INTRODUCTION

The vision in 1986 for CEBAF was to use Synchrotron Radiation to measure the beam emittance [1]. Certain challenges presented in this CEBAF technical note are easily solved now with newer technologies and improved performance. Challenges such as filtering, camera resolution, digitization of the image, and diffraction limitations were all discussed in the note. Now, thirty years and a major energy upgrade later, such devices will be implemented for CEBAF.

The CEBAF machine has several SLMs now, used for monitoring of the beam energy, energy stability, and RF cavity gradient and phase stability. Our principal SLMs are in the high-dispersion regions to monitor energy stability and obtain information about the longitudinal distribution of the beam [2].

The emittance growth for a given Arc depends on the transverse mismatch of the beam to the periodic lattice functions. The proposed four point SLM based measurement should provide an efficient and non-destructive means to measure and monitor the beam properties.

MATCHING TECHNIQUES

Existing Measurement Methods

The present method for measuring and matching the transverse beam properties of the electron beam uses wire profile monitors, or wire scanners. These devices provide great resolution of our small $\sigma < 100 \times 100 \mu\text{m}$ beam sizes. The

profile scans are relatively slow and can take minutes. We vary the strength of a quadrupole in the non-dispersive region upstream of each Arc, and measure the resulting beam size [3]. This process can be time consuming, depending strongly on the speed of wire insertion and details of data collection protocol. We have to balance the insertion velocity against the noise in the measurement. Determination of the range of focusing strength needed can be time consuming. We target measurements spanning the waist (minimum size) and up to a factor of three times greater for both stronger and weaker settings. Upstream optics in some cases must be modified to accommodate strength limitations for the quadrupole being varied. Problematic cases can require several hours to measure and rematch one of the ten Arcs.

Improvements have been made through the years to the process, as well as to software tools for data collection and analysis. The suite of tools, which is called `qsUtility` [4], makes use of Self Describing Data Files (SDDS) [5] to transport the data to `elegant` [6]. The enhancements have improved reproducibility of the measurements, and have improved the speed at which the data can be obtained and analyzed. We plan to use the existing tool suite to analyze the data and compare the measured Twiss parameters for agreement.

Four-point SLM-based Method

The CEBAF accelerator consists of two anti-parallel superconducting RF linacs connected by ten 180° Arc bends to guide the beam successively through the linacs for energy gain. CEBAF is capable of providing up to 12 GeV electrons to experimental Hall D and 11 GeV electrons to halls A, B, and C.

CEBAF can be configured to provide beam to halls A, B or C after each pass through the linacs. Arc 7 contains the second-highest beam energy in the East Arcs. Arc 7 was chosen for this initial SLM installation, as most of the scheduled experimental plans require beam to pass through this Arc. In this Arc, Synchrotron Radiation contributes moderately to emittance growth. Each Arc consists of a periodic focusing structure of single or paired dipole magnets separated by alternating singlet and triplet groups of quadrupole magnets, Arc 7 consists of thirty-three quadrupoles and sixteen pairs of 3 m long dipoles. The homologous points of the four super-periods are chosen to be as close as practical to the horizontal dispersion zeroes just downstream of the 8th, 16th, 24th and 32nd dipoles. The mechanical layout of this Arc allowed for one design to be implemented at all four locations. The horizontal and vertical dispersion and betatron plots for the chosen 7th Arc can be seen in Fig. 1 and Fig. 2

IONIZATION PROFILE MONITOR DESIGN AND EXPERIMENTS IN HIRFL-CSR*

H.M Xie, J.X Wu[†], L.J Mao, Z Du, K.W Gu, Y Wei¹, Z.X Li, Y Zhang, G.Y Zhu, L Jing, X.J Hu
 Institute of Modern Physics, Chinese Academy of Sciences, Lanzhou 730000, China
¹University of Chinese Academy of Sciences, Beijing 100049, China

Abstract

To meet the needs of real-time profile monitoring, injection match optimization, transverse cooling mechanism research in Cooling Storage Ring of Heavy Ion Research Facility of Lanzhou (HIRFL-CSR), and the profile measurement of future intense facilities like High Intensity Heavy-ion Accelerator Facility (HIAF) and China Initiative Accelerator Driven System (CiADS) in Huizhou China, some IPM research and experiments has been proceed since 2013. In 2016, the first IPM was developed with MCPs, phosphor screen and camera acquisition system for vertical profile diagnostics in HIRFL-CSRm. Then another horizontal IPM with new framework and less field distortion was also deployed in CSRm at 2018 summer. Besides, two more IPMs will be installed in HIRFL-CSRe during next summer maintenance. This paper mainly presents the horizontal IPM design concerns, HV settings influence, some experiment anomalies, as well as experiments for transverse electron cooling at HIRFL-CSR in December 2018.

INTRODUCTION

Heavy Ion Research Facility in Lanzhou (HIRFL) [1] is a multi-functional cooling storage ring system, which consists of a main ring (CSRm), an experimental ring (CSRe), and a radioactive beam line (RIBLL2) to connect the two rings. The layout of this accelerator complex is shown in Fig. 1, where two Ionization Profile Monitors (IPMs) and electron cooler are displayed with coloured marks.

As one of the most valuable non-invasive profile instruments in proton and heavy ion accelerator [2–4], IPM measures the distribution of ions or electrons originating from the residual gas ionization during beam passage. Presently many IPMs [5, 6] in the world are designed by electron collecting mode, tandem resistors for bias voltage and anode-electronics acquisition system for the advantage of fast time response, while major drawback is the relative poor spatial resolution due to anode size limitation. Considering the small beam size in HIRFL-CSRm with electron cooling on, the IPM with ion collection mode and optics acquiring system turns out to be our practical choice.

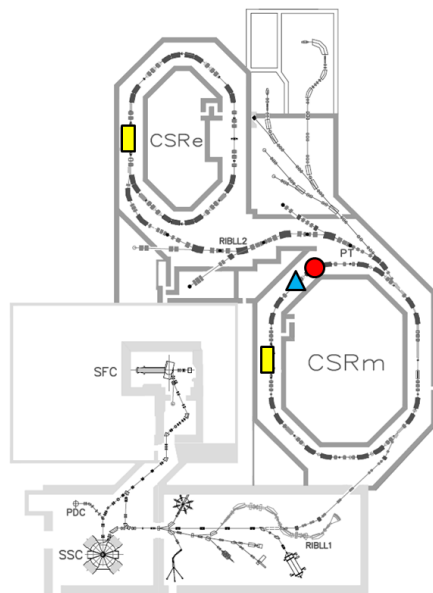


Figure 1: The Layout of HIRFL, the red circle, blue triangle and yellow rectangles representing vertical IPM, new horizontal IPM and electron coolers respectively.

NEW IPM FEATURE AND UPGRADE

Mechanism Design and Data Process

IPM mainly collects ions or electrons resulting from the residual gas ionization during the beam passage. Fig. 2 left is the vertical IPM tested in SSC Linac, which utilizing tandem resistors for bias voltage like most IPMs now. Right is the horizontal IPM with new compact framework design and less electrostatic field distortion. In case of the units degradation under harsh thermal baking and beam loss irradiation, new IPM is determined to use separate electrodes for HV supply instead of tandem resistors. This surely causes voltage supply expenses, while it allows to supply HV on each electrode precisely and controllably for operation or experiments.

Due to small transverse emittance, new IPM is constructed as ion collection mode with dual MCPs, P46 and optics acquisition. The spatial uncertainty from dual MCPs is generally considered to be 2.5–3 times the core diameter of 12 μm, thus the optics system spatial resolution calibrated about 63 μm seems convincing. The 4.2 Megapixels SC-MOS chip using double Camera Link for data transmission achieves 100 fps. Data processing was upgraded by EPICS ioc to realize multiple functions such as ROI selection, data fitting and historical profile display. It also can exploit the

* Supported by the National Natural Science Foundation of China (No. 11805250)

[†] wujx@impcas.ac.cn

Content from this work may be used under the terms of the CC BY 3.0 licence (© 2019). Any distribution of this work must maintain attribution to the author(s), title of the work, publisher, and DOI

TECHNICAL REVIEW OF BEAM POSITION BUTTON DESIGN AND MANUFACTURE

A. F. D. Morgan*, Diamond Light Source, Oxfordshire, UK

Abstract

A workshop in May 2019, hosted by Diamond Light Source (DLS) (UK), reviewed both the design and the manufacturing aspects of beam position monitor (BPM) pick-up buttons with an integrated ultra high vacuum (UHV) feedthrough and coaxial connector. The UHV feedthrough technology (e.g. ceramic brazing vs glass-sealing), the limits on mechanical tolerances, reproducibility and material choices for high reliability were examined by more than 20 users of these devices and a number of reputed manufacturers. Calibration techniques and tools and methods for inspection and testing were also assessed. This paper will present the outcome and conclusions of this workshop and identify challenges and opportunities for future BPM manufacture.

INTRODUCTION

The procurement of beam position monitor buttons was highlighted at Diamond after manufacturing issues were discovered for the buttons made for the single cell DDBA upgrade [1]. A proposed machine upgrade to Diamond-II will require around 1000 buttons to be made [2]. There seemed to be a lack of manufacturers capable of making these devices.

The aim of the workshop was to bring together representatives from the accelerator community along with potential button manufacturers, as well as system integrators who install the buttons into the accelerator vacuum chambers. In total there were seven manufacturers, two system integrators, and representatives from ten facilities.

All the attending manufacturers have made buttons for at least one accelerator facility. However the scale was usually small numbers of prototypes for testing, or small machine upgrades. Based on this new information on the manufacturing base, the workshop focus changed from identifying a manufacturer able to make buttons, to determining which manufacturers would be able to provide buttons at the scale of full machine upgrades.

Three distinct groups of attendees came to the workshop. In order to satisfy all their requirements, the workshop had a slightly different structure than usual. The aim was to have as open a dialog as possible, but the facility representatives also wanted to be able to ask manufacturers deep technical questions. The manufacturers quite understandably did not want to disclose too much information in front of their competitors. As a result, although the majority of the workshop was open at all participants there were also closed sessions for individual manufacturers where the other manufacturers were excluded.

* alun.morgan@diamond.ac.uk

Because of the closed sessions the manufacturers were able to be very open about their processes. The delegates were able to understand the companies processes for designing a button. Detailed discussions were enabled on the limitations of the various techniques and various technologies the manufacturers had at their disposal. The facility representatives also got a feel for the strengths of the various companies, and how each would approach the button fabrication challenge. Some manufacturers viewed it more as a collaboration while other companies were more comfortable with the facilities doing the design and then the company stepping in to do the manufacturing. It was clear that all the companies present were keen, engaged, and interested in this type of problem. They all enjoyed the technical challenge presented, however, the scale of the number of buttons when added up across the various upgrades made it a much more interesting proposition for the companies in general. They realised that the customer demand in the next decade was not just 10s but 1000s of units.

What follows is a summary of the presentations and discussion at the workshop itself. This is designed to give the reader a summary of the main outcomes from the workshop. For more details the reader is directed to the workshop web page [3]. For a previous summary on the complete beam position monitor system readers are directed to [4].

The topics for the workshop fell into two broad categories: design and fabrication.

DESIGN

Smaller chamber dimensions are a common thread for all the machine upgrades. Smaller chambers lead to a smaller button, which has a good effect of having a lower wake loss, but at the cost of signal level.

In order to reduce the signal interference from one bunch to the next the ringing of in the button structure needs to be reduced. Such a reduction can be obtained with careful impedance matching through the design, and is helped by the use of a lower permittivity insulator.

One particular feature of concern is a trapped mode which exists between the button head and the fitting hole or housing. There were various approaches demonstrated to alleviate the effects of this unwanted mode.

There has been a general move away from having a skirt around the button. Originally it was included to simplify installation, and to mitigate against relatively poor installation tolerances. It has been found that this feature can be unhelpful in terms of wake loss and heating and so is not featuring in many of the newer designs as tolerancing improvements have made its utility questionable. Figure 1 shows an example of a skirted and non-skirted design.

PILE-UP EFFECT OF COLD BUTTON BPMS IN THE EUROPEAN XFEL ACCELERATOR

D. Lipka*, B. Lorbeer, DESY, Hamburg, Germany

Abstract

The European XFEL facility is in operation with a maximum of 2700 bunches in one train. The highest bunch repetition rate is 4.5 MHz; this corresponds to a minimum time separation of 222 ns. The measurement of the beam properties for each bunch in a train is required. Therefore the beam position monitor (BPM) system needs to separate the signals from each bunch. All BPM types (button, re-entrant and cavity) fulfill this requirement except a few button BPMS installed inside of the cold accelerator module, where Pile-Up from the train can be observed. To identify the cause of this effect we measured the S-parameters during a shut-down of the accelerator, compared it with a similar BPM at the FLASH accelerator but located in a warm section and finally measured the spectrum of the button signal during beam operation. As a result, resonances were found at about 2.46 GHz with relatively high quality factor that remains within the frequency range accepted by the electronics.

INTRODUCTION

The European XFEL is a user facility generating X-rays in trains with a 222 ns (4.5 MHz) minimum separation [1]. The maximum length of one train is 600 μ s repeat at 10 Hz resulting in a maximum of 2700 bunches per train with energies between 8 and 17.5 GeV [2]. Individual bunches in one train can be redirected to two different beamlines, called the Northern and Southern branch. The Northern branch contains two SASE undulator sections, SASE1 for hard and SASE3 for soft X-rays. Different parts of the train are used to generate the SASE effect in both undulator sections by initiating a betatron oscillation via fast kickers. The Southern branch contains a second hard X-ray undulator section. To be able to control and direct the individual bunches in one train, each bunch position needs to be measured with the Beam Position Monitor (BPM) system [3].

The electron bunches are accelerated by superconducting cavities installed in 98 cryogenic modules. Each module contains 8 cavities followed by a cold quadrupole, a BPM and a higher-order-mode absorber [4] (see Figures 1 and 2).

The accelerator is divided into 3 cryogenic sections, where the longest is about 1 km. Therefore the electron beam diagnostics of the accelerator sections relies mainly on the BPMS, along with beam loss monitors outside the modules.

The BPMS of the 98 cryogenic modules, 74 have wide-band button type [5], in the other 24 modules re-entrant cavity BPMS installed as an in-kind contribution from CEA Saclay [6]. All BPMS are cryogenically tested to be vacuum tight before installation in the modules. Up to now no degradation of the vacuum has been seen from these devices. But

* Dirk.Lipka@desy.de

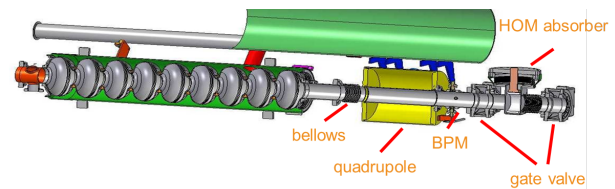


Figure 1: Schematic arrangement of components at the end of a cryogenic module. Beam direction is from left to right.



Figure 2: Photo of components at the end of a cryogenic module before installation; from right: housing of the cavity, housing of the quadrupole, button BPM.

during 4.5 MHz operation about 17 button BPMS showed an unexpected beam charge distribution (see Figure 3). This

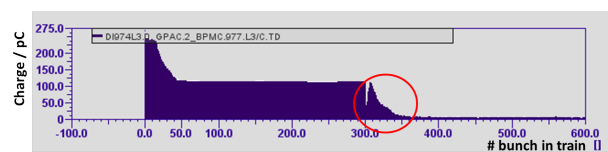


Figure 3: Beam charge reading of a train with 300 bunches. After the 300th bunch the reading indicates a signal which is non-zero.

effect, and the investigations to understand and overcome it, are described in the following.

PILE-UP

The button BPM system consists of the monitor inside the module, Radio Frequency (RF) cables and BPM read-out electronics. The read-out electronics are composed of analog Front-End electronics and digital electronics for data processing. The housing is a so called Modular BPM Unit (MBU) [7]. The 3-dB bandwidth of the analog Front-End electronics is between 1.53 and 2.28 GHz; the lower limit

BEAM MEASUREMENTS AT THE CERN SPS USING INTERFEROMETRIC ELECTO-OPTIC PICKUPS

A. Arteché*, S. E. Bashforth, A. Bosco, S. M. Gibson
John Adams Institute at Royal Holloway, University of London, Egham, UK
M. Krupa, T. Lefèvre, CERN, Geneva, Switzerland

Abstract

Since 2016 a prototype electro-optic pickup has been installed on the SPS as part of the ongoing development of a high bandwidth electro-optic beam position monitor for the High Luminosity LHC. Following the success of initial beam signal observations with the prototype, improvements of the sensitivity and stability of the pickup have become the main focus of the project. A new concept has been developed which uses an interferometric technique to measure the image field of a passing bunch. One arm of an interferometer passes through an electro-optic lithium niobate crystal, embedded in a pickup, whereas the other arm bypasses. The recombination after the pickup results in an interference pattern that changes as a bunch passes by, due to the electro-optic response of the crystal to the image field. This technique enhances the sensitivity to the field and improves control of the working point. Results from high intensity beams at the SPS are presented. These include a comparison between two different interferometric configurations that were tested on different pickups with similar beam conditions. The stability is assessed by frequency scanning interferometry during beam operation.

INTRODUCTION TO CONCEPT

The High Luminosity Large Hadron Collider requires high-bandwidth diagnostics to monitor the crabbed rotation of the proton bunches and to detect rapid, high order bunch instabilities [1, 2]. The solution being developed in the HL-LHC-UK collaboration between Royal Holloway and CERN is an Electro-Optic Beam Position Monitor (EO-BPM), which in essence is an electrostatic BPM that incorporates high bandwidth lithium niobate crystals placed between electrodes in the core of the pickup. As the relativistic proton bunch passes by an electro-optic pickup, the electric field is concentrated by the electrode to interact with the polarised light traversing the crystal by the Pockels effect. The analogue of the longitudinal bunch profile convoluted with the average transverse offset along the proton bunch is imprinted in the phase modulation of light passing through the crystal. In the SPS prototype results presented here, the phase of the modulation of light in the output fibre is transformed into an intensity modulation by combining with an optical path through a second fibre that bypasses the crystal, enabling the rapid beam signal to be recorded by a remote fast photodetector [3].

* alberto.arteché@rhul.ac.uk

This paper reviews various optical configurations that have been tested at the CERN SPS and presents new electro-magnetic simulations based on an upgraded pickup design that is planned to be installed at the LHC for tests during Run-III.

EO-BPM OPTICAL CONFIGURATIONS

Crossed Polarisers

A variety of electro-optic layouts have been investigated in simulation and experiment, and for each configuration the strength of the optical modulation has been assessed. A standard Crossed Polarisers (CP) configuration was employed in the first EO-BPM prototype that was installed and tested in the CERN SPS in 2016 and 2017, which measured the first proton-induced EO signal from a single pickup [4–6]. This arrangement replicates an amplitude modulator where a linearly polarised laser beam is oriented at 45° as it approaches a vacuum-integrated LNB crystal within the pickup, and may be considered as split into two horizontal and vertical component paths through the crystal. Both components are phase-retarded by different amounts due to the crystal birefringence, changing the polarisation, typically to an elliptical state, and where the axes are modified by the passing beam and detected by an analyser oriented perpendicularly to the first one, at -45° .

Single Crystal Interferometer

Soon after the proof of concept delivered by the CP configuration, the optical layout evolved towards the more sensitive ($\times 1.45$) Single Crystal Interferometric (SCI) design shown in Fig. 1. In this case, the laser beam is linearly polarised along

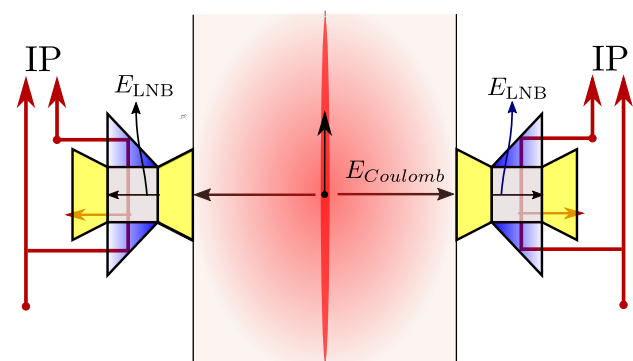


Figure 1: Single Crystal Interferometric layout.

the entire optical path through the crystal and is typically parallel to the extraordinary refractive index n_e . The optical

MicroTCA.4 AT SIRIUS AND A CLOSER LOOK INTO THE COMMUNITY

D. O. Tavares*, G. B. M. Bruno, S. R. Marques, L. M. Russo, H. A. Silva, LNLs, Campinas, Brazil

Abstract

More and more facilities have been adopting MicroTCA.4 as the standard for new electronics. Despite the advertised advantages in terms of system manageability, high availability, backplane performance and supply of high quality COTS modules by industry, the standard still lacks a greater acceptance in the accelerators community. This paper reports on the deployment of MicroTCA.4 systems at Sirius light source, which comprised the development and manufacturing of several open hardware modules, development of a generic gateway/software framework and re-implementation of MMC IPMI firmware as an open source project. A special focus will be given to the difficulties found, unforeseen expansions of the system and general architectural aspects. Based on this experience and on a survey carried out among other MicroTCA.4 adopters, the perceived strengths and weaknesses of the standard will be discussed and a tentative outlook on how it could be evolved to better suit the accelerators community will be presented.

INTRODUCTION

The debate around the adoption of a unified electronics standard for particle accelerators and physics experiments can be traced back to the early days of the International Linear Collider (ILC) project, around 2004 [1]. Taking as reference the successful cases of NIM, CAMAC, FASTBUS and VME standards in the past electronics generations, the ILC collaboration sought to establish a new standard for the years to come, trying to solve not only the pressing issue of the slow parallel buses, but also paving the way to meet the very stringent ILC requirements of communication bandwidth, high availability and remote hardware management [2,3]. After a search among the emerging standards, the collaboration chose PICMG Advanced Telecommunications Computing Architecture (ATCA) as the most promising standard. A series of ATCA workshops and meetings among SLAC, DESY, FNAL, ANL and KEK culminated in a series of technology demonstrations for the ILC, later on joined by other laboratories such as CERN, IHEP, IN2P3, ESS-Bilbao, IPFN, ITER for interests beyond the international collider. In 2009 a PICMG working group called "xTCA for Physics" was formed by several laboratories and companies aiming at extending ATCA and its downscaled version, MicroTCA, for particle accelerators, large HEP detectors and fusion experiments. Those efforts were presented in the upcoming years [4].

As the host of the TESLA Test Facility (TTF) international collaboration, which played a key role in demonstrating the superconducting RF technology required for the ILC, and urged to build superconducting FEL facilities as both

light source facilities and demonstrators of the ILC technologies, DESY soon took a prominent role in the development of ATCA and MicroTCA standard extensions for physics. An evaluation campaign for both standards was launched around 2007 [5] and reported on 2009 [6, 7], with ATCA-based LLRF demonstration and an AMC timing receiver developed in collaboration with the University of Stockholm. In the following years MicroTCA.4 was fully embraced by FLASH and European XFEL projects. More recently, an R&D and technology transfer center has been established, the MicroTCA Technology Lab [8].

CURRENT STATUS

The latest revision of the MicroTCA standard was released on November 2016, MicroTCA.4.1, extending the MicroTCA.4 standard to include auxiliary backplanes, Rear Power Modules (RPMs), MCH-RTM, protective board covers and application classes of RTMs, the later being the ratification of DESY's Zone 3 Connector Pin Assignment Recommendation.

A prominent example of commercially available auxiliary backplane is the RF backplane [9], which was designed by the Institute of Electronic Systems of the Warsaw University of Technology (WUT-ISE) for the European XFEL. It integrates high quality LO signal, clock and interlocks distribution for RTM modules to the crate. The RF backplane has become commonplace in the latest LLRF designs.

In 2017 PICMG released a set of 4 guidelines formulated by the PICMG Software Working Group (SWG) composed of laboratories and industry representatives [10] aiming at the standardization of software interfaces and procedures:

- **SHPP**: hot plug procedure for uninterruptible replacement of modules [11].
- **SHAPI**: common API for configuration and data read-out of addressable register-based devices [12].
- **SPM**: platform-agnostic low-level software interfaces, such as thread-scheduling, inter-thread communication, thread synchronization and timing services [13].
- **SDM**: platform-agnostic access to external devices [14].

An effort to provide EPICS use cases following the above guidelines is being treated by the SWG, but have evolved in slow pace. Another software development that is worth mentioning is the universal PCIe driver available as a common ground for general PCIe functionalities and kept up to date with the SHAPI standard [15].

A mature, although small, ecosystem of companies providing COTS MTCA.4 infrastructure modules (e.g. crates, CPUs, MCHs, power modules) and payload AMC and RTM modules (e.g. picoammeters, high voltage source, fast digitizers, frequency converters, CAN interfaces, scaler/discriminator, Ethernet switches, piezo driver) exist.

* daniel.tavares@lnls.br

DEVELOPMENT OF MTCA.4-BASED BPM ELECTRONICS FOR SPring-8 UPGRADE

H. Maesaka[†], T. Fukui, RIKEN SPring-8 Center, Sayo, Hyogo, 679-5148, Japan
 H. Dewa, T. Fujita, M. Masaki, C. Saji, S. Takano¹, JASRI/SPring-8, Sayo, Hyogo, 679-5198, Japan
¹also at RIKEN SPring-8 Center, Sayo, Hyogo, 679-5148, Japan

Abstract

We have developed a new BPM readout electronics based on the MicroTCA.4 standard for the low emittance upgrade of SPring-8 (SPring-8-II). The main requirements for the BPM system are a highly stable closed-orbit distortion measurement within 5 μm error for 1 month and a high-resolution single-pass BPM better than 100 μm rms for a 0.1 nC injected bunch. We designed an rf front-end rear transition module (RTM), which has band-pass filters, low-noise amplifiers, step attenuators, and pilot tone generators. BPM signals from the RTM are detected by a high-speed digitizer advanced mezzanine card (AMC) developed for the new low-level rf system of SPring-8. The beam position is calculated by the FPGA on the AMC in realtime. We evaluated the performance of the new BPM electronics at the present SPring-8 storage ring with a prototype BPM head for the SPring-8 upgrade. The single-pass resolution was estimated to be better than 30 μm rms for a 0.13 nC single bunch. The long-term stability was confirmed to be within 5 μm peak-to-peak for one or two weeks if the filling pattern was not changed. Thus, the new BPM system satisfies the requirements from SPring-8-II.

INTRODUCTION

To provide much more brilliant X-rays to users, the SPring-8 upgrade project, SPring-8-II [1], was proposed and we are developing accelerator components for the upgrade. Compared with the present SPring-8 ring, the beam energy is reduced from 8 GeV to 6 GeV and the magnet lattice is rearranged from double-bend achromat to 5-bend achromat. As a result, the natural emittance is improved from 2.4 nm rad to ~ 100 pm rad with radiation damping of insertion devices and the X-ray brilliance around 10 keV photons is increased more than 20 times higher than SPring-8.

The beam position monitor (BPM) system for SPring-8-II is required to be more stable and precise than SPring-8 [2]. The beam orbit stability should be 5 μm peak-to-peak for one month to achieve the required optical axis stability of 1 μrad and the source point stability of a few microns. Furthermore, an injected electron beam must be steered within the narrow dynamic aperture of 10 (H) \times 2 (V) mm^2 in the commissioning stage. Therefore, the single-pass BPM resolution is demanded to be 100 μm rms for a 0.1 nC injected beam and the electric center should be accurately

aligned to the field center of quadrupole and sextupole magnets within 100 μm rms (± 200 μm max.).

To fulfill the requirements above, we have developed a stable and precise button-type BPM system consisting of a BPM head, signal cables, and readout electronics. The design and basic performance of the BPM head and cables were already reported in Refs. [2-4]. In this paper, we describe the design and test results of the readout electronics.

DESIGN OF THE BPM ELECTRONICS

Required Functions for the BPM Electronics

For stable and precise BPM measurements, the amplitude from each button electrode must be detected stably and precisely. Since the button-type BPM generates bipolar impulse signals synchronized to the beam, a BPM signal has a main component around the acceleration rf frequency ($f_{\text{rf}} = 508.76$ MHz for SPring-8-II). The beam position is calculated from Δ/Σ ,

$$D_x = \left(\frac{\Delta}{\Sigma}\right)_x = \frac{V_1 - V_2 - V_3 + V_4}{V_1 + V_2 + V_3 + V_4},$$

$$D_y = \left(\frac{\Delta}{\Sigma}\right)_y = \frac{V_1 + V_2 - V_3 - V_4}{V_1 + V_2 + V_3 + V_4},$$

$$\begin{pmatrix} X \\ Y \end{pmatrix} \simeq \begin{pmatrix} k_x D_x \\ k_y D_y \end{pmatrix} \quad (1)$$

where V_n is the amplitude of each electrode (1: top right, 2: top left, 3: bottom left, 4: bottom right) and k_x and k_y are the conversion coefficients. The BPM head for SPring-8-II has a conversion factor of approximately 7 mm [3]. To suppress the BPM drift within 5 μm , the amplitude stability is required to be 0.1% level ($= 2 \cdot 5 \mu\text{m} / 7 \text{mm}$), corresponding to 0.01 dB. To obtain the BPM resolution of 100 μm , a signal-to-noise ratio of more than 35 ($= 0.5 \cdot 7 \text{mm} / 100 \mu\text{m}$) is needed, corresponding to 31 dB. Thus, highly-stable low-noise rf components and analog-to-digital converters (ADC) are necessary. In addition, an in-situ gain correction mechanism, such as a pilot tone method, should be prepared for better stability.

Furthermore, a high-speed closed-orbit distortion (COD) measurement is needed to prevent any damages of accelerator components and X-ray beamline devices from a large orbit deviation. The beam should be aborted within 1 ms in case of an abnormal beam orbit. Therefore, fast COD data with a 10 kHz update rate is required.

[†] maesaka@spring8.or.jp

ENHANCEMENT OF THE S-DALINAC CONTROL SYSTEM WITH MACHINE LEARNING METHODS*

J. Hanten[†], M. Arnold, J. Birkhan, C. Caliari, N. Pietralla, M. Steinhorst
Institut für Kernphysik, TU Darmstadt, Darmstadt, Germany

Abstract

For the EPICS-based control system of the superconducting Darmstadt electron linear accelerator S-DALINAC, supporting structures based on machine learning are currently developed. The most important support for the operators is to assist the beam setup and controlling with reinforcement learning using artificial neural networks. A particle accelerator has a very large parameter space with often hidden relationships between them. Therefore neural networks are a suited instrument to use for approximating the needed value function which represents the value of a certain action in a certain state. Different neural network structures and their training with reinforcement learning are currently tested with simulations. Also there are different candidates for the reinforcement learning algorithms such as Deep-Q-Networks (DQN) or Deep-Deterministic-Policy-Gradient (DDPG). In this contribution the concept and first results will be presented.

INTRODUCTION

The S-DALINAC [1] is a superconducting, thrice recirculating electron linear accelerator at the institute for nuclear physics at the TU Darmstadt (see Fig. 1). It is used for investigation of nuclear structure physics and is operated since 1991 in recirculating mode. The design value of its energy is 130 MeV at a maximum current of 20 μA . The accelerator operates in a continuous wave mode with a frequency of 3 GHz. Its electrons are provided by a thermionic gun or a spin polarized source. The acceleration proceeds, after passing a copper based chopper prebunching system, in an up to 10 MeV superconducting injector and an up to 30 MeV main LINAC. The position and spot size of the electron beam within its pipe is currently controlled with scintillating BeO-Targets and can be manipulated with corrector dipoles and quadrupoles.

It has to be optimized in terms of position, dimension, transmission and energy resolution to suit the proposed experiment. However, due to partly unknown fluctuations, set points from previous beam times can not be used again without adaption. At the moment, beam setup is done manually by operators and can take up to several weeks for the most complex systems. To improve this situation, it is planned to use deep reinforcement learning algorithms to support this process.

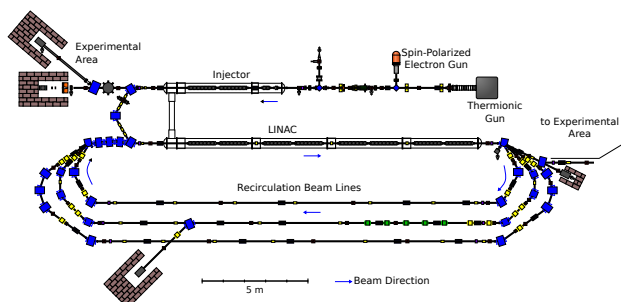


Figure 1: Accelerator hall floorplan of the thrice recirculating S-DALINAC.

DEEP REINFORCEMENT LEARNING

Deep Learning with the use of artificial neural networks (NN) as function approximators is used more frequently in the last years for sensory processing and computer vision [2]. There were also accelerator physics-related applications such as image based diagnostics of particle beam parameters [3]. More recently, there was a significant progress in combining deep learning with reinforcement learning, resulting in the “Deep Q Network” (DQN) algorithm [4]. This was capable to perform human level performance in many Atari games, having only the pixel data as its input. Because of the big parameter space and the nonlinear connection between these, machine learning and especially NNs are also proposed to be suited for modeling and control of particle accelerators [5].

At present, different algorithms are tested with a simple simulated pair of corrector magnets with the electron beam tracking algorithm *elegant* [6].

Parameters and Basic Functions

The standard reinforcement learning setup consists of an agent interacting with an environment E , in a sequence of actions a_t , observations of states s_t and rewards r_t , where $t = \{1, \dots, T\}$ is the index for one discrete time step. In general E can also be stochastic. The values s_t can be represented by the beam center coordinates, beam width, target position, magnet set points, etc. When used with the accelerator, it is planned to use the *areaDetector* [7], a plugin for the EPICS based control system [8] to obtain this information from the images produced by the scintillating targets. It is also possible to add additional environment parameters like temperature or vacuum pressure to s_t . At each time step the agent chose an action a_t from a set of set-point changes of corrector or quadrupole magnets. Depending on the chosen algorithm, the action space can be discrete or continuous.

* *Work supported by DFG through GRK 2128

[†] jhanten@ikp.tu-darmstadt.de

CHARACTERISATION OF CLOSED ORBIT FEEDBACK SYSTEMS

G. Rehm*, Diamond Light Source, Oxfordshire, UK

Abstract

Closed orbit feedback is applied at nearly all synchrotrons. Detailed investigations continue to be performed on the mathematical modelling of the spatial part (i.e. related to Orbit Response Matrix) and the dynamic part (i.e. the controller). This talk will serve as a summary of the ARIES workshop on Next Generation Beam Position Acquisition and Feedback Systems in November 2018. Benefits of recent advances compared to the traditional implementations will be highlighted.

INTRODUCTION

Closed orbit feedback (COFB) systems have been installed in most synchrotrons, both light sources and hadron accelerators. This contribution aspires to take a brief view at closed orbit feedback system from the perspective of *control theory*, which is useful as an integral part in the modern synchrotron design process. Furthermore, it will try to highlight some of the recent approaches to the spatial and dynamic processes used in closed orbit feedback with examples from the ARIES workshop "Next Generation Beam Position Acquisition and Feedback Systems" organised and held at ALBA in November 2018 [1]. While COFB has a long legacy in synchrotrons, digital real-time feedback systems operating at rates of 10 kHz and above have become widespread, so particular aspects affecting their performance will be focused on. It should be noted that most theoretical aspects are excellently covered in PhD thesis [2, 3], so this paper can only serve to give a brief introduction.

Motivation for Closed Orbit Feedback

Synchrotrons store relativistic charged particle beams for various reasons: the origins lie in high energy physics and storage rings for rare species, but also synchrotron light sources have become a widespread scientific tool globally. Whichever the motivation for the operation of a synchrotron ring, there will frequently be a desire to control the closed orbit of the particle beam, since disturbances of the magnetic guide fields are hard to limit to the degree that would allow operation without feedback control.

In practice, a specification on the standard deviation of orbit is set and this is frequently expressed as a an absolute distance or a fraction of beam size (or angle) in a relevant location. In light sources, this will provide an electron beam that is not significantly deteriorated by orbit motion so that photon beams are produced stably. In a particle collider it might help to ensure a constant collision rate, while in a ramping synchrotron it will be required to enable predictable extraction trajectories independent of hysteresis or other

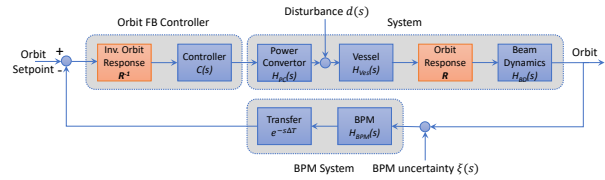


Figure 1: Block diagram of a simplified closed orbit feedback system: blue blocks signify dynamic processes, while red blocks show spatial processes.

disturbances. This orbit stability deviation needs to be accompanied by a frequency or time duration range over which the specified deviation should be integrated. This range will lead to further considerations on the requirements for beam position monitors (BPMs), like electronic noise, impact of thermal expansion or ground motion of the support.

CONTROL THEORY

COFB is an excellent fit with the common definition of a control loop in the context of control theory. Readers unfamiliar with terms like disturbance rejection, unity gain crossover frequency, open loop gain etc. can find an introduction in this tutorial aimed specifically at physicists [4]. For the purposes of COFB, the sources of orbit distortions in synchrotrons are well enough described by the following equation [5]:

$$\Delta x = \Delta x' R_{ij} = \Delta x' \frac{\sqrt{\beta_i \beta_j}}{2 \sin \pi \nu} \cos (|\Psi_i - \Psi_j| - \pi \nu)$$

In each transverse plane a kick $\Delta x'$ creates an orbit Δx and $\beta_{i,j}$, $\Psi_{i,j}$ are the respective beta function and phase advance at the location of the kick and observation. The presence of the betatron fractional tune ν in the denominator acts as a reminder to minimise orbit distortions during magnetic lattice design, by keeping ν near 0.5. The Orbit Response Matrix (ORM) is assembled from the elements R_{ij} by iterating through all the locations of dipole disturbances and observables. For use in COFB this is limited to corrector magnets and BPM locations.

Dynamic and Spatial Processes

Figure 1 attempts to map the generic feedback structure of controller, system, monitor to the typical implementation in the case of COFB. Inside this block diagram dynamic and spatial processes are identified:

- Dynamic processes: these are systems with the ability to store energy or information and thus display a dynamic response to the input on the output. If we limit

* guenther.rehm@diamond.ac.uk

TOWARDS AN ADAPTIVE ORBIT-RESPONSE-MATRIX MODEL FOR TWISS-PARAMETER DIAGNOSTICS AND ORBIT CORRECTION AT DELTA

S. Kötter*, T. Weis

Center for Synchrotron Radiation (DELTA), TU Dortmund, 44227 Dortmund, Germany

Abstract

At DELTA, a 1.5-GeV electron storage ring operated by the TU Dortmund University, preliminary tests of an adaptive orbit-response-matrix model were conducted. Closed orbit perturbations corrected by the slow orbit feedback can be buffered and used to update a fit of the bilinear-exponential model with dispersion (BE+d model). This model is a representation of the orbit-response matrix depending on the beta functions, the betatron phases and the tunes in both planes. This work introduces a new fitting recipe to obtain good estimates of the aforementioned quantities and evaluates a BE+d-model represented orbit-response matrix for orbit correction. Numerical studies are shown along with measurement results.

A NEW BEAM-STEERING AND DIAGNOSTICS TOOL

A new slow-orbit-feedback software [1] is under development at DELTA, a 1.5-GeV synchrotron radiation light source operated by the TU Dortmund University. Based on the bilinear-exponential model with dispersion (BE+d model) [2], this work explores integrating the new software with an adaptive orbit-response-matrix model for recovering optical functions according to the ideas presented in [3] and maintaining a well working orbit-response matrix to estimate orbit correction steps when switching beam optics.

The storage ring at DELTA is equipped with $J = 54$ capacitive beam-position monitors (BPMs) to measure the transverse beam position in $W = 2$ planes [4]. The majority of read-out electronics are Bergoz MX BPMs [5]. Their resolution is limited by the CAN-BUS modules digitizing the measurement signal to about $4.9 \mu\text{m}$ (12 bit for $\pm 10 \text{mm}$). The remaining BPMs are equipped with Libera Electron and Libera Brilliance read-out electronics which achieve a resolution of $<5 \mu\text{m}$ for typical beam currents [6].

For beam steering, 30 horizontal and 26 vertical steering magnets, $K = 56$ in total, are available [7]. The maximum deflection angles are up to 3.13 mrad for horizontal steering magnets and 1.13 mrad for vertical steering magnets.

The new slow-orbit-feedback software applies global correction steps with a maximum rate of about 0.1 Hz [1]. The basic idea for integrating the adaptive orbit-response-matrix model is to store the corrected orbit displacements $\Delta \vec{\kappa}$ ($W \cdot J$ elements) and the applied changes in steering angles $\Delta \vec{\theta}$ (K elements) in a ring buffer of length N while a subprocess continuously updates the BE+d model on this buffer.

* stephan.koetter@tu-dortmund.de

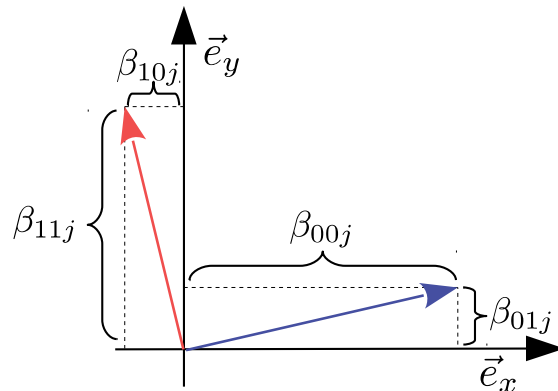


Figure 1: Beta function values β_{mwj} of coupled betatron oscillations at BPM j . The first mode ($m = 0$) is mostly horizontal. The second mode ($m = 1$) is mostly vertical.

THE BILINEAR-EXPONENTIAL MODEL WITH DISPERSION (BE+D MODEL)

According to the BE+d model [2], the orbit displacement $\Delta \kappa_{wj}$ at BPM j in plane w divided by the steering angle $\Delta \theta_k$ at steering magnet k

$$\frac{\Delta \kappa_{wj}}{\Delta \theta_k} = \sum_{m=0}^{M-1} \Re \left\{ Z_{mwj} A_{mk}^* e^{-i\pi q_m S_{jk}} \right\} + d_{wj} b_k,$$

is determined by the sum over $M = 2$ modes of betatron motion and dispersion. The plane index w refers to either the horizontal or the vertical plane. The separation of the indices m and w incorporates coupled betatron oscillations into the model. These are not confined to a single plane. For this reason, the phasor

$$Z_{mwj} = \sqrt{I_m \beta_{mwj}} e^{i\Phi_{mwj}}$$

is indexed with both m and w . It encodes the amplitude and phase of the betatron oscillation of the m -th mode where β_{mwj} is the projection of the beta function into the w -th plane at BPM j (Fig. 1) and Φ_{mwj} is the corresponding betatron phase. The invariant of motion I_m is proportional to the Courant-Snyder invariant [3].

The remaining model parameters are the tune of the m -th mode q_m , the factor S_{jk} , which is either -1 if the k -th steering magnet is downstream of the j -th BPM or 1 otherwise, an unnormalized dispersion d_{wj} , which is related to the dispersion function by an unknown factor, the corrector parameters A_{mk} and the dispersion coefficients b_k .

TUNE COMPUTATION VIA MODEL FITTING TO SWEPT MACHINE RESPONSE MEASUREMENT

M.G. Abbott*, G. Rehm, Diamond Light Source, UK

Abstract

At Diamond Light Source we compute the horizontal and vertical tunes by fitting a simple multi-pole resonator model to the measured electron beam frequency response. The transverse (and longitudinal) tune response is measured by sweeping an excitation across the range of possible tune frequencies and synchronously measuring the IQ response.

The multi-pole resonator model is a good fit to the measured behaviour, but the fitting process is surprisingly challenging. Problems include noisy measurements, very complex beam responses in the presence of increasing chromaticity, poor data when the beam is close to instability, and a number of challenges with the stability of the algorithm.

The tune fitting algorithm now in use at Diamond has been developed and refined over many years. It is finally stable enough to work reliably throughout most beam operating conditions. The algorithm involves alternating peak finding and non-linear fitting, with a fairly naive mathematical approach; the main focus is on providing reliable results.

INTRODUCTION

The synchrotron beam has natural frequencies of oscillation in the horizontal, vertical, and longitudinal directions: transverse “betatron tunes” and longitudinal “synchrotron tunes”. The precise betatron tune frequencies are of considerable interest to machine physicists, and need to be measured at various stages during machine operation.

At Diamond Light Source the storage ring configuration has evolved into a state where movement of the tunes (driven mainly by insertion device movements affecting machine optics) can result in loss of beam lifetime and injection efficiency, so it is necessary to actively measure and correct the betatron tunes in both transverse axes. This therefore requires a reliable measurement of the tunes, during both machine startup conditions and normal operation.

A complicating factor when computing the tunes arises from interference between transverse and longitudinal oscillations, depending on the chromaticity settings of the synchrotron. This interaction can result in significant side-lobes at (roughly) multiples of synchrotron frequency offset either side of the main tune measurement. Depending on machine conditions it can become difficult to identify the central tune frequency. This is addressed by the process described here, but there remain some operating conditions that can be surprisingly difficult to interpret.

We are able to take advantage of phase and magnitude measurement to fit a reasonably sophisticated model.

* michael.abbott@diamond.ac.uk

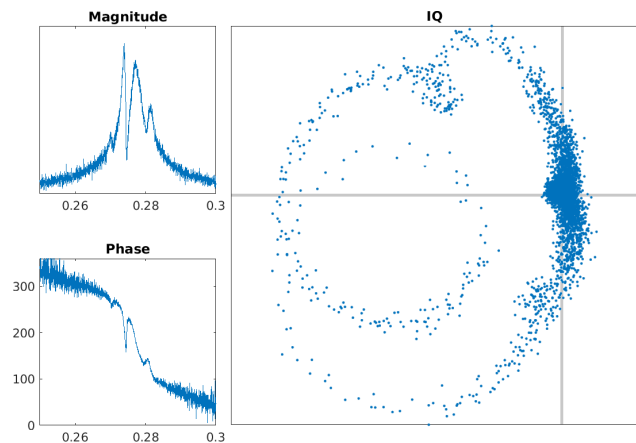


Figure 1: Illustration of swept response, showing magnitude (in arbitrary units) and phase (in degrees) against fractional tune, and the corresponding complex IQ measurements. This sweep shows a typically complex response with multiple lobes, illustrating the problem of identifying the true tune in the presence of large synchrotron side-lobes.

RESPONSE MEASUREMENT

Tune measurement at Diamond is integrated into the operation of the Multi-Bunch Feedback (MBF) system [1], and is done by exciting the beam with a swept sinusoidal oscillation and synchronously measuring the response. The result is a complex number $z(\omega)$ at each sampled frequency ω representing the phase and magnitude of the machine response, computed thus:

$$z(\omega) = \sum_{t \in \text{dwell}(\omega)} e^{-iK\omega t} x(t)$$

where $\text{dwell}(\omega)$ is typically 100 turns per frequency step, and K is a frequency scaling factor.

Because measurement and stimulus are both confined to a single location in the machine, we are only able to see the fractional part of the machine tune, but in practice this is the only part that needs to be measured. For convenience, all frequencies ω are scaled to fractions of machine revolution frequency.

When using the MBF system for tune sweeping we have a number of options, including which bunches to excite and measure, which overall phase advance between bunches to apply (this is referred to as the “mode”), strength of excitation, and the dwell time at each frequency. At present we excite and measure all bunches at a mode of 80, and typically sweep 4096 points of a frequency range of 0.1 around the nominal tune point over a period of about 780 ms. From this the tune measurement is updated at just over 1 Hz.

A typical measurement is shown in Fig. 1.

Content from this work may be used under the terms of the CC BY 3.0 licence (© 2019). Any distribution of this work must maintain attribution to the author(s), title of the work, publisher, and DOI

COMMISSIONING OF THE NON-INVASIVE PROFILE MONITORS FOR THE ESS LEBT

C.A. Thomas*, R. Tarkeshian, J. Etxeberria, S. Haghtalab, H. Kocevar,
N. Milas, R. Miyamoto, T. Shea,
European Spallation Source ERIC, Lund, Sweden

Abstract

In the Low Energy Beam Transport (LEBT) of the European Spallation Source (ESS) Linac, a specific Non-invasive Profile Monitor (NPM) has been designed to primarily monitor beam position monitor with 100 μm accuracy, and in addition enable beam profile and size measurement. We present the first measurement results using NPM during the commissioning of the LEBT. The measurement results conclude the beam position as well as the angle of the beam. The performance of the measurement is discussed and compared to the required accuracy for the position measurement. In addition, the profile of the beam along the propagation axis is reported, as measured for part or the full pulse transported in the LEBT. The fidelity of the reported profile will be discussed as function of the system sensitivity and image signal to noise ratio.

INTRODUCTION

The Non-invasive Profile Monitors in the ESS LEBT have been design to be primarily beam position monitors [1]. However, this instrument acquires an image of the residual gas fluorescence, and therefore it is capable of measuring the beam centroid angle, and the beam size as well [2]. In order to achieve the required accuracy, we have designed the instrument to be fiducialised, permitting the imaging system to be aligned on the beam reference axis within specified requirements. In this case, the accuracy of the beam position measurement is $\pm 100 \mu\text{m}$. The method to align the optical axis with the beam axis reference is described in the first section, together with the qualification measurements. Two NPMs, one for each transverse plane, have been installed in the Permanent Tank of the ESS LEBT, i.e. between the two solenoids of the LEBT. The commissioning of the LEBT has started in 2018, and continued through the first part of 2019. The NPMs were commissioned and the result of beam position measurement is presented and the accuracy and the precision of the measurement is discussed in the second session. In addition, it has been shown that the instrument is capable of measuring also the angle of the beam centroid. Processing the images to retrieve beam angles has been done successfully, and the performance on the measurement is shown and discussed also in the second section. Finally, the beam emittance can also be measured by fitting the beam size variation along the instrument longitudinal axis. Since the beam profile in the LEBT is not always Gaussian and also composed by a different species (mainly H^+ and H_2^+) the

beam emittance can be calculated only in a specific condition. In the last part of the second section, the results for emittance estimation based on Gaussian function are discussed. Finally, concluding remarks are drawn for the use of this diagnostic for the LEBT and the rest of the ESS linac.

INSTRUMENT QUALIFICATION

This NPM-LEBT is capable of measuring beam position by imaging the beam induced Fluorescence in the background gas. In order to have precise measurement precise setup of image magnification as well as knowledge of the image coordinates are required.

The NPM is equipped with a motorized lens, with an encoder to read out focusing position of the camera sensor with respect to the focal plane of the lens. Magnification m is given with the lens equation $m = X/F$, where X is the image sensor distance to the focal plane and F is the focal lens. The motor of the lens has limit switches to ensure the it is in the correct position. This introduces an additional offset that has to be determined.

The magnification at various lens positions are measured for all NPM units. Figure 1 shows measurements for one of the NPM units with a target positioned along the optical axis at various distances. In each position, the lens is adjusted and the target lens offset is found by minimizing the difference between the measured magnifications and the predicted ones using the lens equation with $X = \text{offset} + x_{\text{enc}}$. The minimization results in finding the offset with an average difference of less than 1%.

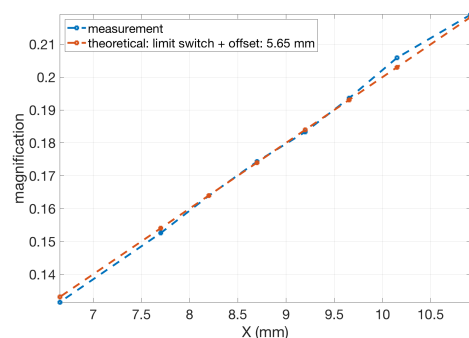


Figure 1: Magnification of the vertical unit of the first NPM set in the LEBT. Its focal length is $F = 50 \text{ mm}$.

The object coordinates relative to the image are given by the fiducialisation of the optical axis of the camera. The procedure consists in aligning the corner cube of the laser tracker in the centre of the image, and then recording several

* cyrille.thomas@ess.se

STUDY AND CHARACTERIZATION OF SPIRAL2 BPMs

V. Langlois, M. Lewitowicz, C. Jamet, S. Leloir, T. Andre, G. Ledu, P. Legallois, F. Lepoittevin,
S. Loret, C. Potier de courcy, GANIL, Caen, France

Abstract

The SPIRAL2 facility currently under commissioning at GANIL in France will deliver high-intensity up to 5mA 20MeV/n light and heavy-ion beams. SPIRAL2 beams are accelerated by a Radio Frequency Quadrupole (RFQ) and a LINAC composed of 26 superconducting cavities. A tuning of the SPIRAL2 LINAC relies mainly on Pick-up Beam Profile Monitors (BPM). 20 BPMs are mounted inside the warm sections between superconducting cavities. They serve to measure a beam transverse position to center the beam, a phase to tune cavities and an ellipticity to adjust beam optics along the LINAC. The phase and ellipticity measurements require high acquisition accuracy of the BPM signals.

This paper deals with an analytical study and CST code simulations of the BPM performed in order to determine correction coefficients for the ellipticity measurements. The results of calculations were compared to experimental ones obtained with two BPMs located on a “diagnostic plate” after the RFQ and a BPM located in the MEBT. Finally, the BPM acquisition chain was carefully characterized to identify its uncertainties and to ensure that it meets initial specifications.

INTRODUCTION

SPIRAL2 LINAC [1] is composed of 19 cryomodels that contains accelerating cavities. Warm sections are installed between cryomodels. These sections contain two quadrupoles and a pick-up type BPM inside the first quadrupole of each warm section.

SPIRAL2 BPM are designed to monitor beam position, phase and ellipticity with the following specifications: (Table 1)

Table 1: BPM Specifications

Parameter	Resolution	Range
Position	+/- 150µm	+/-20 mm
Phase	+/-0.5 deg.	+/-180 deg.
Ellipticity	+/-20 % or +/- 1.2 mm ²	

The BPM probes are composed of 4 squared electrodes (Fig. 1) connected with 23 meters long cables to the BPM acquisition electronics. The electronic modules were constructed by the Electronics Division of “Bhabha Atomic Research Centre” (BARC) in the framework of collaboration with the SPIRAL2 project. The French laboratory IPN Orsay and GANIL are in charge of the global BPM installation and commissioning [2].

The BPM electronics process the signal at two frequencies: the accelerating frequency 88MHz and its

harmonic 176MHz. The beam position, ellipticity phase and bunch length are calculated from the 4 BPM signals [3].

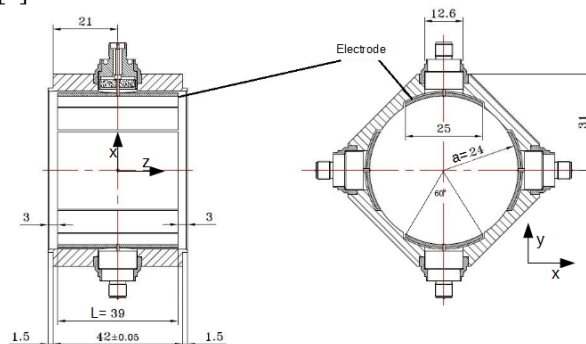


Figure 1: SPIRAL2 BPM Mechanics.

The tuning of the SPIRAL2 LINAC will be performed in two steps. In the first one, the beam will be centered using the BPM position measurements and the phase of each cavity will be tuned using the beam phases measured by BPM. In the second step, the beam will be matched along the LINAC using ellipticity and position measurements from BPM.

The proton beam velocity will increase along the LINAC from $\beta=0.04$ to about $\beta=0.26$. Position and ellipticity sensitivities depend on the beam velocity and the processed frequency. This dependence should be taken into account in order to obtain the absolute values of the measured parameters.

BEAM MODELIZATION

Let's consider a beam traveling through the BPM along the beam axis. The beam intensity can be expanded in a Fourier series [4].

$$I_b(t) = \langle I_b \rangle \left[1 + 2 \sum_{n=1}^{\infty} A_n \cos(n\omega_0 t + \phi_n) \right]$$

With:

- I_b the beam intensity
- $\langle I_b \rangle$ the average beam intensity
- A_n the Fourier component amplitude
- ω_0 the fundamental pulsation
- ϕ_n the Fourier component phase

A wall current density i_w induced by the beam is calculated by solving the Laplace equation [5]:

$$i_w = \frac{A_n \langle I_b \rangle}{\sqrt{2\pi a}} \left[\frac{I_0(g r_0)}{I_0(g a)} + 2 \sum_{m=0}^{\infty} \frac{I_m(g r_0)}{I_m(g a)} \cos(m(\varphi - \varphi_0)) \right]$$

DEVELOPMENT OF A LOW-BETA BPM FOR MYRTE PROJECT*

M. Ben Abdillah[†], F. Fournier, P. Blache, Institut de Physique Nucléaire, Orsay, France

Abstract

MYRTE (MYRRHA Research Transmutation Endeavour) performs research to support the development of the MYRRHA (Multi-Purpose Hybrid Research Reactor for High-Tech Applications) research facility, which aims to demonstrate the feasibility of high-level nuclear waste transmutation at industrial scale. MYRRHA Facility aims to accelerate 4mA proton beam up to 100 MeV. The accurate tuning of LINAC is essential for the operation of MYRRHA and requires measurement of the beam transverse position and shape, the phase of the beam with respect to the radiofrequency voltage with the help of Beam Position Monitor (BPM) system. MYRTE aims to qualify beam operation at 1.5MeV. Two BPMs were realized for MYRTE operation. This paper addresses the design, realization, and calibration of these two BPMs and their associated electronics. The characterization of the beam shape is performed by means of a test bench allowing a position mapping with a resolution of 0.02mm.

GENERAL DESCRIPTION OF MYRTE

The MYRTE project was launched in 2015 to perform the necessary research to support the development of the MYRRHA (Multi-Purpose Hybrid Research Reactor for High-Tech Applications) facility, which aims to demonstrate the feasibility of high-level waste transmutation at industrial scale.

MYRRHA LINAC is accelerating a beam with characteristics sketched in Table 1.

Table 1: Beam Specifications

Particle	Current (mA)	Energy (MeV/u)
Proton	0.1-5	1.5-600

MYRTE addresses the topics that have been identified as priority ones to successfully pursue the research, design and development of the MYRRHA accelerator and prepare for its actual construction. Among the topics, beam characterization would deliver data of fundamental importance in all beam dynamics simulation tools.

The characterization is performed at the injector.

The injector is constituted by an ECR proton source, a low energy beam transfer line followed by a Radiofrequency Quadrupole (RFQ) which accelerates beam up to 1.5MeV/u. RFQ frequency is set to $f_{acc}=176.1$ MHz

Beam Position Monitors (BPM) measures beam position, phase shift regarding the accelerating signal and an indication on the beam transverse shape. This paper details the steps of design, fabrication and qualification of these two BPMs.

* This work is supported by the European Atomic Energy Community's (Euratom) H2020 Program under grant agreement n°662186186 (MYRTE Project).

[†] abdillah@ipno.in2p3.fr

GENERAL DESCRIPTION OF BPM

BPMs allow measuring the vertical and horizontal coordinates of the center of gravity of the beam position and assessing the transverse size of the beam. Capacitive BPMs are used. Each BPM is equipped with 4 probes formed by a sealed 50Ohm feedthroughs attached to an electrode. The probes (feedthrough + electrode) should be as identical as possible and they should be symmetrical regarding the center of the BPM.

BPM must meet a set of constraints (vacuum, magnetism, positioning, steaming, resistance to ionizing radiation) in order to ensure its integration into the machine.

The beam induces electrical signal on each electrode, beam position, transverse shape and energy are induced from these electrical signals. The electronic module provides the following information by processing the electrical signals delivered by the electrodes:

- The horizontal and vertical position of the center of gravity of the beam.
- Beam phase shift with respect to the main reference signal. Beam velocity and energy are processed from this measurement.
- Beam quadrupole moment figuring in the second order moment of the beam transverse distribution.

BPM SPECIFICATIONS

- In the scope of MYRRHA project, IPN is in charge of the realization of BPMs for the 17MeV-100MeV section. In the scope of MYRTE project, two BPMs partially characterize the beam emerging of the RFQ.
- The specifications are similar for both MYRRHA and MYRTE. The precision on the position should be less than 100µm on both axes. The beam phase shift relative to the accelerating signal should be measured with a precision less than 1 degree. The beam quadrupole moment should be less than 1.6mm² for circular beam or within 20% precision for elliptical beams. Table 2 summarizes the BPM specifications.

Table 2: BPM Specifications

Parameter	Range	Precision
Position	±5 mm	100µm
Phase	360degrees	1degree
Quadrupole moment	±5mm	Max(1.6mm ² ;20%)

BPM DESIGN

The way both projects were held was to focus on the design of the BPM for the 17-100MeV/u section and to simulate the said design at beam energy equal to 1.5MeV.

A NEW BUTTON-TYPE BEAM POSITION MONITOR FOR BESSY II AND BESSY VSR*

J.-G. Hwang[†], G. Schiwietz[‡], A. Schällicke, M. Ries, V. Dürr, D. Wolk, F. Falkenstern
 Helmholtz-Zentrum Berlin für Materialien und Energie GmbH (HZB), Berlin, Germany

Abstract

The implementation of the variable pulse length storage ring upgrade BESSY VSR involves more than one order-of-magnitude differences in the total charge of adjacent short and long bunches within the bunch train. Thus, any signal ringing beyond a nanosecond in time will cause a misreading of beam position and current, specifically for low bunch charges. This calls for a significantly improved performance of the beam-position-monitor (BPM) system for bunch-selective operation. We report on the corresponding design and fabrication of a new button BPM with advanced features, such as impedance matching inside the button as well as optimization of insulator material, button size, and position, for reduced crosstalk between buttons.

INTRODUCTION

There is a strong scientific motivation to generate sub-to picosecond level short X-ray pulses, a timescale on which chemical reactions or phase transitions take place, for investigating the dynamics of fast reactions [1]. The time resolution of experiments in storage rings is typically, however, limited fundamentally in time resolution by the electron bunch length of 30 ~ 100 ps full width at half-maximum (FWHM) apart from several sophisticated methods such as short pulse generation scheme from transversal chipped long bunches [2] and Femtoslicing [1, 3]. The BESSY Variable-pulse-length Storage Ring (BESSY VSR) project was launched to establish picosecond short pulses for covering the future increasing demands for short X-ray pulses. This is feasible by installing superconducting cavities with resonance frequencies of 1.5 GHz and 1.75 GHz [4] in addition to the fundamental mode 0.5 GHz NC cavities, which generates a beating pattern of the sum voltage, thereby creating alternating buckets for long and short bunches [5]. This provides the capability of user accessible picosecond pulses at a high repetition rate, up to 250 MHz [6]. For a sophisticated operation mode as shown in Fig. 1, in order to preserve the present average brilliance of BESSY II, BESSY VSR has about ten times more beam current in long bunch buckets than short bunch buckets to avoid the longitudinal microwave instability that occurs above a certain threshold current. Due to this disparity in the beam current of long and short bunches, it is particularly difficult to measure the position of the short bunches precisely when there is signal ringing beyond a nanosecond in time [7, 8]. It can cause the

performance deterioration of the bunch-by-bunch feedback system. This stimulates the development of new button-type beam position monitor (BPM).

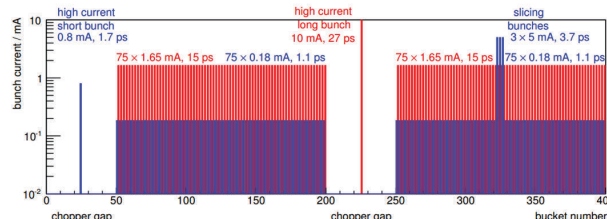


Figure 1: Possible complex filling pattern for BESSY VSR operation with short bunches (blue) and long bunches (red). Trains of low charges short bunches are added to relax beam lifetime and to supply THz power as well as short X-ray pulses at high repetition rate.

LONG-RANGE SIGNAL RINGING

Helmholtz-Zentrum Berlin (HZB) operates the 3rd generation synchrotron radiation facility, BESSY II, since 1999. The BESSY II standard button-type BPMs were developed and installed during construction of the storage ring. We observed a completely different signal shape in the measurements of the BESSY II standard BPM with 1 mA single bunch and multi-bunch train [9]. This can occur because trapped modes inside the insulation of the BPM are not fully damped within 2 ns, which corresponds to the bunch spacing in the storage ring. When the frequency of the trapped mode is a harmonic of the fundamental beam frequency $f_{RF} = 500$ MHz, the accumulative effect over the multi-bunch train can cause significant distortion of not only the shape of the signal but also the amplitude although the amplitude of the signal ringing is small. The spectrum of measured BPM signal during single-bunch operation is shown in Fig. 2.

In the spectrum of the measured BPM signal, two strong trapped modes are present at the frequencies of 5.2 GHz and 5.5 GHz. To confirm the effect of the long-range signal ringing, the evolution of the signal can be calculated by superimposing the measured single-bunch signal V_{single} with bunch spacing Δt_b which can be expressed as

$$V_{accum}(t) = \sum_n V_{single}(t-n\Delta t_b) \int_{-\infty}^{t-n\Delta t_b} ds \delta(s), \quad (1)$$

By using Eq. (1) with 2 ns equi-spaced and equi-populated without concerning transient beam loading effects, the expected signal shape with a multi-bunch filling is calculated.

* Work supported by German Bundesministerium für Bildung und Forschung, Land Berlin, and grants of Helmholtz Association.

[†] ji-gwang.hwang@helmholtz-berlin.de

[‡] schiwietz@helmholtz-berlin.de

CONCEPT OF A BEAM DIAGNOSTICS SYSTEM FOR THE MULTI-TURN ERL OPERATION AT THE S-DALINAC*

M. Dutine[†], M. Arnold, T. Bahlo, R. Grewe, L. Jürgensen, N. Pietralla, F. Schließmann, M. Steinhorst
 Institut für Kernphysik, Darmstadt, Germany

Abstract

The S-DALINAC is a thrice-recirculating linear electron accelerator operating in cw-mode at a frequency of 3 GHz. A path-length adjustment system in the second recirculation beam line allows to shift the beam phase by 360° and thus to operate in ERL mode. For the multi-turn ERL operation, the beam will be accelerated twice and subsequently decelerated twice again (not demonstrated yet). For this mode, it is necessary to develop a nondestructive beam diagnostics system in order to measure the beam position, phase and beam current of both, the accelerated and the decelerated beam, simultaneously in the same beamline. The conceptual study of a 6 GHz resonant cavity beam position monitor will be presented together with alternative solutions.

INTRODUCTION

The Superconducting Darmstadt Linear Accelerator (S-DALINAC) is a thrice-recirculating linear electron accelerator operating in cw-mode at a frequency of 3 GHz [1]. It has been upgraded in 2016 by the installation of a third recirculation beamline. A path length adjustment system included in the newly built beamline allows an increase of the path length by up to 100 mm corresponding to a phase shift of 360° in beam phase. It is therefore possible to operate the S-DALINAC as an Energy-Recovery-Linac (ERL) by shifting the beam phase by 180° which was demonstrated in 2017 [2]. A floorplan of the S-DALINAC is shown in Fig. 1.

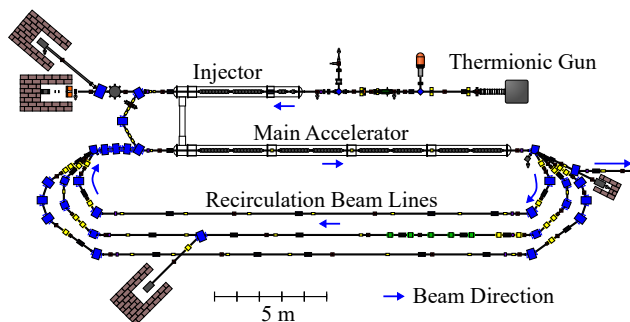


Figure 1: Floorplan of the S-DALINAC

For the upcoming multi-turn ERL operation, the beam will be accelerated twice and subsequently decelerated twice again. In this mode, the once accelerated beam and the once decelerated beam will share the same beamline (first recirculation) but do not necessarily have the same orbit

* Work supported by BMBF through grant No. 05H18RDRB2 and DFG through GRK 2128.

[†] mdutine@ikp.tu-darmstadt.de

in this beamline. Therefore, a beam position measurement capable of determining the beam positions of both beams simultaneously is required. In addition, a beam phase and current measurement is desired. The measurement has to be nondestructive as it would otherwise interrupt the ERL mode. A particular challenge will be the operation at low beam currents of 100 nA, which corresponds to bunch charges of about 30 aC while the beam is tuned. As conventional pickups are not suitable for these low bunch charges, the following solutions are under investigation:

1. A resonant cavity beam position monitor (BPM) operated at 6 GHz.
2. A resonant cavity beam position monitor operated at 3 GHz together with a pulsed beam of about 1.7 MHz.
3. A wire scanner measurement.

6 GHz RESONANT CAVITY BEAM POSITION MONITOR

In ERL mode, the beam has an effective bunch repetition frequency of 6 GHz in the first recirculation beamline. The first concept is a position measurement using a resonant cavity BPM with its TM₁₁₀ mode at a frequency of 6 GHz. The TM₁₁₀ mode is the so called dipole mode. It can be used for position measurement as the field strength depends linearly on the beam current and the transverse offset to the cavity center for small offsets. In order to distinguish between a change of the beams position and its current, a nondestructive current measurement is necessary. When the beam crosses the cavity center the signal will show a phase shift of 180°. Therefore, a beam phase measurement is required whereby the BPM can be calibrated to the transverse side. Both measurements can be conducted using another type of cavity located close to the cavity BPM. This type of cavity is routinely used at the S-DALINAC [3] and its TM₀₁₀ mode is excited independent of the beams transverse position.

Electromagnetic Conception

The required cavity radius R_{res} for a simple pillbox cavity without beampipes can be calculated to

$$R_{\text{res}}^{110} = \frac{c_0 \cdot a_{mn}}{2\pi \cdot f_{\text{res}}} \approx 30.5 \text{ mm}, \quad (1)$$

where $f_{\text{res}} = 6 \text{ GHz}$ is the resonance frequency, c_0 is the speed of light and a_{mn} is the n th zero of the Bessel function of m th order. The beampipe at the S-DALINAC has a radius of 17.5 mm which leads to a decrease of the resonance frequency which in turn has to be compensated by

BPM RESOLUTION STUDIES AT PETRA III

G. Kube, J. Neugebauer, F. Schmidt-Föhre, DESY, Hamburg, Germany

Abstract

In order to measure the noise level of a BPM system from beam generated orbit data, the correlated beam jitter has to be removed from the position signals. There exist different ways to extract the BPM noise, as the “three-BPM” correlation method or the model-independent principal components analysis (PCA). Both methods will shortly be reviewed. Based on a PCA, the resolution of the PETRA III *Libera Brilliance* based BPM system was measured. The results are presented together with first measurements in view of an updated BPM system for the future PETRA IV project at DESY.

INTRODUCTION

PETRA III is a third-generation synchrotron light source currently operated at 6 GeV by DESY Hamburg, Germany [1, 2]. Since 2016 DESY has been pursuing R&D towards upgrading the machine to a fourth-generation one, PETRA IV, being diffraction limited up to X-rays of about 10 keV [3] and expected to start operation in 2027. For this new machine a good resolution of the button-type BPMs of about 10-20 μm in turn-by-turn and 100 nm in stored beam mode (at 300 Hz bandwidth) will be required [4].

The position resolution $\sigma_{x,y}$ of a button-type BPM is determined by two factors, the monitor constant $K_{x,y}$ and the signal-to-noise ratio SNR [5]:

$$\sigma_{x,y} \propto K_{x,y} / \sqrt{SNR}. \quad (1)$$

While $K_{x,y}$ is defined by the pickup geometry (mainly beam pipe diameter, but also button size), SNR depends on geometry (button size defines signal strength), infrastructure (cable length, attenuators. . .), and quality of the read-out electronics. In the following, the main focus will be on the performance of the read-out electronics. As first step towards a new BPM system for PETRA IV it was decided to measure the achievable resolution of the existing PETRA III *Libera Brilliance* electronics from the commercial supplier Instrumentation Technologies [6].

Usually the design of modern ADCs integrated in electronic devices is driven by the telecommunication market, therefore they are well adapted for cw signals. Beam generated signals from a button-type pickup however are far away from being comparable to a cw signal, therefore it is preferable to perform the resolution study based on orbit data from the electron beam. Beam generated signals however contain two different kinds of jitter. For one thing it is the beam jitter, i.e. a real change of beam angle and position caused by fluctuations in the accelerator (caused by ground motion, energy fluctuation. . .). This kind of jitter is seen by several or even all BPMs simultaneously because of the correlation established by the particle beam optics. On the

other hand it is the noise of the BPM electronics which is the quantity of interest and has to be measured. In case of BPM noise there exist no correlation between adjacent BPM readings. Consequently a correlation analysis is a powerful tool in order to disentangle both jitter sources. In the next section, two common methods which are in use in the accelerator community are briefly described, hereafter a principal component analysis is applied for the determination of the PETRA III BPM resolution.

CORRELATION ANALYSIS

Two schemes are sometimes used for BPM investigations, the “three BPM” correlation method and the Principal Component Analysis (PCA). Examples can be found in Refs. [7] from KEK-B (Tsukuba, Japan) and [8] from SSRF (Shanghai, China). Their underlying ideas will briefly be sketched hereafter. A further method described in Ref. [9] is an extension of the “three BPM” method, but will not be covered.

“Three BPM” Correlation Method

In the “three BPM” method, position readings from three adjacent BPMs are considered, assuming that no non-linear elements are inbetween the monitors. As indicated in Fig. 1, the readings are connected by the transport matrices according to

$$\begin{pmatrix} y_3 \\ y'_3 \end{pmatrix} = M_\alpha \begin{pmatrix} y_1 \\ y'_1 \end{pmatrix}, \quad \begin{pmatrix} y_2 \\ y'_2 \end{pmatrix} = M_\gamma \begin{pmatrix} y_1 \\ y'_1 \end{pmatrix}, \quad M_\alpha = \begin{pmatrix} \alpha_{11} & \alpha_{12} \\ \alpha_{21} & \alpha_{22} \end{pmatrix},$$

and M_γ respectively. While a BPM delivers only position information, position readings from both transport equations can be combined in order to get rid of y'_1 , resulting in

$$\tilde{y}_2 = \left(\gamma_{11} - \frac{\alpha_{11}\gamma_{12}}{\alpha_{12}} \right) y_1 + \frac{\gamma_{12}}{\alpha_{12}} y_3 = X_{21}y_1 + X_{23}y_3.$$

The tilde indicates that the position at location 2 is an estimated one. It can be calculated from the readings of BPM₁ and BPM₃ with knowledge of the transport matrix elements which are comprised in the coefficients X_{21}, X_{23} . At the other hand, y_2 can directly be measured at BPM₂, the difference

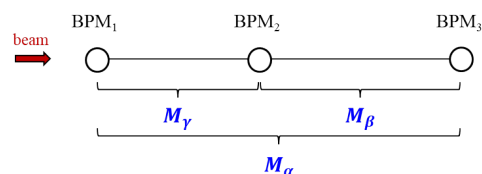


Figure 1: Principle scheme of the “three BPM” correlation method. In order to eliminate the beam correlated jitter in BPM measurements, N position readings of three adjacent BPMs have to be recorded.

Content from this work may be used under the terms of the CC BY 3.0 licence (© 2019). Any distribution of this work must maintain attribution to the author(s), title of the work, publisher, and DOI

OPERATIONAL PERFORMANCE OF NEW DETECTION ELECTRONICS FOR STRIPLINE-TYPE BEAM POSITION MONITORS AT THE SuperKEKB INJECTOR LINAC

F. Miyahara[†], K. Furukawa, M. Satoh, Y. Seimiya, T. Suwada, High Energy Accelerator Research Organization (KEK), Tsukuba, Japan

Abstract

SuperKEKB injector linac delivers four different beam modes modulated pulse by pulse at 50 Hz, which have 100-times different beam charges, and a pulse may contain two bunches only 96-ns apart. Required low-emittance beams for SuperKEKB rings would need precise beam orbit controls in order to suppress the transverse wakefield in the accelerating structures. A new detection electronics with a wide dynamic range of 40 dB with a high resolution based on a 180-MHz narrow-band detection technique for stripline-type beam position monitors (BPMs) has been developed for the SuperKEKB injector linac. Position resolutions of 5-7 micrometer in one standard deviation were successfully achieved in a normal operation. The self-calibration system is also installed in order to monitor or compensate gain drifts for each input channel with accuracy down to 0.1%, by using test pulses going through stripline heads between 50-Hz beam pulses. The design concept of the new detection electronics is described, as well as operational performance of synchronized measurement with 100 BPMs for injection beams to four electron/positron storage rings.

INTRODUCTION

The linac is required to inject electron/positron beams with bunch charge of 4 nC and normalized emittance of $(\epsilon_x, \epsilon_y) = (40, 20) \mu\text{m}$ for e^- , $(100, 15) \mu\text{m}$ for e^+ , to SuperKEKB HER/LER circular accelerator [1] and 0.3 nC/bunch beams into PF/PF-AR rings. Thus, there are multiple beam modes that can be switched ever 20 ms [2, 3]. Because beam injection energies for those rings are different, 64 pulsed magnets with dedicated power supply system with energy recovery circuit have been installed [4].

To deliver the low emittance e- beam which is generated by an rf-gun[5] to the HER, suppressing emittance growth in the linac is very important. The main source of the emittance growth is transverse wakefield generated in misaligned quadrupole magnets and accelerating structures[5], and it can be mitigated by an orbit correction. For this purpose, a high resolution, less than 10 μm , beam position monitor had been required. Then, we have developed a stripline BPM read system with high position resolution, high dynamic range and self-calibration system [6, 7]. Because the linac has double bunch operation with 96 ns spacing, a full width of the signal output from bandpass filters, 4th-order Butterworth and 2nd-order Bessel filter, used in the readout board less than 90 ns.

[†] fusashi.miyahara@kek.jp

The dynamic range can be ensured by attenuation of the of the BPM signal for every beam modes. The attenuator value of each BPM board is determined by the beam mode and the amount of the bunch charge passing through, and a calibration coefficient is given for each attenuator value. There are about 100 BPMs in the linac, and all readout systems were updated in 2017.

PERFORMANCE OF THE BPM SYTEM

Position Resolution

The BPM readout system has a position resolution of 3 μm if the attenuator is set optimally [6], but in the current operation, the strength of the attenuation is set so that it has a wide dynamic range with respect to position and the position resolution is 10 μm or less. Position resolutions of BPMs are shown in Fig. 1 with the linac layout. The resolution is estimated by 3-bpm method using data obtained by changing strength of a quadrupole at the A-sector. Except for points, J-Arc and a chicane in 3-sector, with a large dispersion function because energy jitter and variation of the energy distribution affect the measurement at that point, the position resolution is much better than the requirement. Since stripline BPMs in 3-sector to 5-sector has small inner radius, resolutions are better than others.

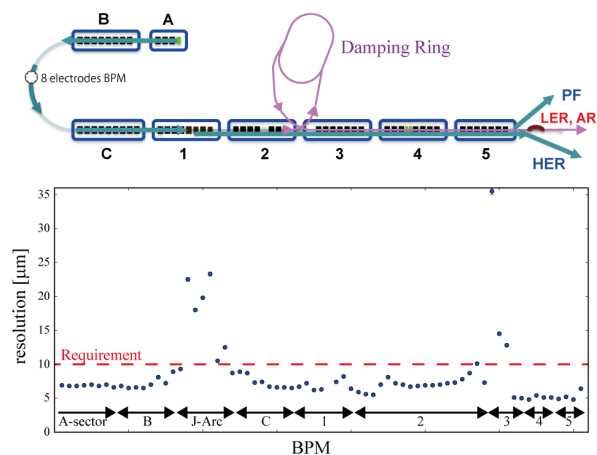


Figure 1: Linac layout and position resolution.

Self-Calibration System

The self-calibration system is used to calibrate gain balance between two signals from opposite electrodes and monitor the gain drift or cable connection stability. Figure 2 shows a gain balance calibration of the x-direction. First, the calibration pulse is sent from the channel Y+

Content from this work may be used under the terms of the CC BY 3.0 licence (© 2019). Any distribution of this work must maintain attribution to the author(s), title of the work, publisher, and DOI

CALIBRATION OF THE BEAM ENERGY POSITION MONITOR SYSTEM FOR THE RIKEN SUPERCONDUCTING ACCELERATION CAVITY

T. Watanabe*, H. Imao, O. Kamigaito, N. Sakamoto, N. Fukunishi,
M. Fujimaki, K. Yamada, Y. Watanabe, RIKEN, Wako, Japan
T. Toyama, T. Miyao, KEK/J-PARC, Tokai, Japan
A. Miura, JAEA/J-PARC, Tokai, Japan

K. Hanamura, T. Kawachi, Mitsubishi Electric System & Service Co., Ltd., Tokai, Japan
R. Koyama, SHI Accelerator Service Ltd., Wako, Japan
A. Kamoshida, National Instruments Japan Corporation, Tokyo, Japan

Abstract

Upgrades for the RIKEN Heavy-ion Linac that involve a new Superconducting Linac are currently underway to promote super-heavy element searches and radioactive isotope (RI) production of astatine (^{211}At) for medical use. We have developed a beam energy position monitor (BEPM) system that can simultaneously measure not only the beam position but also the beam energy by measuring the time of flight of the beam. By using parabolic-shaped electrodes, we realized the ideal linear response of the quadrupole moments while maintaining good linear position sensitivity. We fabricated 11 BEPMs and the position calibration system employing a wire method that we used to obtain the sensitivity and offset of the BEPMs. Here, we present details concerning the BEPM system, calibration system, and measured results.

INTRODUCTION

Nihonium is a synthetic super-heavy element that was discovered at RIKEN and is the first such element named by Japan. We aim to search for even heavier synthetic elements by using the upgraded Superconducting Linac (SRILAC) at the RIKEN RI Beam Factory (RIBF). Furthermore, the short-lived radio isotope ^{211}At , which emits α particles, attracts a lot of attention as a strong candidate for use in cancer therapy. Recently, ^{211}At has been produced by using an α -beam accelerated by the Azimuthally Varying Field (AVF) cyclotron at RIKEN [1, 2]. The production rate of ^{211}At increases with the energy of the α -beam when the beam energy exceeds 22 MeV/u. However, production of polonium (^{210}Po), which is very toxic to humans, starts to increase after the beam energy is raised above 30 MeV/u. Therefore, measuring and controlling the α -beam energy are crucially important. An absolute accuracy of the beam energy measurement better than 0.1% should be achieved.

Destructive monitors generate outgassing; if they are used, it becomes difficult to maintain the Q value and surface resistance required to monitor the performance of the superconducting radio frequency (SRF) cavities over a long period of time. It is therefore crucial to develop nondestructive beam measurement diagnostics. With the aim to measure the beam position to an accuracy of ± 0.1 mm overall, a calibration measurement was performed at the KEK campus in Tokai.

* wtamaki@riken.jp

BEAM ENERGY AND POSITION MONITOR

The RIKEN Heavy-ion Linac (RILAC) at the present facility, and the beam transport lines and the SRILAC, which are under construction, are shown in Fig. 1. Heavy-ion beams accelerated by the SRILAC are used by the GAs-filled Recoil Ion Separator (GARIS III) to search for super-heavy elements and to produce radioisotopes for medical use. If further acceleration is necessary, the beams are transported to the rear stage Riken Ring Cyclotron (RRC).

Here, depending on the installation location, 3 types of BEPM (Types I, II, and III) were designed and 11 BEPMs were fabricated [3] by Toyama Co., Ltd. [4]. BEPMs are installed in the center of the quadrupole magnets (Fig. 1), which are located between the SRF cavities. Photographs of the 3 types of BEPMs and a cross section of a BEPM are shown in Fig. 2, and the mechanical dimensions of each type of BEPM are summarized in Table 1.

By using a parabolic cut, the ideal linear response of the quadrupole moments is realized while maintaining a good linear position sensitivity [5]. The shape of an electrode is represented by $y = (L/2) \cos 2\theta$, where θ is the angle in cylindrical coordinate system, y is the longitudinal axis, and L is the length of the electrode. During electrode processing, a mill cuts the end of the cylinder perpendicularly. Consequently, the edge plane of the electrode maintains a

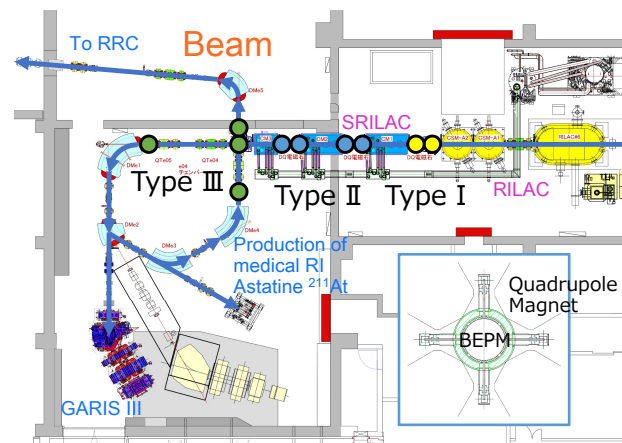


Figure 1: Schematic drawing of the RIKEN Heavy-ion Linac (RILAC), the upgraded Superconducting Linac (SRILAC), and the installation locations of the 3 types of BEPM.

DESIGN AND SIMULATION OF A CAVITY BPM FOR HUST PROTON THERAPY FACILITY*

J.Q. Li, K.J. Fan†, Q.S Chen, Kai Tang, P. Tian,

State Key Laboratory of Advanced Electromagnetic Engineering and Technology,
 School of Electrical and Electronic Engineering, Huazhong University of Science and Technology,
 Wuhan 430074, China

Abstract

In a proton therapy facility, non-destructive beam diagnostic devices are essential for the promise of precise beam dose to a patient during treatment. A high dynamic range of beam intensity, which varies from the order of nano-ampere to micro-ampere, is required to meet the clinical requirement. However, it creates challenges to the design of non-destructive beam diagnostics system particularly for the extremely weak beam current. A cavity-type beam position monitor (BPM) device is being developed for the Huazhong University of Science and Technology Proton Therapy Facility (HUST-PTF), which has the advantage of high shunt impedance and can induce sufficient diagnostic signal. The device consists of three cavities, a reference cavity and two position-cavities placed orthogonally. Both CST Microwave Studio and Particle Studio are used to achieve an optimum design.

INTRODUCTION

With more and more success of proton therapy reported, attention to proton therapy has dramatically increased in recent years. Compared with traditional radiation therapy, proton therapy shows a clear advantage of improving clinical outcomes for cancer patients because of the Bragg peak of proton dose distribution [1]. A dedicated cyclotron based proton therapy facility, Huazhong University of Science and Technology Proton Therapy Facility (HUST-PTF), is being developed [2]. As shown in Fig.1, it mainly consists of a 250MeV superconducting cyclotron, an energy selection system, one fixed treatment room, two rotatable gantries, and the corresponding transport lines.

An energy degrader and selection system must be employed to obtain variable energy beams from the cyclotron for treatment, which reduces the beam intensity remarkably. Tab.1 shows the key beam parameters after the energy selection system. In order to ensure the precise dose delivery to the tumor volume, high sensitive BPMs are needed to monitor the beam accurately while it is being delivered to the patient. Currently, the ionization chambers are widely used to monitor the beam position with such low intensity. However, excessive ionization chambers in the beamline will cause beam scattering

* Work supported by national key R&D program, 2016YFC0105303

† kjfan@hust.edu.cn.

leading to worse beam quality. Non-destructive beam diagnostics with high sensitivity are preferable in such cases to avoid deteriorating the beam performance.

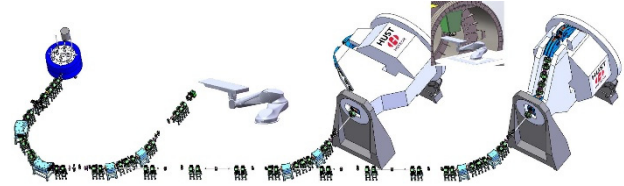


Figure 1: Layout of HUST-PTF.

A cavity-BPM device with the capability of monitoring the feeble proton beam is being developed, which consists of one reference-cavity and two position-cavities placed orthogonally. The reference-cavity is used to measure the charge-dependent signal to normalize the position signal, and the two orthogonal positioned cavities are used to measure the transverse beam position directly.

Table 1: Beam Parameters After a Degradier

Parameters	Value
Bunch length	~200mm
Bunch frequency	73MHz
Bunch radius	2-10mm
Beam energy	70-230MeV
Average current	0.4-4nA

THEORETICAL BASIS

When a bunch passes through a cavity, a series of eigenmodes will be excited, which can be extracted by a coupler. The output signal is given by [3]:

$$V_0 = \frac{1}{2} q \omega \sqrt{\frac{Z}{Q_{ext}}} (R/Q) \exp\left(-\frac{\omega^2 \sigma_z^2}{2c^2}\right)$$

(1)

where q is the bunch charge, ω is the working mode frequency, Z is the impedance of the detector, R is the shunt impedance, Q is the quality factor of the cavity itself, Q_{ext} is an external quality factor, c is the speed of light and σ_z is the bunch length. In case of multiple bunches, if the signal decay time τ of a single bunch is

BEAM COMMISSIONING OF BEAM POSITION AND PHASE MONITORS FOR LIPAc*

I. Podadera[†], D. Gavela, A. Guirao, D. Jiménez-Rey, L. M. Martínez,
J. Molla, C. Oliver, R. Varela, V. Villamayor, CIEMAT, Madrid, Spain
P. Cara, IFMIF/EVEDA Project team, Rokkasho, Japan
Y. Carin, H. Dzitko, D. Gex, A. Jokinen, A. Marqueta,
I. Moya, F. Scantamburlo, Fusion for Energy, Garching, Germany
T. Akagi, K. Kondo, Y. Shimosaki, T. Shinya, M. Sugimoto, QST, Rokkasho, Japan
A. Rodríguez, ESS Bilbao, Zamudio, Spain
L. Bellan, M. Comunian, F. Grespan, INFN Legnaro, Italy

Abstract

The LIPAc accelerator is 9-MeV, 125-mA CW deuteron accelerator that aims to validate the technology that will be used in the future IFMIF accelerator (40-MeV, 2×125 -mA CW). LIPAc is presently under beam commissioning of the second acceleration stage (injector and Radio Frequency Quadrupole) at 5 MeV. In this stage two types of BPM's are used: four stripline-type to control the transverse position and phase at the Medium Energy Beam Transport line (MEBT), and three other stripline-type mainly for the precise measurements of the mean beam energy at the Diagnostics Plate. All the BPM's have been successfully tested and served to increase the duty cycle and the average power of the beam delivered down to the beam dump. Moreover, the BPM's were key devices for the transverse beam positioning and longitudinal beam tuning and validation of the RFQ and re-buncher cavities at the MEBT.

INTRODUCTION

Beam position and phase monitors have been used during the beam commissioning of the 5 MeV and 125 mA pulsed deuteron beam in LIPAc for beam transport and characterization. This is the first stage towards the goal of achieving an average power of 625 kW up to LIPAc's final energy of 9 MeV once the superconducting accelerator is installed later on. Now, the beam from the ion source is accelerated from the low energy ion source by a RadioFrequency Quadrupole and then transported by a Medium Energy Beam Transport Line down to a Low Power Beam Dump, able to sustain up to 0.1% of the nominal deuteron current. The BPM's have been used both to measure the transverse position of the bunch centroid and the longitudinal one, by measuring the phase of the bunches with respect to an absolute reference and is fulfilling the beam dynamics requirements.

INSTALLATION

Pickups

Firstly, the vacuum chambers of the Beam Position Monitors were positioned in their mechanical supports at the

beamline (Fig. 1). Each pickup was aligned to the general coordinate frame of the accelerator with an accuracy lower than $150 \mu\text{m}$ [1]. To obtain this accuracy several reflector holders for laser tracker alignment were used in each pickup. The position of each holder was previously referenced to the mechanical center of each pickup in a CMM and the values obtained were used. Once the BPM's were perfectly aligned, they were tightened to the other components and vacuum leak tests were performed to ensure the goodness of the vacuum connection and the status of the vacuum chamber.

Cabling

The connection between the electrodes and the acquisition electronics was performed using several types of coaxial cables: 1) Flexible coaxial cables to connect the electrodes to a patch panel aside the beamline. 2) Low losses cables for the long connections between the accelerator vault and the electronics cabinet. In this case, low losses RFS cable with double shielding has been used, with attenuation of less than 3 dB each 100 m.

To minimize the effect of the RF noises and imbalances between each channel, several mitigation measures were carried out: 1) Low losses cables were used for the big distance cables, 2) Cabinets with high EMC shielding (up to 60 dB below 1 GHz) and 3) Long cables were phase matched down to 1° by adjusting the cable length for the bunch of four cables in each BPM using Time Domain Reflectometry to each cable.

In parallel, the status of the cabling and pickup was finally checked by analyzing the coupling measurement between the electrodes and the measurements at the test bench using a vector network analyzer.

ACQUISITION ELECTRONICS

As further explained in [2], the acquisition electronics is based in two main components: 1) an analog front-end (AFE) which conditions the RF signal coming from the BPM electrodes, and 2) a digital board which provides a fast digital treatment of the signal and communicates with the control system. The system uses an analog front-end to house the system calibration switches and an intermediate frequency stage, plus ancillary boards such as timing and clock distribution, on CompactPCI. As such, all parameters

* Work partially supported by the Spanish Ministry of Economy and Competitiveness under project AIC-A-2011-0654 and FIS2013-40860-R

[†] ivan.podadera@ciemat.es

A REPORT ON DEVELOPMENTS OF THE BCM AND BPM PICKUPS OF THE ESS MEBT

S. Varnasseri, I. Bustinduy, A. Ortega, I. Rueda, A. Zugazaga, A. Conde, J. Martin
ESS-Bilbao, Bilbao, Spain
R.A. Baron, H. Hassanzadegan, T. Shea
European Spallation Source - ERIC, Lund, Sweden

Abstract

In the framework of the Spanish In-Kind Contribution (IKC) to the construction of the European Spallation Source (ESS-ERIC), ESS-Bilbao is in charge of providing some key systems for the accelerator. In this paper, design and pre-delivery measurements of two non-interceptive devices of Medium Energy Beam Transport (MEBT) (e.g. Beam Position Monitor pick-ups, shielded ACCT and FCT) are reported. Overall there are eight (8) BPMs distributed in MEBT, seven (7) of them are used for the beam position and phase measurements and one BPM is used for the fast timing characterization. The latter is used mainly to characterize the partially chopped bunches and rise/fall time of the Beam Chopper. Furthermore, there are two ACCTs, one just attached to the beam dump and the other at the end of the MEBT. One FCT combined with the second ACCT gives the complementary information on the fast timing characteristics of the beam pulses.

INTRODUCTION

ESS MEBT (Medium Energy Beam Transport) with energy of 3.62 MeV is part of the European Spallation Source (ESS) which is delivered recently and to be operational at Lund, Sweden early 2020 [1]. In order to monitor and characterize the beam parameters, various beam diagnostics instruments including the position, phase and intensity measurement devices have been incorporated in the MEBT. In this paper, the developments of stripline beam position monitors (BPM) and beam current transformers are reported. The processing frequency for the BPM readout is the 2nd harmonic of RF frequency. Furthermore, the bunch length (rms) varies from 60 ps to 180 ps during its passage across MEBT, which introduces slightly varied signal amplitudes on BPM pick-ups. Table 1 shows the related beam parameters of the MEBT.

Table 1: MEBT Various Beam Parameters

Parameter	Value	Unit
Beam energy	3.62	MeV
Beam current (avg.)	62.5	mA
Particles/bunch	$1.1e9$	
Readout frequency	704	MHz
RF frequency	352	MHz
Bunch length (σ_z)	60-180	ps
Pulse length (max.)	2.86	ms
Repetition rate	14	Hz

There are eleven (11) quadrupole magnets within the MEBT, eight (8) of them housing BPM pick-ups inside.

Thus, the main mechanical restriction for the BPMs was the quadrupole magnets yoke profile and overall spaces, including the space for the BPM feedthroughs. BPMs are designed and installed in eight out of eleven quadrupole magnets of the MEBT. Seven of the BPMs are used for the beam position and phase measurements and one of them is used for the fast timing characterization of the beam. It is specifically used for the beam chopper rise/fall time measurements.

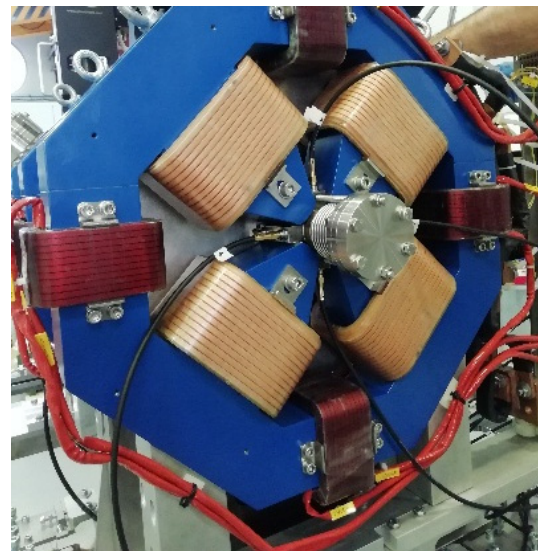


Figure 1: A BPM installed inside quadrupole before integration into the MEBT.

For the beam current with slow and fast timing characteristics, two ACCTs and one FCT are installed in the MEBT. Due to mechanical space limitations, the FCT is combined with one ACCT and located at the end of the MEBT.

BPM DESIGN

Electromagnetic design and various choices of the BPMs are explained in a previous paper [2]. Each BPM has four pick-ups, one pair in horizontal and one pair in vertical planes. The BPM pick-ups are of stripline type which are embedded inside quadrupole magnets (see Fig. 1). The main reason is due to lack of mechanical space within compact MEBT to install the BPMs in the dedicated spaces outside magnets [3,4]. The BPM sensitivity to displacement, voltage signal level, frequency response, impedance matching, and mechanical restrictions are the main factors in the design of stripline. The 3D models of several types including button type, short-end stripline and matched stripline are analyzed for low- β beam (see Fig. 2).

ESS BEAM POSITION AND PHASE MONITOR SYSTEM

R. A. Baron, H. Hassanzadegan, T.J. Shea, A. Jansson, H. Kocevar, K.E. Rosengren, European Spallation Source - ESS, Lund, Sweden

I. Bustinduy, S. Varnasseri, ESS-Bilbao, Bilbao, Spain

S. Vilcins, D. Lipka, Deutsches Elektronen-Synchrotron - DESY, Hamburg, Germany

T. Gräber - Deutsches Elektronen-Synchrotron - DESY, Zeuthen, Germany

M. Poggi, F. Grespan, Istituto Nazionale di Fisica Nucleare – INFN, Legnano, Italy

Abstract

The European Spallation Source (ESS) is a neutron facility under construction in Lund, Sweden, and established as a European collaboration between different member countries. The machine is a 2 GeV proton LINAC with a nominal beam current of 62.5 mA, 2.86 ms of pulse length and a bunch repetition rate of 352 MHz. The Beam Position and Phase Monitors (BPM) at ESS were designed to satisfy the specifications for the different beam modes, which span from 5 μ s pulse length and 6.3 mA beam until the nominal beam condition. The system is designed for standard beam position measurements for beam trajectory correction and for beam phase measurements for cavity phase tuning, imposing restrictions on the sensor design and electronics architecture. Approximately a hundred BPM's were manufactured and are being installed by partners in collaboration with ESS. The BPM system comprises a MicroTCA.4 electronics based in COTS AMC and RTM modules with custom FPGA firmware implementation and a custom Front-End electronics. In this work, the system architecture, implementation, and test results are presented and discussed.

INTRODUCTION

The ESS beam position monitor system is an RF receiver system based on a superheterodyne architecture with high speed IF sampling designed for improved RF phase measurements.

Table 1: ESS BPM system specifications. The precision numbers are provided with the bandwidth specified in the table.

Parameter	Value
Phase precision for nominal beam	0.2 °
Phase accuracy for 6.3 mA beam / 5 us pulse length	+/- 2 °
Phase precision for 6.3 mA beam / 5 us pulse length	2 °
Phase stability over 8 hours for nominal beam	+/- 1°
Beam position precision for nominal beam	20 μ m
Position accuracy at 6.3 mA / 5 us pulse length	+/- 400 μ m
Position precision at 6.3 mA / 5 us pulse length	200 μ m
Position accuracy stability over 8 hours	1 mm
Phase and Position bandwidth	1 MHz

The ESS BPM system is composed by approximately 100 BPM stripline and button BPM sensors which were designed in a collaboration between ESS beam diagnostics team and collaborations across several European institutes.

RF phase measurements are most stringent than amplitude measurements in the ESS BPM system and a phase stable reference line is distributed along the accelerator for both BPM and LLRF systems. The RF phase of the signals excited to the BPM sensors are compared to the phase of the reference line to provide the user with phase measurements on each BPM relative to the phase of the reference line. The specifications for the ESS BPM system is shown on Table 1.

ESS BPM System Architecture

The BPM signals are transmitted through cables ranging from 20-80 meters, from the sensor to the electronics, and are bundled together along its extension with the reference RF cables. The receiver channels are digitized separately and phase and amplitudes are measured independently in the digital domain. Comparison of the digitized phase and amplitudes are performed in the FPGA firmware to provide the user with beam X and Y positions and relative phases between BPM sensor inputs and the reference signal.

Near-IQ is used on the BPM receiver with an IF/CLK ratio of 4/15 providing a bandwidth of approximately 11.7 MHz around the IF without having nonlinear higher order frequency components lying within the first Nyquist zone of the digitized signal [1].

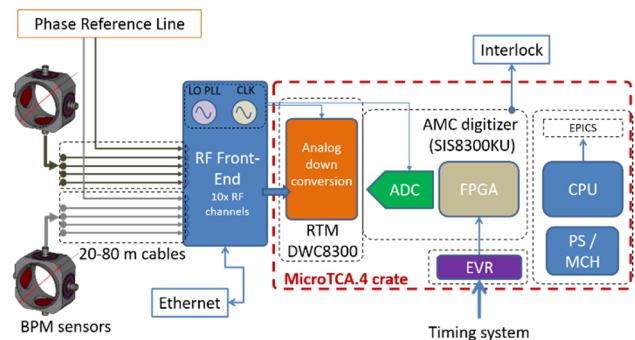


Figure 1: BPM system block diagram.

Every pair of BPM sensors are digitized in the same digitizer board as shown in Fig. 1, allowing strong noise correlation between channels and also improved relative thermal drifts between pairs of BPM's. The ESS BPM

Any distribution of this work must maintain attribution to the author(s), title of the work, publisher, and DOI

REAL-TIME SYNCHRONIZED CALIBRATION AND COMPUTING SYSTEM WITH EPICS BASED DISTRIBUTED CONTROLS IN THE TPS XBPM SYSTEM

J. Y. Chuang[†], Y. M. Hsiao, Y. Z. Lin, Y. C. Liu, Y. T. Cheng, C. Shueh, C. M. Cheng, Y. C. Yang, C. C. Chang, C. K. Chan, National Synchrotron Radiation Research Center, Hsinchu, Taiwan

Abstract

In synchrotron facilities, X-ray beam position monitor (XBPM) is an important detector for photon beam position monitoring and must be calibrated to ensure reliability and precision. However, light source operating conditions, such as beam orbit, injection and insertion device parameters, etc., can influence the sensitivity and specific weighting of photoemission current from the XBPM diamond blades. In the Taiwan Photon Source (TPS), Experimental Physics and Industrial Control System (EPICS) was utilized to implant an automatic calibration process. By using EPICS, we can ensure a seamless integration between the different front ends (FEs) and direct all data stream into a centralized server, creating a distributed XBPM calibration system. The XBPM performance indicators are analyzed to evaluate the validity of calibration parameters by input/output controller (IOC) in each FE computing system. This paper will discuss the benefits of implanting this distributed control system into a working environment such as the TPS.

INTRODUCTION

The XBPM is obviously a standardized diagnostic sensor for orbit feedback or beam alignment [1, 2]. However, due to the blade-type design and the measurement object being a photon beam, calibration must be done more frequently than for other commercial sensors such as temperature or pressure sensors, etc. Many studies have shown that the accuracy of an XBPM is greatly affected by the conditions of synchrotron radiation operation [3, 4]. According to these studies, we define the XBPM as a time-varying system with varying responses to different light source conditions. In order to prove this concept and optimize the performance of XBPMs, we describe in this study the development of an XBPM dedicated control system. Considering of the TPS is composed of 48 segments, each with a FE. This generates a large system control issue and a real-time synchronized XBPM calibration process to perform rapid and remote scanning becomes desirable. This system is required to determine all XBPM coefficient calibrations and data analysis. The XBPM system should be able to provide high precision and reliable beam position information for a number of applications which is the main purpose to develop this control system.

THE XBPM SCANNING CONTROL SYSTEM

The XBPM scanning control system consists of a two-dimensional translation stage to move the XBPM along the

X and Y-axis. The signals from the four-diamond blades transmit photoemission current signals by standard 50-ohm coaxial cables to the data acquisition Libera photon controller which calculates the X and Y positions to be published as process variables (PVs) by the EPICS on the TPS instrument control intranet [5]. The control software which is programmed with the LabVIEW object-oriented software will be described in this section.

Programming Method

Considering program flexibility, the architecture utilizes the queue message handler (QMH) structure which is composed of event-triggered producer-consumer, state machine and functional global variables (FGV). The advantages are easy maintenance and readability as well as high expandability and supporting multiplex executions. Parameters, which need to be matched with corresponding states, are triggered by the event handling loop and are passed to the "Message Handling Loop" by the queue method for physical actions.

After the XBPM calibration process in the QMH architecture is completed, the authenticity and independence of data transfer requires that all instruments and devices, which are used in this process, must be classified and encapsulated. Each instrument must follow the required rules in three steps: open (initialize), configuration, read/write and close. Encapsulating the motor control parameters of the translation stage into an object and its reference, established during the "Open" process, is transferred by the shift register in the main program architecture. Thereafter, the reference from the shift register is updated when activating the "Read/Write" status. In order to make the calibration process simpler, each axis is used separately. The axis control parameters of each axis are encapsulated in the cluster which can be regarded as a "Struct" in C++ and then placed in an array. When operating a specific axis, only an element in the array changes the parameters to make it more convenient to use, as shown in Fig. 1.

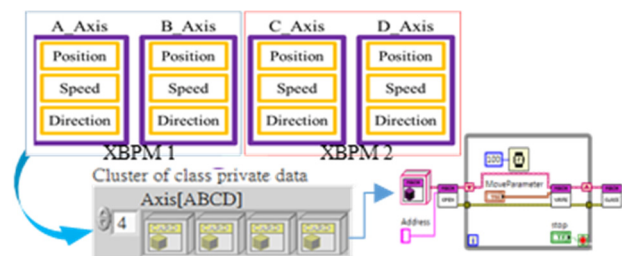


Figure 1: Encapsulating the axis control parameters in the clusters.

CURRENT MONITOR AND BEAM POSITION MONITOR PERFORMANCE FOR HIGH CHARGE OPERATION OF THE ADVANCED PHOTON SOURCE PARTICLE ACCUMULATOR RING*

A. R. Brill[†], J. R. Calvey, K. C. Harkay, R. T. Keane, N. Sereno, U. Wienands, K. P. Wootton, C. Yao
Argonne National Laboratory, Lemont, IL 60439, USA

Abstract

A design choice for the Advanced Photon Source Upgrade (APS-U) to inject into the storage ring using bunch swap out rather than off-axis accumulation means that the Advanced Photon Source (APS) injectors are required to accelerate much higher electron bunch charge than originally designed. In the present work, we outline upgrades to the current monitor and beam position monitor (bpm) diagnostics for the Particle Accumulator Ring (PAR) to accommodate bunch charges of 1-20 nC. Through experiments, we compare and characterize the system responses over the range of bunch charge.

INTRODUCTION

The APS injector consists of a linac, PAR, and booster synchrotron. The linac provides a series of 1-nC bunches at a 30-Hz repetition rate. The pulses are accumulated and damped in the PAR at the fundamental rf frequency. Approximately 230 ms before extraction, the single bunch is captured in a 12th harmonic rf system which further compresses the bunch. The APS injector was originally designed to provide a maximum bunch charge of 6 nC at a 2-Hz extraction rate.

The APS-U design requires on-axis injection to meet emittance performance goals. For APS-U, on-axis injection will be implemented using a swap-out scheme. In swap-out injection, the injectors are required to produce enough single-bunch charge to perform a complete bunch replacement. Swap-out places high demands on the injector bunch charge. For APS-U timing mode operations, the PAR will be required to provide 20 nC in a single bunch [1], which exceeds the original design parameters of the PAR by a factor of greater than three.

Operating at the default accumulation period of 0.5 s, the PAR is limited to providing approximately 10 nC per bunch. To provide up to 20 nC of charge, the injector cycle must be extended to at least 1 s allow sufficient time to accumulate and compress the required linac bunches [2].

CURRENT MONITOR PERFORMANCE

Several techniques have been used to measure the amount of charge in the PAR. The combination of high revolution rate and wide range of signal levels used in the PAR present unique challenges for measuring the stored beam charge.

One option is to use the sum signal from the bpm electronics. Another option is to use the installed integrating current transformer (ICT). Each method has its own advantages and disadvantages.

Beam Position Monitor Sum

The simplest method of observing the PAR charge is to use the sum signal of one of sixteen 352-MHz stripline bpps to calculate the estimated charge present. By comparing the the readings of the linac-to-PAR (LTP) and PAR-to-booster (PTB) current transformers, the amount of charge in the PAR can be determined. By applying a calibration factor to the sum signal, a reasonable estimate of charge is calculated. There are some important limitations of this method. As the stored charge increases well beyond the initial design parameters, the sum signal from the bpm electronics begin to saturate, providing nonlinear results if the input signal is not sufficiently attenuated. The bpm sum signal also varies inversely with bunch length throughout the cycle, limiting the useful range of this measurement.

Integrating Current Transformer

An ICT produces an output signal that is very linear with charge but almost independent of the input bunch duration [3]. The original beam current monitor electronics were implemented with a gated integrator to measure the ICT pulse. However, due to the 9.78-MHz repetition rate and changes in bunch length and beam phase through the injection cycle, the gated integrator proved to provide unreliable readings. The gated integrator electronics were replaced with an FPGA-based data acquisition system around 2008 [4]. Using interleaved sampling, the FPGA processor digitizes the output waveform of the ICT to calculate the rms values in 10 user-defined time windows throughout the injection cycle. With these windows, injection efficiency can be observed in stages throughout the accumulation, damping, and harmonic capture portions of the PAR injection cycle.

A drawback of using an ICT in the PAR is that as the repetition rate of the input to an ICT increases, the baseline of the output waveform shifts. The baseline shift between a 1-MHz repetition rate and the PAR repetition rate is shown in Fig. 1. After subtracting the baseline offset, the shape of the waveform is almost identical. To evaluate the linearity of the ICT response through charge levels greater than 20 nC at the PAR repetition rate, the measured charge plotted in Fig. 2 is calculated using different methods, with baseline subtraction as the preferred method.

* Work supported by U.S. Department of Energy, Office of Science, Office of Basic Energy Sciences, under Contract No. DE-AC02-06CH11357.

[†] abrill@anl.gov

THz GENERATION BY OPTICAL RECTIFICATION FOR A NOVEL SHOT TO SHOT SYNCHRONIZATION SYSTEM BETWEEN ELECTRON BUNCHES AND FEMTOSECOND LASER PULSES IN A PLASMA WAKEFIELD ACCELERATOR*

S. Mattiello[†], A. Penirschke, Technische Hochschule Mittelhessen, Friedberg, Germany
H. Schlarb, DESY, Hamburg, Germany

Abstract

We investigate the influence of the optical properties and of the theoretical description of the THz generation on the conversion efficiency of the generation of short THz pulses. The application is a feedback system for SINBAD with a time resolution of less than 1 fs for the synchronization of the electron bunch and of the plasma wake field in a laser driven plasma particle accelerator. Here stable THz pulses are generated by optical rectification of a fraction of the plasma generating high energy laser pulses in a nonlinear lithium niobate crystal. Then the generated THz pulses will energy modulate the electron bunches shot to shot before the plasma to achieve the required time resolution. In this contribution we compare different approximations for the modeling of the generation dynamics using second order or first order equations as well as considering pump depletion effects. Additionally, the dependence of the efficiency of the THz generation on the choice of the dielectric function has been investigated.

INTRODUCTION

Achieving new discoveries, e.g. the Higgs boson or the strong interacting Quark Gluon Plasma, or cancer treatment with the high-energy particle beams are two of several application fields of particle accelerators. Because of their extremely large accelerating electric fields [1], plasma-based particle accelerators driven by laser beam can overcome the limit of the standard accelerators given by the physical-chemical properties of the material used for the construction as well as by the huge size and the financial costs. In fact, the acceleration gradients of conventional linear accelerators are limited to 10 MVm^{-1} [2], whereas for laser-driven particle accelerators values in the order of 1 TVm^{-1} can be achieved. Nevertheless, the period of the fields in this method known as plasma wakefield acceleration (PWA) is in the range of 10 fs. Consequently, an optimal acceleration requires stable synchronization of the electron bunch and of the plasma wakefield in the range of few femtoseconds.

For this purpose, we are developing a new shot to shot feedback system for SINBAD with a time resolution of less than 1 fs. We plan to generate stable THz pulses by optical rectification of a fraction of the plasma generating high energy laser pulses in a periodically poled lithium niobate

crystal (LiNbO_3) (PPLN). These pulses allow to energy modulate the electron bunches shot to shot before the plasma in order to achieve the time resolution [3].

This paper focuses on the generation of THz pulses. We present our investigation of the influence of the optical properties as well as the theoretical description of the THz generation on the conversion efficiency as well on the optimum crystal length for the generation length of short THz pulses.

The paper is organized as follows. First, we derive the general equations for the description of the THz generation and then we introduce two different methods in order to include the effects of the laser pump on the crystal. Therefore we compare the corresponding results for the efficiency as well as for optimum crystal length of the THz generation. The conclusions finalize this work.

MODELING THE THz GENERATION

Starting from the Maxwell equations the following one dimensional system of coupled differential equations for the laser pulse $E_L(\omega_L, z) = A_L(\omega_L)e^{-ik(\omega_L)z}$ and for the THz wave $E_T(\omega_T, z) = A_T(\omega_T)e^{-ik(\omega_T)z}$

$$\left(\frac{\partial^2}{\partial z^2} + \frac{\omega_T^2}{c^2} \varepsilon(\omega_T) \right) E_T(\omega_T, z) = G_T(\omega_T, \omega_L, z) \quad (1)$$

$$\left(\frac{\partial^2}{\partial z^2} + \frac{\omega_L^2}{c^2} \varepsilon(\omega_L) \right) E_L(\omega_L, z) = G_L(\omega_L, \omega_T, z), \quad (2)$$

can be derived [4–7]. Here $\varepsilon(\omega)$ denotes the generalized (complex) dielectric function and the inhomogeneous term G_L and G_T are related to the nonlinear polarizations in the optical and THz frequency range respectively.

A simplification for this system is the slope varying approximation (SVA), where the second spatial derivatives of the amplitudes A_m with $m \in L, T$ are neglected. This approach is used in almost all investigations [4, 8–10] and leads to coupled system of linear differential of the first order,

$$\left(\frac{\partial}{\partial z} + \frac{\alpha_m(\omega_m)}{2} \right) A_m(\omega_m, z) = G_m^{\text{SVA}}(\omega_T, \omega_L, z) \quad (3)$$

where α_m indicates the adsorption coefficient in the optical ($m = L$) and in the THz range ($m = T$) respectively and the inhomogeneous terms become [11]

$$G_m^{\text{SVA}} = iG_m \frac{e^{ik(\omega_m)z}}{2k(\omega_m)}. \quad (4)$$

The assumption $G_L = 0$ leads to the decoupling of the system and only Eq. (1) or Eq. (3) with $m = T$ has to be

* The work of S. Mattiello is supported by the German Federal Ministry of Education and Research (BMBF) under contract no. 05K16ROA.

[†] stefano.mattiello@iem.thm.de

CONCEPT OF A NOVEL HIGH-BANDWIDTH ARRIVAL TIME MONITOR FOR VERY LOW CHARGES AS A PART OF THE ALL-OPTICAL SYNCHRONIZATION SYSTEM AT ELBE*

A. Penirschke[†], Technische Hochschule Mittelhessen (THM), Friedberg, Germany
M. K. Czwalinna, H. Schlarb, Deutsches Elektronen-Synchrotron (DESY), Hamburg, Germany
M. Kuntzsch, Helmholtz-Zentrum Dresden-Rossendorf (HZDR), Dresden, Germany
W. Ackermann, Technische Universität Darmstadt, Darmstadt, Germany

Abstract

Numerous advanced applications of X-ray free-electron lasers require pulse durations and time resolutions in the order of only a few femtoseconds or better. The generation of these pulses to be used in time-resolved experiments require synchronization techniques that can simultaneously lock all necessary components to a precision in the range of a few fs only. The CW operated electron accelerator ELBE at the Helmholtz-Zentrum Dresden-Rossendorf uses an all-optical synchronization system to ensure a timing stability on the 10-fs scale of the reference signal.

ELBE requires a minimum beam pipe diameter of 43mm that limits the achievable output voltage of the pickup structure to drive the attached electro-optical modulator.

This contribution presents a concept for a novel high-bandwidth arrival time monitor with sufficient output signal for the attached EOMs for very low charges as a part of the all-optical synchronization system at ELBE.

INTRODUCTION

In order to investigate dynamical processes down to the femtosecond time scale, free electron lasers (FELs) are conducted to deliver ultrashort x-ray pulses for pump-probe experiments [1,2]. These time-resolved measurements require synchronization between an external pumping laser and the FEL pulse for probing lower than the pulse duration, i.e., a few femtoseconds. The FEL pulse timing can be determined by high-resolution arrival-time measurements of electron bunches at the undulators [3].

In recent years, the interest for ultrashort x-ray pulses is continuously rising which requires for the accelerator an ultra-low bunch charge operation down to a few pC only [4,5]. Different schemes for bunch arrival time measurements have been implemented so far allowing for single-shot detection with a resolution of a few fs and below [6-10].

At the free-electron lasers European XFEL and FLASH in Hamburg, pickup-based bunch arrival-time monitors (BAM) with electro-optical detection schemes have been implemented.

As part of a laser-based synchronization system, bunch arrival-time monitors (BAMs) measure the arrival time with a sub-10 fs time resolution for bunch charges higher

than 500 pC [11]. A beam-induced signal modulates the amplitude of an external laser pulse in a Mach-Zehnder type electro-optic modulator (EOM). This laser pulse is delivered through a stabilized optical fiber link with a drift stability of around 10 fs per day. Thus, as a direct client of this highly stable optical reference, the current BAM, based on standard telecom EOMs at 1550 nm has an intrinsic low drift feature, in addition to the high resolution. The reference timing is the zero crossing of the pickup signal, where the sampling laser pulse has no modulation. The EOM DC bias is chosen in such a way that without an external RF modulation the amplitude of the sampling laser pulses is halved. Any deviation from the zero crossing of the pickup transient, i.e. bunch arrival-time jitter, results in an amplitude modulation of the reference laser pulse. With a proper calibration with a precession delay line, this amplitude modulation is directly converted to arrival-time information with a dynamic range corresponding to the linear part of the pickup slope. More details are given in [11-12]. The slope steepness at the zero crossing defines the modulation voltage which the laser pulse experiences in the presence of an arrival-time jitter. This determines the time resolution as well as the sensitivity of the BAMs. The slope steepness reduces proportionally with the bunch charge leading to a BAM performance degradation for charges lower than 200 pC [3,13].

The cone shaped pickups are part of the synchronization systems at European XFEL, FLASH and ELBE (Helmholtz-Zentrum Dresden- Rossendorf) [14-16].

The first facility-wide evaluation of the optical synchronization system at the European XFEL demonstrated a performance of the optical synchronization infrastructure on the single-digit femtosecond timescale with the existing BAMs [17].

In order to achieve a time resolution down to a few pC for a low charge operation mode, the bandwidth of the current BAMs need to be increased from 40 GHz up to 80 GHz or higher.

This paper presents a concept of an ultra-wideband pickup structure frequencies up to 80 GHz or higher with sufficient output signal for driving the attached EOMs.

CONE SHAPED PICKUP DESIGN

The RF properties of the pickup are defined by its shape, the material, the used connectors, and the cables connected to the pickup. However, the pickup shape has the largest influence on the performance of the system.

* This work is supported by the German Federal Ministry of Education and Research (BMBF) under contract no. 05K19RO1.

[†] andreas.penirschke@iem.thm.de

FIRST RESULTS ON FEMTOSECOND LEVEL PHOTOCATHODE LASER SYNCHRONIZATION AT THE SINBAD FACILITY

M. Titberidze*, M. Felber, T. Kozak, T. Lamb, J. Müller, H. Schlarb, S. Schulz, F. Zummack
Deutsches Elektronen-Synchrotron (DESY), Hamburg, Germany
C. Sydlo, Paul Scherrer Institut (PSI), Villigen, Switzerland

Abstract

SINBAD, the "short-innovative bunches and accelerators at DESY" is an accelerator research and development facility which will host various experiments. SINBAD-ARES linac is a conventional S-band linear accelerator which will be capable of producing ultra-short electron bunches with duration of few femtoseconds and energy of up to 100 MeV. In order to fully utilize the potential of ultra-short electron bunches while probing the novel acceleration techniques (e.g. external injection in LWFA), it is crucial to achieve femtosecond level synchronization between photocathode laser and RF source driving the RF gun of the ARES linac. In this paper we present the first results on the synchronization of the near-infrared photocathode laser to the RF source with the residual timing jitter performance of ~ 10 fs rms. These results were obtained using a conventional laser-to-RF synchronization setup employing heterodyne detection of an RF signal generated by impinging the laser pulses to a fast photodetector. In addition, we describe an advanced laser-to-RF phase detection scheme as a future upgrade; promising even lower timing jitter and most importantly the long-term timing drift stability.

INTRODUCTION

The accelerator research experiment at sinbad (ARES) linac is a conventional S-band RF accelerator which is currently in the construction and commissioning phase [1, 2]. It consists of S-band ($f_{RF} = 2.998$ GHz) normal conducting accelerating structures: a 1.5 cell RF gun [3] and two travelling wave structures (TWS1, TWS2), capable of accelerating electron bunches up to 100 MeV energy in nominal operating mode [1, 2, 4]. The electron bunches are produced by impinging ultra-short UV laser pulses on a photocathode inside the RF gun. The ARES linac is schematically shown in Fig. 1. The final electron beam parameters at ARES are defined in [2] and require an arrival time jitter of < 10 fs rms. In order to meet this requirement it is crucial to achieve a precise laser-to-RF synchronization between the pulsed injector laser and the 2.998 GHz RF reference signal from the RF master oscillator (MO). The injector laser is a commercial system from Light Conversion¹ with a fundamental wavelength of 1030 nm and variable pulse duration of 0.16 ps to 10 ps. The laser oscillator of this system is designed such that the repetition rate of the optical pulses $f_{rep} = 83.28$ MHz is the 36th sub-harmonic of the RF

reference frequency $f_{RF} = 2.998$ GHz. The following section covers the general concept of direct conversion based laser-to-RF synchronization using heterodyne detection and presents the technical implementation as well as first measurement results.

DIRECT CONVERSION BASED LASER-TO-RF SYNCHRONIZATION

General Concept of Heterodyne Detection

One of the most common techniques to synchronize a mode-locked laser to an RF signal is using a fast photodetector [5–8]. The pulsed optical signals are converted to electrical pulses which are composed of high spectral purity harmonics of the laser repetition rate. The cutoff frequency of the RF comb is given by the bandwidth of the photodetector. The desired frequency component of the RF comb can be filtered out using an RF band-pass filter (BPF) and amplified until the signal level is sufficient for downconversion or heterodyning. The downconverted signal is digitized using an analog-to-digital converter (ADC) employing so called non-IQ sampling [5, 9, 10]. The amplitude and phase information is extracted in the digital domain. The obtained phase error information is fed back to the piezo actuator of the laser oscillator using a piezo driver to establish the phase locked loop (PLL).

There are several advantages of downconverting the photodetected signal to an intermediate frequency (IF) instead of baseband. Baseband signals are often degraded by undesired DC offsets due to imperfections of the electronics and they are highly susceptible to electromagnetic interference (EMI). Both effects limit the overall PLL performance potentially leading to a poor synchronization performance. These problems are mitigated by direct sampling the IF signal and using digital phase detection.

Fundamental Limitations

There are still fundamental limitations related to the photodetection process, such as the AM-PM effect, where optical power fluctuations are converted to phase fluctuations of each frequency component of the generated frequency comb [11, 12] while low signal levels from the photodetector together with the intrinsic thermal and shot noise sources lead to a limited signal-to-noise ratio (SNR).

One can estimate the thermal noise limited timing jitter for a 50Ω terminated photodetector using the following

* mikheil.titberidze@desy.de

¹ Pharos SP-06-200-PP

MACHINE LEARNING IMAGE PROCESSING TECHNOLOGY APPLICATION IN BUNCH LONGITUDINAL PHASE DATA INFORMATION EXTRACTION*

X.Y.Xu[†], Y.M.Zhou, Shanghai Institute of Applied Physics, CAS, Shanghai, China
also at University of Chinese Academy of Sciences, Beijing, China
Y.B.Leng[#], Shanghai Advanced Research Institute, CAS, Shanghai, China

Abstract

To achieve the bunch-by-bunch longitudinal phase measurement, Shanghai Synchrotron Radiation Facility (SSRF) has developed a high-resolution measurement system. We used this measurement system to study the injection transient process, and obtained the longitudinal phase of the refilled bunch and the longitudinal phase of the original stored bunch. A large number of parameters of the synchronous damping oscillation are included in this large amount of longitudinal phase data, which are important for the evaluation of machine state and bunch stability. The multi-turn phase data of a multi-bunch is a large two-dimensional array that can be converted into an image. The convolutional neural network (CNN) is a machine learning model with strong capabilities in image processing. We hope to use the convolutional neural network to process the longitudinal phase two-dimensional array data and extract important parameters such as the oscillation amplitude and the synchrotron damping time.

INTRODUCTION

With the enhancement of computer computing performance, machine learning technology has been greatly developed in recent years. In particular, the concept of deep learning allows us to use algorithms to deal with the complex problem with a large amount of data. Accelerator scholars have also begun to gradually apply machine learning technology to beam measurement and diagnosis, have achieved some remarkable results [1].

The development of machine learning in image processing is obvious to all, such as face recognition, automatic driving and so on. Using image processing techniques such as convolutional neural networks, we can give machines the ability to process image data. In our field of beam measurement, we collect huge amounts of data every day. These data are often stored in two-dimensional or even multi-dimensional arrays. If the two-dimensional array is restored according to the storage method of the grey value image, it can be drawn into a greyscale image. So can we use cutting-edge deep learning techniques such as multi-layer convolutional neural networks to process such data in the form of multi-dimensional arrays and extract the infor-

mation we need from it? In this regard, we made a preliminary attempt. The object we are dealing with is the electrical signal data of the BPM electrode at the instant of the accelerator injection. We hope to use this data to extract the relevant parameters of synchrotron damping oscillation when injecting transients.

The study of the injection transient is helpful for optimizing the state parameters of the injector and understanding the physical process of the fusion of the stored charge and the refilled charge during the injection [2]. Therefore, starting from 2012, the BI group of SSRF (Shanghai Synchrotron Radiation Facility) performs bunch-by-bunch phase measurement analysis, and uses phase multi-channel delay sampling technology and table look-up method to achieve phase acquisition. These phase data are fitted by gradient descent method or the fitting function library in commercial data software such as Matlab to obtain the synchronous damping oscillation parameters. The most primitive data is the BPM electrical signal obtained using a digital acquisition board. These electrical signals are stored in the form of multi-dimensional arrays. If we treat these data as multiple images and deal with it with deep learning multi-layer convolutional neural networks, we can directly extract the synchrotron damping oscillation parameters of the injection transients, which will greatly streamline the data processing process and provide a viable solution for instant online processing [3].

CONVOLUTIONAL NEURAL NETWORK

Convolutional Neural Networks (CNN) is a type of feed-forward neural network with convolutional computation and deep structure. It is one of the representative algorithms of deep learning [4-5]. Convolutional neural networks have the ability to represent learning, and can shift-invariant classification of input information according to their hierarchical structure. Therefore, it is also called "Shift-Invariant Artificial Neural Networks, SIANN" [6].

Convolutional neural networks are inspired by the visual organization of living things. Visual cortical cells receive signals from photoreceptors on the retina, but a single visual cortical cell does not receive all of the signals from the photoreceptor, but only accepts the signal from the stimulus region it dictates. Only by feeling the stimulation in the field can the neuron be activated. Multiple visual cortical cells systematically superimpose the receptive field, completely receiving signals transmitted by the retina and establishing a visual space.

*Work supported by National Natural Science Foundation of China (No.11575282) and Ten Thousand Talent Program and Chinese Academy of Sciences Key Technology Talent Program

[†]xuxingyi@sinap.ac.cn

[#]lengyongbin@sinap.ac.cn

A METHOD OF CORRECTING THE BEAM TRANSVERSE OFFSET FOR THE CAVITY BUNCH LENGTH MONITOR*

Qian Wang, Qing Luo[†], Baogen Sun[‡]

NSRL, University of Science and Technology of China, 230029 Hefei, China

Abstract

Cavity bunch length monitor uses monopole modes excited by bunches within the cavities to measure the bunch longitudinal root mean square (rms) length. It can provide a very high accuracy and high resolution. However, when the bunch passes through the cavities with transverse offset (that is, the bunch moves off the cavity axis), the amplitude of the monopole modes will change and cannot reflect the bunch length precisely. In this paper, a method of correcting the beam transverse offset is proposed. Simulation results show that the method can reduce the error of the bunch length measurement significantly.

BACKGROUND

The cavity bunch length monitor was widely used for the past few years because of its high accuracy, high resolution and nondestructive measurement [1-4].

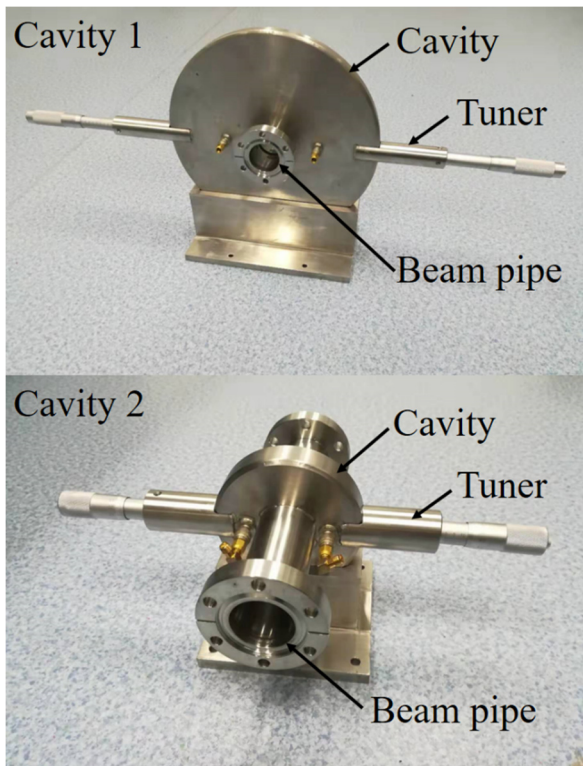


Figure 1: The cavity bunch length monitor.

When a bunch passes through the cavity, the monopole modes will be excited. At least two monopole modes in different frequencies are needed, and the bunch length σ can be obtained by solving the equation [5]

$$\sigma = \sqrt{\frac{2}{\omega_2^2 - \omega_1^2} \ln \frac{k_2 V_1}{k_1 V_2}} \quad (1)$$

Where k_1 and k_2 are constants, ω_1 and ω_2 are the working frequencies, and V_1 and V_2 are the output voltage of the two monopole modes respectively. As shown in Fig. 1, the cavity bunch length monitor in the National Synchrotron Radiation Laboratory infrared free-electron laser facility (FELiChEM) is composed of two cavities. The TM_{010} mode resonating at 0.9515 GHz in the cavity 1 and the TM_{020} mode resonating at 6.1847 GHz in the cavity 2 are used to measure the bunch length. The radii of the two cavities are 123.3 mm and 46.1 mm respectively. Each cavity has two coaxial probes with axial symmetry that are used to extract the signal of the monopole modes.

ERROR OF BEAM OFFSET

The output voltage of the monopole mode excited by a bunch within a cavity can be written as [6,7]

$$V = \frac{1}{2} \omega q \sqrt{\frac{Z(R/Q_0)}{Q_{ext}}} \exp\left(-\frac{\omega^2 \sigma^2}{2}\right) \quad (2)$$

Where q is the bunch charge, Z is the impedance of the detector, and Q_{ext} is the external quality factor of the mode. (R/Q_0) is the normalized shunt impedance, which can be described as

$$\frac{R}{Q_0} = \frac{\left| \int \mathbf{E} ds \right|^2}{\omega U} \quad (3)$$

Where U is the stored energy of the mode in the cavity, and the numerator indicates integration of the electric field of the mode along the beam orbit. The bunch will "see" different electric fields when it passes through the cavity in different transverse positions, so the monopole modes amplitudes excited by the bunch are different. Monopole modes are axially symmetric and have a field maximum on the cavity axis. The electric field intensity distributions of TM_{010} mode within cavity 1 and TM_{020} mode within cavity 2 along the diameter are shown in Fig. 2 and Fig. 3, respectively.

* Work supported by National Key R&D Program of China (Grant No. 2016YFA0401900 and No. 2016YFA0401903) and The National Natural Science Foundation of China (Grant No. U1832169, 11575181).

[†] Corresponding author (email: luoqing@ustc.edu.cn)

[‡] Corresponding author (email: bgsun@ustc.edu.cn)

A TRANSVERSE DEFLECTING CAVITY PROTOTYPE FOR THE MAX IV LINAC

D. Olsson*, A. Bjeremo, L. Christiansson, J. Lundh, D. Lundström, E. Mansten, M. Nilsson, E. Paju, L. Roslund, K. Åhnberg, MAX IV Laboratory, Lund, Sweden

Abstract

The MAX IV LINAC operates both as a full-energy injector for two electron storage rings, and as a driver for a Short Pulse Facility (SPF). There are also plans to build a Soft X-ray Laser (SXL) beamline at the end of the existing LINAC. For SPF and SXL operation, it is important to characterize beam parameters such as bunch profile, slice energy spread and slice emittance. For these measurements, two 3 m long transverse deflecting RF structures are being developed. The structures are operating at S-band, and it is possible to adjust the polarization of the deflecting fields. In order to verify the RF concept, a short 9-cell prototype was constructed. The measurements results of the prototype are presented in this paper.

INTRODUCTION

When the MAX IV LINAC [1] will be upgraded to a driver for an SXL [2], it becomes increasingly important to measure beam parameters such as bunch profile, slice energy spread and slice emittance. For these measurements, transverse deflecting structures are being designed. It is possible to change the polarization of the deflecting TM_{110} mode between horizontal and vertical by adjusting the phases of the RF signals that are fed to the structures. This is illustrated in Figure 1. Each structure is 3 m long, and consists of 91 cells, including 2 coupler cells. Two deflecting structures will be installed in the second half of 2019, and the RF concept is further presented in [3]. In order to verify the RF and mechanical concepts, a shorter prototype was constructed in early 2019.

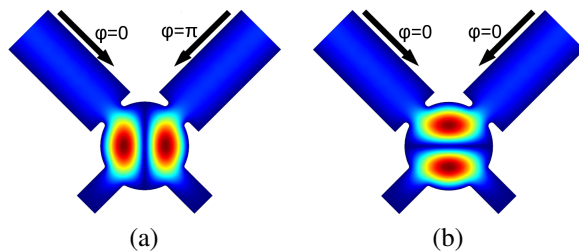


Figure 1: The magnitude of the electric field $|E|$ in the coupler cell when deflecting the beam in the horizontal plane (a), and in the vertical plane (b). φ is the relative phase of the incoming RF signal.

* Corresponding author: david.olsson@maxiv.lu.se

PROTOTYPE

The inner volume of the prototype is almost identical to those of the final structures. The only major difference is that the prototype has two coupler cells and 7 regular cells, while the final structures will have 2 coupler cells and 89 regular cells each. Figure 2 shows a CAD model of the prototype, and Figure 3 shows its inner volume.

The prototype was assembled using an in-house developed heat-shrink method. Here, each part is cooled in liquid nitrogen before it is mounted. The vacuum seal and RF contact to the rest of the assembly is then created when the part expands as it reaches room temperature. Unfortunately, some vacuum leaks were detected after all the parts were assembled. The copper was softened by heating the complete prototype in a bracing oven after it was assembled. This was necessary to create sufficient RF contact around the coupler cells. The heat-shrink assemble method will not be used when making the final structures. Instead, the coupler cells will be braced together, and the regular cells will be clamped together with a method similar to those presented in [4].

MEASUREMENT SET-UP

The prototype and the test set-up can be seen in Figure 4. The fields are perturbed using a cylindrical bead attached to fishing line. The cylinder is moved along the structure by a stepper motor that is controlled from a MATLAB program via a Raspberry Pi. This set-up will also be used to characterize the final TDC structures, but longer rails are of course needed.

The mixed-mode S-parameters are measured with a 4-port network analyzer. As seen in Figure 1, the polarization is

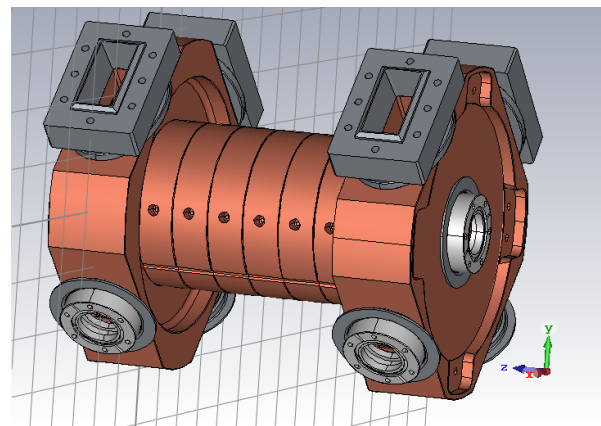


Figure 2: A CAD model of the 9-cell prototype.

ELECTRON BUNCH COMPRESSION MONITORS FOR SHORT BUNCHES - COMMISSIONING RESULTS FROM SwissFEL

F. Frei*, R. Ischebeck, Paul Scherrer Institut, Villigen, Switzerland

Abstract

In SwissFEL, by using three magnetic chicanes, 1–3 ps long electron bunches can be compressed by a factor of more than 100 down to a few fs in order to generate ultra short X-ray pulses. In order to meet the envisaged beam performance, noninvasive longitudinal diagnostic after each compression stage is essential. These bunch compression monitors measure relative bunch length changes on a shot-to-shot basis by detecting coherent edge, synchrotron or diffraction radiation emitted by the electron bunches. Here, we will report on the first commissioning results of the bunch compression monitors for the ultra short bunch mode.

INTRODUCTION

The Aramis beam line at the compact free electron laser user facility SwissFEL [1] at the Paul Scherrer Institut (PSI) in Villigen (Switzerland) produces tunable and coherent X-ray pulses in the wavelength range of 0.1–0.7 nm and is designed to run at 100 Hz.

As depicted in Fig. 1, SwissFEL is based on an S-band radio frequency (RF) photoinjector. An S-band injector in combination with an X-band structure is simultaneously generating the acceleration as well as the necessary linear energy chirp for the first bunch compression stage (BC1). To ensure the proper setup of the injector, the longitudinal electron bunch profile can be measured by means of S-band transverse deflection cavity (TDC).

Thereafter, the electron beam is further accelerated in C-band LINACs to the beam energy of 2.1 GeV. After a second bunch compressor (BC2), a C-band TDC is also providing the possibility to measure the longitudinal electron bunch profile. Two electron bunches with a time delay of 28 ns might be transported up to the switch-yard, where they are directed to the Aramis and Athos beam line respectively. The electron beam in the Aramis beam line can further be

accelerated up to a beam energy of 5.8 GeV, before reaching the energy collimator (EC) and hence the undulators.

As indicated in Fig. 1, for one of the four nominal operation modes of SwissFEL (Aramis), the energy collimator can be used as a third bunch compressor to achieve electron bunch lengths of less than 1 fs (rms) (ultra short bunch mode).

The lasing performance of SwissFEL highly depends on the electron beam quality, in particular on the compression along the whole machine as well as on the stability over time. Therefore, an electron bunch compression monitor is installed after each possible compression stage (BC1, BC2 and EC).

While the first two monitors are used to stabilize the compression phase of the injector and LINAC1, respectively, the signal of the bunch compression monitor after the EC is expected to be used for an indication of full compression in the ultra short bunch mode.

In the subsequent sections, we provide first commissioning results on the electron bunch compression monitors (BCM) for the ultra short bunch mode at 10 pC. To study the sensitivity of the monitors with respect to small changes in bunch length, the compression phases are scanned around the working point where the machine was set up to. In the injector (BC1), this is achieved by varying the off-crest phases of the last two S-band structures simultaneously, while keeping the beam energy via an energy feedback constant.

In contrast, the compression after BC2 is varied by alternately shifting all RF stations of LINAC1 with respect to a fixed off-crest phase. This, to minimize multipacting in the RF structures.

Each of the three electron bunch compression monitors is briefly outlined and the experimental results are presented following the order along the machine.

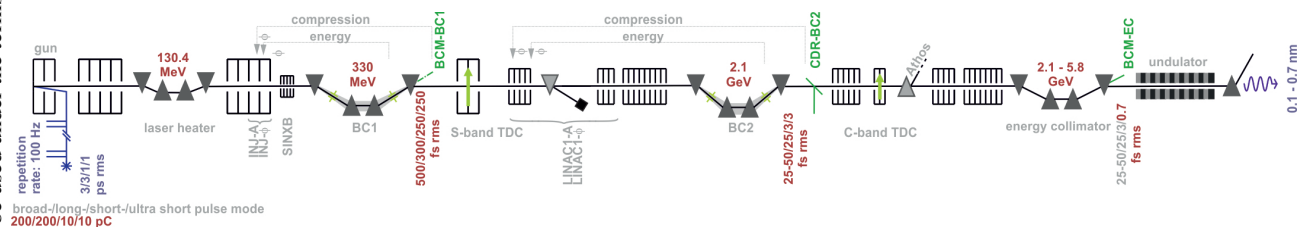


Figure 1: Layout of SwissFEL. After each possible compression stage, there is an electron bunch compression monitor installed. While BC1 (flexible bending angle to cover: 3–4°) and BC2 (flexible bending angle to cover: 1.5–3.8°) are constantly used for compression, the energy collimator (fixed bending angle of 1°) is only used as a third bunch compressor in the ultra short pulse mode. But only after the first two compression stages, the longitudinal electron bunch profile can be measured using a transverse deflecting cavity (destructively).

* franziska.frei@psi.ch

Content from this work may be used under the terms of the CC BY 3.0 licence (© 2019). Any distribution of this work must maintain attribution to the author(s), title of the work, publisher, and DOI

LASER COMPTON BACKSCATTERING SOURCE FOR BEAM DIAGNOSTICS AT THE S-DALINAC*

M. G. Meier^{1,†}, M. Arnold¹, V. Bagnoud², J. Enders¹, N. Pietralla¹ and M. Roth¹

¹Institut für Kernphysik, TU Darmstadt, Darmstadt, Germany

²GSI Helmholtzzentrum für Schwerionenforschung, Darmstadt, Germany

Abstract

The Superconducting DARMstadt electron LINear ACcelerator S-DALINAC is a thrice-recirculating linear accelerator providing electron beams with energies up to 130 MeV and beam currents up to 20 μA for nuclear-physics experiments. A new setup for Laser Compton Backscattering (LCB) will provide a quasi-monochromatic X-ray photon beam for nuclear photonics applications, in photonuclear reactions, and for beam diagnostics. The expected energies of a LCB source at the S-DALINAC extend from about 28 keV to 180 keV with a flux of about 17 ph/s at an expected bandwidth of 0.3 % with a collimated beam. This project is aimed at accelerator physics development in the field of artificial γ -sources. In the first step it will be used at the S-DALINAC for non-destructive beam diagnostics to measure energy and energy bandwidth. General considerations for the setup are presented.

INTRODUCTION

For a wide range of applications in nuclear photonics it is necessary to have a brilliant quasi-monochromatic high-energy photon beam. Hence, the development of artificial γ -sources is important. While bremsstrahlung produced by an electron linear accelerator (LINAC) has a broadband spectrum, novel γ -ray sources use Laser Compton Backscattering (LCB) [1], where photons, produced from a laser, scatter with relativistic electrons at 180° . The scattered photons are Lorentz boosted in the direction of the electrons. LCB provides a sharp energy spectrum at 180° . In a ring accelerator, the energy distribution of the scattered photons is typically limited by the emittance to $\geq 3\%$. To go below this limit, the use of a LINear ACcelerator (LINAC) with LCB was proposed [2]. The γ -ray intensity and / or the experimental count rate are limited by the collision rate and the intensities of both laser and electron beam. A setup combining high electron beam currents with low-emittance beams and high repetition rates could therefore be considered as an ideal driver of an LCB source. Superconducting Energy-Recovery LINACs (ERLs) can provide such electron beams. A secondary application of LCB, useful for all kind of accelerators, is non-destructive beam diagnostic, to measure e.g. beam energy [3].

The thrice-recirculating [4] Superconducting DARMstadt electron LINear ACcelerator S-DALINAC [5] delivers energies up to 130 MeV with average currents of up to 20 μA

* Supported in part through the state of Hesse (LOEWE research center Nuclear Photonics) and DFG through GRK 2128 "AccelencE"

[†] mmeier@ikp.tu-darmstadt.de

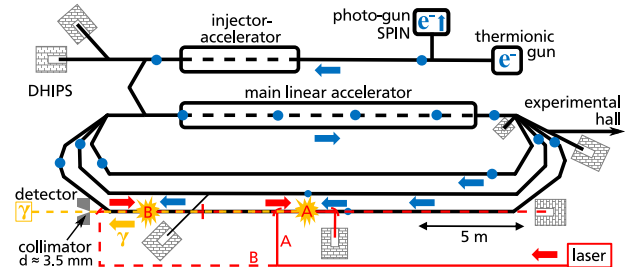


Figure 1: Schematic view of the S-DALINAC, with two (A,B) possible LCB interaction points. The 3 GHz pulsed electron beam collides with laser pulses at the third recirculation. The boosted photons will be detected behind the dipole magnet.

with 3 GHz repetition frequency. It was operated as Germany's first ERL in 2017 [6]. Current investigations are focused on multi-turn ERL operation. Figure 1 shows a floor plan of the accelerator, its sources, injector LINAC as well as the main LINAC with the three recirculation paths.

We propose to install an LCB setup in the third recirculation beam line, where the electrons may reach a maximum energy of about 99 MeV. At the proposed section, the ERL operation is not possible, however, the setup will allow the synchronization of laser pulses and electron bunches to be optimized, the beam-transport lattice to be adapted, and the transmission through the main LINAC after inverse Compton scattering to be studied. The LCB photons will be used for first applications in nuclear photonics as well as non-destructive beam diagnostics.

LASER COMPTON BACKSCATTERING

The Compton effect describes the elastic scattering of a photon with a free electron, where the X-ray photon typically loses recoil energy to the electron. The inverse process to this is Compton backscattering, where the photon is scattered off an relativistic electron at 180° , see Fig. 2. In most cases

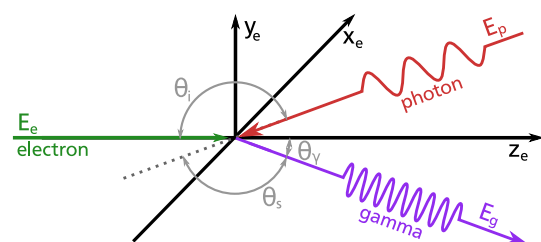


Figure 2: Schematic view of Laser Compton Backscattering.

VIRTUAL PEPPER-POT TECHNIQUE FOR 4D PHASE SPACE MEASUREMENTS

G. Z. Georgiev, M. Krasilnikov, Deutsches Elektronen-Synchrotron DESY, Zeuthen, Germany

Abstract

A novel method for 4-dimensional transverse beam phase space measurement is proposed at the Photo Injector Test facility at DESY in Zeuthen (PITZ) for ongoing beam coupling studies. This method is called Virtual Pepper-Pot (VPP), because key principles of the pepper-pot mask scheme are applied. The latter approach is of limited use in high-brightness photo injectors, because of technical reasons. At PITZ a slit scan method instead is the standard tool for reconstruction of horizontal and vertical phase spaces. The VPP method extends the slit scan technique with a special post-processing. The 4D transverse phase space is reconstructed from a pepper-pot like pattern that is generated by crossing each measured horizontal slit beamlet with all measured vertical slit beamlets. All elements of the 4D transverse beam matrix are calculated and applied to obtain the 4D transverse emittance, 4D kinematic beam invariant and coupling factors. The proposed technique has been applied to experimental data from the PITZ photo injector optimization for 0.5 nC bunch charge. Details of the VPP technique and results of its application will be discussed.

INTRODUCTION

Good knowledge of particle beam properties is required in many scientific experiments. For example, of particular importance for FEL electron sources is the optimization of the beam emittance. Transverse beam phase space is under ongoing studies at the Photo Injector Test Facility at DESY in Zeuthen (PITZ) towards improving the electron source for the European XFEL and detailed understanding of beam dynamics in photo injectors.

Electron beam asymmetries have been observed at PITZ and gun quadrupoles are installed to correct them to a large extend [1]. Slit scans are used to provide 2-dimensional phase space information, but 4-dimensional phase space characterization is needed to understand beam asymmetries and transverse coupling in details. More sophisticated methods are required, e.g. imaging with a pepper-pot mask [2]. While the aforementioned method should provide the desired information, a pepper-pot mask method has limitations in its applicability to the PITZ setup.

A new technique called Virtual-Pepper Pot is proposed at PITZ. It is extension of the slit scan analysis by using a pair of complementary slit scan measurements. Despite it is inspired by the pepper-pot mask principles, most limitations of the latter are not present. The results of the application of the Virtual-Pepper Pot technique on data of experimental studies using gun quadrupoles provide a view on its usability in practice.

TRANSVERSE BEAM PHASE SPACE

The particle motion in the transverse plane is described by the 4D transverse phase space of two position coordinates x and y and their corresponding angles x' and y' . The 4D transverse beam matrix (4D TBM) σ^{4D} is defined as [2, 3]

$$\sigma^{4D} = \begin{pmatrix} \langle xx \rangle & \langle x'x \rangle & \langle yx \rangle & \langle y'x \rangle \\ \langle xx' \rangle & \langle x'x' \rangle & \langle yx' \rangle & \langle y'x' \rangle \\ \langle xy \rangle & \langle x'y \rangle & \langle yy \rangle & \langle y'y \rangle \\ \langle xy' \rangle & \langle x'y' \rangle & \langle yy' \rangle & \langle y'y' \rangle \end{pmatrix} \quad (1)$$

with the corresponding variances and covariances. The beam matrices of the horizontal and vertical phase spaces are respectively the top-left and bottom-right two by two submatrices of the 4D TBM. The 4D transverse emittance of the particle beam is in relation with the determinant of the 4D TBM:

$$\epsilon_{4D}^2 = \det(\sigma^{4D}) = \epsilon_x^2 \epsilon_y^2 - C_{xy}^4, \quad (2)$$

where ϵ_x and ϵ_y are the horizontal and vertical emittances and C_{xy} is the coupling term, which is related to the correlations between the horizontal and vertical phase spaces of the beam.

The measured scaled normalized RMS emittance is defined as $\epsilon_{x,n} = f_{\text{scaling}} \beta \gamma \epsilon_x$, where γ is the relativistic factor of the beam defined from the mean beam energy $\gamma = 1/\sqrt{1-\beta^2}$ and $\beta = v/c$ with v as the beam velocity. The scaling factor f_{scaling} is introduced to correct systematic errors of slit scan measurements. It is described in [4].

RELATED METHODS

Before introducing the VPP technique it is of benefit to present key points of the slit scan technique that are extended by the VPP technique and a few other methods of performing 4D beam measurements.

A standard procedure for measuring projected emittance at PITZ is the single slit scan method [4, 5]. A detailed description of this approach and the experimental setup used at PITZ can be found in Chapter 5 of [6]. Briefly, a space charge dominated electron beam is masked with a horizontal or vertical movable slit. After the slit an emittance dominated beamlet continues its propagation. Downstream of the slit is a scintillating screen that images the beamlet. The beam profile at the slit position is also measured with a scintillating screen for reference, yielding an information on the local beam size. A reconstruction of the phase space of the beam is possible from multiple shots of the beam scanned with a movable slit. The sets of horizontal and vertical shots are separated and require a change of the slit orientation and scanning direction. It should be also noted, that the slice emittance can also be measured by slit scan with a time deflecting structure [7].

BETATRON PHASE ADVANCE MEASUREMENTS USING THE GATED TURN-BY-TURN MONITORS AT SuperKEKB

G. Mitsuka*, K. Mori, M. Tobiya, KEK, Ibaraki, Japan

Abstract

In the SuperKEKB commissioning Phases 2 (Feb.-Jul. 2018) and 3 (from Mar. 2019), the betatron phase advances between adjacent beam position monitors have been measured using a total of 138 gated turn-by-turn monitors. A fast RF gating of the monitors enables turn-by-turn beam position detection by focusing only on an artificially-excited non-colliding bunch, while leaving colliding bunches unaffected. Betatron phase advances measured by the gated turn-by-turn monitors and accordingly obtained betatron functions were consistent with the closed orbit measurements. High signal-to-noise ratio were achieved by advanced signal extraction methods such as NAFF, SVD, and independent component analysis.

INTRODUCTION

Since SuperKEKB aims at very high luminosity $8 \times 10^{35} \text{ cm}^{-2}\text{s}^{-1}$, transverse beam sizes at the interaction point (IP) must be squeezed down to $10 \mu\text{m}$ and 50 nm in horizontal and vertical plane, respectively. Therefore minimization of betatron coupling (X-Y coupling) and vertical dispersion, causing an increase in beam size, is crucial at SuperKEKB. Additionally, betatron function measurements and its corrections are of importance, since a disturbance of the betatron function leads to a dynamic aperture reduction and a vertical emittance growth.

At SuperKEKB we usually estimate X-Y coupling and vertical dispersion by closed orbit analysis for a beam artificially excited by steering magnets. However, these measurements need few tens of minutes in total and are limited to be performed in low-current operation ($\leq 30 \text{ mA}$) with no collision to avoid an accidental system quench. Therefore, fast beam-optics measurements during beam-beam collision and/or high-current operation are desired to compensate close orbit analysis.

For measurements during collisions, we utilize the injection kickers or the transverse feedback kickers to excite a specific non-colliding bunch, while leaving colliding bunches unaffected. Electrode signals from beam position monitors (BPMs) for only a non-colliding bunch are specially processed by the gated turn-by-turn beam position monitors (GTBTs) [1]. Main purposes of the GTBTs are as follows.

- Beam optics measurements using a non-colliding bunch during beam-beam collisions and high-current operation
- Beam study such as measurements for betatron function or X-Y coupling at IP
- Beam diagnostics during beam injection

* gaku.mitsuka@kek.jp

GATED TURN-BY-TURN MONITORS

Shown in Fig. 1 is the top view of the GTBT detector circuit contained in a 1U rack-mount case. A GTBT detector has four-channel BPM inputs. Incoming BPM electrode signals first go to a fast RF gating switch [3] where signals from only a non-colliding bunch (pilot bunch) are accepted, and other bunch signals are rejected. Rejected BPM signals return to four-channel BPM outputs connecting to an external 508 MHz narrow-band detector circuit in charge of a closed orbit analysis. Accepted pilot bunch signals are processed in a GTBT by 508 MHz band pass filters, low-noise amplifiers (HMC616, total gain 40 dB), log-ratio amplifier (ADL5513), peak hold circuit, and are finally analog-digital converted by a 14 bits ADC (ADS850). Timing to control these processes is issued by the Xilinx FPGA (Spartan-6, XC6SLX100T-3FGG484).

Figure 2 indicates the RF gating response, where the one-bunch signal (bottom red) is cut from the input all-bunch signals (top blue, -20 dBm). Switching noise is suppressed to 2 mVpp . Both rise time and fall time are 0.6 ns , which are well shorter than the bunch separation (4 ns). Insertion loss

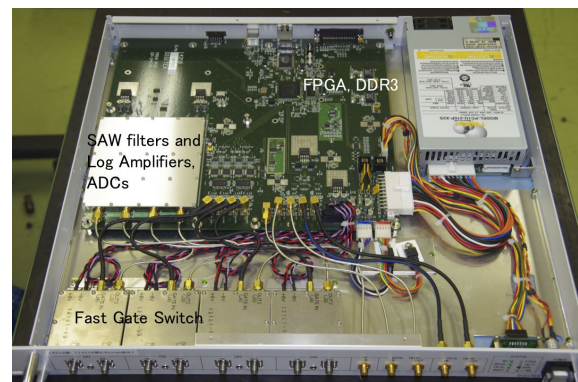


Figure 1: Top view of the GTBT detector.

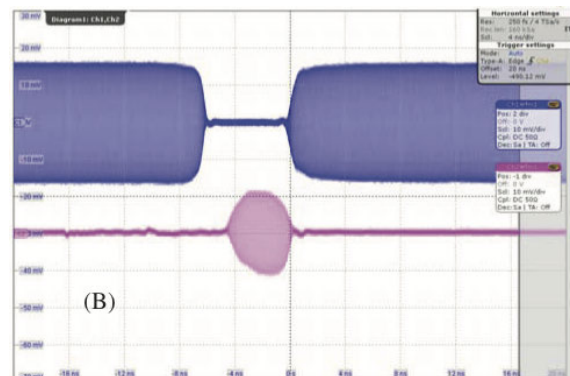


Figure 2: Switch response for a 4 ns gate input.

LONG BEAM PULSE EXTRACTION BY THE LASER CHARGE EXCHANGE METHOD USING THE 3-MeV LINAC IN J-PARC*

H. Takei†, K. Hirano, Shin-ichiro Meigo, J-PARC Center, Japan Atomic Energy Agency, Tokai, Ibaraki, Japan

K. Tsutsumi, Nippon Advanced Technology Co., Ltd., Tokai, Ibaraki, Japan

Abstract

The Accelerator-driven System (ADS) is one of the candidates for transmuting long-lived nuclides, such as minor actinide (MA), produced by nuclear reactors. For efficient transmutation of the MA, a precise prediction of neutronics of ADS is required. In order to obtain the neutronics data for the ADS, the Japan Proton Accelerator Research Complex (J-PARC) is planning the Transmutation Physics Experimental Facility (TEF-P), in which a 400-MeV negative proton (H^-) beam will be delivered from the J-PARC linac. Since the TEF-P requires a stable proton beam with a power of less than 10 W, a stable and meticulous beam extraction method is required to extract a small amount of the proton beam from the high power beam of 250 kW. To fulfil this requirement, the Laser Charge Exchange (LCE) method has been developed. To demonstrate the long beam pulse extraction using the bright continuous laser beam with a power of 196 W, we installed the LCE device at the end of a 3-MeV linac. As a result of the experiment, a charge-exchanged proton beam with a power of 0.70 W equivalent was obtained under the J-PARC linac beam condition, and this value agreed well with the theoretical value.

INTRODUCTION

The Accelerator-driven System (ADS) is one of candidates for transmuting long-lived nuclides such as minor actinide (MA) produced by nuclear reactors [1]. For the efficient transmutation of MA, precise prediction of the neutronic performance of ADS is required. In order to obtain the neutronics data for the ADS, the Japan Proton Accelerator Research Complex (J-PARC) is planning the Transmutation Physics Experimental Facility (TEF-P) [2], which is one of two facilities of the Transmutation Experimental Facility (TEF) [3]. TEF-P is a critical assembly, that is, a low power nuclear reactor, and is operated at most 500 W to prevent excessive activation of the core. To perform the experiments at the TEF-P with such a reactor power with an effective neutron multiplication factor (k_{eff}) of approximately 0.97, the incident proton beam power must be less than 10 W. In the subcritical core of the TEF-P, two kinds of operation modes are existed, the short pulse mode and the long pulse mode. For the short pulse mode, the subcriticality of the core was measured using the low power proton beam with a pulse time width of several ns. For the long pulse, the neutron flux distribution in the subcritical core was measured using the low power proton beam with a

pulse time width of 500 μ s. The power of the incident proton beam ranges from 5 W to less than 10 W for the short pulse mode, and less than 1 W for the long pulse.

On the other hand, the ADS Target Test Facility (TEF-T) [3], another experimental facility of the TEF, equips with a liquid lead-bismuth spallation target bombarded by a 400 MeV-250 kW proton beam. A proton beam provided by the J-PARC linac is shared by TEF-P and TEF-T. These two facilities are connected by one beam line from the J-PARC linac. Because the 250 kW proton beam directed to TEF-T is intense, a technique to extract a low power proton beam of 10 W with high reliability for TEF-P is indispensable.

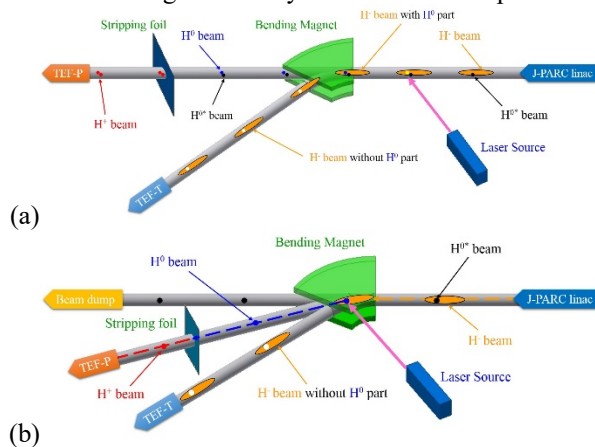


Figure 1: Conceptual diagram of the LCE device for TEF-P. For (a), the laser light is injected in the straight section of the H^- beam line. On the other hand, for (b), the laser light is injected in the bending section of the magnet. The neutralized proton due to interaction by the laser light is written as “ H^{0+} ”, and the pre-neutralized proton due to interaction by the remaining gas in accelerator tubes is written as “ H^{0*} ”.

A stripping foil has traditionally been used to extract low power proton beams from high power proton beams [4]. There is a problem of an unexpectedly high power beam extraction due to the deformation of the stripping foil, and it is difficult to extract a very weak proton beam according to the pulse time width. Hence we applied the laser charge exchange (LCE) technique, which is one of non-contact beam extraction techniques, to extract the low power proton beam. Another advantage for the LCE technique is that it is relatively easier to extract the low power proton beam with different pulse time width by exchanging the laser light source. The technique was originally developed to measure proton beam profiles [5] and has been applied to beam forming devices [6]. Recently, the LCE injection for

* This paper summarizes results obtained with the Subsidy for Research and Development on Nuclear Transmutation Technology.

† takei.hayanori@jaea.go.jp

BEAM BASED ALIGNMENT OF ELEMENTS AND SOURCE AT THE ESS LOW ENERGY BEAM TRANSPORT LINE

N. Milas*, M. Eshraqi, B. Gålnander, Y. Levinsen, R. Miyamoto, E. Nilsson and D. C. Plostinar
 European Spallation Source ERIC, Lund, Sweden

Abstract

The European Spallation Source (ESS), currently under construction in Lund, Sweden, will be the world's most powerful linear accelerator driving a neutron spallation source, with an average power of 5 MW at 2.0 GeV. The first protons were accelerated at the ESS site during the commissioning of the ion source and low energy beam transport (LEBT), that started in September 2018 and ran until July 2019. Misalignments of the elements in the LEBT can have a strong impact on the final current transmission of the low energy part. In this paper, we present a way to isolate and measure tilts of the elements and the initial centroid divergence of the source. We also present initial test measurements for the ESS LEBT and discuss how to extend the method to other facilities.

INTRODUCTION

The low energy beam transport (LEBT) section of the ESS linac was commissioned at ESS between September 2018 and June 2019. This section has two focusing solenoids and two sets of dipole correctors (steerer) and is responsible for transporting and focusing the beam that will be delivered to the following radio frequency quadrupole (RFQ) [1]. It is crucial not only that the beam entering the RFQ has the correct Twiss parameters, but also that it enters centered and with minimum centroid angular component. For the latter, it is necessary that the elements along the LEBT as well as the source extraction point are well aligned. For the solenoids in the LEBT, tilts creates dipole components and thus trajectory excursions. In order to correct the beam trajectory in the best possible way it is necessary to have, in addition to a good model, knowledge of the elements tilts and also of the initial beam conditions at the extraction point. In this work we present a method to isolate angular misalignments for the LEBT solenoids and also a way to estimate the initial beam centroid angles. The presented method uses the readings from a Non-invasive Profile Monitor [2] (NPM), but we will also discuss a possibility to use an Allison Scanner type Emittance Measurement Unit (EMU) to perform the same measurement. Finally, measurements performed during the LEBT commissioning and their comparisons with beam transmission simulations, taking into account the reconstructed errors, will be shown.

METHOD

In a perfect machine the trajectory should be on the reference axis, however that is seldom the case. Many different

* natalia.milas@esss.se

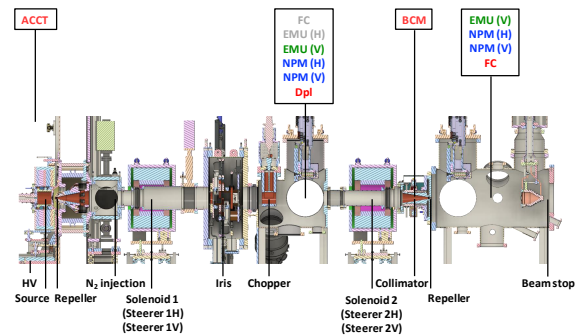


Figure 1: LEBT layout.

errors contribute to offsets in beam trajectory and we face questions of how to identify and make effective estimations of most relevant error sources. For the case of the trajectory in the ESS LEBT (Fig. 1), knowledge of errors in the two solenoids and initial conditions at the source extractions are the keys.

Assuming offsets can be neglected, as assessed in the next section, there are six major error sources to account for: initial centroid angles at the source and tilts around two transverse planes for each solenoid. On the other hand, we have access to only two variables, namely (x, y) positions, at two locations of NPMs downstream of each solenoid. This requires multiple solenoid measurements at different strengths in order to characterize all the six error sources. In this paper, we will use pitch (θ) and yaw (ϕ) as elements tilts, which correspond to a rotation around the vertical and horizontal axis respectively.

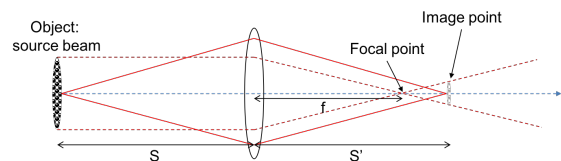


Figure 2: Schematics of the optics of the source and first solenoid at the ESS linac.

The principle of the technique to identify the aforementioned errors, used throughout this paper, is sketched in Fig. 2. When the strength of the solenoid lens is as such to produce the image point at the measurement location, e.g. at the NPM location, the measured position offset is insensitive against the initial errors at the source and dictated by the errors of the solenoid lens itself. In the ESS LEBT, the image point can be easily placed at the first NPM by simply scanning Solenoid 1 strength and finding a value to minimize the beam size at the same NPM. Once this condition is

POSITION BASED PHASE SCAN

N. Milas^{*}, R. Miyamoto, M. Eshraqi, D. C. Plostinar and Y. Levinsen
European Spallation Source ERIC, Lund, Sweden
Y. Liu, J-PARC, Japan

Abstract

Knowledge of the longitudinal beam parameters is important for understanding beam dynamics in linacs. As well as with transverse optics, the settings for the RF cavities have to be established and phase and amplitude seen by the beam must be determined in order to guarantee a stable motion in the longitudinal plane. This work presents an extension of the most widely used phase scan method, relying on time-of-flight, using only transverse positions measured at a few selected BPMs downstream of the cavity being scanned. In principle, the method can be applied both to normal conducting and SC. The suggested method is fast and relatively simple and is capable to provide the values for the cavity transverse misalignment (offsets and tilts) at the same time. It can be a useful part of the initial longitudinal beam tuning.

INTRODUCTION

The European Spallation Source (ESS), currently under construction in Lund, Sweden, will be a spallation neutron source driven by a superconducting proton linac [1]. The linac in its final configuration will accelerate a beam with a 62.5 mA peak current and 4% duty cycle (2.86 ms pulse length at 14 Hz) up to 2 GeV and thus produces an unprecedented 5 MW average beam power.

One important issue at ESS, as in many other hadron linacs, is to set the correct phase and amplitude for the cavities to ensure that the proton bunches receive the desired acceleration and energy gain. The settings for the RF cavities have to be established and phase and amplitude seen by the beam must be determined in order to guarantee a stable motion in the longitudinal plane. This work presents a novel method to determine the RF phase and amplitude using only position measurement at a few selected beam position monitors (BPMs) downstream of the cavity being scanned. In addition to the calibration it is also possible to extract the transverse offsets and tilts (pitch and yaw angles) of the cavities which can then be fed back into the machine model.

A series of measurement using the position based cavity tuning were performed at J-PARC in March 2019 and compared with conventional ToF and signature matching measurements [2–5] for the first buncher cavity in the MEBT1 section. Those measurements corresponds the a first proof of principle for the method and will be presented in this work.

^{*} natalia.milas@esss.se

THE METHOD

Consider a simple lattice setup composed of a drift-cavity-drift. When the beam goes through an RF cavity off centered it feels a transverse force proportional to the offset, which could be focusing or defocusing depending on the phase of the cavity. The amplitude of this effect depends both of the cavity phase and amplitude and thus affects the beam trajectory accordingly, in the thin-lens approximation

$$\begin{bmatrix} x \\ x' \end{bmatrix} = \begin{bmatrix} 1 & 0 \\ 1/f(\phi, V) & 1 \end{bmatrix} \begin{bmatrix} x_0 \\ x'_0 \end{bmatrix}, \quad (1)$$

for the horizontal plane only, where $f(\phi, A)$ is the RF focusing which for a linear model can be expressed as

$$\frac{1}{f(\phi, V)} = -\frac{\pi qVT \sin(\phi)}{mc^2 \lambda (\gamma\beta)^3} = F(V) \sin \phi, \quad (2)$$

where T is the cavity transit time factor, λ the wavelength, ϕ the RF phase seen by the beam and $V = E_0 L$ is the gap voltage, with E_0 the cavity field and L the gap length. Now calculating the transverse transfer matrix of the whole setup drift-cavity-drift it is possible to find the following relations

$$\begin{bmatrix} x \\ x' \end{bmatrix} = \begin{bmatrix} x_0 + L_d x_0 / f + L_d x'_0 \\ x_0 / f + x'_0 \end{bmatrix}, \quad (3)$$

where L_d is the length of the drift between cavity and the observations points, which in most cases will be a beam position monitor (BPM) and for this reason will be referred as such from this point on. By scanning the cavity phase and looking at the trajectory it is possible to calibrate the phase of the RF fields.

There are two ways of calibrating the cavity amplitude. The first one is to run several phase scans for different amplitudes and record the maximum trajectory displacement, which happens when the cavity phase is at maximum focusing in the longitudinal plane. The trajectory deviation is connected to the cavity amplitude through the second term in Eq. (3) as $\Delta x_{\max} = L_d x_0 F(V)$. Since L_d and x_0 are known parameters and the calibration between Δx_{\max} and the cavity amplitude, given by the function $F(V)$, can be resolved from simulation.

Another way to calibrate the amplitude, easier to visualize however with a more difficult setup, is to measure the real focal length of the cavity transverse focusing component. In this method the initial trajectory angle has to be correctly set to zero and it is also assumed that a previous beam based alignment of the nearby BPMs was performed and the remaining trajectory errors are small. An amplitude scan is then perform for two different initial trajectory offsets x_0^1 and

OPTICS-MEASUREMENT-BASED BPM CALIBRATION

A. García-Tabarés Valdivieso*, R. Tomás García, CERN, 1217 Meyrin, Switzerland

Abstract

Beam position monitors (BPMs) are key elements in accelerator operation, providing essential information about different beam parameters that are directly related to the accelerator performance. In order to obtain an accurate conversion from an induced voltage to the position of the centre of mass of the charge distribution, the BPMs have to be calibrated prior to its installation in the accelerator. This calibration procedure can only be performed when the accelerator is in a period of non-activity and does not completely reproduce the exact conditions that occur during the machine operation. Discrepancies observed during the optics measurements at the Large Hadron Collider show that the impact of the BPM calibration factors on the optics functions was greater than expected from the design values and tolerances. Measurement of the optics functions allows obtaining extra information on BPM calibration together with its associated uncertainty and resolution. The optics measurement based calibration allows computing optics functions that are biased by a possible calibration error such as beta function, dispersion function and beam action.

INTRODUCTION

Accurate optics measurements are an essential step performed during the commissioning of present and future colliders such as LHC [1–4], its upgrades HL-LHC [5] and HE-LHC [6] or the FCC [7, 8]. The requirements of increasing the luminosity moves the LHC into more challenging operational regimes with lower β^* . Optics measurements and corrections will play an important role in this scenario, aiming to correct strong localized magnetic errors to achieve the design value of the β function at the interaction point (IP), called β^* , to provide the design high luminosity within the 5% tolerance limits to the experiments: ATLAS, located in the Interaction Region 1 in the LHC (IR1) [9] and CMS [10], located in the Interaction Region 5 in the LHC (IR5). These corrections rely on the accuracy that can be achieved in the β^* measurements and it has been the primary motivation for further developing β -function reconstruction methods.

Most common optics reconstruction approaches are based on driven turn-by-turn measurements recorded at each BPM location [11–15]. The excitation induced by an external source moves the beam in phase space, allowing to record larger betatron oscillations, improving the resolution of the β reconstruction. The motion of the beam, when subjected to an external periodic force, is denoted as driven oscillation. In driven turn-by-turn measurement mode, BPMs record the centre-of-charge position of a given bunch excited by an external source every time it passes through the BPM [16].

Advanced Fourier analysis tools allow transforming turn-by-turn data from the time domain to the frequency domain [17]. Information contained in the frequency spectra: frequency, phase and amplitude, is used for optics functions reconstruction around the ring.

On the one hand, relative phase advances between a reference BPM and at least two other BPMs allow reconstructing the values of the β functions at the reference BPM. This method, known as β from phase (β^ϕ), was first used in LEP [18] and has been further developed in LHC, ALBA and ESRF [19–22]. This approach is very sensitive to errors for values of the BPMs phase advance close to $n\pi$. Those values match the phase advance between consecutive BPMs for certain BPMs in the LHC and the entire BPM range in the Proton Synchrotron Booster (PSB).

On the other hand, the amplitude of the transverse motion at a given position is proportional to $\sqrt{\beta}$, and this can be used for β measurements. This approach is known as β from amplitude (β^A). Nonetheless, a possible calibration error of each BPM will directly propagate to the measured amplitude. This β -function reconstruction does not allow to separate the contribution of BPM calibration errors from the real driven amplitude. The β^A approach has been used in the past [18, 22–24], it is currently implemented as part of the OMC software [25], but it has not been as widely used as β^ϕ . The lack of resolution in the β -function calculation when using β^ϕ for specific values of the phase advance triggered further development of an alternative method for computing the calibration factors.

Knowledge of BPM calibration factors would allow to accurately measure β function using β^A approach where the performance of β^ϕ is limited.

This paper introduces an optics-based-BPM calibration measurement method based on β function measurements using the ratio $\sqrt{\beta^\phi/\beta^A}$. Calibration factors are calculated in an optics configuration where the systematic lattice errors affect as less as possible β^ϕ and dispersion measurements. In case of LHC, an optics that is suitable for this method is the Ballistic or Alignment optics, characterised by having the triplets switched off [26].

CALIBRATION PROCEDURE

β -function Measurements Based on Amplitude Analysis

The parameters obtained after applying Fourier transformation to turn-by-turn data- frequency, phase and amplitude- are the base of optics functions reconstructions: β^ϕ, β^A .

Linear optics studies are especially focused on the analysis of amplitude and phase corresponding to the main line of the spectrum, associated to the driven tune. For the i^{th} BPM,

* ana.garcia-tabares.vvaldivieso@cern.ch

USING TUNE MEASUREMENT SYSTEMS BASED ON DIODE DETECTORS FOR QUADRUPOLEAR BEAM OSCILLATION ANALYSIS IN THE FREQUENCY DOMAIN

M. Gasior, T. Levens, CERN, Geneva, Switzerland

Abstract

Requirements for diagnostics of injection matching and beam space charge effects have driven studies at CERN using high sensitivity tune measurement systems based on diode detectors for the observation of quadrupolar beam oscillations in the frequency domain. This has led to an extension of such tune systems to include a channel optimised for quadrupolar oscillation measurements. This paper presents the principles of such measurements, the developed hardware and example measurements.

INTRODUCTION

The unprecedented requirements for the sensitivity of the tune measurement system in the Large Hadron Collider (LHC) triggered an extensive research program, resulting in the development of the direct diode detection technique [1]. Its operational implementation, the Base-Band Tune (BBQ) system, was already proven in several accelerators before the LHC start-up [2]. The large dynamic range of these systems and their complete suppression of beam orbit signals made them excellent candidates for new attempts of obtaining quadrupolar signals from standard four-electrode beam position pick-ups (PUs) for beam diagnostic purposes. The first BBQ system used to observe quadrupolar signals was in the CERN Super Proton Synchrotron (SPS). The system was configured for quadrupolar studies in 2006 and was used for successful observation of beam quadrupolar oscillations during injection matching studies. Following this, a similar setup was used at GSI for studying space charge [3]. In 2014 the BBQ system in the CERN Proton Synchrotron (PS) was upgraded with a sensitive strip-line PU and since then space charge studies based on quadrupolar signals have continued at CERN [4]. Finally, in 2018 these studies led to an extension of the PS BBQ system in order to provide the spectra of beam quadrupolar signals in parallel to regular tune measurement operation. This paper briefly describes the BBQ systems, beam quadrupolar oscillation signals and the setups that have been used for their observation in the frequency domain. Finally, the new BBQ front-end providing both tune and quadrupolar signals is described along with example measurements performed with this setup.

BASE-BAND TUNE SYSTEMS

A simplified block diagram of a BBQ system is shown in Fig. 1. The four signals L , R , T and B correspond to the left, right, top and bottom pick-up electrodes, respectively. The signals are first processed by diode detectors (DD) installed directly on the PU output terminals. The detectors provide envelope demodulation around the maxima of the

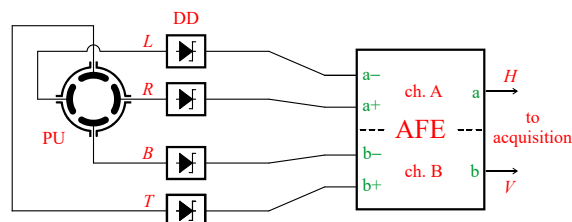


Figure 1: A sketch of a BBQ system in its standard tune measurement configuration.

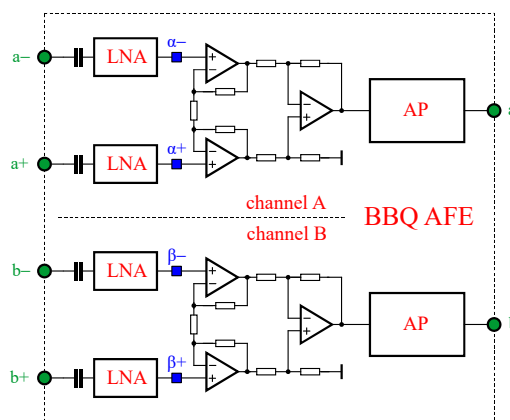


Figure 2: Simplified signal processing of the BBQ analogue front-end (AFE).

beam pulses. In this process, any modulation carried by the short beam pulses is converted into an envelope signal superimposed on a DC level that is related to the beam pulse amplitude that does not change from one pulse to another. The subsequent analogue front-end (AFE), installed close to the PU in the accelerator tunnel, processes only the envelope signals. The large DC background is suppressed at the input of the AFE by series capacitors, as shown on the block diagram in Fig. 2. The envelope signals are first amplified by low-noise amplifiers (LNA) before going to the inputs of differential amplifiers built in the classical instrumentation configuration with three operational amplifiers (op-amps). Two differential amplifiers provide subtraction of the amplified envelope signals from the opposing PU electrodes for both the horizontal and vertical planes. The subsequent analogue processing (AP) consists of a chain of filters and amplifiers, as described in more detail in [2].

The two AFE output signals are base-band signals that are sent over long cables to a dedicated VME acquisition system with 16-bit ADCs sampling synchronously to the beam revolution frequency (f_{rev}). The acquisition system

Content from this work may be used under the terms of the CC BY 3.0 licence (© 2019). Any distribution of this work must maintain attribution to the author(s), title of the work, publisher, and DOI

APPLICATION OF THERMOELECTRIC OSCILLATIONS IN A LITHIUM NIOBATE SINGLE CRYSTAL FOR PARTICLE GENERATION

A.N. Oleinik[†], John Adams Institute at Royal Holloway, University of London, Egham, UK and Laboratory of Radiation Physics, Belgorod State University, Belgorod, Russia

P.V. Karataev, John Adams Institute at Royal Holloway, University of London, Egham, UK

K. Fedorov, Tomsk Polytechnic University, Tomsk, Russian Federation and John Adams Institute at Royal Holloway, University of London, Egham, UK

O.O. Ivashchuk, A.A. Klenin, A.S. Kubankin, A.S. Shchagin, Laboratory of Radiation Physics, Belgorod State University, Belgorod, Russia

Abstract

Thermoelectric oscillations in lithium niobate single crystals include oscillations of temperature and pyroelectric current. The possibility of generating electrons and positive ions in vacuum conditions is shown. The results of the first experiments are presented. The possibilities and development prospects of the particle generation method are discussed.

INTRODUCTION

The absence of a centre of symmetry in certain materials, as lithium tantalate or lithium niobate, leads to the appearance of a constant dipole moment of each crystal cell [1]. In thermal equilibrium, an induced surface charge is completely screened. Presence of surface charge can be registered at changing of temperature of pyroelectric sample. It is called a pyroelectric effect. In standard atmosphere conditions this charge is screened very quickly, but in vacuum surroundings screening time can be about a few months.

This fact favours to collection of surface charge, which is enough to generate high electric field with strength of about 10^5 V/cm [2]. It is high enough to eject particles from the surface of the crystal and ionize residual gas molecules. Thus, electrons and positive ions can be generated and accelerated due to the pyroelectric effect [3-6].

In this paper, a method for generating electrons and positive ions based on thermoelectric oscillations at pyroelectric effect is presented and discussed. The frequency dependences of the amplitudes of the generated pyroelectric current and the current of the generated particles are also presented.

THERMOELECTRIC OSCILLATIONS

The generated pyroelectric current can be expressed as

$$i_{pyr} = pA \frac{dT}{dt} \quad (1)$$

where p is the pyroelectric coefficient, A is the area of polar surface, $\frac{dT}{dt}$ is the time derivative of the temperature. If the temperature changes as

$$T(t) = T_0 + T_1 \sin \omega t \quad (2)$$

where T_0 is an initial temperature of sample, ω is the frequency of oscillations, T_1 is an amplitude of temperature oscillation. In this case, the generated current could be rewritten in following form

$$i_{pyr} = pAT_1 \cos \omega t \quad (3)$$

Such mode of current generation implies that there are oscillations of current on the polar surface induced by oscillation of the temperature. In vacuum condition the oscillating current is accumulated on the polar surface of pyroelectric sample. It leads to the oscillations of the amount of charge, and hence oscillations of the strength of the electric field. Thus, a stable mode of periodic generation of electric field can be achieved. Such conditions should provide stable generation of electrons or positive ions at each half-wave, which was previously unattainable for pyroelectric particle sources.

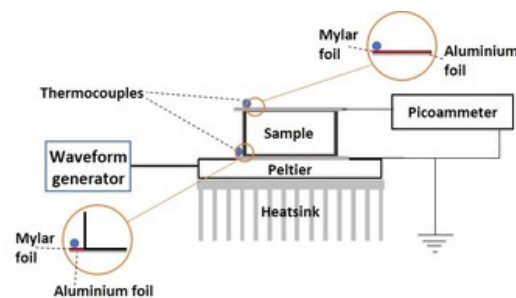


Figure 1: The scheme of experimental setup.

Analysis of literature shows that such oscillations in the bulk samples of lithium niobate are not investigated yet at all. The theory of sinusoidal temperature waves in the ferroelectrics as a way of determining pyroelectric coefficient of the sample, and also as a way of separation of the contribution of pyroelectric current from other currents stimulated by temperature, is being consistently developed in Garn and Sharp's works [7]. An experimental investigation of thermoelectric oscillations in a 50 μm thick LN sample shows that only pyroelectric current observed without any other contributions [8]. Due to the sinusoidal temperature change, it is possible to precisely determine the sample's pyroelectric coefficient [9] and its distribution [10] along

[†] andrey.oleynik.2017@live.rhul.ac.uk

FIRST MEASUREMENTS OF CHERENKOV-DIFFRACTION RADIATION AT DIAMOND LIGHT SOURCE

D. M. Harryman*, P. Karataev, JAI, Royal Holloway, University of London, Egham, Surrey, UK
M. Apollonio, L. Bobb, Diamond Light Source, Oxfordshire, UK
M. Bergamaschi, R. Kieffer, M. Krupa, T. Lefevre, S. Mazzoni, CERN, Geneva, Switzerland
A.P. Potylitsyn, Tomsk Polytechnic University, Tomsk, Russia

Abstract

Cherenkov-Diffraction Radiation (ChDR), appearing when a charged particle moves in the vicinity of a dielectric medium with speed faster than the speed of light inside the medium, is a phenomenon that can be exploited for a range of non-invasive beam diagnostics. By using dielectric radiators that emit photons when in proximity to charged particle beams, one can design devices to measure beam properties such as position, direction and size. The Booster To Storage-ring (BTS) test stand at Diamond Light Source provides a 3 GeV electron beam for diagnostics research. A new vessel string has been installed to allow the BTS test stand to be used to study ChDR diagnostics applicable for both hadron and electron accelerators. This paper will discuss the commissioning of the BTS test stand, as well as exploring the initial results obtained from the ChDR monitor.

INTRODUCTION

Diamond Light Source is a 3rd generation synchrotron light source storage ring facility in the U.K [1]. Recently the conceptual design report was published for the 4th generation upgrade to Diamond-II [1]. Such an upgrade would feature a Multi-Bend Achromat (MBA) lattice, requiring more dipole magnets with lower magnetic field strength. This creates new straight sections for more insertion devices to be installed, and also reduces the horizontal emittance as

$$\epsilon_x \propto \frac{1}{N_{\text{Bending}}^3} \quad (1)$$

where ϵ_x is the horizontal emittance, and N_{Bending} is the number of dipole magnets [1]. From a diagnostics perspective, one drawback of such a design is that the shallower bends provided by the dipole magnets reduce the space available for synchrotron radiation extraction.

For ultra-low emittance rings, monitoring the beam position inside the dipole could be advantageous. Previous results have shown that Cherenkov Diffraction Radiation (ChDR) offers the ability to design non-invasive optical diagnostics that could be used for monitoring a variety of beam parameters, such as; position, size, and bunch length [2–5].

As part of the ChDR collaboration, research is being undertaken at Diamond into the feasibility of using a ChDR radiator as an optical Beam Position Monitor (BPM) pickup. These investigations could lead to an optical BPM design to be used on Diamond-II.

* daniel.harryman.2018@live.rhul.ac.uk

BEAM TEST STAND

The Diamond accelerator chain has three accelerators: a linac, a booster synchrotron, and a storage-ring [1]. On the Booster to Storage-ring (BTS) transfer line is a test stand that is used for beam diagnostics research [6]. Figure 1 shows the vacuum vessel string recently installed on the BTS test stand, this features: three Optical Transition Radiation (OTR) monitors, an Inductive Beam Position Monitor (IBPM) [7], and a ChDR monitor. The OTR monitors and IBPM are used for cross referencing the results from the ChDR monitor. The IBPM is used for beam position and charge measurements [7], whereas the OTR monitors are used to obtain the size and position of the beam. By monitoring OTR monitors upstream and downstream of the ChDR radiator, the trajectory through the test stand, and the beam's distance from the radiator can be found.

Nominal beam parameters in the BTS test stand will set the booster to extract 3 GeV electrons in a train of 120 bunches at a rate of 5 Hz. These have approximately 0.2 nC of charge per train, and a bunch spacing of 2 ns. The transverse beam size in the test stand has a Gaussian distribution with a σ_x of 1.4 mm and a σ_y of 0.5 mm.

The beam parameters of the BTS test stand can be changed to enable a variety of experimental studies. For example, the transverse beam position can be changed, and a horizontal or vertical waist can be introduced onto the beam and moved along the test stand. The beam can also be extracted in either a multi-bunch train, or a single bunch train. The charge can be varied up to 1.3 nC for a multi-bunch train, or 0.3 nC for a single bunch.

THEORY

ChDR is a type of radiation emitted from a dielectric when a highly relativistic charged particle moves in the vicinity of the dielectric at a speed faster than the speed of light through that medium [8]. This happens due to the effect of the charged particles external field producing a polarisation effect on the material [9]. As with Cherenkov radiation, ChDR is emitted at the angle Θ_{Ch} , given by

$$\cos(\Theta_{Ch}) = \frac{1}{n\beta} \quad (2)$$

where n is the refractive index for the dielectric medium, and β is the particles velocity relative to the speed of light [8]. As the charged particle is not moving through the material, the distance between the charged particle and the dielectric, known as the impact parameter, h , must be considered [8].

OBSERVATION OF MICROBUNCHING INSTABILITIES USING THz DETECTOR AT NSLS-II*

W. Cheng[#], B. Bacha, G. L. Carr

NSLS-II, Brookhaven National Laboratory, Upton, NY 11973

Abstract

Microbunching instabilities have been observed in several light sources with high single bunch current stored. The instability is typically associated with threshold beam currents. Energy spread and bunch length are increasing above the thresholds. Recently, a terahertz (THz) detector was installed at the cell 22 infrared (IR) beamline at NSLS-II storage ring to study the micro-bunch instabilities. The IR beamline has wide aperture allowing long-wavelength synchrotron radiation or microwave signal propagate to the end station, where the detector was installed. The detector output signal has been analyzed using oscilloscope, spectrum analyzer and FFT real-time spectrum analyzer. Clear sidebands appear as single bunch current increases and the sidebands tend to shift/jump. We present measurement results of the THz detector at different nominal bunch lengths and ID gaps.

INTRODUCTION

Microbunching instabilities have been observed at several storage rings [1-3], in earlier 2000. Bursts of coherent synchrotron radiation (CSR) in terahertz (THz) range were observed when beam current was above a certain threshold. Microstructure in the bunch, typically in the millimeter range (THz), is formed. The microstructure in the longitudinal phase space causes a sideband frequency component detectable with broadband THz detectors. More recent measurements [4-8] in low-alpha mode show stable CSR measured with broadband detectors. Schottky barrier diode (SBD) and quasi-optical detector (QoD) are easy to use with fast responses and high sensitivity.

NSLS-II storage ring has seen significant bunch lengthening and energy spread increases [9]. Earlier measurement of the beam spectrum shows higher order synchrotron motion sidebands appearance, indicating possible microstructure in the high current single bunch. To further understand the issue, a Quasi-optical detector (QoD) [10] has been prepared and setup at the visible diagnostic beamline and cell 22 infrared beamline (22-IR) at NSLS-II. The QoD has integrated broadband amplifier with 4GHz bandwidth. This allows bunch-to-bunch measurement with 2-ns bunch spacing. Recent observations from single bunch studies, as well as multi-bunch normal operations, are presented. It is worth to point out that most of the measurements were carried out with

normal lattice with momentum compaction factor of 3.63×10^{-4} . RMS bunch lengths are around 10-40ps, depending on the RF voltages, ID gaps and bunch lengthening.

EXPERIMENT SETUP

The 22-IR beamline at NSLS-II has been commissioned in 2018, collects bending magnet radiation from a large gap dipole in cell 23 (90mm magnet gap height, 76mm vacuum chamber inner height). The beamline is typically called 22-IR as it takes the experimental floor space facing cell 22 straight section. The beamline accepts synchrotron radiation fans of ~ 48 mrad horizontally. The vertical acceptance angle varies from 34-76 mrad along the dipole trajectory. The light is then guided through a series of Aluminum coated mirrors. The beamline layout is shown in Figure 1.

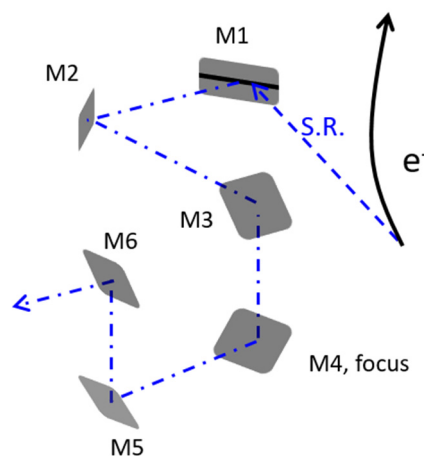


Figure 1: 22-IR beamline layout. Large gap dipole radiations are first reflected by the slotted first mirror (M1), then relayed to outside hutch through a series of mirrors. The concrete shielding wall is in-between M4/M5 mirrors.

The first mirror M1 locates at 2250mm from the dipole entrance. It has a wedge-shaped slot in the middle to let high power x-ray pass through. The slot has a vertical opening of 3mm at the location where electrons enter the dipole field, and increases linearly to about 6mm near the downstream edge. This is corresponding to open angle of 1.3 – 6 mrad for the slot. The wedge angle then increases so that the mirror profile matches the nominal vacuum chamber cross section (an octagon shape with 25mm high and 76mm wide). Long wavelength synchrotron radiations, including visible light, IR and far IR, are reflected by the M1 mirror and guided to the hutch on the experimental floor through other mirrors, as shown in Figure 1. M4 is a

*Work supported by DOE contract No: DE-SC0012704

[#]Weixing Cheng is now at Argonne National Laboratory, Email: wcheng@anl.gov

SINGLE-SHOT DIAGNOSTICS OF MICROBUNCHED ELECTRONS IN LASER-DRIVEN PLASMA ACCELERATORS AND FREE-ELECTRON LASERS*

Alex H. Lumpkin[†], Fermi National Accelerator Laboratory, Batavia, IL 60510 USA
Donald W. Rule, Silver Spring MD, 20904 USA

Abstract

In general, the inherent statistical variances in the laser-driven plasma accelerators (LPAs) and self-amplified spontaneous emission (SASE) free electron lasers (FELs) motivate the use of single-shot diagnostics. In addition, the microbunching phenomenon in each is also variable, so coherent optical transition radiation (COTR) techniques also warrant single-shot evaluations. In both cases, the enhancements of the signals enable optical beam splitters to be used to direct light to the different measuring devices for electron beam size, divergence, spectral content, and/or bunch length as appropriate. COTR Interferometry (COTRI) modelling results for the pre-buncher case at 266 nm and for the LPA case at 633 nm are presented. In addition, examples of few-micron beam size and sub-mrad beam divergence measurements from a single shot of an LPA are reported.

INTRODUCTION

The need for single-shot diagnostics of the periodic longitudinal density modulation of relativistic electrons at the resonant wavelength (microbunching) in a free-electron laser (FEL) or at broadband visible wavelengths as in a laser-driven plasma accelerator (LPA) has been reaffirmed. In the self-amplified spontaneous emission (SASE) FEL case, statistical fluctuations in the microbunching occur in the start-up-from-noise process. In the LPA, the plasma itself is chaotic and varies shot to shot. Fortunately, we have shown that coherent optical transition radiation (COTR) techniques, can assess beam size, divergence, spectral evolution, and z-dependent gain (10^5) of microbunched electrons in a past SASE FEL experiment at 530 nm [1]. We consider a potential use of such diagnostics for the microbunched electrons following a pre-buncher involving a seed laser, modulator, and chicane for 266 nm. Recently, the application of COTR-based diagnostics to LPAs has been demonstrated with single-shot near-field (NF) and far-field (FF) COTR imaging done at the exit of an LPA for the first time [2,3]. Both configurations will be described with modelling of COTRI for the first and second cases with examples of data for the second.

* This manuscript has been authored by Fermi Research Alliance, LLC under Contract No. DE-AC02-07CH11359 with the U.S. Department of Energy, Office of Science, Office of High Energy Physics.

[†] lumpkin@fnal.gov

EXPERIMENTAL ASPECTS

The APS Linac

The APS linac is based on an S-band thermionic cathode (TC) rf gun which injects beam into an S-band linear accelerator with acceleration capability currently up to 450 MeV. This is an S-band pulse train with about 10 ns macropulse duration and 28 micropulses, presently delivering 1 to 1.5 nC per macropulse. Beam diagnostics in the linac include imaging screens, rf BPMs, loss monitors, and coherent transition radiation (CTR) autocorrelators.

For possible experiments for imaging microbunched electrons due to a pre-buncher, the beam is transported to the Linac Experimental Area (LEA) tunnel [4] where the pre-buncher is staged as schematically shown in Fig. 1. In the considered case, a 266-nm wavelength seed laser is co-propagated with the 375-MeV electron beam through a modulator to energy modulate the beam. A small chicane magnet array is used to provide the R_{56} term for converting this to the longitudinal modulation, or microbunching at 266 nm. An insertable foil is used to block the seed laser for the COTR measurements. A NF image of the beam size is obtained from forward COTR emitted from the back surface. In addition, a mirror rotated at 45° to the beam direction and located 6.3 cm downstream redirects the light to the optics. This same mirror is the source for backward COTR that interferes with the COTR from the first source to form interference patterns in the angular distribution patterns recorded in the FF camera.

Due to the enhancements of the COTR, the signal may be split among the five measurement options as indicated in Fig. 2. For this case the NF image, FF image, spectral content, COTR gain, and bunch length could be assessed on a single shot. Even with the sampling entrance slits of the spectrometer and streak camera, the signals should be strong enough for statistically relevant data.

Laser-driven Plasma Accelerator Aspects

For the LPA, the basic arrangement is shown in Fig. 3 with the 150 TW laser of central wavelength 800 nm, gas jet, the foil wheel, and the downstream mirror at 45° to the beam direction. A similar two source geometry is used as in the pre-buncher scenario, only $L=18.5$ mm in this case, and the beam energy is about 215 MeV [3]. In the experiment the FF image is filtered with a 633 ± 5 nm bandpass filter (BPF) which is narrow enough so that the fringe visibility is dependent on only the beam divergence.

OPTIMIZATION OF ANTIPROTON CAPTURE FOR ANTIHYDROGEN CREATION IN THE ALPHA EXPERIMENT

S. Fabbri*, W. Bertsche, University of Manchester, Manchester, England

Abstract

At the ALPHA Experiment at CERN, thin foils of material are used to slow down and trap antiprotons in a Penning trap, where they can be used for antihydrogen creation and measurements. Historically, over 99% of antiprotons are lost during the capture process as a result of the 5.3 MeV initial kinetic energy of the beam delivered by the Antiproton Decelerator. This places a limit early on in the achievable number of antihydrogen. ELENA is a new storage ring coming online which will lower this initial kinetic energy of the beam to 100 keV, improving this efficiency but requiring experiments to update their infrastructure. We present Monte Carlo and particle tracking simulation results for the optimization of the new degrading foil material, thickness, and location in the ALPHA catching Penning trap. From these results, we expect an upper capture efficiency of approximately 50%.

INTRODUCTION

As charged particles pass through a degrader, they are slowed down through inelastic collisions with the electrons of the target's atoms, referred to as 'electronic', and elastic collisions, referred to as 'nuclear' where the atom as a whole recoils. The antimatter experiments at CERN rely on this phenomena to slow the 5.3 MeV antiproton beam delivered by the Antiproton Decelerator (AD) [1] to trapable energies. A combination of the high initial kinetic energy of the antiproton beam and limitations on the particle trapping voltages has meant that in typical cases less than 1% of the antiproton beam is trapped. The ASACUSA collaboration achieved a higher capture efficiency by employing an additional RF decelerating cavity at the entrance to their experiment [2], at the expense of a device with added complexity, cost, and size.

ELENA is a new ring which will decelerate the antiproton beams from the AD to 100 keV [3]. The reduced initial kinetic energy of the beam will increase the percentage of trapable antiprotons by up to two orders of magnitude. To accommodate for ELENA, experiments need to upgrade their particle apparatus. The following paper presents a portion of the proposed modifications for the ALPHA Experiment, but applicable to other Penning trap based experiments.

Particles exiting the ALPHA degrader enter into a Penning-Malmberg charged particle trap [4], termed the 'Catching Trap' (CT), as shown in Fig. 1. Such a trap uses a strong axial magnetic field B_z for radial confinement and an electrostatic well for axial confinement that is limited to a longitudinal energy depth of ~ 5 keV for practical reasons. The trap has 18 low voltage electrodes, and two high

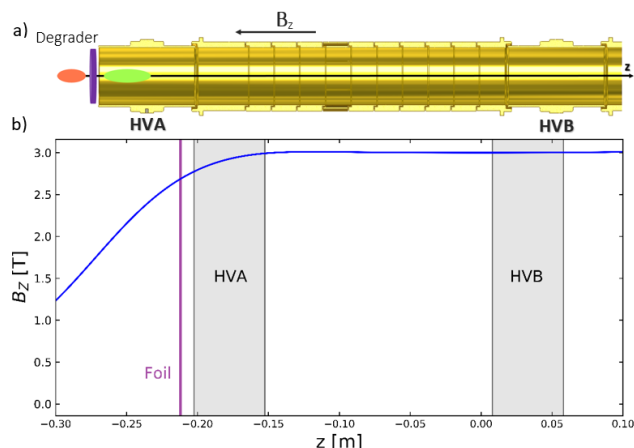


Figure 1: a) Partial schematic of the ALPHA degrader and catching trap electrodes (2012-2018). An example antiproton beam passes through the degrading foil from high energy (red) to low energy (green), and enters into the electrically-isolated cylindrical electrodes. HVA and HVB are special high voltage electrodes of inner diameter 29.6 mm. b) The longitudinal magnetic field B_z (blue) in the ALPHA catching trap, with $z = 0$ corresponding to its center.

voltage (HV) electrodes, HVA and HVB, used for capturing incoming antiproton bunches [5]. Particles emerging from the foils with energy less than 5 keV are reflected by a potential barrier of -5 kV (this is HVB in Fig. 1). Before these reflected particles can return to the degrader, a -5 kV potential is switched onto HVA and the capturing process is completed. Trapped particles then undergo sympathetic cooling and manipulation with preloaded electrons, until they are cold and dense enough for antihydrogen formation. Once this occurs, they are extracted to the atom trap, where they form antihydrogen through recombination with cold positron plasmas [6].

We present an optimization study of the new degrading foil material, thickness, and location in the ALPHA CT for slowing future ELENA beams. A combination of analytic models, Monte Carlo simulation codes, and a particle tracking code have been employed to model the antiproton energy loss process and capture in the trap.

DEGRADING APPARATUS MATERIAL AND THICKNESS

The stopping power, $S(E)$, of a material is defined as the ion's mean energy loss per travelled path length, $-dE/dx$. Figure 2 displays the electronic stopping power for degrading materials considered in this study. We utilized two primary Monte Carlo simulation packages, SRIM-2013 [7] and

* siara.sandra.fabbri@cern.ch

MEASUREMENT OF THE SECOND MOMENTS OF TRANSVERSE BEAM DISTRIBUTION WITH SOLENOID SCAN*

I. Pinayev[†], Brookhaven National Laboratory, Upton, U.S.A.

Abstract

Measurement of the dependence of the beam size on profile monitor vs. strength of a focusing element is widely used for measurement of the beam parameters. Such measurements are mostly used for the separate planes and assumption that beam satisfied Gaussian distribution. In many linear accelerators the transverse beam dynamics is coupled between planes and distribution is far from the Gaussian. We developed measurement technique of the second moments of beam distribution which does not rely on any assumptions. The theory and experimental results are presented.

INTRODUCTION

The charged beam in the accelerator is usually is described by Twiss parameters α , β , γ , and emittance ϵ . Transverse motion in each plane is considered decoupled and parameters at particular point (α_0 , β_0 , γ_0 , ϵ_0) can be found by solving a set of n linear equations:

$$\begin{pmatrix} \sigma_x^2(1) \\ \sigma_x^2(2) \\ \dots \\ \sigma_x^2(n) \end{pmatrix} = \begin{bmatrix} S_{11}^2(1) & -2S_{11}(1)S_{12}(1) & S_{12}^2(1) \\ S_{11}^2(2) & -2S_{11}(2)S_{12}(2) & S_{12}^2(2) \\ \dots & \dots & \dots \\ S_{11}^2(n) & -2S_{11}(n)S_{12}(n) & S_{12}^2(n) \end{bmatrix} \begin{pmatrix} \beta_0 \epsilon_x \\ \alpha_0 \epsilon_x \\ \gamma_0 \epsilon_x \end{pmatrix} \quad (1)$$

where S is a transfer matrix between the point of interest and observation point (profile monitor).

$$\begin{pmatrix} x_1 \\ x'_1 \\ y_1 \\ y'_1 \end{pmatrix} = S \begin{pmatrix} x_0 \\ x'_0 \\ y_0 \\ y'_0 \end{pmatrix} \quad (2)$$

The index in the parentheses indicates measurement with varying transfer matrix by the strength of focusing element and/or utilized profile monitor. All four parameters can be resolved using equation connecting Twiss parameters

$$\beta\gamma = 1 + \alpha^2$$

In general case Twiss parametrization is not applicable and one can utilize only the measurements of the second moments of the transverse distribution $\langle x^2 \rangle$, $\langle x'^2 \rangle$, $\langle xx' \rangle$, $\langle y^2 \rangle$, $\langle y'^2 \rangle$, $\langle yy' \rangle$, $\langle xy \rangle$, $\langle xy' \rangle$, $\langle x'y \rangle$, and $\langle x'y' \rangle$ (here we assume that all the first moments are equal zero). Profile monitor provides three observables $\langle x^2 \rangle$, $\langle y^2 \rangle$, and $\langle xy \rangle$. For the n measurements Eq. 1 transforms into

$$\begin{pmatrix} \sigma_x^2(1) \\ \sigma_y^2(1) \\ \sigma_{xy}(1) \\ \dots \\ \sigma_x^2(n) \\ \sigma_y^2(n) \\ \sigma_{xy}(n) \end{pmatrix} = \mathbf{R} \begin{pmatrix} \langle x^2 \rangle \\ \langle xx' \rangle \\ \langle x'^2 \rangle \\ \langle y^2 \rangle \\ \langle y'^2 \rangle \\ \langle yy' \rangle \\ \langle xy \rangle \\ \langle x'y' \rangle \\ \langle x'y \rangle \\ \langle xy' \rangle \end{pmatrix} \quad (3)$$

where \mathbf{R} is $3n \times 10$ matrix formed using elements of the transfer matrix S in a manner similar used in [1] (we do not show it explicitly due to its size). On the left size of the Eq. (3) is columnar vector with experimental observables, and on the right side ten seconds moments of the beam at the point of interest. For the illustration we show the dependence of σ_x^2 from transport matrix and ten moments:

$$\sigma_x^2 = S_{11}^2 \langle x^2 \rangle + 2S_{11}S_{12} \langle xx' \rangle + S_{12}^2 \langle x'^2 \rangle + S_{13}^2 \langle y^2 \rangle + 2S_{13}S_{14} \langle yy' \rangle + S_{14}^2 \langle y'^2 \rangle + 2S_{11}S_{13} \langle xy \rangle + 2S_{12}S_{14} \langle x'y' \rangle + 2S_{11}S_{14} \langle xy' \rangle + 2S_{12}S_{13} \langle x'y \rangle \quad (4)$$

Now one can find the second moments by solving the system of linear equations when at least four measurements were performed. However, matrix \mathbf{R} is rank deficient. No matter how many experimental points we have its rank is 9. Analysis showed that this is a fundamental feature of the system containing only solenoids and drifts. Neither transfer matrix of solenoid [2] nor transfer matrix of drift does not change $x'y - xy'$. To resolve these moments, we need to add a quadrupole into the transport line. We do not have any quadrupole in the transport, therefore in the analysis of the experimental results we assumed that $\langle x'y \rangle = \langle xy' \rangle$.

It should be noted that the approach we used is suitable for emittance dominated beams. The substantial space charge forces will introduce systematic errors which are behind the scope of this paper.

EXPERIMENTAL RESULTS

The proposed approach was tested on the two accelerators in the RHIC complex: the first one used for coherent electron cooling (CeC) experiment [3, 4], and the second one for the low energy RHIC electron cooler (LEReC) [5, 6].

The measurements performed at CeC accelerator utilized electron beam generated by 1.25 MeV superconducting RF gun. Bunch length was 375 ps and bunch charge 0.6 nC. The measurements results are shown in Fig. 1. This beam is close to round.

* Work supported by Brookhaven Science Associates, LLC under Contract No. DE-AC02-98CH10886 with the U.S. Department of Energy

[†] pinayev@bnl.gov

TIME-OF-FLIGHT TECHNIQUE FOR MATCHING ENERGIES IN ELECTRON COOLER*

I. Pinayev†, R. Hulsart, K. Mernick, R. Michnoff, BNL, Upton, U.S.A.
Z. Sorrell, ORNL, Oak Ridge, U.S.A.

Abstract

Electron cooler with bunched electron beam is being commissioned at the Relativistic Heavy Ion Collider at BNL. For the cooler to operate the energies of the hadron and electron beams should be matched with high accuracy. We have developed time-of-flight technique based on the phase measurement of the beam induced signal in the beam position monitors separated by a drift. We present the method description and experimental results.

INTRODUCTION

The purpose of the low energy RHIC electron cooler is (LEReC) is to provide luminosity improvement for the operation at low energies [1]. Unlike other electron coolers LEReC uses bunched electron beam accelerated to the desired energy using RF cavities [2].

For the successful cooler operation, the energy match between hadrons and the electrons should be better than 10-3. Such accuracy is hard to achieve with low-energy beams (relativistic factor $\gamma=4-6$). For this purpose, for redundancy three techniques have been developed. The 180-degree magnet and recombination monitor are described in [3]. This paper is focused on the approach based on measurement of the phase difference of two signals excited by the beams on two beam position monitors (BPMs) with RF processing.

For the two BPMs separated by distance L_{drift} the propagation time t of the bunch depends on its relativistic factor

$$t = \frac{L_{drift}}{c\sqrt{1-1/\gamma^2}} \quad (1)$$

where c is speed of light and phase difference ϕ at processing frequency F_{proc}

$$\phi = 2\pi t F_{proc} \quad (2)$$

Measured phase difference is affected by the delays in the cables and shifts in the electronics which makes it difficult to use this technique for absolute measurement of the beam relativistic factor. However, if the drifts are small then phase information can be used for matching of the beam velocities. For difference in relativistic factor $\Delta\gamma$ the phase difference will be

$$\Delta\phi = \frac{2\pi F_{proc} L_{drift}}{c\sqrt{1-1/\gamma^2}} \frac{1}{\gamma^2} \frac{\Delta\gamma}{\gamma} \quad (3)$$

* Work supported by Brookhaven Science Associates, LLC under Contract No. DE-AC02-98CH10886 with the U.S. Department of Energy

† pinayev@bnl.gov

From Eq. 3 one can see that sensitivity to the energy change quickly goes down with beam energy and this technique is applicable for not very relativistic beams. Having long distance between pick-up electrodes increases sensitivity, therefore they were placed at the ends of the cooling sections. For the highest energy the accuracy

The layout of the LEReC accelerator is shown in Fig. 1. The electron beam is generated by a DC gun with photocathode and then accelerated with superconducting 704 MHz booster cavity. The electron beam structure is defined by a drive laser and the structure is formed by trains of the 30 bunches separated by 1.4 nsec and repetition frequency of 9.4 MHz to match the hadron beams circulating in RHIC.

There are five implemented time-of-flight (ToF) subsystems. The first one is in the injection line and uses two BPMs separated by 2.273 meters. The signal is processed at 713.4 MHz frequency to avoid interference from the RF field from the booster cavity. Each cooling section has two subsystems one at high frequency (704.0 MHz) to monitor energy stability of the electron beam and one at low frequency (9.4 MHz) to perform matching of the relativistic factors. In the yellow ring distance between pick-up electrodes is 17.857 meters and in the blue ring it is 18.958 meters.

Signal processing is performed in the BPM modules [4] with modified firmware. The two raw signals pass from separate pick-up electrodes through the analogue filters and digitally processed in the same module to the desired bandwidth. Processing in the same module is critical to avoid systematic errors introduced by different ADC clocks.

Since the signal level is sufficiently high then the Johnson noise is well below the noise due to the ADC clock jitter σ_{clock} . The signal to noise ratio in the phase is

$$S/N = \frac{\phi}{2\pi\sigma_{clock}F_{proc}} = \frac{t}{\sigma_{clock}} \quad (4)$$

As one can see it does not depend on the processing frequency. Choosing the low processing frequency reduces the cable losses and phase shifts.

We have utilized the specialized modules but signal processing can be done in the regular BPMs – the amplitude of the signal used for position and phase for relativistic factor monitoring.

EXPERIMENTAL RESULTS

Verification of the proposed method was done using measurement of the phase difference between two BPM

Content from this work may be used under the terms of the CC BY 3.0 licence (© 2019). Any distribution of this work must maintain attribution to the author(s), title of the work, publisher, and DOI

BEAM POSITION MONITORING SYSTEM FOR FERMILAB'S MUON CAMPUS*

N. Patel†, P. Prieto, J. Diamond, D. Voy, C. McClure, N. Eddy,
 Fermi National Accelerator Laboratory, Batavia, USA

Abstract

A Beam Position Monitor (BPM) system has been designed for Fermilab Muon Campus. The BPM system measures Turn-by-Turn orbits as well as Closed Orbits (average of multiple turns). While in the early commissioning phase of this program, preliminary measurements have been made using these BPMs. This paper discusses the design and implementation of these BPMs.

INTRODUCTION

A BPM system is required for providing transverse position to transport proton bunches through the Muon Campus beam lines shown in Figure 1. Ninety-four split plate style BPMs are placed along the transport lines and 120 split plate BPMs are in the Delivery Ring.

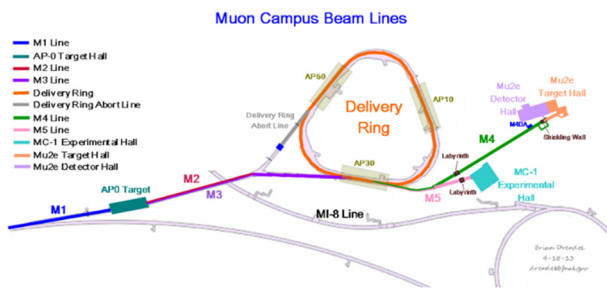


Figure 1: Map of muon campus beam lines.

Table 1: Beam Specifications

Parameter	Requirement	Units
Maximum Intensity	1×10^{12}	protos
Revolution Frequency (central orbit)	590018	Hz
Bunch Length (rms)	35	nsec

DESIGN OVERVIEW

The BPM system block diagram is shown in Figure 2. Each BPM has 2 ports corresponding to each of the pickups of the split plate style BPM. All of the 94 transfer-line and 120 Delivery Ring BPMs were already installed for previous experiments. As such, it was found that 4 different types of split plate BPMs were used throughout the transfer line. The majority of them are cylindrical with 4.5" diameter, however a few of the split-plates are rectangular.

Figure 3 shows a picture of the most common BPM used. There are 5 service buildings along the transport line which house the electronics. The BPMs have a type-N connector welded on the housing. The coaxial cables connecting these to electronics in the service buildings can vary in length from 100 to 900 feet. The variation of cable type and length used results in a 4dB variation in loss across all the channels.

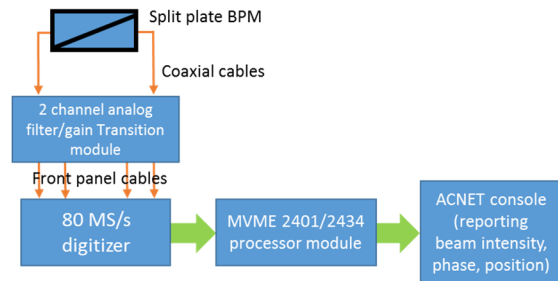


Figure 2: Muon campus BPM system block diagram.

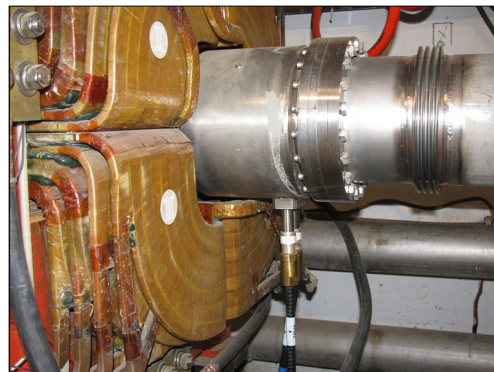


Figure 3: Picture of split-plate BPM implemented.

A stretch wire scanning test was performed to map out the BPM pick up response versus position. In this test, a wire is stretched longitudinally within the beam pipe. The response of the BPM pick-ups was measured as the wire was swept in the transverse direction. Data from this test is shown in Figure 4. The good linearity from this split-plate style BPM can be observed in this plot. The scaling

DEVELOPMENT OF AN AUTOMATED BPM TEST BENCH

M. Schwarz*¹, D. Strehl², H. Höltermann², B. Koubek², H. Podlech¹,
U. Ratzinger², W. Schweizer², C. Trageser²

¹IAP, Goethe University, Frankfurt am Main, Germany

²BEVATECH GmbH, Frankfurt am Main, Germany

Abstract

The Institute for Applied Physics (IAP) of Goethe University Frankfurt has a long history in developing DTL-cavities and further essential components of particle accelerators from design and simulation up to tuning and final testing. In recent times, the development of beam diagnostic components for the hadron accelerator projects has become increasingly important. BEVATECH is designing and setting up linear accelerators, RF and vacuum technology for research laboratories and enterprises worldwide. In a joint effort a simple, efficient and mobile beam position monitor (BPM) test bench has been developed and will be further improved for future tests and the calibration of beam position monitors. It is fully automated using single-board computers and microcontrollers to obtain the essential calibration data like electrical offset, button sensitivity and the 2D response map. In addition, initial tests with the implementation and evaluation of the Libera signal processing units Single Pass H and Spark were promising.

INTRODUCTION

Beam position monitors are an essential tool for the operation of a particle accelerator. As a non-destructive diagnostic device, they are used very frequently in nearly all linacs, cyclotrons and synchrotrons worldwide. Providing the beam's center of mass position as well as a monitor for longitudinal beam position and shape, the BPM is an indispensable component of beam diagnostic strategies.

BPMs for several projects and a corresponding BPM test bench (see Fig. 1) have already been developed or are currently under development by IAP and BEVATECH. These include for example the MYRRHA (Multipurpose hYbrid Research Reactor for High-end Applications) project [1] which aims at realizing a pre-industrial Accelerator Driven System (ADS) to explore the transmutation of long lived nuclear waste. Furthermore, it will also be used as multipurpose irradiation facility applying fast neutrons. The linac for this ADS will be a high-power proton accelerator delivering 2.4 MW CW beam at 600 MeV [2, 3].

Further BPM developments are related to NICA (Nuclotron-based Ion Collider fAcility) at JINR (Joint Institute for Nuclear Research) in Dubna, Russia. The NICA facility aims to perform a wide program of fundamental and applied research with ion beams from p to Au at energies from a few hundred MeV/u up to a few GeV/u. As an injector for heavy ions into the Booster synchrotron of the NICA accelerator facility the Heavy Ion Linac (HILac)



Figure 1: View of the BPM test bench with Libera Spark for data acquisition.

has recently been put into operation. The HILac consists of three accelerating sections (RFQ and two DTL sections based on IH-DTL cavities) and a medium energy beam transport (MEBT) section [4].

In the frame of the NICA ion collider upgrade a new light ion frontend linac (LILac) for protons and ions with a mass-to-charge ratio of up to 3 will be built [5–7]. Consisting of three parts - a normal conducting linac up to 7 MeV/u, a normal conducting energy upgrade up to 13 MeV/u and a superconducting section - the first part will be built in collaboration between JINR and BEVATECH. This also includes beam diagnostic devices like beam position monitors.

After manufacturing of a BPM, it should be tested to measure the button's sensitivity, the deviation of its mechanical and electrical center as well as non-linearities in the format of a 2-dimensional response map. The latter is used to determine the differences between the theoretical and measured beam positions. For these calibration measurements, many laboratories worldwide use a wire-based approach [8–24]. By feeding the copper wire with an RF-sine signal, which

* schwarzz@iap.uni-frankfurt.de

TECHNOLOGY AND FIRST BEAM TESTS OF THE NEW CERN-SPS BEAM POSITION SYSTEM

M. Wendt*, A. Boccardi, M. Barros Marin, T. Bogey, I. Degl’Innocenti, A. Topaloudis
 CERN, Geneva, Switzerland

Abstract

The CERN Super Proton Synchrotron (SPS) uses 215 beam position monitors (BPMs) to observe the beam orbit when accelerating protons or ions on a fast ramp cycle to beam energies of up to 450 GeV/c. In the frame of the CERN LHC Injector Upgrade (LIU) initiative the aged, and difficult to maintain homodyne-receiver based BPM read-out system is currently being upgraded with A Logarithmic Position System – ALPS. As the name indicates, this new BPM electronics builds upon the experience at CERN with using logarithmic detector amplifiers for beam position processing, and is well suited to cover the large range of beam intensities accelerated in the SPS. The system will use radiation tolerant electronics located in close proximity to the split-plane or stripline beam position monitor with GB/s optical data transmission to the processing electronics located on the surface. Technical details of the analog and digital signal processing, the data transmission using optical fibers, calibration and testing, as well as first beam tests on a set of ALPS prototypes are presented in this paper.

INTRODUCTION

After more than 20 years of operation, the Multi-turn Orbit Position System (MOPOS) [1, 2] will be replaced by A Logarithmic Position System (APLS) to monitor the beam orbit and provide beam trajectory information of the Super Proton Synchrotron (SPS) at CERN. Figure 1 gives an overview of the new ALPS BPM read-out electronics in the form of a simplified block schematic, with more details in terms of BPM system requirements, beam conditions in the SPS and the initial R&D on ALPS found in [3].

Of the 215 BPM pickups distributed around the 6.7 km circumference of the SPS, most are single-plane “shoe-box” (split-plane) style BPMs, with a few stripline monitors in special locations. Apart from the mechanical structure of these BPMs themselves, all the existing BPM read-out hardware will be replaced, with a dedicated optical fiber infrastructure added. Due to the large variety of beam formats, intensities, particle species and operational modes of the SPS, a dynamic compression in the form of a set of logarithmic power detectors is applied to condition the BPM pickup signals to accommodate the required dynamic range of 90 dB without gain switching, see also [3]. Here the intensity normalization of the BPM electrode signals is based on the well-known principle:

$$\begin{aligned} \text{pos} &= \frac{1}{S_{\text{dB}}k} 20 \log_{10} \left(\frac{A}{B} \right) \\ &= \frac{1}{S_{\text{dB}}} \left[\frac{1}{k_A^{\text{rg}}} 20 \log_{10}(A^{\text{rg}}) - \frac{1}{k_B^{\text{rg}}} 20 \log_{10}(B^{\text{rg}}) \right], \end{aligned} \quad (1)$$

where A and B are the signals of the BPM pickup electrodes of a single plane and S_{dB} is the sensitivity of the BPM pickup. For the SPS $S_{\text{dB}}^{\text{hor}} = 0.2 \text{ dB/mm}$ and $S_{\text{dB}}^{\text{vert}} = 0.4 \text{ dB/mm}$ for the split-plane BPMs. Once the BPM pickup signals are detected, post-amplified and digitized, a linear calibration constant k (unit: ADC counts/dB) represents the transfer characteristic between the analog input and the digital output of the read-out electronics.

A key element of the analog front-end-electronics is the *Analog Devices ADL5519* dual logarithmic detector amplifier. This is preceded by two matched 200 MHz band-pass filters, and has its outputs connected to ADC driver amplifiers followed by anti-aliasing low-pass filters. A calibration signal circuit is also present. The analog and digital front-end are assembled in a 19-inch, 1U housing that is installed

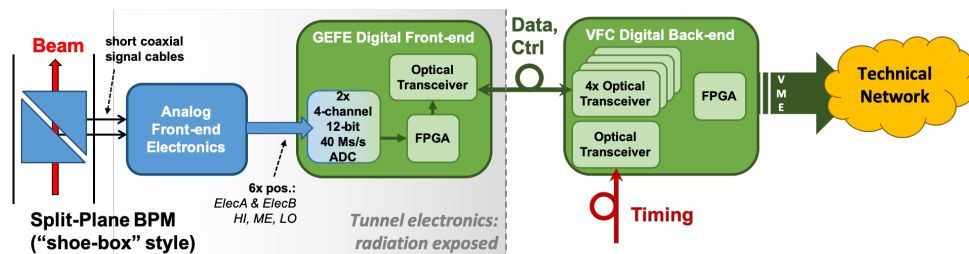


Figure 1: Simplified layout of the new CERN-SPS BPM read-out electronics (ALPS) – one channel shown.

* manfed.wendt@cern.ch

CHERENKOV DIFFRACTION RADIATION AS A TOOL FOR BEAM DIAGNOSTICS

D. Alves, M. Bergamaschi, A. Curcio, R.O. Jones, R. Kieffer, T. Lefèvre* S. Mazzone,
 N. Mounet, E. Senes, A. Schloegelhofer, CERN, Geneva, Switzerland
 K. Fedorov, P. Karataev, D. Harryman, K. Lekomtsev
 JAI, Royal Holloway University of London, Egham, UK
 V.V. Bleko, S.Y. Gogolev, A.S. Konkov, J.S. Markova, A.P. Potylitsyn, D.A. Shkitov
 Tomsk Polytechnic University, Tomsk, Russia
 M. Billing, J. Conway, Y. Padilla Fuentes, J. Shanks, Cornell University, Ithaca, USA
 M. Apollonio, L. Bobb, Diamond Light Source, Oxfordshire, UK
 A. Aryshev, N. Terunuma, KEK, Tsukuba, Japan
 J. Gardelle, CEA, Le Barp, France
 K. Lasocha, Jagiellonian University, Krakow, Poland

Abstract

Over the past 3 years, the emission of Cherenkov Diffraction Radiation (ChDR), appearing when a relativistic charged particle moves in the vicinity of a dielectric medium, has been investigated as a possible tool for non-invasive beam diagnostics. ChDR has very interesting properties, among which is the emission of a large number of photons in a narrow and well-defined solid angle which provides excellent conditions for signal detection with very little background. This contribution will present a collection of recent beam measurement results performed at several facilities such as the Cornell Electron Storage Ring (CESR), the Advanced Test Facility 2 (ATF2) at KEK and the CLEAR test facility at CERN. These results, complemented by simulations, are showing that both the incoherent and coherent emission of Cherenkov Diffraction radiation could open the path for a new kind of beam diagnostic technique for relativistic charged particle beams.

INTRODUCTION

The emission of Cherenkov radiation by charged particles travelling through matter was discovered in 1934 [1,2] and, due to its fascinating properties (i.e. the emission of a large number of photons in a narrow and well-defined solid angle), has found numerous applications in many fields including astrophysics [3], and particle detection and identification [4,5]. Recently, a first experiment was performed to investigate the possibility of non-invasive beam diagnostic techniques based on the detection of incoherent Cherenkov diffraction radiation (ChDR) [6]. The latter refers to the emission of Cherenkov radiation by charged particles travelling not inside, but in the vicinity of, a dielectric material. This combines the already well-known advantages of Cherenkov radiation with non-invasive photon generation, making it an ideal technique for beam instrumentation. In this paper we present a summary of the work performed by our team in developing both incoherent and coherent ChDR techniques

over the past 3 years. This includes the development of a theoretical model to predict the characteristics of the emitted radiation for a given geometry and 3D electromagnetic simulations that can be used to simulate coherent radiation emitted at mm wavelength for any geometry. We also present an overview of the experimental results to date from several different beam facilities.

PHYSIC MODEL AND SIMULATIONS

Cherenkov diffraction radiation can be considered as Polarization Radiation (PR) resulting from polarization currents in the volume of a dielectric induced by the electromagnetic field of a passing particles. The model developed in [7,8] predicts that the photons radiated by a relativistic particle in a simple geometry such as the one presented on Fig. 1 are emitted at the Cherenkov angle all along the dielectric before being refracted out at the end of the radiator. An example of the calculated angular spectral density for such a case is given in Fig. 2, which shows the horizontal and vertical polarization content of the radiation emitted by a 5.3 GeV positron propagating at a distance of 0.8 mm from the surface of a 2 cm long dielectric made out of fused silica.

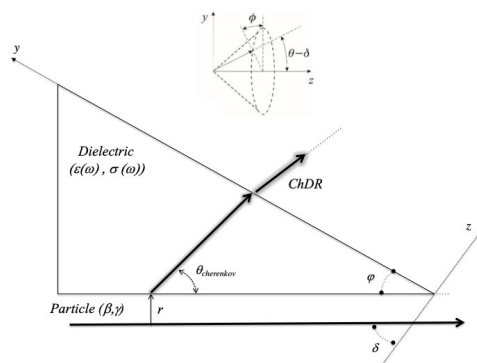


Figure 1: Emission of Cherenkov diffraction radiation by a charged particle propagating at a distance ρ from the surface of a dielectric material.

* thibaut.lefevre@cern.ch

TOWARDS FULL 4H-SiC BASED X-RAY BEAM MONITORING

M. Carulla† and M. Camarda, Paul Scherrer Institute, Villigen, Switzerland
 M. Birri, B. Meyer, D. Grolimund, C. Pradervand, O. S. Nida¹, A. Tsibizov¹, T. Ziemann¹,
 U. Grossner¹, Paul Scherrer Institute, Villigen, Switzerland
¹also at Advanced Power Semiconductor Laboratory, ETH Zurich, Switzerland

Abstract

In this work, we present a systematic theoretical and experimental investigation of the use of Silicon Carbide thin (thicknesses between 500 nm and 10 μm) low-doped large area ($>10\text{ mm}^2$) membranes as X-ray sensors for beam position monitoring (XBPM) applications at synchrotron light sources (SLS).

INTRODUCTION

SLS generates high brilliance ($>1\text{ kW/cm}^2$) coherent and polarized X-ray beam for e.g. diffraction experiments conducted at the different beamlines. Beam stability is a key issue to increase throughput and resolution, especially in the case of small ($<100\text{ nm FWHM}$) beams [1]. This drove the demand for in-line, continuous, accurate and reliable monitoring. Semiconductor based X-ray Beam Position Monitors (XBPMs) are front to back quadrant detectors (Fig. 1) which provide continuous spatial and intensity information allowing, e.g. implementation of feedback loops to correct for example mirrors instabilities. Until recently, state-of-the-art commercial XBPMs were made of diamond, thanks to its excellent thermal conductivity, high melting point, wide bandgap and low absorption coefficient, i.e. high transparency (see Table 1) [2]. Diamond is not available as large single crystal wafers so the material availability and quality limit the sensor performance, thus the applications [3]. Nowadays, diamond XBPM are commercially available as small ($<25\text{ mm}^2$) single crystal or polycrystalline sensors [4, 5].

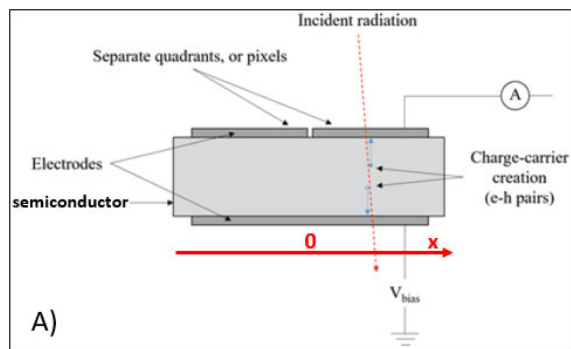


Figure 1: A schematic of a semiconductor based XBPM.

Table 1: Comparison of the Main Properties of Sc-Diamond and 4H-SiC

Property	Sc-Diamond	4H-SiC
Effective Quantum Yield per photon energy [1/eV]	0.077	0.128
X-ray attenuation length at 8keV [μm]	650	70
Thermal Conductivity [W/cmK]	22	4.9
Shottky Barrier Height (to nickel) [eV]	1.5	1.56

4H-SiC XBPM

Thanks to the mechanical and electrical properties of 4H-SiC (see Tab.1), as well as the 4H-SiC material maturity due to the power device industry, represents a superior alternative to diamond. However SiC was never tested for X-ray beam monitor application due to its high absorption coefficient (see Tab.1) and the thickness of the available substrates, i.e. $>350\text{ }\mu\text{m}$. In the last years, a newly developed/patented [2018P04211EP] doping selective electrochemical etching process makes possible the thinning of 4H-SiC substrates. 4H-SiC XBPM produced using doping selective electrochemical etching show superior optical (transparency) and electrical (dynamics, linearity and signal strength) properties in comparison to state-of-the-art commercial single crystal and polycrystalline diamond sensors, respectively [6].

Pink Beam and White Beam

Pink beam is the beam delimited by the region between the front-end and the monochromator, while whitebeam is the beam in the front-end region, just after the insertion device, as PSI beamline convention. The pink beam expected power is in the order of several hundred watts, so it is mandatory to have as-thin-as-possible XBPMs, to reduce the absorbed power and thus avoid thermal run-aways. Furthermore, a Rapid Thermal Annealing (RTA) of the XBPM metallization should be done, in order to form an alloy with silicon and so increase the evaporation temperature of the contacts.

In the other hand the expected power of white beam will be on the order of several thousand watts, for such applications a new XBPM design without membrane and a pinhole

† maria.carulla@psi.ch

ROSE - A ROTATING 4D EMITTANCE SCANNER

M.T. Maier†, L. Groening, C. Xiao

GSI Helmholtzzentrum für Schwerionenforschung GmbH 64291 Darmstadt, Germany

A. Bechtold, J. Maus, NTG Neue Technologien GmbH & Co. KG, 63571 Gelnhausen, Germany

Abstract

The detector system ROSE [1, 2], allowing to perform 4D emittance measurements on heavy ion beams independent of their energy and time structure, has been built and successfully commissioned in 2016 at GSI in Darmstadt, Germany. This method to measure the four dimensional emittance has then been granted a patent in 2017. The inventors together with the technology transfer department of GSI have found an industrial partner to modify ROSE into a fully standalone, mobile emittance scanner system. This is a three step process involving the ROSE hardware, the electronics ROBOMAT* and the software working packages. The electronics was commissioned at the ECR test bench of the Heidelberg ion therapy facility HIT in June 2019. Currently our main focus is on the development of the 4D software package FOUROSE**. This contribution presents the actual status and introduces the multiple possibilities of this 4D emittance scanner.

MOTIVATION

Usually just separated measurements of two-dimensional $x-x'$ and $y-y'$ sub phase-spaces (planes) are measured, as for simplicity correlations between the two planes, i.e. $x-y$, $x-y'$, $x'-y$, and $x'-y'$ are often assumed as zero. However, such inter-plane correlations may be produced by non-linear fields such as dipole fringes, tilted magnets or just simply by beam losses. An example for matching the round transverse phase space of a linac beam to the flat acceptance of a synchrotron is shown in Figure 2. To accomplish this, inter-plane correlations are a prerequisite [3, 4].

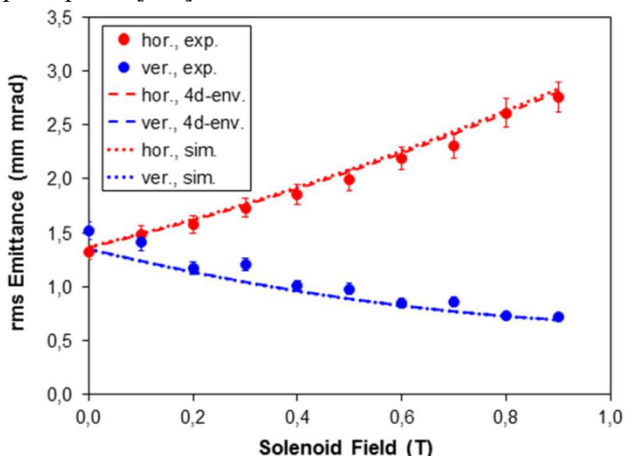


Figure 1: One knob emittance transfer using EMTEX [3].

In order to remove correlations that do increase the projected rms-emittances they must be quantified by measurements. This applies especially if space charge effects are involved as they cannot be calculated analytically.

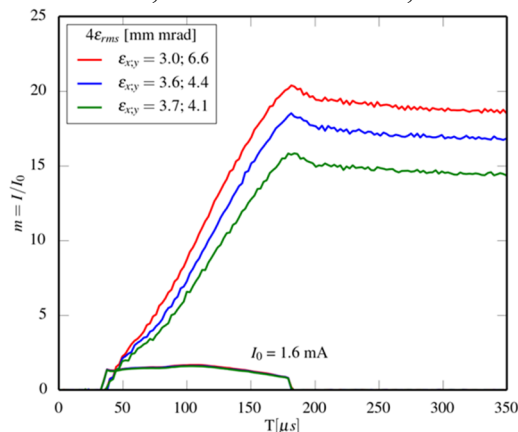


Figure 2: The emittance transfer using EMTEX directly translates in increased injection efficiency into SIS18 [4].

Using the skew triplet of the EMTEX setup we have measured the increase of the projected rms-emittance of a U28+ beam with 11.4 MeV/u to be in the order of 75%. Removing this inter-plane coupling could increase the beam brilliance and thus the injection efficiency into SIS18 [5].

THEORY OF ROSE

ROSE is a standard slit-grid emittance scanner using only one measuring plane which is rotatable around the beam axis. In combination with a magnetic doublet it allows to determine the full 4D beam matrix C with a minimum of four emittance measurements at three different angles.

$$C = \begin{bmatrix} \langle XX \rangle & \langle XX' \rangle & \langle XY \rangle & \langle XY' \rangle \\ \langle X'X \rangle & \langle X'X' \rangle & \langle X'Y \rangle & \langle X'Y' \rangle \\ \langle YX \rangle & \langle YX' \rangle & \langle YY \rangle & \langle YY' \rangle \\ \langle Y'X \rangle & \langle Y'X' \rangle & \langle Y'Y \rangle & \langle Y'Y' \rangle \end{bmatrix} \quad (1)$$

Figure 3 shows that the emittance measurements are done using a quadrupole doublet setting (a) for the 0° , 45° , and 90° measurement and a setting (b) for another 45° measurement.

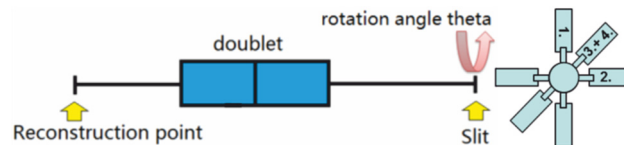


Figure 3: To obtain the beam matrix C at the reconstruction point four emittance measurements are done using ROSE behind a quadrupole doublet.

Work supported by:
* Bundesministerium für Wirtschaft und Energie - WIPANO
** Land Hessen - Innovationsförderung Hessen LOEWE 3
† m.maier@gsi.de

TRANSVERSE EMITTANCE MEASUREMENT USING UNDULATOR HIGH HARMONICS FOR DIFFRACTION LIMITED STORAGE RINGS*

K. P. Wootton[†], J. L. McChesney, F. Rodolakis, N. S. Sereno, B. X. Yang
 Argonne National Laboratory, Lemont, USA

Abstract

A particular challenge for diagnostics in diffraction limited storage ring light sources is the measurement of electron beam transverse emittances. In the present work, we present measurements and simulations of vertical electron beam emittance using high harmonics from an electromagnetic undulator in the present Advanced Photon Source storage ring. Based on these results, using simulation we motivate an undulator-based horizontal and vertical transverse emittance monitor for diffraction limited storage rings, using the Advanced Photon Source Upgrade as an example.

INTRODUCTION

Over the coming years, the Advanced Photon Source Upgrade (APS-U) project will convert the existing Advanced Photon Source (APS) facility to a high brilliance diffraction limited electron storage ring (DLSR) light source [1]. The horizontal emittance of the APS-U storage ring lattice will be 41.7 pm rad [1]. In that regard, measurement of the horizontal emittance at DLSRs presents similar challenges to measurement of the vertical emittance measurement at existing third generation storage rings [2–8].

Dedicated emittance and electron beam energy spread monitors have been designed for the APS-U storage ring employing bending magnet radiation sources [9]. These monitors have been optimised to confirm the small transverse horizontal and vertical emittances of the proposed APS-U storage ring.

A technique that has previously been used to measure pm rad scale vertical emittances employs a vertical undulator undulator by mapping the energy and spatial profile of the ID beam by coordinated scans of the monochomator and aperture [10–14]. In the present work, we use the Intermediate Energy X-ray (IEX) beamline to measure the vertical emittance of the existing APS storage ring. Based on these results, using simulations we motivate that this technique could be used to measure transverse emittances of DLSRs, using the APS-U as an example.

IEX BEAMLINE

This experiment was conducted using the APS storage ring and the Angle-Resolved Photoemission Spectroscopy branch line of the IEX beamline [15, 16]. The IEX beamline is a user beamline at the APS storage ring. A schematic of the IEX beamline is given in Fig. 1.

* Work supported by the U.S. Department of Energy, Office of Science, Office of Basic Energy Sciences, under Contract No. DE-AC02-06CH11357.

[†] kwootton@anl.gov

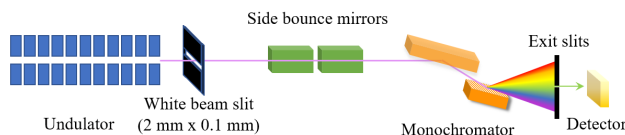


Figure 1: Schematic of IEX beamline components used in the present experiment.

The IEX undulator is an electromagnetic insertion device (ID), able to operate in horizontal, vertical and left and right-hand circular polarisation modes [16–19]. It is possible to operate the ID in quasi-periodic mode [19, 20], but for this experiment the ID was operated with full periodicity. Parameters of the electron beam and ID for both experiment and simulations are summarised in Table 1.

The white beam slits correspond to the first optical element of the beamline and are located at a longitudinal position of 28.8 m downstream of the centre of the ID and was used to define the portion of the ID radiation being sampled [15]. This is the longitudinal position at which all simulations and measurements in this work are evaluated. The photon beam is horizontally deflected by two gold coated planar mirrors which are located just downstream of the white beam slits. The second mirror has the largest angle of incidence, 1.5 degrees, and is responsible for maximum energy cutoff of ~3000 eV. Downstream of these mirrors is a variable line-spacing plane grating monochromator which focuses the beam on the exit slit for all photon energies.

Table 1: Parameters of electron beam and undulator for APS (experiment and simulations), and APS-U (simulations)

Parameter		APS	APS-U	Units
Electron beam				
Energy	E	7.0	6.0	GeV
Horiz. emittance	ϵ_x	3100	41.7	pm rad
Horiz. beta	β_x	19.1	5.19	m
Vert. beta	β_y	3.20	2.40	m
Horiz. dispersion	η_x	167	0.39	mm
Energy spread	$\Delta E/E$	0.096	0.135	%
IEX undulator				
Peak magnetic field	B_x	0.322	-	T
Peak magnetic field	B_y	-	0.322	T
Undulator period	λ_u	0.125	0.125	m
Number of periods	n_u	38	38	-
First harmonic	ϵ_1	461	339	eV
IEX beamline				
White beam slits		28.8	28.8	m

MACHINE LEARNING-BASED LONGITUDINAL PHASE SPACE PREDICTION OF TWO-BUNCH OPERATION AT FACET-II*

C. Emma[†], A. Edelen, M. Alverson, A. Hanuka, M. J. Hogan, B. O'Shea,
D. Storey, G. White, V. Yakimenko
SLAC National Accelerator Laboratory, Menlo Park, USA

Abstract

Machine learning (ML) based virtual diagnostics predict what the output of a measurement would look like when that diagnostic is unavailable [1]. This is especially useful for cases when a particular measurement is destructive. In this paper, we report on the application of ML methods for predicting the longitudinal phase space (LPS) distribution of the FACET-II linac operating in two-bunch mode. Our approach consists of training a ML-based virtual diagnostic to predict the LPS using only nondestructive linac and e-beam measurements as inputs. We validate this approach with a simulation study including the longitudinal smearing of the bunch profile which occurs as a result of measuring the LPS using a Transverse Deflecting Cavity (TCAV). We find good agreement between the simulated LPS as measured by the TCAV and the prediction from the ML model. We discuss how the predicted LPS profile compares to the actual beam LPS distribution extracted from simulation and how the resolution limits of the TCAV measurement are reflected in the ML prediction. We discuss important challenges that need to be addressed, such as quantifying prediction uncertainty, for this diagnostics to be implemented in routine accelerator operation. Finally, we report on the use of the ML-based prediction in conjunction with a standard optimizer for tuning the accelerator settings to generate a desired two-bunch LPS profile at the exit of the FACET-II linac.

INTRODUCTION

The main running configuration for PWFAs experiments at FACET-II will involve accelerating two bunches from the photocathode to the interaction point (IP) at the plasma entrance with specific longitudinal profile properties and drive-witness bunch separation. For a full description of PWFAs experiments at FACET-II see Ref. [2]. The major goals for the PWFAs experiments will be to demonstrate pump depletion of the 10-GeV drive beam and acceleration of the witness beam to approximately 20-GeV while preserving good beam quality. The figures of merit for the beam quality will be preservation of energy spread and emittance of the witness bunch, and these will need to be measured on a shot-to-shot basis for both the incoming distribution and the accelerated witness beam. To this end, accurate measurements of the bunch profile entering the plasma are essential for the success of the experimental campaign. Previous work has demonstrated the feasibility of using Machine Learning

(ML) models as virtual diagnostics to predict the LPS distribution of FACET-II single bunch operation (in simulation) and at LCLS (in experiment) [3].

At FACET-II we plan to measure the LPS distribution of the electron bunch at the entrance of the plasma with an X-band TCAV operating at a peak voltage of 20 MV. This introduces a challenge for accurately characterizing the longitudinal bunch profile, as the accelerator is expected to produce very short bunches ($\sigma_z \sim 1 \mu\text{m}$) beyond the TCAV resolution. In this work we examine the effect of the TCAV measurement on the performance of the ML-based virtual diagnostic and discuss its application in the FACET-II two-bunch operation mode.

In the following section we describe the TCAV measurement of the two-bunch configuration at FACET-II and compare the measured LPS distributions with the actual LPS which we extract directly from particle tracking simulations. The results show very good agreement between the LPS distribution measured by the TCAV and the LPS distribution predicted by the ML model. Due to TCAV resolution limits there is some discrepancy when we use the projection of the measured LPS distribution to infer the current profile at the entrance of the plasma. This discrepancy affects the accuracy of the ML-based virtual diagnostic, which predicts the LPS using the output of the TCAV measurement as training data. We present results from 3,125 simulations of the FACET-II linac from the exit of the injector to the end of the linac with induced jitter of key accelerator and beam parameters described in Table 1. The simulations include longitudinal space charge, incoherent and coherent synchrotron radiation and wakefields and are performed using the Lucretia particle tracking code [4].

SIMULATED TCAV MEASUREMENTS OF LONGITUDINAL PHASE SPACE AT FACET-II

Two-bunch Simulations

Three examples of the simulated LPS profiles as measured by the TCAV are shown in Fig. 1 with corresponding current profiles and prediction from the ML model. The three distributions shown represent an under-compressed, over-compressed and nearly fully-compressed (nominal) beam respectively. Note that the head of the bunch is on the left of the images. The ML model we used was a three-layer fully-connected neural network with (500,200,100) neurons in each successive hidden layer and a rectified linear unit activation function for each neuron. The network was trained using the open source ML library Tensorflow, and two sepa-

* This work was supported by the U.S. Department of Energy under Contract No. DEAC02-76SF00515

[†] cemma@slac.stanford.edu